

2009

A Study of E=C Compound Reactivity: Alkyne Addition and Polymerization

Laura C. Pavelka

Follow this and additional works at: <https://ir.lib.uwo.ca/digitizedtheses>

Recommended Citation

Pavelka, Laura C., "A Study of E=C Compound Reactivity: Alkyne Addition and Polymerization" (2009).
Digitized Theses. 3779.
<https://ir.lib.uwo.ca/digitizedtheses/3779>

This Thesis is brought to you for free and open access by the Digitized Special Collections at Scholarship@Western. It has been accepted for inclusion in Digitized Theses by an authorized administrator of Scholarship@Western. For more information, please contact wlsadmin@uwo.ca.

A Study of E=C Compound Reactivity: Alkyne Addition and Polymerization

(Spine Title: E=C Compound Reactivity: Alkyne Addition and Polymerization)
(Thesis Format: Integrated-Article)

By

Laura C. Pavelka

Graduate Program
in
Chemistry

A thesis submitted in partial fulfillment
of the requirements for the degree of
Doctor of Philosophy

The School of Graduate and Postdoctoral Studies
The University of Western Ontario
London, Ontario, Canada

© Laura C. Pavelka, 2009

THE UNIVERSITY OF WESTERN ONTARIO
SCHOOL OF GRADUATE AND POSTDOCTORAL STUDIES

CERTIFICATE OF EXAMINATION

Supervisor

Dr. Kim Baines

Supervisory Committee

Examiners

Dr. Mel Usselman

Dr. Mark Workentin

Dr. Paul Charpentier

Dr. Don Berry

The thesis by

Laura C. Pavelka

entitled:

**A Study of E=C Compound Reactivity: Alkyne Addition and
Polymerization**

is accepted in partial fulfillment of the
requirements for the degree of
Doctor of Philosophy

Date _____

Chair of the Thesis Examination Board

Abstract

In this thesis, various aspects of E=C compound reactivity are reported. Alkyne addition to three different phosphalkenes and a germene has been investigated. The results were compared to those reported from previous work on the addition of alkynes to silenes. Formal [2+2] cycloaddition does not appear to be a general pathway for the addition of alkynes to E=C compounds. Some cycloadducts were observed; however, ene-addition and CH-insertion of the terminal alkynyl bond across the E=C bond were also prominent. The favoured pathway of addition depends heavily on the polarity of the E=C bond, which varies with the main group element (E) and the electronic nature of the substituents.

Alkyne cycloaddition and CH-insertion pathways were modeled for silenes and germenes using computational chemistry. Cycloaddition involving the formation of a diradical intermediate was found to be the lowest energy pathway for both silenes and germenes.

Addition polymerization of a silene, $\text{Mes}_2\text{Si}=\text{C}(\text{H})\text{CH}_2t\text{Bu}$, and germene, $\text{Mes}_2\text{Ge}=\text{C}(\text{H})\text{CH}_2t\text{Bu}$, has also been investigated. The use of anionic and radical initiators is reported. The polymers contain a regularly alternating metalloid-carbon backbone.

Conditions for the living anionic polymerization of $\text{Mes}_2\text{Ge}=\text{C}(\text{H})\text{CH}_2t\text{Bu}$ have been explored. Low molecular weight polygermene can be synthesized in a controlled fashion in an ether-THF cosolvent using $t\text{BuLi}$ as the initiator. The conditions developed for the radical polymerization of $\text{Mes}_2\text{Ge}=\text{C}(\text{H})\text{CH}_2t\text{Bu}$ have been applied to the synthesis of germene-styrene copolymers.

Keywords

Addition Polymerization

Alkyne Addition

CH-Insertion

Copolymer

Cycloaddition

1,2-Dihydrophosphinine

DFT

Ene-addition

Germacyclobutene

Germene

Germylacetylene

Inorganic Polymer

Mechanism

Phosphaalkene

Polycarbogermane

Polycarbosilane

Silacyclobutene

Silene

Co-Authorship Statement

A version of section 5.2 has been published as a communication: Pavelka, L. C.; Holder, S. J.; Baines, K. M. *Chem. Commun.* **2008**, 2346. I am the primary author and conducted all synthetic experiments under the supervision of Prof. Simon Holder (University of Kent) and Prof. Kim Baines. The written work was a collaborative effort between all three authors.

A version of section 5.3 has been published as a communication: Pavelka, L. C.; Milnes, K. K.; Baines, K. M. *Chem. Mat.* **2008**, *20*, 1580. I am the primary author and conducted all synthetic experiments under the supervision of Prof. Kim Baines. NMR spectroscopic data for one compound was obtained by Kaarina Milnes, a previous graduate student in the Baines lab. The written work was a collaborative effort between Prof. Kim Baines and myself.

Acknowledgements

My acknowledgements must begin with my Ph. D. supervisor Kim Baines, who has been a great mentor and friend. I found my love of chemistry (and NMR spectroscopy) while working with Kim. I am forever grateful for her guidance and understanding, especially through the difficult times.

I would also like to thank all the people that I have worked with over the years in the Baines lab. From a casual chat over coffee to an in depth chemistry discussion, I have enjoyed all the time we have spent together. I would especially like to thank Kaarina, Krysten, Jen, Paul, and Julie for always lending an ear when it was needed, for chemistry questions or otherwise. I would also like to thank Margaret for help in reading this thesis and her contributions to my computational chemistry work. The faculty and staff in the chemistry department have also been a huge support.

I am grateful for the opportunity that I had to spend some time in England at the University of Kent thanks to the ASPIRE program and my host supervisor Simon Holder. I learned many invaluable techniques on polymer purification and characterization. I also thank NSERC and OGSST for funding support over the years.

I would also like to thank my friends and family outside the chemistry world. You keep me grounded. In particular, I need to give a special thanks to my mom, who has been my one true source of strength and inspiration.

Table of Contents

Certificate of Examination.....	ii
Abstract.....	iii
Keywords.....	iv
Co-Authorship Statement.....	v
Acknowledgements.....	vi
Table of Contents.....	vii
List of Tables.....	xiii
List of Figures.....	xiv
List of Schemes.....	xvi
List of Abbreviations.....	xix
Chapter 1	
1.1 Why Study E=C Compounds?.....	1
1.2 A Brief History of E=C Compounds.....	2
1.3 Properties and Reactivity of Phosphaalkenes.....	5
1.4 Properties and Reactivity of Silenes and Germanes.....	7
1.5 Research Objectives.....	11
1.6 Alkyne Addition to E=C Compounds.....	12
1.6.1 Outline of Alkyne Reactivity Study.....	14
1.7 E=C Compounds as Precursors for Inorganic Polymers.....	15
1.7.1 Outline of Polymerization Study.....	19
1.8 Determination of Polymer Molecular Weights.....	20
1.9 Synthesis of E=C Compounds.....	21

1.10	References.....	24
Chapter 2		
2.1	Introduction.....	30
2.2	Results: Addition of Alkynes to Phosphaalkenes	33
2.2.1	Addition of Aromatic Alkynes to Phosphaalkene 2.1	34
2.2.2	Addition of Aromatic Alkynes to Phosphaalkenes 2.2 and 2.3	40
2.2.3	Addition of Non-aromatic Alkynes to Phosphaalkenes 2.1 , 2.2 , and 2.3 ...	41
2.2.4	Addition of Alkynes to Phosphaalkenes 2.1 , 2.2 , and 2.3 under Photochemical Conditions.....	43
2.3	Discussion.....	44
2.3.1	Reactivity of Phosphaalkenes towards Alkynes.....	44
2.3.2	Properties of 1,2-Dihydrophosphinines 2.4a-c	48
2.3.3	Comparison of Phosphaalkene Reactivity to Silenes and Alkenes	50
2.4	Conclusions.....	51
2.5	Experimental.....	52
2.5.1	General Experimental Details	52
2.5.2	General Procedure for the Addition of Aromatic Alkynes to Phosphaalkene 2.1	53
2.5.3	Oxidation of 1,2-Dihydrophosphinine 2.4a-c with Sulfur	56
2.5.4	General Procedure for the Addition of Other Alkynes to Phosphaalkenes 2.1 , 2.2 , and 2.3	59
2.5.5	General Procedure for the Addition of Alkynes to Phosphaalkenes 2.1 , 2.2 , and 2.3 under Photochemical Conditions.....	60
2.6	References.....	60

Chapter 3

3.1	Introduction.....	64
3.2	Results: Addition of Alkynes to Germene 3.3	68
3.3	Determination of Regiochemistry of Germacyclobutenes.....	77
3.4	Discussion of Germene 3.3 Reactivity.....	80
	3.4.1 Cycloaddition	80
	3.4.2 Ene-Addition	84
	3.4.3 CH-Insertion.....	89
	3.4.4 Summary of Alkyne Addition Pathways.....	90
3.5	Conclusions.....	92
3.6	Experimental	93
	3.6.1 General Experimental Details	93
	3.6.2 General Procedure for the Reaction of Alkynes with Germene 3.3	93
	3.6.3 General Reaction of Germacyclobutenes 3.9a-c with NaOH	100
3.7	References.....	102

Chapter 4

4.1	Introduction.....	106
4.2	Methods.....	112
4.3	Computational Results.....	113
	4.3.1 Energies and Geometries of the Reactants.....	114
	4.3.2 Energies and Geometries of the Products.....	114
	4.3.3 Summary of Acetylene Addition Pathways	116
	4.3.4 Open-Shell Cycloaddition Pathways.....	118

4.3.4.1	Cycloaddition through Diradical Pathway 1 (DR1).....	119
4.3.4.2	Cycloaddition through Diradical Pathway 2 (DR2).....	123
4.3.5	Closed-Shell Cycloaddition Pathways.....	126
4.3.5.1	Cycloaddition through a Zwitterionic Pathway (ZW).....	126
4.3.5.2	Cycloaddition through a Concerted Pathway (CT).....	129
4.3.6	CH-insertion Pathways (CH).....	131
4.4	Discussion of Pathway Selectivity.....	133
4.5	Comparison to Experiment.....	136
4.5.1	Addition to Silene.....	136
4.5.2	Addition to Germene.....	138
4.6	Conclusions.....	139
4.7	References.....	140

Chapter 5

5.1	Introduction.....	145
5.2	Synthesis of a Polygermene.....	147
5.2.1	Polymerization of 1,1-Dimesitylneopentylgermene (5.1).....	147
5.2.2	NMR Spectroscopic Characterization of Polygermene 5.4	150
5.2.3	Polymerization Mechanism.....	151
5.2.4	Polymerization of Germene 5.1 in the Absence of an Initiator.....	151
5.3	Synthesis of a Polysilene.....	153
5.3.1	Polymerization of 1,1-Dimesitylneopentylsilene (5.2).....	154
5.3.2	NMR Spectroscopic Characterization of Polysilene 5.8	155
5.3.3	Polymerization Mechanism.....	158

5.3.4	Polymerization of Silene 5.2 in the Absence of an Initiator	159
5.4	Towards the Living Polymerization of Germene 5.1	160
5.5	Summary.....	167
5.6	Experimental.....	167
5.6.1	General Experimental Details	167
5.6.2	Synthesis of Polygermene 5.4 from Germene 5.1	169
5.6.3	Synthesis of Polygermene 5.4 from Vinylgermane 5.3	170
5.6.4	Synthesis of Polygermene 5.4 from Germene 5.1 in the Absence of an Initiator	170
5.6.5	Synthesis of Polysilene 5.8 from Silene 5.2	172
5.6.6	Synthesis of Polysilene 5.8 from Vinylsilane 5.7	173
5.6.7	Synthesis of $\text{Mes}_2\text{Si}(\text{OMe})\text{CH}_2\text{CH}_2t\text{Bu}$	173
5.6.8	Synthesis of Silane 5.9	174
5.6.9	Synthesis of Silane 5.10	175
5.6.10	Synthesis of Polysilene 5.8 from Silene 5.2 in the Absence of an Initiator.....	176
5.7	References.....	177

Chapter 6

6.1	Introduction.....	181
6.2	Synthesis of Germene Homopolymers	183
6.2.1	Radical-Initiated Polymerization of Germene 6.2 : Thermal Conditions	184
6.2.2	Radical-Initiated Polymerization of Germene 6.1 : Photochemical Conditions.....	186

5.3.4	Polymerization of Silene 5.2 in the Absence of an Initiator	159
5.4	Towards the Living Polymerization of Germene 5.1	160
5.5	Summary.....	167
5.6	Experimental.....	167
5.6.1	General Experimental Details	167
5.6.2	Synthesis of Polygermene 5.4 from Germene 5.1	169
5.6.3	Synthesis of Polygermene 5.4 from Vinylgermane 5.3	170
5.6.4	Synthesis of Polygermene 5.4 from Germene 5.1 in the Absence of an Initiator	170
5.6.5	Synthesis of Polysilene 5.8 from Silene 5.2	172
5.6.6	Synthesis of Polysilene 5.8 from Vinylsilane 5.7	173
5.6.7	Synthesis of $\text{Mes}_2\text{Si}(\text{OMe})\text{CH}_2\text{CH}_2t\text{Bu}$	173
5.6.8	Synthesis of Silane 5.9	174
5.6.9	Synthesis of Silane 5.10	175
5.6.10	Synthesis of Polysilene 5.8 from Silene 5.2 in the Absence of an Initiator.....	176
5.7	References.....	177

Chapter 6

6.1	Introduction.....	181
6.2	Synthesis of Germene Homopolymers	183
6.2.1	Radical-Initiated Polymerization of Germene 6.2 : Thermal Conditions	184
6.2.2	Radical-Initiated Polymerization of Germene 6.1 : Photochemical Conditions.....	186

6.2.3	Characterization of Polygermene 6.2	190
6.2.4	Polymerization Mechanism	190
6.3	Synthesis of Germene/Styrene Copolymers	191
6.4	Conclusions	196
6.5	Experimental	197
6.5.1	General Experimental Details	197
6.5.2	Polymerization of Germene 6.1 with AIBN under Thermal Conditions	198
6.5.3	Polymerization of Germene 6.1 with AIBN under Photochemical Conditions	199
6.5.4	Irradiation of Germene 6.1 with Styrene and AIBN	200
6.6	References	201
Chapter 7		
7.1	Summary	203
7.2	Conclusions	207
7.3	Future Work	209
7.4	References	213
Appendix 1: Molecular Structure Analysis		
		216
Appendix 2: Energies and Coordinates of Calculated Structures		
		225
Appendix 3: Copyrighted Material and Permissions		
		237
Curriculum Vitae		
		241

List of Tables

Table 2.1	Selected bond lengths (Å) and angles (deg) for 2.6a-c	38
Table 2.2	Absorption and fluorescence data for 2.4a-c in THF	39
Table 3.1	Product ratios from the reactions of terminal alkynes with germene 3.3	70
Table 4.1	Calculated bond lengths, angles, and relative energies of the (a) metallacyclobutenes and (b) metallylacetylenes.....	115
Table 4.2	Calculated energies and spin densities along DR1 for the addition of acetylene to silene and germene.....	120
Table 4.3	Calculated energies and spin densities along DR2 for the addition of acetylene to silene and germene.....	125
Table 4.4	Calculated energies and bond orders along ZW for the addition of acetylene to silene and germene.....	128
Table 4.5	Calculated energies and bond orders along CT for the addition of acetylene to silene and germene.....	130
Table 4.6	Calculated energies and bond orders along CH for the addition of acetylene to silene and germene.....	132
Table 5.1	Polymerization of germene 5.1 in ether	163
Table 5.2	Polymerization of germene 5.1 in ether-THF	165
Table 6.1	Radical polymerization of germene 6.1	184
Table 6.2	Radical copolymerization of germene 6.1 with styrene.....	193
Table A1.1	X-Ray Crystallographic Data for 2.6a	217
Table A1.2	X-Ray Crystallographic Data for 2.6b	219
Table A1.3	X-Ray Crystallographic Data for 2.6c	221
Table A1.4	X-Ray Crystallographic Data for 5.5a	223

List of Figures

Figure 1.1	Representative substituted silenes.....	8
Figure 1.2	Phosphaalkenes and germene studied.....	15
Figure 2.1	Phosphaalkenes 2.1 , 2.2 , and 2.3	33
Figure 2.2	Thermal ellipsoid plot (50% probability surface) of 2.6a-c	37
Figure 2.3	UV-vis spectra of 2.4a-c in THF.....	39
Figure 2.4	Emission spectra of 2.4a-c in THF.....	40
Figure 3.1	Alkynyl mechanistic probes.....	65
Figure 3.2	Digermacyclobutane 3.14 , vinylgermane 3.15 , and digermoxane 3.16	73
Figure 3.3	Resonance structures of ring-opened anions.....	80
Figure 4.1	Representative optimized geometries: (a) silacyclobutene and (b) silylacetylene.....	115
Figure 4.2	B3LYP gas-phase free energy profiles at 298 K and 1 atm for the addition of acetylene to silene.....	117
Figure 4.3	B3LYP gas-phase free energy profiles at 298 K and 1 atm for the addition of acetylene to germene.....	118
Figure 4.4	Optimized geometries of intermediates and transition-states along DR1 for the addition of acetylene to (a) silene and (b) germene.....	119
Figure 4.5	Isosurface plot of the net spin density of (a) DR1-SiC-a[†] and (b) DR1-SiC-b	121
Figure 4.6	Optimized geometries of intermediates and transition-states along DR2 for the addition of acetylene to (a) silene and (b) germene.....	124
Figure 4.7	Optimized geometries of intermediates and transition-states along ZW for the addition of acetylene to (a) silene and (b) germene.....	127
Figure 4.8	Optimized transition-state geometries along CT for the addition of acetylene to (a) silene and (b) germene.....	129

Figure 4.9	Optimized geometries of transition-state along CH for the addition of acetylene to (a) silene and (b) germene	131
Figure 5.1	¹³ C NMR spectrum of polygermene 5.4	150
Figure 5.2	Cyclic dimers (5.5a,b) and isomeric germane (5.6) of germene 5.1	152
Figure 5.3	Thermal ellipsoid plot (50% probability surface) of 5.5a	153
Figure 5.4	¹³ C NMR spectrum of polysilene 5.8	158
Figure 5.5	Isomeric silane (5.11) of silene 5.2	159
Figure 5.6	Representative GPC trace of polygermene 5.12	162
Figure 5.7	Representative GPC trace of polygermene 5.13	164
Figure 6.1	¹ H NMR spectrum of 6.9c	194

List of Schemes

Scheme 1.1	Synthesis of phosphacyanines.....	2
Scheme 1.2	Synthesis and reactivity of 1,1-dimethylsilene	3
Scheme 1.3	Synthesis of the first isolable phosphalkenes.....	3
Scheme 1.4	Synthesis of the first isolable germenes.....	4
Scheme 1.5	Addition of MeOH to phosphalkenes	6
Scheme 1.6	Pericyclic reactions of phosphalkenes	6
Scheme 1.7	Hydrogenation and epoxidation of metal-coordinated phosphalkenes	7
Scheme 1.8	Generalized mechanism of alcohol addition to silenes.....	9
Scheme 1.9	General reactivity of silenes and germenes	10
Scheme 1.10	Addition of alkynes to Brook silenes.....	13
Scheme 1.11	Addition of alkynes to polar silene 1.11	13
Scheme 1.12	Overview of addition polymerization	16
Scheme 1.13	Examples of condensation polymerization in inorganic chemistry	17
Scheme 1.14	Examples of ring-opening polymerization in inorganic chemistry.....	18
Scheme 1.15	Polymerization of MesP=CPh ₂	19
Scheme 1.16	Synthesis of Becker phosphalkene 1.13	21
Scheme 1.17	Synthesis of phosphalkene 1.6	22
Scheme 1.18	Synthesis of MesP(SiMe ₃) ₂	23
Scheme 1.19	Synthesis of phosphalkene 1.14	23
Scheme 1.20	Synthesis of silene 1.11 and germene 1.12	24
Scheme 2.1	Cycloaddition of silenes with alkynes	31
Scheme 2.2	Known examples of alkyne addition to phosphalkenes	32
Scheme 2.3	Addition of aromatic alkynes to phosphalkene 2.1	34

Scheme 2.4	Formation of cycloadducts 2.4a-c	36
Scheme 2.5	Oxidation of 2.4a-c with sulfur.....	36
Scheme 2.6	Attempted addition of phenylacetylene to phosphalkenes 2.2 and 2.3	41
Scheme 2.7	Addition of non-aromatic alkynes to phosphalkene 2.1	42
Scheme 2.8	Addition of non-aromatic alkynes to phosphalkene 2.2	42
Scheme 2.9	Addition of non-aromatic alkynes to phosphalkene 2.3	43
Scheme 2.10	Irradiation of phosphalkenes 2.1 , 2.2 , and 2.3 with alkynes.....	44
Scheme 2.11	Addition of benzophenone to a Brook silene.....	45
Scheme 2.12	Addition of an aldehyde to dimesitylfluorenylidengermane.....	45
Scheme 2.13	Cycloaddition reactions of non-aromatic 1-phosphabutadienes with alkynes	46
Scheme 2.14	Proposed mechanism of 2.4a-c formation	47
Scheme 2.15	Typical routes to 1,2-dihydrophosphinines.....	48
Scheme 3.1	Mechanism of alkyne addition to Brook silenes.....	65
Scheme 3.2	Addition of alkynyl probes to silene 3.2	66
Scheme 3.3	Addition of simple alkynes to silene 3.2	67
Scheme 3.4	Reactions of terminal alkynes with germene 3.3	69
Scheme 3.5	Ring-opening of germacyclobutenes 3.9a-c	78
Scheme 3.6	Proposed mechanism of cycloaddition with aromatic alkynes	82
Scheme 3.7	Proposed mechanism of cycloaddition with ethoxyacetylene	84
Scheme 3.8	Lewis acid-base complexes of $\text{Mes}_2\text{Ge}=\text{CR}_2$	84
Scheme 3.9	Proposed mechanism for vinylgermanes 3.10a-d formation.....	85
Scheme 3.10	Proposed mechanism for vinylgermane 3.13 formation.....	88
Scheme 3.11	Metallene-catalyzed aldehyde dimerization	88

Scheme 4.1	Overview of possible mechanisms for the addition of alkynes to (di)metallenes to form (di)metallocyclobutenes	107
Scheme 4.2	Alkynyl mechanistic probe	109
Scheme 4.3	Addition of the alkynyl mechanistic probe to non-polar and polar silenes.....	110
Scheme 5.1	Polymerization of germene 5.1	148
Scheme 5.2	Polymerization of silene 5.2	154
Scheme 5.3	Synthesis of silane 5.9	156
Scheme 5.4	Synthesis of silane 5.10	156
Scheme 5.5	Polymerization of germene 5.1 in ether	161
Scheme 5.6	Uninitiated, ionic polymerization of germene 5.1	165
Scheme 5.7	Solvent effect on reactivity of dimesitylfluorinyldenegermane	166
Scheme 6.1	Anionic polymerization of germene 6.1 and silene 6.3	182
Scheme 6.2	Polymerization of germene 6.1 and silene 6.3 in the absence of an initiator	183
Scheme 6.3	Synthesis of polygermene 6.2 under thermal conditions.....	185
Scheme 6.4	Synthesis of polygermene 6.2 under photochemical conditions.....	187
Scheme 6.5	Synthesis of copolymer 6.9	192
Scheme 7.1	Addition of methylated alkynyl probe to transient polar silenes	209
Scheme 7.2	Addition of alkynyl probe to 1,1-dimesitylfluorenyldenegermane	210

List of Abbreviations

1-D	one dimensional
AIBN	azobisisobutyronitrile
Ad	adamantyl
Ar	aryl
<i>n</i> BuLi	<i>n</i> -butyllithium
<i>t</i> BuLi	<i>t</i> -butyllithium
<i>t</i> Bu	<i>tert</i> -butyl
B3LYP	Becke's hybrid exchange-correlation DFT functional
Bi-Ar	bicyclic aryl
br	broad
C	Celsius
calc	calculated
CCSD	coupled cluster singles and doubles
d	doublet (NMR); day
DBU	1,8-diazabicyclo[5.4.0]undec-7-ene
D _{calc}	density
dd	doublet of doublets
ddd	doublet of doublet of doublets
dddd	doublet of doublet of doublet of doublets
DFT	density functional theory
dq	doublet of quartets
diphos	diphenylphosphinoethane
DSC	differential scanning calorimetry

e	electron
E	generic main group element
EDX	energy dispersive x-ray spectroscopy
EI-MS	electron impact mass spectrometry
ES TOF-MS	electrospray time of flight mass spectrometry
Et	ethyl
eV	electron volts
FT	fourier transform
G	relative free energy
gCOSY	gradient correlation spectroscopy
GPC	gel permeation chromatography
gHMBC	gradient heteronuclear multiple bond correlation
gHSQC	gradient heteronuclear single quantum coherence
h	hour
HOMO	highest occupied molecular orbital
Hz	hertz
IR	infrared
IRC	intrinsic reaction coordinate
<i>J</i>	coupling constant
K	Kelvin
kcal	kilocalories
LUMO	lowest unoccupied molecular orbital
m	multiplet (NMR); medium (IR)
M ⁺	molecular ion

Me	methyl
MeO	methoxy
MeOH	methanol
Mes	mesityl (2,4,6-trimethylphenyl)
MHz	megahertz
min	minutes
M:I	monomer to initiator ratio
M_n	number-average molecular weight
M_w	weight-average molecular weight
m/z	mass to charge ratio
NaOMe	sodium methoxide
NBO	natural bond orbital
nm	nanometer
NMR	nuclear magnetic resonance
OEt	ethoxy
OTf	triflate (SO_2CF_3)
PDI	polydispersity index
Ph	phenyl
ppm	parts per million
q	quartet
R or R'	generic substituent
ROE	rotating-frame Overhauser enhancement
RT	room temperature
s	singlet (NMR); strong (IR)

t	triplet
T_g	glass transition temperature
TGA	thermal gravimetric analysis
THF	tetrahydrofuran
UV	ultraviolet
vis	visible
w	weak
ZPE	zero-point energy
Å	angstroms
χ	electronegativity symbol (Pauling scale)
δ	chemical shift in ppm
ϵ	extinction coefficient
λ	wavelength (nm)
h ν	irradiation

Chapter 1

E=C Compounds: Reactivity and Prospects in Polymer Chemistry

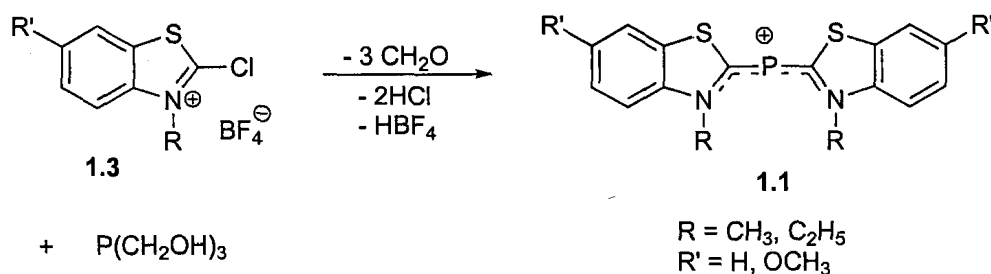
1.1 Why Study E=C Compounds?

From synthesis to plastics, the chemistry of multiply bonded organic compounds is ubiquitous. Alkenes, in particular, are fundamental building blocks in organic chemistry. The reactive carbon-carbon double bond undergoes a multitude of addition reactions, many of which can be performed under regio- and/or stereochemical control, and thus, alkenes are useful and versatile starting materials in a variety of transformations. However, once an alkene is incorporated into a more complex structure, the resulting saturated carbon centres are, in general, unreactive. Although much is known about the functionalization of saturated carbons, the chemistry is difficult in the absence of a good leaving group or a catalyst. The quest for even greater and varied reactivity encouraged chemists to look past the first row elements towards multiply-bonded inorganic species. Compounds that contain a multiple bond to a heavier element would introduce functionality not possible with purely organic species since the heavier element would be available for modifications after a reaction. Furthermore, double bonds involving the heavier elements are more reactive, which may lead to new modes of reactivity. Compounds containing a double bond between carbon and a heavier main group element (denoted as E=C) are of particular interest due to the similarities between their chemistry and that of alkenes while maintaining the functionality and added reactivity of an inorganic double bond.

1.2 A Brief History of E=C Compounds

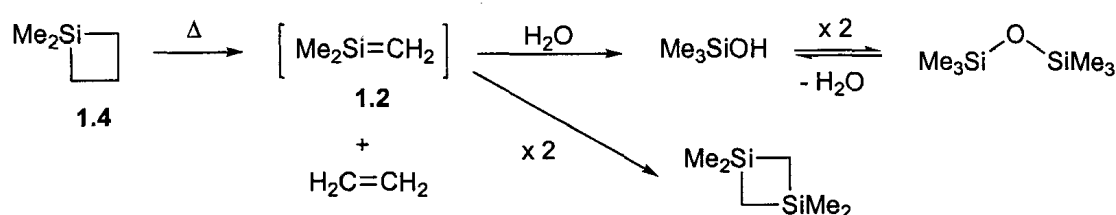
Compounds that contain multiple bonds to the heavier main group elements have long been an interest within inorganic chemistry, beginning with the work of Fredrick Stanley Kipping in the late nineteenth century.¹ For the greater part of the twentieth century, multiply bonded main group compounds were elusive. Numerous researchers attempted and subsequently failed to synthesize these types of compounds; singly bonded dimers and oligomers were usually obtained. The struggle to synthesize unsaturated, heavy main group species lead to the formulation of the “double bond rule”, which stated that elements with a principle quantum number greater than two could not form double bonds with themselves or with other elements.²

This rule held until the 1960's when several compounds were synthesized as exceptions. The synthesis of a series of phosphacyanines, **1.1**,³ containing P=C bonds, as well as a transient silene, $\text{Me}_2\text{Si}=\text{CH}_2$, **1.2**,⁴ were reported. The phosphacyanines were synthesized from the corresponding 2-chlorobenzothiazolium salts, **1.3**, and tris(hydroxymethyl)phosphine (Scheme 1.1). Alternatively, the 2-chloroquinolinium salts could be used.



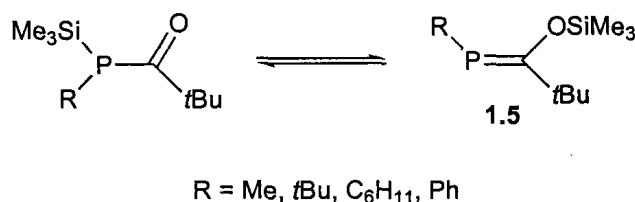
Scheme 1.1 Synthesis of phosphacyanines.

1,1-Dimethylsilene, **1.2**, was prepared, along with ethene, upon the pyrolysis of 1,1-dimethyl-1-silacyclobutane, **1.4** (Scheme 1.2). In the absence of a trap, the silene dimerized to yield 1,1,3,3-tetramethyl-1,3-disilacyclobutane, whereas in the presence of water, trimethylsilanol and hexamethyldisiloxane were produced. In the years that followed, a wide variety of transient, doubly bonded, main group compounds were synthesized;⁵ evidence for a transient germene ($R_2Ge=CR_2$) was not reported until 1973.⁶



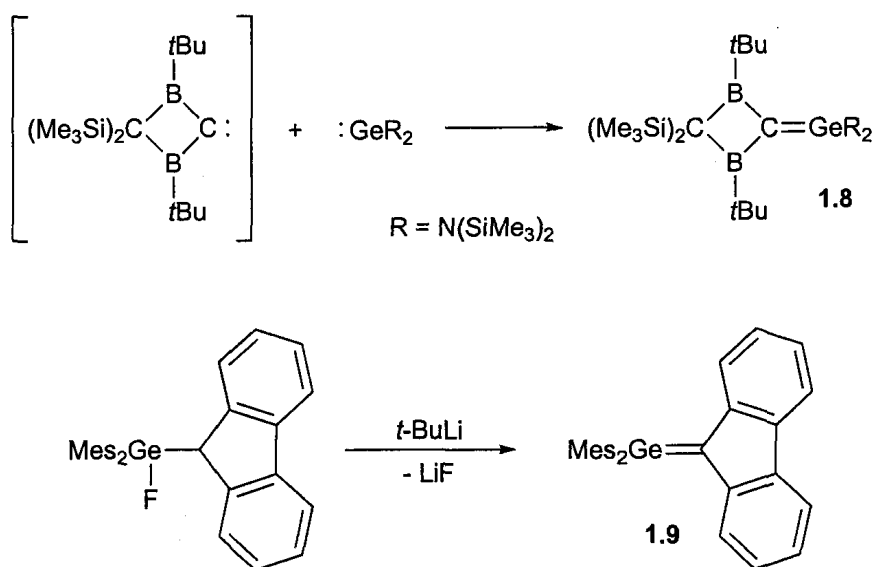
Scheme 1.2 Synthesis and reactivity of 1,1-dimethylsilene.

The use of bulky substituents, to kinetically stabilize the double bond from self-reaction, lead to the synthesis of isolable $E=C$ compounds. Becker reported the first stable, acyclic phosphalkene ($RP=C(OSiMe_3)(tBu)$), **1.5**, in 1976 (Scheme 1.3);⁷ the use of the electronically-stabilizing trimethylsiloxy group, in addition to other large substituents, allowed for isolation of this compound in the absence of oxygen and water. A few years later, a stable phosphalkene with only carbon substituents, $MesP=CPh_2$, **1.6**, was reported.⁸



Scheme 1.3 Synthesis of the first isolable phosphalkene.

Around the same time, Brook *et al.* synthesized the first isolable silene, $(\text{Me}_3\text{Si})_2\text{Si}=\text{C}(\text{OSiMe}_3)(1\text{-Ad})$, **1.7**.⁹ The similarity between the Becker phosphalkene and the Brook silene is striking; both were synthesized from similar precursors and the $\text{E}=\text{C}$ compound was generated by a 1,3-silyl shift to a carbonyl oxygen upon heating or irradiation. The heavier group 14 element analogues (metallenes) took longer to synthesize; it was not until 1987 when the first stable germene $(\text{R}_2\text{Ge}=\text{CR}_2)$ ¹⁰ and stannene $(\text{R}_2\text{Sn}=\text{CR}_2)$ ¹¹ were prepared. In fact, within a year, two different research groups published their results on very different germenes (Scheme 1.4).¹⁰ Germene **1.8** was synthesized from the reaction between an electrophilic carbene with a germylene, while the second germene, 1,1-dimesitylfluorenylidengermane, **1.9**, was formed by salt elimination.



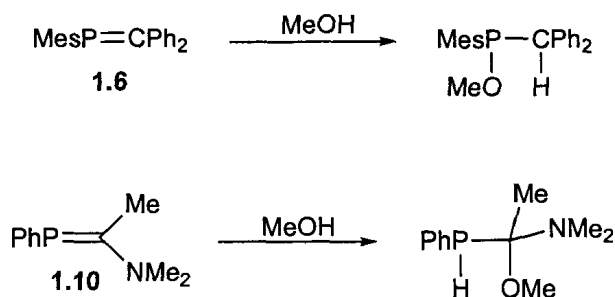
Scheme 1.4 Synthesis of the first isolable germenes.

The majority of isolable E=C compounds can be readily synthesized in good yield, which allowed for extensive studies into the reactivity of these species. Such detailed work was extremely difficult with the transient analogues. Thus, it was the synthesis of the stable E=C compounds that lead to the wide spread study of these species in main group inorganic chemistry.

1.3 Properties and Reactivity of Phosphaalkenes

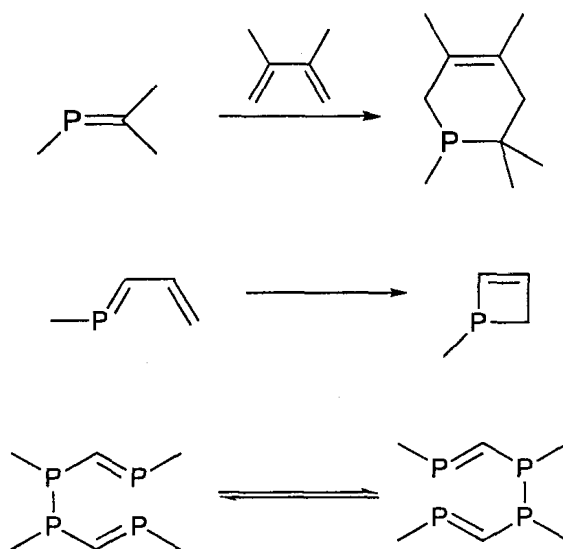
In general, the reactivity of phosphaalkenes has been shown to parallel the reactivity of alkenes.^{12,13} The P=C π -bond is relatively non-polar; the electronegativity difference between carbon and phosphorus is quite small ($\chi = 2.5$ vs. 2.1, respectively, on the Pauling scale). Using UV photoelectron spectroscopy, the HOMO of the parent phosphaethylene (HP=CH₂) has been shown to be the P=C π -bond rather than the lone pair on phosphorus.¹⁴

The substituents on a phosphaalkene can have a significant effect on the polarity of the P=C bond. As a result, the regiochemistry of the addition of polar reagents can be controlled by varying the substituents on the phosphaalkene. In the absence of any polarizing substituents, the bond is weakly polarized towards carbon; however, the presence of π -donating substituents on carbon can reverse the natural polarity and greatly influence the outcome of a reaction. For example, addition of MeOH to MesP=CPh₂, **1.6**, leads to C-H bond formation, as expected from the natural polarization of the P=C π -bond,⁸ whereas addition of MeOH to the amino-substituted phosphaalkene **1.10** leads to P-H bond formation (Scheme 1.5).¹⁵



Scheme 1.5 Addition of MeOH to phosphalkenes.

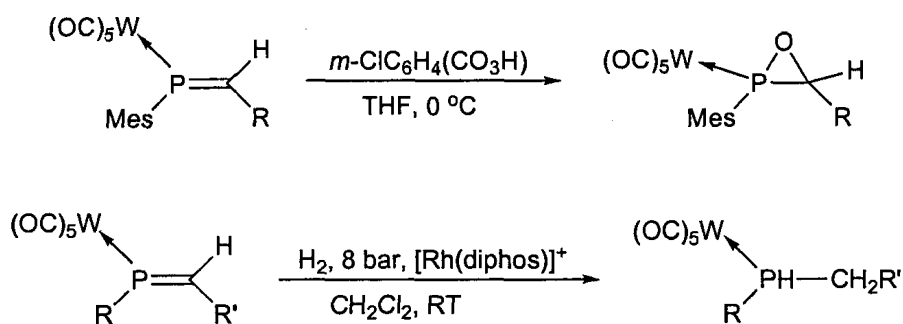
The similarity in the reactivity between phosphalkenes and alkenes is particularly apparent when reviewing pericyclic reactions; for example, they undergo standard $[4n+2]$ cycloadditions, electrocyclic ring closures, and sigmatropic shifts (Scheme 1.6).¹²



Scheme 1.6 Pericyclic reactions of phosphalkenes.

There are some notable exceptions that reflect the increased reactivity of the phosphalkene and the tendency for the lone pair to participate in the reaction. In the absence of bulky substituents, phosphalkenes dimerize head-to-tail or head-to-head to form diphosphacyclobutanes.¹⁶ However, like alkenes these reactions appear to follow

the Woodward-Hoffmann rules¹⁷ as they are proposed to proceed via a stepwise mechanism.¹⁶ Certain classes of reactions, such as epoxidation¹⁸ and hydrogenation¹⁹, can only be performed on phosphalkenes that have the reactivity of their lone pairs moderated by complexation to transition metals (Scheme 1.7).



Scheme 1.7 Hydrogenation and epoxidation of metal-coordinated phosphalkenes.

1.4 Properties and Reactivity of Silenes and Germanes

The electronegativity difference between carbon ($\chi = 2.5$) and silicon ($\chi = 1.8$) or germanium ($\chi = 1.9$) is greater than that between carbon and phosphorus ($\chi = 2.1$), which imparts a greater polarity to the π -bond in a silene or germene, relative to a phosphalkene. However, like phosphalkenes, the polarity is strongly influenced by the nature of the substituents at the metalloid and at carbon. A detailed computational study performed by Apeloig *et al.* demonstrated the effect of the substituents on the polarity of the Si=C bond.²⁰ The length of the Si=C double bond as well as the charge density at silicon and carbon were used as measures of bond polarity. A reduction in polarity leads to an increase in bond length, for example, the Si=C bond lengthened when σ -donating or π -withdrawing groups were placed on silicon and when there were π -donating or σ -

withdrawing groups on carbon. In fact, it is even possible to reverse the natural polarity of a Si=C bond when strongly π -donating substituents are placed on carbon,²¹ silenes with reversed polarity are best described as singly bonded, zwitterionic compounds. Recently, an extensive computational investigation using higher levels of theory and focusing on silenes of reversed polarity confirmed the existence of a correlation between Si=C bond length as well as the charge density on silicon and silene polarity (Figure 1.1).^{21b}

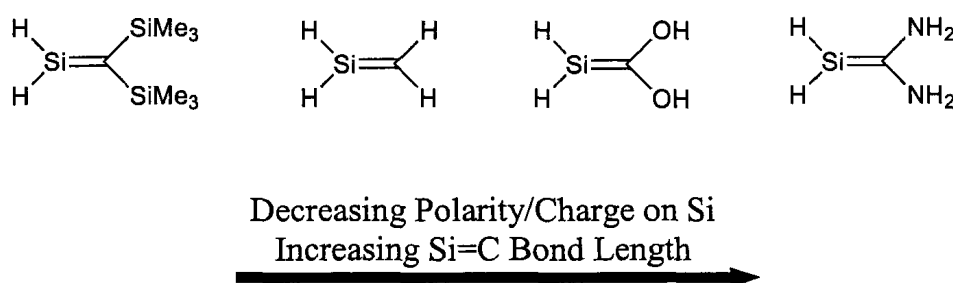
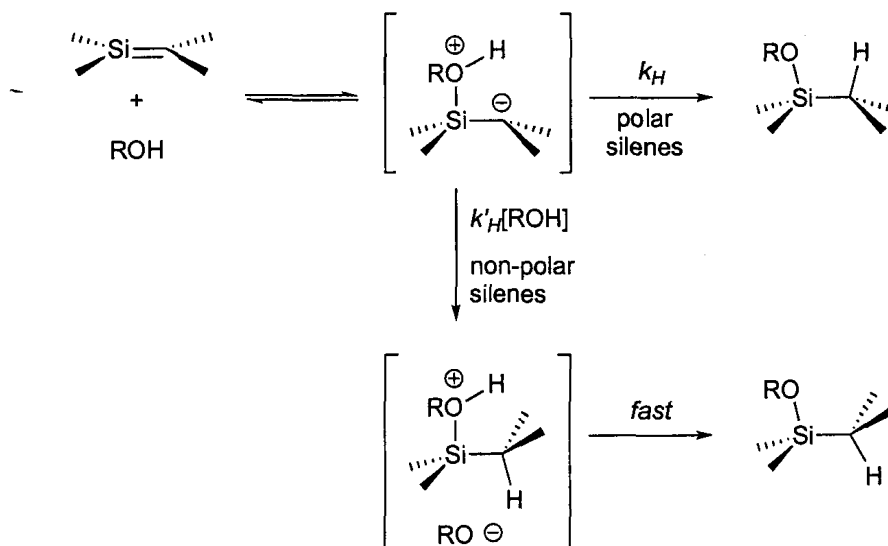


Figure 1.1 Representative substituted silenes.

Computational work has also been performed on germenes;²² however, studies that examined the effects of substitution primary focused on fluorinated germenes such as $\text{H}_2\text{Ge}=\text{CF}_2$, $\text{F}_2\text{Ge}=\text{CH}_2$, and $\text{F}_2\text{Ge}=\text{CF}_2$.^{22b,c} Consequently, there is much less known about the relationship between the substituents and the polarity of the Ge=C bond. The charge distributions for $\text{H}_2\text{Si}=\text{CH}_2$ and $\text{H}_2\text{Ge}=\text{CH}_2$ were calculated,^{22a} the charge difference, between carbon and silicon/germanium, was much larger for silene than germene indicating a greater intrinsic polarity, which is in agreement with expectations based on electronegativity differences.

The computational work performed by Apeloig *et al.* also determined that silenes with low Si=C bond polarity had significantly lower π and π^* orbital energies, and thus,

the reactivity of these silenes is expected to be reduced.²⁰ Leigh and co-workers verified these results experimentally. The reactivity of transient silenes, with various substituents at silicon and carbon, towards alcohols was examined by laser flash photolysis (Scheme 1.8).²³ The relatively non-polar silenes with σ -donating groups on silicon showed a dramatic decrease in the reactivity of the Si=C bond; the rate constant of the reaction with alcohols was approximately 9 orders of magnitude lower than that of the polar silenes. In addition, the mechanism of alcohol addition was fundamentally different between polar and non-polar silenes. Although alcohols add to both types of silenes via nucleophilic attack at silicon, the reactions proceed with second order kinetics for polar silenes, while they proceed with overall third order kinetics for non-polar silenes, being second order in alcohol concentration (Scheme 1.8).

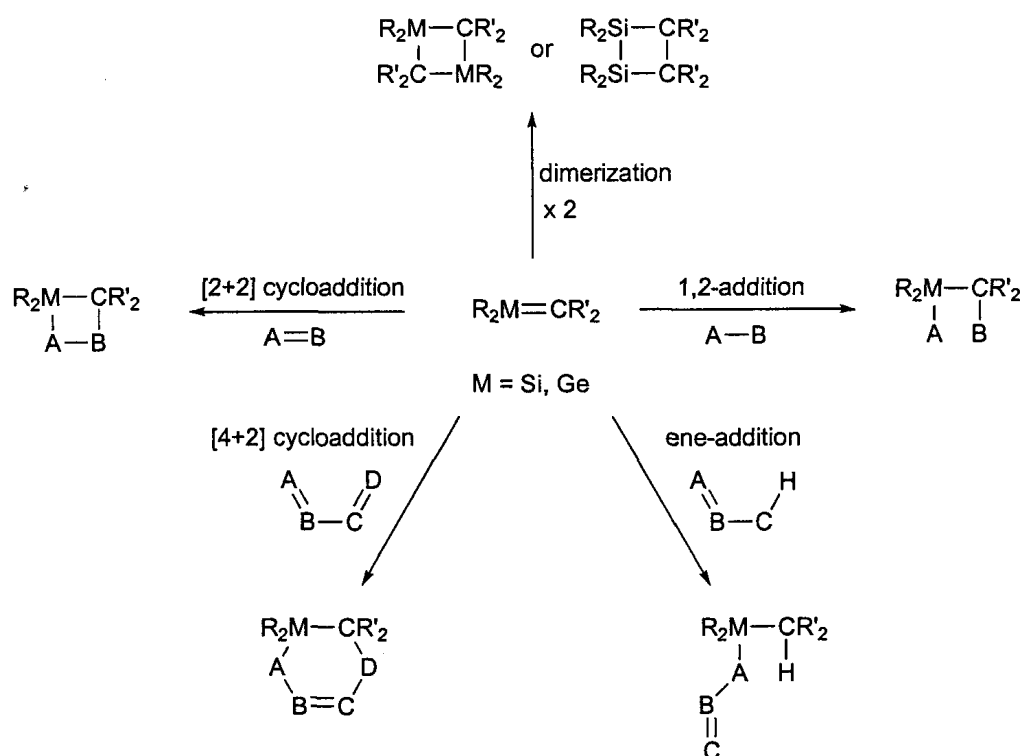


Scheme 1.8 Generalized mechanism of alcohol addition to silenes.

Similar experiments assessing the reactivity of germenes with alcohols were also performed. Interestingly, germenes without substituents that would dramatically influence the polarity of the Ge=C bond behaved like the non-polar silenes: they were

shown to have overall third order kinetics in the reaction with alcohols and the rate constants were 2-3 orders of magnitude lower than those for the analogous silenes.²⁴ Thus, germenes are indeed much less polar than silenes, as evidenced by their decreased reactivity towards nucleophilic addition in comparison to naturally polarized silenes.

The reactivity of silenes has been studied extensively.²⁵ A general scheme depicting several typical reactions of silenes is shown below (Scheme 1.9). Silenes undergo a variety of regioselective 1,2-additions with polar reagents such as water, alcohols, amines, and inorganic acids. In general, the more electronegative atom of the polar reagents adds to the silicon. A number of π -bonded species, such as aldehydes, ketones, alkenes, and alkynes, have been shown to react with silenes; however, depending on the nature of the reagent, different modes of reactivity may be possible including [2+2] and [4+2] cycloaddition and/or ene-addition.



Scheme 1.9 General reactivity of silenes and germenes.

The reactivity of germenes, on the other hand, has not been studied to the same extent.²⁶ Some similarities to silene chemistry have been observed (Scheme 1.9). For example, analogous 1,2-addition products are formed regioselectively when germenes are treated with polar reagents; here, the main difference is in the rates of reaction. In contrast, the addition of π -bonded reagents leads to some more significant differences. For example, the addition of benzophenone to 1,1-dimesitylneopentylsilene yields a mixture of a [2+2] cycloadduct (major) and an ene-addition product, whereas addition to the analogous germene leads exclusively to the ene-addition product.

1.5 Research Objectives

Our group has long been interested in the reactivity and the mechanistic chemistry of multiply bonded main group species. We have focused on their cycloaddition chemistry for a number of years, particularly on carbonyl and alkyne additions.^{27,28} The work presented in this thesis will focus on two different areas of E=C compound chemistry.

1) Alkyne Addition

- a. Reactivity of phosphalkenes towards alkynes (Chapter 2)
- b. Reactivity of a germene towards alkynes (Chapter 3)
- c. Computational study of the mechanism of alkyne addition to polar silenes and germenes (Chapter 4)

Surprisingly, the addition of alkynes to germenes and phosphalkenes has not been well studied. Thus, the first part of this thesis will focus on the product studies of the reactions between phosphalkenes or germenes and alkynes. There are no reports on

the mechanism of alkyne addition to polar group 14 metallenes. Thus, to help understand the observed reactivity, a computational study of the mechanism of alkyne addition to polar silenes and germenes was performed. An introduction of alkyne addition to E=C compounds is presented in section 1.6 and an outline of this study is presented in section 1.6.1.

2) Group 14 Metallenes as Precursors for Inorganic Polymers

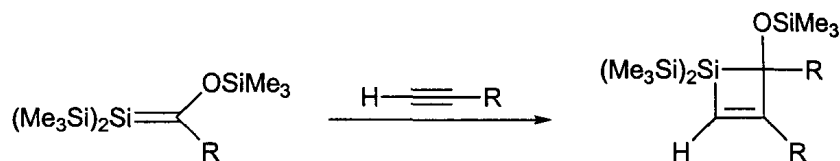
- a. Anionic Addition Polymerization of Group 14 Metallenes (Chapter 5)
- b. Radical Addition Polymerization of a Germene (Chapter 6)

During the course of the alkyne reactivity studies, a relatively simple method for the polymerization of germenes was discovered. Thus, in the second part of this thesis, the addition polymerization of germenes is presented. The polymerization of silenes was also investigated. An introduction of the use of E=C compounds as precursors for inorganic polymers will be presented in section 1.7 and the approach for this study is presented in section 1.7.1.

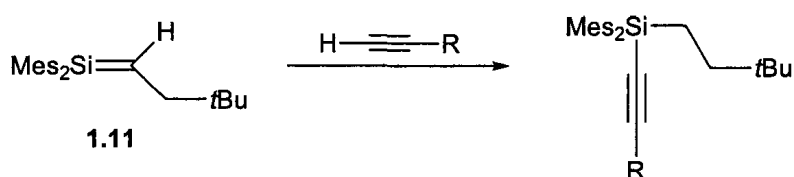
1.6 Alkyne Addition to E=C Compounds

The regioselective addition of alkynes to the relatively non-polar Brook silenes to give silacyclobutenes is a well-known reaction (Scheme 1.10).^{29,30} Surprisingly, much less is known about the addition of alkynes to polar silenes.²⁵ The reaction between polar silenes and alkynes predominantly gives silacyclobutenes; however, ene-addition also occurs.^{31,32,33} In a recent study, we examined the addition of a variety of terminal alkynes to a stable, naturally polarized silene, 1,1-dimesitylneopentylsilene, **1.11**; significant differences in reactivity were observed (Scheme 1.11).³⁴ Although cyclo- and ene-

adducts were observed, silylacetylenes, from insertion of the alkynyl C-H across the Si=C bond, were formed as the major products.



Scheme 1.10 Addition of alkynes to Brook silenes.



Scheme 1.11 Addition of alkynes to polar silene 1.11.

Clearly, the polarity of the silene dramatically influences the outcome of the reaction with alkynes. In general, the relationship between bond polarity and reactivity of the E=C bond has been demonstrated for both silenes and germenes: the more polar the double bond, the more reactive the metallene. When the same argument is extended to phosphaaalkenes it follows that silenes and germenes should be more reactive than comparable phosphaaalkenes due to the decreased electrophilicity of phosphorus and the low intrinsic polarity of the P=C bond.

We were interested in comparing the alkyne reactivity of silenes with that of germenes and phosphaaalkenes. Would the inherently less polar Ge=C bond of the analogous germene, $\text{Mes}_2\text{GeC(H)CH}_2t\text{Bu}$, **1.12**, favour cycloaddition over CH-insertion? How would the reactivity of phosphaaalkenes towards alkynes compare to silenes? Can substitution on the phosphaaalkene influence the reactivity towards alkynes?

According to the Woodward-Hoffmann rules,¹⁷ thermal $[2\pi_s+2\pi_s]$ cycloaddition reactions of alkenes are forbidden. The addition of alkynes to Brook silenes to give silacyclobutenes, under thermal conditions, appears to violate the Woodward-Hoffmann rules; however, the low-lying, diffuse orbitals of the silene may be able to participate in a $[2\pi_s+2\pi_a]$ cycloaddition, which would be thermally allowed, or the addition may be stepwise. Baines and co-workers have recently demonstrated that the cycloaddition of terminal alkynes to Brook silenes proceeds through a diradical intermediate.^{28d,e} The mechanism of the cycloaddition of alkynes to polar silenes has not been determined. Thus, we were interested in examining the mechanism of alkyne addition to polar silenes through computational methods. A parallel study into the mechanism of alkyne addition to germenes was also performed.

1.6.1 Outline of Alkyne Reactivity Study

The reactivity of three different phosphalkenes towards alkynes will be examined: P-mesityl[(*t*-butyl)(trimethylsiloxy)]methylenephosphine, **1.13**, P-mesityl-diphenylmethylenephosphine, **1.6** and bis(trimethylsilyl)amino(trimethylsilyl)methylenephosphine, **1.14** (Figure 1.2). These are representative of a non-polarized, naturally polarized, and a highly polarized phosphalkene, respectively. The reactivity of these phosphalkenes towards a variety of terminal alkynes, with different electronic properties, was examined and the results are presented in Chapter 2.

The reactivity of a naturally polarized germene, 1,1-dimesitylneopentylgermene, **1.12**, towards a variety of terminal alkynes was also examined and the results were

compared to those obtained for the analogous 1,1-dimesitylneopentylsilene, **1.11**. The results of this study are presented in Chapter 3.

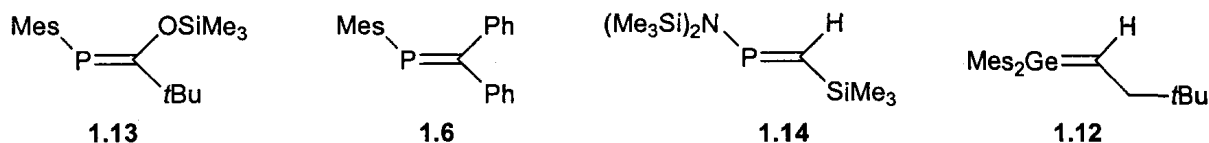


Figure 1.2 Phosphaalkenes and germene studied.

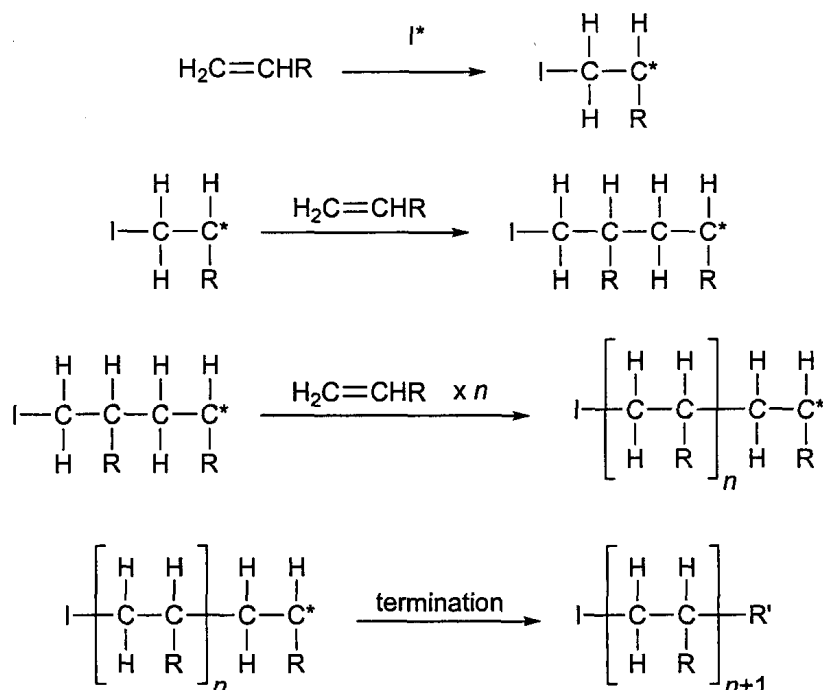
The mechanism of alkyne addition to polar silenes and germenes was investigated using Density Functional Theory. Pathways for the addition of acetylene to the parent silene, H₂Si=CH₂, or germene, H₂Ge=CH₂, were examined at the B3LYP/6-311++G(d,p) level of theory. The findings of the computational study are presented in Chapter 4.

1.7 E=C Compounds as Precursors for Inorganic Polymers

Multiply bonded organic compounds have been used as precursors for polymeric materials for nearly a century.³⁵ The most common monomers employed are the alkenes. Today, some of our most important commodity materials such as plastics, synthetic rubbers, and synthetic clothing fibers are synthesized from the addition polymerization of alkenes.

The addition polymerization of alkenes proceeds via a chain-growth mechanism. There are three stages to the chain-growth mechanism: initiation, propagation, and termination (Scheme 1.12). Initiation involves the addition of a reactive species (radical, cation, or anion) to the monomer. The newly formed reactive intermediate then adds to another monomer. The same process occurs repeatedly during the propagation stage thereby extending the length of the chain. The chain continues to grow until all

monomers are depleted or until propagation is terminated by some other means. Termination can occur spontaneously or upon addition of a quenching reagent, depending on the nature of the initiator.

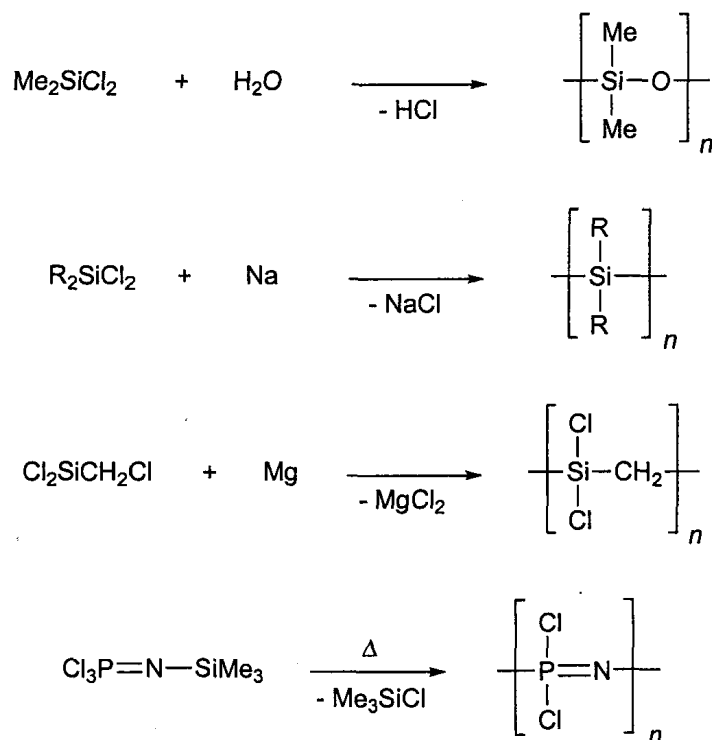


Scheme 1.12 Overview of addition polymerization.

Polymers that contain inorganic elements in the backbone can be expected to have different properties and functionalities compared to organic materials. Given the wide variety of inorganic elements available, the possibility for inorganic polymers with tunable properties is intriguing. Inorganic elements can be incorporated into the side chains of organic polymers or into the backbone. This thesis will focus on polymers with inorganic elements in the main chain.

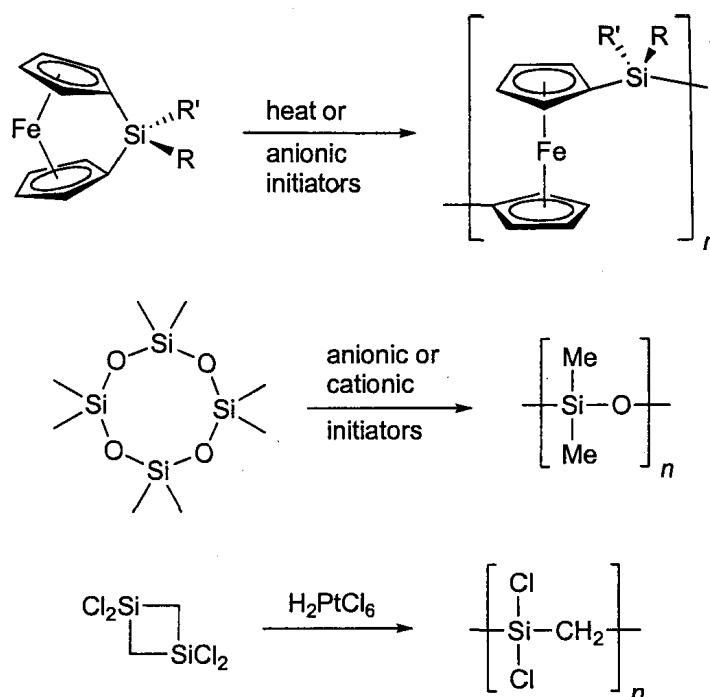
Both addition and condensation polymerizations have been applied to the synthesis of inorganic polymers. Many inorganic polymers such as polysiloxanes,

$[R_2SiO]$, polysilanes, $[R_2Si]$, polysilylenemethylenes, $[R_2SiCH_2]$, and polyphosphazenes, $[R_2P=N]$, (Scheme 1.13) can be made by condensation polymerization.^{36,37}



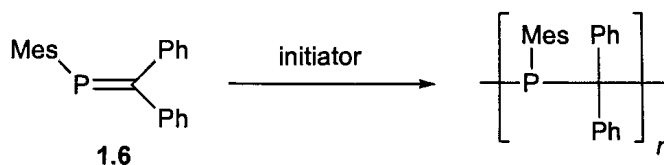
Scheme 1.13 Examples of condensation polymerization in inorganic chemistry.

Addition polymerization has also been used extensively to prepare inorganic polymers; however, cyclic inorganic compounds, for use in ring-opening polymerizations, have been the predominant monomers rather than doubly bonded inorganic species.^{36,37} The use of multiply bonded inorganic compounds as monomers is rare. Some common examples of inorganic polymers synthesized via ring-opening polymerization include the poly(ferrocenylsilane)s and polydimethylsiloxane (Scheme 1.14).



Scheme 1.14 Examples of ring-opening polymerization in inorganic chemistry.

The spontaneous polymerization of a phosphalkyne ($\text{Ph-C}\equiv\text{P}$) was investigated in 1999; however, only low molecular weight, mostly saturated oligomers were produced rather than polymeric material.³⁸ Recall that the formation of dimers and other cyclic oligomers was one of the main problems that plagued the initial attempts at isolating inorganic multiply-bonded compounds due to their low kinetic and thermal stability. Phosphaalkene **1.6**, $\text{MesP}=\text{CPh}_2$, was the first inorganic multiply bonded species to be successfully polymerized (Scheme 1.15).³⁹ Many of the stable $\text{E}=\text{C}$ compounds, and other inorganic multiply-bonded compounds, have bulky substituents that would make propagation unfavourable, and thus, the compounds are inappropriate for use as polymeric precursors. Phosphaalkene **1.6** proved to have an appropriate degree of kinetic stabilization to be isolated and purified, while still maintaining enough reactivity to allow for polymerization.



Scheme 1.15 Polymerization of MesP=CPh₂.

Phosphaalkene **1.6** can be polymerized using either anionic or radical initiators. Random copolymers with styrene can be prepared with a radical initiator.⁴⁰ Conditions have also been developed for the living anionic polymerization of phosphaalkene **1.6**;⁴¹ these conditions have been utilized in the synthesis of block copolymers with vinylic monomers. Some aspects of the chemistry of poly(methylenephosphine)s have been investigated. The coordination chemistry of the backbone phosphine with gold and palladium has been studied.⁴² Complexation of an isoprene-phosphaalkene block copolymer to gold has led to the formation of micelles with gold cores through self-assembly of the block copolymer in solution.⁴³

The goal of this study is to determine whether other E=C compounds, particularly those containing silicon or germanium, can act as precursors for inorganic polymers. The addition polymerization of the silenes and germenes would provide a new approach for the synthesis of silicon- and germanium-containing inorganic polymers.

1.7.1 Outline of Polymerization Study

Couret's 1,1-dimesitylneopentylsilene, **1.11**, and 1,1-dimesitylneopentylgermene, **1.12**, were chosen as monomers for our polymerization study. They are both relatively simple to prepare in near quantitative yields and have only a moderate degree of kinetic stabilization, which should enable polymerization.

The polymerization of silene **1.11** and germene **1.12** was examined with anionic initiators in pentane. In addition, alternative conditions to achieve a living anionic polymerization of germene **1.12** were explored. The results from the anionic polymerization studies are presented in Chapter 5.

The polymerization of germene **1.12** using radical initiators was also investigated. AIBN was chosen as the free-radical source. The synthesis of random copolymers with styrene using a radical initiator was also studied. The results from the radical polymerization studies are presented in Chapter 6.

1.8 Determination of Polymer Molecular Weights

Unlike molecular compounds, a sample of polymeric material will consist of many macromolecules with varying chain lengths of different molecular weights. Thus, the molecular weight of a polymer sample represents an average. Furthermore, the distribution of molecular weights within a polymer sample must also be evaluated. The number average molecular weight (M_n) and the weight average molecular weight (M_w) are the most common measures used to characterize the molecular weight of a polymer. M_n is the mean molecular weight value, taken from the total weight of all the molecules divided by the total number of molecules (Equation 1.1). The M_w is a weighted average; the higher molecular weight molecules are weighted more heavily (Equation 1.1). The distribution of molecular weights in a given polymer sample is represented by the polydispersity index (PDI). PDI is determined by dividing the M_w by the M_n ; a monodisperse polymer sample, where all polymer chains are the same length, would have a PDI of one.

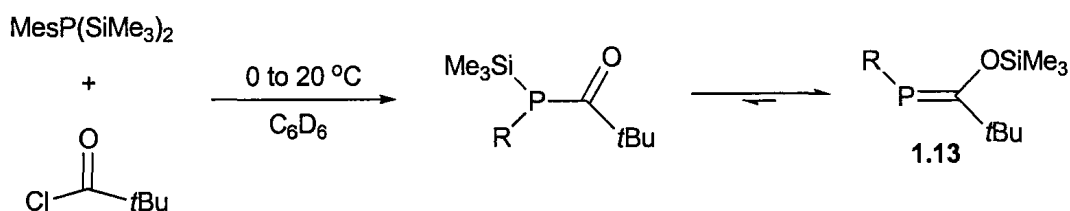
$$M_n = \frac{\sum N_i \times M_i}{\sum N_i} \quad M_w = \frac{\sum N_i \times (M_i)^2}{\sum N_i \times M_i}$$

Equation 1.1 M_n and M_w

1.9 Synthesis of E=C Compounds

Although there are many ways to synthesize E=C compounds, only those that are the focus of this thesis are presented.

Becker phosphalkenes, $RP=C(OSiMe_3)R'$, are easily prepared from the addition of an acid chloride to a bis(trimethylsilyl)phosphine.⁷ The reaction first generates an acylphosphine, which then rearranges to a phosphalkene via a 1,3-silyl shift upon mild heating. A variety of phosphalkenes with different substituents have been synthesized using this general procedure.^{7,44} Mesitylbis(trimethylsilyl)phosphine was allowed to react with pivaloyl chloride at 0 °C; upon warming to room temperature, phosphalkene **1.13** formed quantitatively (Scheme 1.16). A mixture of *E*- and *Z*-isomers of phosphalkene

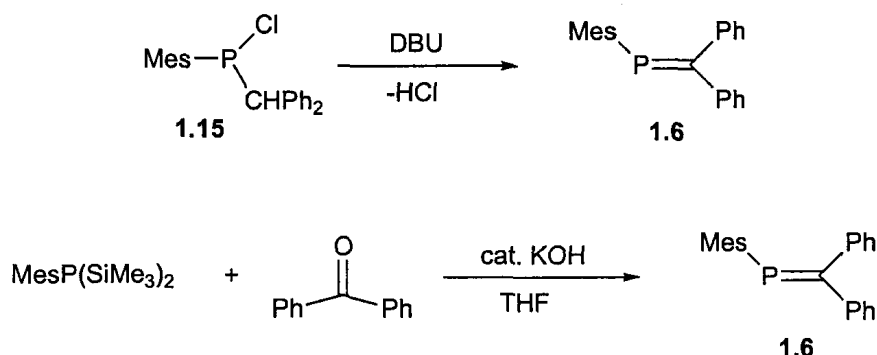


Scheme 1.16 Synthesis of Becker phosphalkene **1.13**.

1.13 are synthesized initially; however, the *Z*-isomer can be isomerized to the *E*-isomer upon irradiation with long wavelength UV light. Similar behaviour has been observed with other asymmetrically substituted phosphalkenes.⁴⁵ The conversion is readily

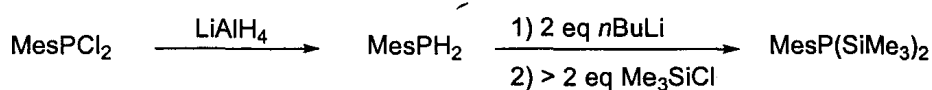
monitored by ^{31}P NMR spectroscopy. Phosphaalkenes have strongly deshielded ^{31}P chemical shifts (> 100 ppm) whereas three coordinate phosphines have ^{31}P resonances that are significantly shifted upfield (generally less than 0 ppm).⁴⁶

Phosphaalkene **1.6** was originally synthesized from chlorophosphine **1.15** by treatment with DBU, a strong base.⁸ However, an alternative approach has been developed that gives the phosphaalkene in higher yield from more readily available reagents: the addition of benzophenone to mesitylbis(trimethylsilyl)phosphine, in the presence of a catalytic amount of base, yields phosphaalkene **1.6** via a phospha-Peterson reaction (Scheme 1.17).⁴⁵



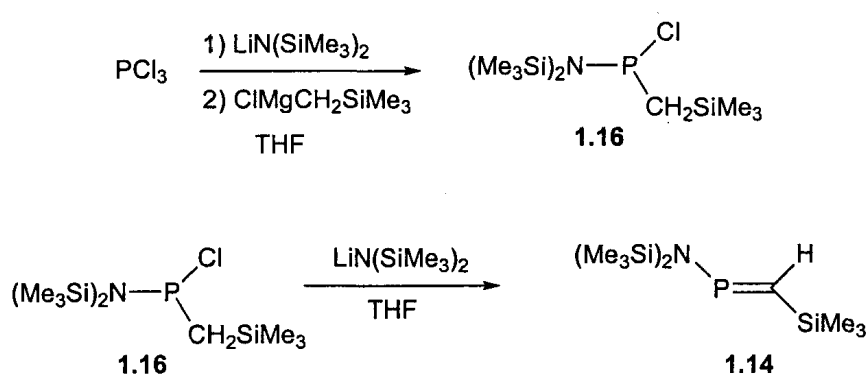
Scheme 1.17 Synthesis of phosphaalkene **1.6**.

Mesitylbis(trimethylsilyl)phosphine, the required starting material for both phosphaalkene **1.13** and **1.6**, can easily be prepared in large quantities from the addition of excess trimethylsilyl chloride to dilithiated mesitylphosphine,⁴⁷ which is synthesized by the deprotonation of mesitylphosphine using two-equivalents of *n*-BuLi (Scheme 1.18). The dilithiophosphine is generated *in situ* and used immediately.



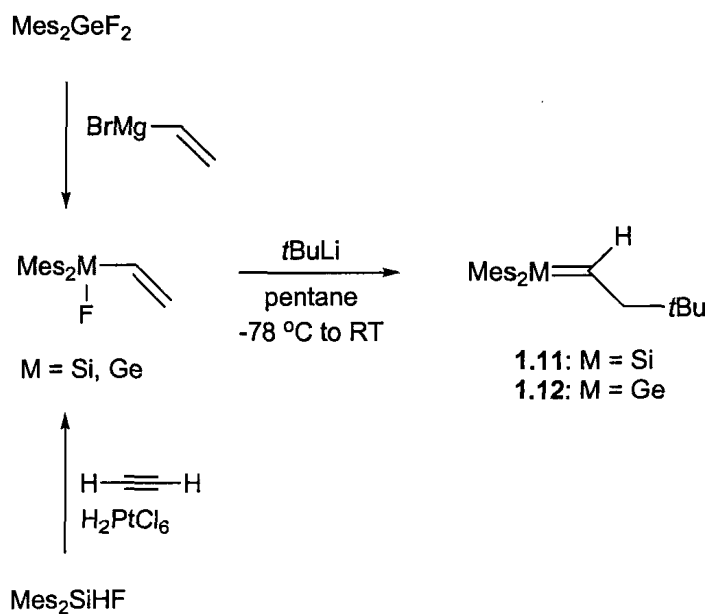
Scheme 1.18 Synthesis of MesP(SiMe₃)₂.

P-amino-substituted phosphalkene **1.14** was synthesized using a dehydrohalogenation reaction. Treatment of chlorophosphine **1.16** with LiN(SiMe₃)₂ leads to deprotonation of the chlorophosphine followed by the elimination of LiCl to yield phosphalkene **1.14** (Scheme 1.19). Chlorophosphine **1.16** is synthesized in two steps from PCl₃ by the addition of LiN(SiMe₃)₂, to yield a dichlorophosphine, followed by the addition of ClMgCH₂SiMe₃ (Scheme 1.19).



Scheme 1.19 Synthesis of phosphalkene **1.14**.

Silene **1.11** and germene **1.12** are synthesized from fluorodimesitylvinylsilane or -germane, respectively, by the addition of *t*BuLi and subsequent elimination of LiF (Scheme 1.20). Fluorodimesitylvinylsilane is prepared by the platinum-catalyzed hydrosilylation of fluorodimesitylsilane, whereas fluorodimesitylvinylgermane is synthesized from the addition of vinylmagnesium bromide to difluorodimesitylgermane.



Scheme 1.20 Synthesis of silene 1.11 and germene 1.12.

1.10 References

1. (a) Kipping, F. S.; Sands, J. E. *J. Chem. Soc. Trans.* **1921**, 119, 830; (b) Kipping, F. S. *Proc. R. Soc. London Ser A.* **1937**, 159, 139.
2. (a) Pitzer, K. S. *J. Am. Chem. Soc.* **1948**, 70, 2140; (b) Mulliken, R. S. *J. Am. Chem. Soc.* **1950**, 72, 4493.
3. (a) Dimroth, K.; Hoffmann, P. *Angew. Chem., Int. Ed. Engl.* **1964**, 3, 384; (b) Dimroth, K.; Hoffmann, P. *Chem. Ber.* **1966**, 99, 1325.
4. Gusel'nikov, L. E.; Flowers, M. C. *J. Chem. Soc., Chem. Commun.* **1967**, 864.
5. Jutzi, P. *Angew. Chem. Int. Ed.* **1975**, 14, 232.
6. Barton, T. J.; Kline, E. A.; Garvey, P. M. *J. Am. Chem. Soc.* **1973**, 95, 3078.
7. Becker, G. *Z. Anorg. Allg. Chem.* **1976**, 423, 242.
8. Klebach, T. C.; Lourens, R.; Bickelhaupt, F. *J. Am. Chem. Soc.* **1978**, 100, 4886.

9. (a) Brook, A. G.; Abdesaken, F.; Gutekunst, B.; Gutekunst, G.; Kallury, R. K. M. R. *J. Chem. Soc., Chem. Commun.* **1981**, 191; (b) Brook, A. G.; Nyburg, S. C.; Abdesaken, F.; Gutekunst, B.; Gutekunst, G.; Kallury, R. K. M. R.; Poon, Y. C.; Chang, Y. M.; Wong-Na, W. *J. Am. Chem. Soc.* **1982**, *104*, 5667.
10. (a) Meyer, H.; Baum, G.; Massa, W.; Berndt, A. *Angew. Chem. Int. Ed. Engl.* **1987**, *26*, 798; (b) Lazraq, M.; Escudié, J.; Couret, C.; Satgé, J.; Dräger, M.; Dammel, R. *Angew. Chem. Int. Ed. Engl.* **1987**, *27*, 828.
11. Meyer, H.; Baum, G.; Massa, W.; Berger, S.; Berndt, A. *Angew. Chem. Int. Ed. Engl.* **1987**, *26*, 546.
12. Dillon, K. B.; Mathey, F.; Nixon, J. F. *Phosphorus: The Carbon Copy*; John Wiley & Sons: New York, 1998.
13. Mathey, F. *Angew. Chem. Int. Ed.* **2003**, *42*, 1578.
14. Mathey, F. *Multiple Bonds and Low Coordination in Phosphorus Chemistry*, Regitz, M., Scherer, O. J., Ed.; Thieme, Stuttgart, 1990, p 38.
15. Meriem, A.; Majoral, J.-P.; Revel, M.; Navech, J. *Tetrahedron Lett.* **1983**, *24*, 1975.
16. Markovskii, L. N.; Romanenko, V. D. *Tetrahedron* **1989**, *45*, 6019.
17. (a) Woodward, R. B.; Hoffman, R. *J. Am. Chem. Soc.* **1965**, *87*, 395. (b) Woodward, R. B.; Hoffman, R. *Conservation of Orbital Symmetry*; Academic: New York, 1970.
18. Bauer, S.; Marinetti, A.; Ricard, L.; Mathey, F. *Angew. Chem. Int. Ed. Engl.* **1990**, *29*, 1166.
19. de Vaumas, R.; Marinetti, A.; Mathey, F. *J. Organomet. Chem.* **1991**, *413*, 411.
20. Apeloig, Y.; Karni, M. *J. Am. Chem. Soc.* **1984**, *106*, 6676.
21. (a) El-Sayed, I.; Guliashvili, T.; Hazell, R.; Gogoll, A.; Ottosson, H. *Org. Lett.* **2002**, *4*, 1915; (b) Ottosson, H. *Chem. Eur. J.* **2003**, *9*, 4144.

22. (a) Trinquier, G.; Barthelat, J. C.; Satgé, J. *J. Am. Chem. Soc.* **1982**, *104*, 5931; (b) Gowenlock, B. G.; Hunter, J. A. *J. Organomet. Chem.* **1976**, *111*, 171; (c) Gowenlock, B. G.; Hunter, J. A. *J. Organomet. Chem.* **1977**, *140*, 265.
23. (a) Leigh, W. J.; Stuggett, G. W. *J. Am. Chem. Soc.* **1994**, *116*, 10468; (b) Leigh, W. J.; Bradaric, C. J.; Kerst, C.; Banisch, J. H. *Organometallics* **1996**, *15*, 2246; (c) Owens, T. R.; Grinyer, J.; Leigh, W. J. *Organometallics* **2005**, *24*, 2307; (d) Leigh, W. J.; Owens, T. R.; Bendikov, M.; Zade, S. S.; Apeloig, Y. *J. Am. Chem. Soc.* **2006**, *128*, 10772.
24. (a) Tolti, N. P.; Leigh, W. J. *J. Am. Chem. Soc.* **1998**, *120*, 1172; (b) Leigh, W. J.; Potter, G. D.; Huck, L. A.; Bhattacharya, A. *Organometallics* **2008**, *27*, 5948.
25. For reviews on silene see: (a) Gusel'nikov, L. E.; Nametkin, N. S. *Chem. Rev.* **1979**, *79*, 529; (b) Raabe, G.; Michl, J. *Chem. Rev.* **1985**, *85*, 419; (c) Brook, A. G.; Baines, K. M. *Adv. Organomet. Chem.* **1986**, *25*, 1; (d) Brook, A. G.; Brook, M. A. *Adv. Organomet. Chem.* **1996**, *39*, 71; (e) Müller, T.; Ziche, W.; Auner, N. *The Chemistry of Organic Silicon Compounds*; Rappoport, Z.; Apeloig, Y., Eds.; Wiley & Sons: New York, 1998; Vol. 2, Chapter 16; (f) Morkin, T. L.; Owens, T. R.; Leigh, W. J. *The Chemistry of Organic Silicon Compounds*; Rappoport, Z.; Apeloig, Y., Eds.; Wiley & Sons: New York, 2001; Vol. 3, Chapter 17; (g) Ottosson, H.; Eklöf, A. M. *Coord. Chem. Rev.* **2008**, *252*, 1287.
26. For reviews on germenes see: (a) Wiberg, N. *J. Organomet. Chem.* **1984**, *273*, 141; (b) Barrau, J.; Escudié, J.; Satgé, J. *Chem. Rev.* **1990**, *90*, 283; (c) Escudie, J.; Couret, C.; Ranaivonjatovo, J. *Coord. Chem. Rev.* **1998**, *180*, 565.
27. (a) Baines, K. M.; Cooke, J. A.; Vittal, J. J. *Heteroat. Chem.* **1994**, *5*, 293; (b) Baines, K. M.; Stibbs, W. G. *Adv. Organomet. Chem.* **1996**, *39*, 275; (c) Dixon, C. E.; Hughes, D. W.; Baines, K. M. *J. Am. Chem. Soc.* **1998**, *120*, 11049; (d) Baines, K. M.; Dixon, C. E.; Samuel, M. S. *Phosphorus, Sulfur, Silicon Relat. Elem.* **1999**, *150-151*, 393; (e) Mosey, N. J.; Baines, K. M.; Woo, T. K. *J. Am. Chem. Soc.* **2002**, *124*, 13306; (f) Samuel, M. S.; Jenkins, H. A.; Hughes, D. W.; Baines, K. M. *Organometallics* **2003**, *22*, 1603; (g)

Samuel, M. S.; Baines, K. M. *J. Am. Chem. Soc.* **2003**, *125*, 12702; (h) Milnes, K. K.; Baines, K. M. *Organometallics* **2007**, *26*, 2392.

28. (a) Baines, K. M.; Dixon, C. E.; Langridge, J. M.; Liu, H. W.; Zhang, F. *Organometallics* **1999**, *18*, 2206; (b) Gottschling, S. E.; Grant, T. N.; Milnes, K. K.; Jennings, M. C.; Baines, K. M. *J. Org. Chem.* **2005**, *70*, 2686; (c) Gottschling, S. E.; Milnes, K. K.; Jennings, M. C.; Baines, K. M. *Organometallics* **2005**, *24*, 3811; (d) Gottschling, S. E.; Jennings, M. C.; Baines, K. M. *Can. J. Chem.* **2005**, *83*, 1568; (e) Milnes, K. K.; Jennings, M. C.; Baines, K. M. *J. Am. Chem. Soc.* **2006**, *128*, 2491; (f) Hurni, K. L. MSc Thesis, UWO, 2007; (g) Milnes, K. K.; Baines, K. M. *Can. J. Chem.* **2009**, *87*, 307.

29. (a) Brook, A. G.; Harris, J. W.; Lennon, J.; El Sheikh, M. *J. Am. Chem. Soc.* **1979**, *101*, 83; (b) Brook, A. G.; Baumegeger, A.; Lough, A. J. *Organometallics* **1992**, *11*, 3088; (c) Lassacher, P.; Brook, A. G.; Lough, A. J. *Organometallics* **1995**, *14*, 4359.

30. (a) Naka, A.; Ishikawa, M.; Matsui, S.; Ohshita, J.; Kunai, A. *Organometallics* **1996**, *15*, 5759; (b) Naka, A.; Ishikawa, M. *Organometallics* **2000**, *19*, 4921; (c) Naka, A.; Ishikawa, M. *J. Organomet. Chem.* **2000**, *611*, 248; (d) Naka, A.; Ikadai, J.; Shingo, M.; Yoshizawa, K.; Kondo, Y.; Kang, S.-Y.; Ishikawa, M. *Organometallics* **2002**, *21*, 2033; (e) Yoshizawa, K.; Kondo, Y.; Kang, S.-Y.; Naka, A.; Ishikawa, M. *Organometallics* **2002**, *21*, 3271; (f) Naka, A.; Ishikawa, M. *Chem. Lett.* **2002**, *3*, 364; (g) Naka, A.; Ohnishi, H.; Miyahara, I.; Hirotsu, K.; Shiota, Y.; Yoshizawa, K.; Ishikawa, M. *Organometallics* **2004**, *23*, 4277; (h) Naka, A.; Ohnishi, H.; Ohshita, J.; Ikadai, J.; Kunai, A.; Ishikawa, M. *Organometallics* **2005**, *24*, 5356; (i) Ohshita, J.; Ohnishi, H.; Naka, A.; Senba, N.; Ikadai, J.; Kunai, A.; Kobayashi, H.; Ishikawa, M. *Organometallics* **2006**, *25*, 3955; (j) Naka, A.; Motoike, S.; Senba, N.; Ohshita, J.; Kunai, A.; Yoshizawa, K.; Ishikawa, M. *Organometallics* **2008**, *27*, 2750.

31. Wiberg, N.; Preiner, G.; Schieda O. *Chem. Ber.* **1981**, *114*, 3518.

32. Conlin, R. T.; Kwak, Y.-W.; Huffaker, H. B. *Organometallics* **1983**, *2*, 343.

33. (a) Auner, N.; Seidenschwarz, C.; Herdtweck, E. *Angew. Chem. Int. Ed.* **1991**, *30*, 1151; (b) Auner, N.; Heikenwälder, C.-R.; Wagner, C. *Organometallics* **1993**, *12*, 4135; (c) Auner, N. *Organosilicon Chemistry, From Molecules to Materials*; Auner, N.; Weis, J., Eds.; Weinheim: New York, 1994, 103; (d) Auner, N.; Grasmann, M.; Herrschaft, B.; Hummer, M. *Can. J. Chem.* **2000**, *78*, 1445.
34. Milnes, K. K.; Pavelka, L. C.; Baines, K. M. *manuscript in preparation*.
35. Saunders, K. J. *Organic Polymer Chemistry*; Springer: New York, 1988.
36. (a) Manners, I. *Angew. Chem., Int. Ed. Engl.* **1996**, *35*, 1602; (c) Manners, I. *Angew. Chem., Int. Ed.* **2007**, *46*, 1565.
37. (a) Archer, R. D. *Inorganic and Organometallic Polymers*; Wiley & Sons: New York, 2001; (b) Mark, J. E.; Allcock, H. R.; West, R. *Inorganic Polymers*; Oxford University Press: Oxford, 2005.
38. Loy, D. A.; Jamison, G. M.; McClain, M. D.; Alam, T. M. *J. Polym. Sci. Part A: Polym. Chem.* **1999**, *37*, 129.
39. Tsang, C.-W.; Yam, M.; Gates, D. P. *J. Am. Chem. Soc.* **2003**, *125*, 1480.
40. Tsang, C.-W.; Baharloo, B.; Riendl, D.; Yam, M.; Gates, D. P. *Angew. Chem. Int. Ed.* **2004**, *43*, 5682.
41. Noonan, K. J. T.; Gates, D. P. *Angew. Chem. Int. Ed.* **2006**, *45*, 7271.
42. Gillon, B. H.; Patrick, B. O.; Gates, D. P. *Chem. Commun.* **2008**, 2161.
43. Noonan, K. J. T.; Gillon, B. H.; Cappello, V.; Gates, D. P. *J. Am. Chem. Soc.* **2008**, *130*, 12876.
44. Becker, G. Z. *Anorg. Allg. Chem.* **1977**, *430*, 66.
45. Yam, M.; Chong, J. H.; Tsang, C.-W.; Patrick, B. O.; Lam, A. E.; Gates, D. P. *Inorg. Chem.* **2006**, *45*, 5225.

46. Quin, L. D. *A Guide to Organophosphorus Chemistry*; Wiley & Sons: New York, 2000.
47. Becker, G; Mundt, O.; Rössler, M.; Schneider, E. *Z. Anorg. Allg. Chem.* **1978**, *443*, 42.

Chapter 2

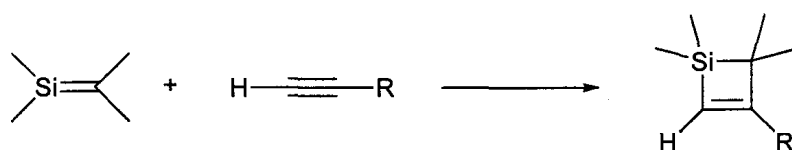
Reactivity of Phosphaalkenes towards Terminal Alkynes

2.1 Introduction

The properties and reactivity of phosphaalkenes (P=C) are very similar to those of their carbon analogues, the alkenes.¹ This so called “phosphorus-carbon analogy” has been attributed to the diagonal relationship between P and C, which focuses on the similar electronegativities of carbon ($\chi = 2.5$) and phosphorus ($\chi = 2.1$) rather than the number of valence electrons.^{1a,b} Surprisingly, comparisons between multiply bonded compounds containing elements with the same valency, for example silenes and alkenes or phosphaalkenes and imines, do not tend to exhibit the same degree of relation that is observed between phosphaalkenes and alkenes.

Given the numerous applications of alkene chemistry in organic synthesis and materials chemistry, the development and expansion of the corresponding phosphaalkene chemistry has become a growing area of research. The cycloaddition chemistry of phosphaalkenes is of particular interest since it holds much potential for the synthesis of a wide variety of phosphorus heterocycles. Several cycloaddition reactions of phosphaalkenes have been investigated; however, the majority of the reactions have focused on 6π electron cycloadditions and 1,3-dipolar additions, where striking similarities have been observed between the reactivity of phosphaalkenes and alkenes.^{1,2} In contrast, formal [2+2] cycloaddition reactions of phosphaalkenes have not been well-studied. Although these types of reactions are thermally forbidden in alkene chemistry,

there have been some reports of phosphalkenes undergoing [2+2] cycloaddition reactions. A common example is the dimerization of simple phosphalkenes, which highlights the increased reactivity of the P=C bond over the C=C bond. [2+2] Cycloaddition reactions are quite common with other heavy alkene analogues, such as silenes ($R_2Si=CR_2$).³ The reaction between silenes and alkynes, in particular, has been studied for several decades; the regioselective cycloaddition, most often, gives silacyclobutenes cleanly and in high yields (Scheme 2.1).

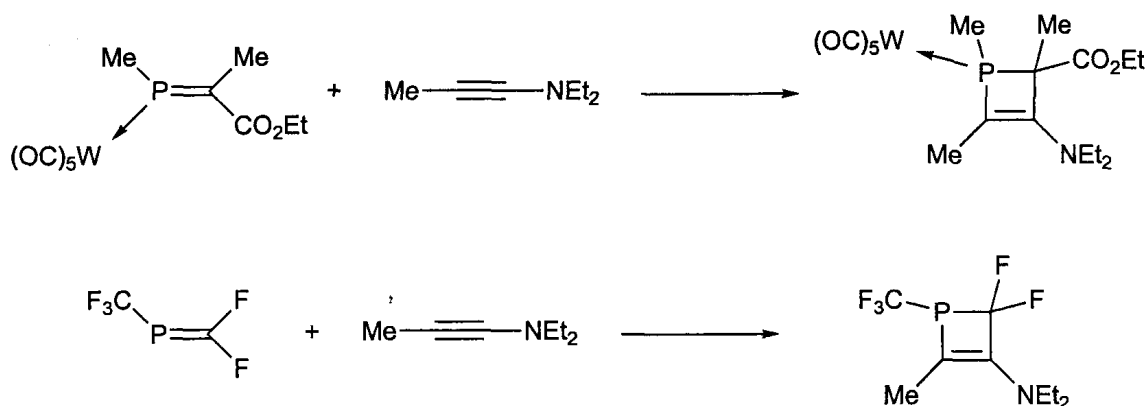


Scheme 2.1 Cycloaddition of silenes with alkynes.

The analogous reaction between a phosphalkene and an alkyne would produce a phosphacyclobutene, otherwise known as a 1,2-dihydrophosphete. The chemistry of these phosphorus-containing, unsaturated ring systems has been of interest over the last 20 years as they can be utilized as masked 1-phosphabutadienes.⁴ Like carbon-based dienes, the 1-phosphabutadienes play an important role in the synthesis of larger phosphorus heterocycles,⁵ which are, in turn, used as starting materials for more complex molecules or as P-ligands.⁶ Furthermore, 1-phosphabutadienes have the potential to be utilized as precursors in the expanding field of phosphorus materials chemistry.⁷

1,2-Dihydrophosphetes are commonly prepared via an electrocyclic ring closure of a transient 1-phosphabutadiene;^{8,9,10} the ring system is thermodynamically favoured in most cases although the 1-phosphabutadiene can usually be regenerated. 1,2-Dihydrophosphetes can also be synthesized from the ring expansion of a phosphirene¹¹ or

from the reaction of a dichlorophosphine with a titanocyclobutene.¹² The cycloaddition of alkynes with phosphalkenes could provide an alternative, regioselective method for the synthesis of a variety of new 1,2-dihydrophosphetes. This approach has successfully been employed; however, only reactions between electron deficient P=C species, such as metallophosphaalkenes,¹³ phosphoranes,⁸ metal-coordinated phosphalkenes,^{14a} 1,2-thiaphospholes,^{14b} or fluorinated phosphalkenes,^{14c} and electron rich alkynes have been examined (Scheme 2.2). Alkyne addition to organo-substituted phosphalkenes has not yet been studied.



Scheme 2.2 Known examples of alkyne addition to phosphalkenes.

In this study, the reactivity of three different phosphalkenes with varying electronic properties will be examined: P-mesityldiphenylmethylenephosphine, **2.1**,¹⁵ bis(trimethylsilyl)-amino(trimethylsilyl)methylenephosphine, **2.2**,¹⁶ and P-mesityl[(*t*-butyl)-(trimethylsiloxy)]methylenephosphine, **2.3** (Figure 2.1).¹⁷ Phosphalkene **2.1** contains only carbon substituents, and thus, the P=C bond is naturally polarized, with a slight partial negative charge on carbon. The absence of any strongly electron withdrawing substituents leaves the P=C bond of **2.1** relatively electron rich. Both phosphalkene **2.2** and **2.3** have substituents that greatly influence the electronic nature of

the P=C bond. Both the P-amino group and the C-silyl group on **2.2** enhance the natural polarity of the P=C bond by increasing the electron density at carbon. The C-siloxy group on **2.3** diminishes the polarity of the P=C bond through π -donation of electron density from oxygen to phosphorus.

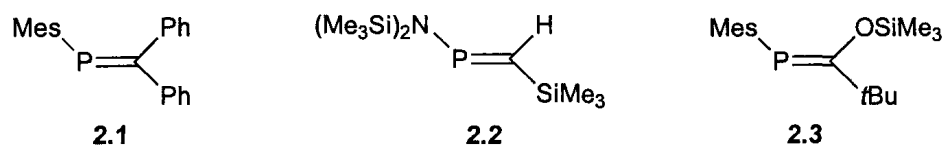


Figure 2.1 Phosphaalkenes **2.1**, **2.2**, and **2.3**.

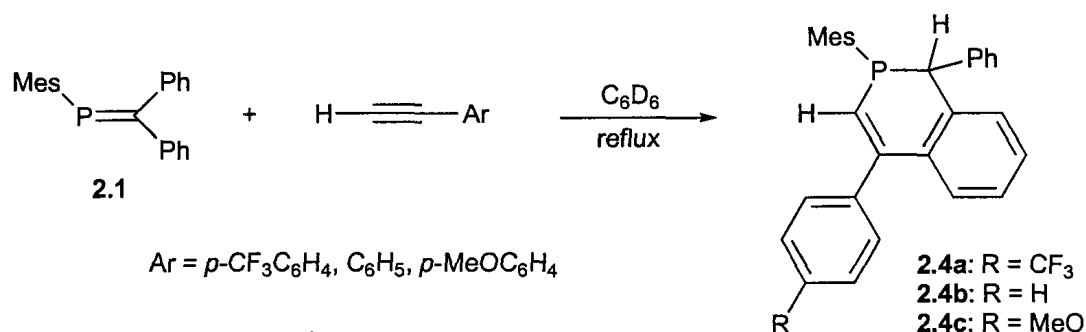
The reactivity of each of these phosphaalkenes with a number of different alkynes has been investigated. Both electron rich and electron deficient, aromatic and non-aromatic, alkynes were examined to study the influence of the electronic properties of the alkyne, in addition to the nature of the phosphaalkene, on cycloaddition reactivity. The reactivity of phosphaalkenes towards alkynes will be compared to that of silenes.

2.2 Results: Addition of Alkynes to Phosphaalkenes

The reactivity of phosphaalkenes **2.1**, **2.2**, and **2.3** towards alkynes was investigated using both thermal and photochemical conditions. The results of the reactions performed under thermal conditions are presented first. Details from the addition of aromatic alkynes to **2.1** are presented in section 2.2.1, those from the addition of aromatic alkynes to **2.2** and **2.3** are presented in section 2.2.2, and the results from the reactions of all three phosphaalkenes (**2.1**, **2.2**, and **2.3**) with aliphatic alkynes are presented in section 2.2.3. Reactions under photochemical conditions are described in section 2.2.4.

2.2.1 Addition of Aromatic Alkynes to Phosphaalkene 2.1

A solution of P-mesityldiphenylmethylenephosphine, **2.1**, in C_6D_6 was treated with excess alkyne ($Ar\equiv H$; $Ar = p\text{-CF}_3C_6H_4$, Ph, $p\text{-MeOC}_6H_4$). The solution was heated to reflux and the reaction was monitored by 1H and ^{31}P NMR spectroscopy. In each case, a 1-phosphacyclohexa-2,4-diene (or 1,2-dihydrophosphinine), **2.4a-c**, was obtained quantitatively (Scheme 2.3). A difference was noted, however, in the reaction times. The addition of $p\text{-CF}_3C_6H_4\equiv H$ to **2.1** was complete after 16 hours, whereas the addition of $Ph\equiv H$ and $p\text{-MeOC}_6H_4\equiv H$ required 4 and 6 days, respectively, to go to completion. 1,2-Dihydrophosphinines **2.4a-c** were purified by chromatography; however, it was difficult to obtain samples of high purity (>95 %) due to their tendency to oxidize in air.



Scheme 2.3 Addition of aromatic alkynes to phosphoalkene **2.1**.

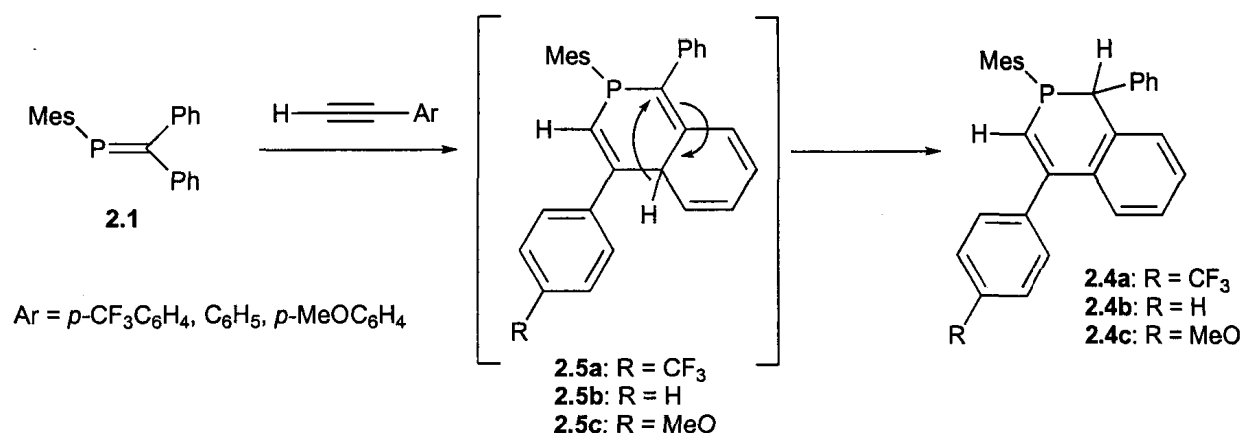
The structures of 1,2-dihydrophosphinines **2.4a-c** were identified by 1H , ^{13}C , ^{31}P , gCOSY, $^1H\text{-}^{13}C$ gHSQC and gHMBC NMR spectroscopy, and mass spectrometry. A molecular ion consistent with a 1:1 (**2.1** to alkyne) adduct was observed in the mass spectra for all addition products.

The ^{31}P signals of **2.4a-c** (-27 to -26 ppm) were significantly shifted upfield in comparison to the ^{31}P signal of phosphoalkene **2.1** (234 ppm), which is consistent with a

change from two-coordinate phosphorus(III) to three-coordinate phosphorus(III).¹⁸ The ¹H NMR spectra of **2.4a-c** all showed a doublet in the vinylic region (~6.5 ppm) with a coupling constant that ranged from 17 – 19 Hz, consistent with a geminal coupling between a vinylic ¹H and a ³¹P(III) centre.¹⁸ The presence of a vinylic ¹H geminal to a P(III) centre suggested that the terminal end of the alkyne has added to the phosphorus centre of the phosphalkene.

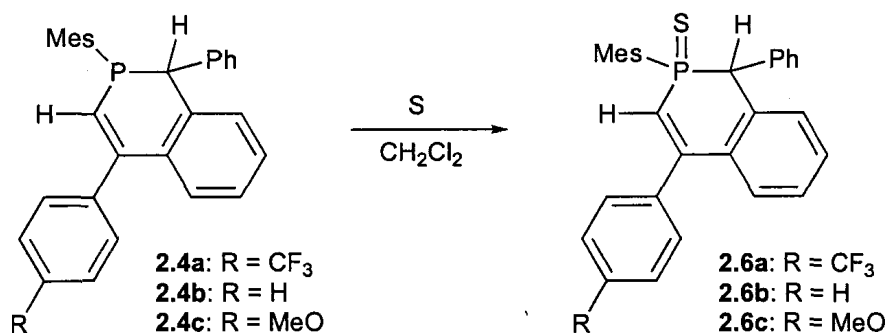
The ¹³C NMR spectra of **2.4a-c** showed the presence of a saturated carbon adjacent to the P(III) centre; a doublet at ~ 46 ppm with a coupling constant of 11 – 13 Hz was observed in all cases.¹⁸ This carbon signal showed a correlation in the ¹H-¹³C gHSQC spectra of **2.4a-c** to a signal at ~ 5.5 ppm in the ¹H dimension, which integrated for one ¹H. Thus, this ¹H was situated two bonds from the ³¹P(III) centre; however, there was no visible splitting of the ¹H signal due to the proximal ³¹P(III). In addition to the saturated CH, the phosphorus was substituted with an unsaturated CH and a mesityl group to give a MesP(CH=CR₂)(CHR₂) moiety.

Upon close examination of the ¹H NMR spectra of **2.4a-c**, the integration value of the signals in the aromatic region did not correspond to the number of aromatic hydrogens present in the starting materials; there was one unaccounted for aromatic hydrogen. To account for the low integration value in the aromatic region, along with the presence of a ¹H signal on a saturated carbon next to the ³¹P(III) centre, regioselective cycloaddition between phosphalkene **2.1** and the alkyne to initially give 1,4-dihydrophosphinine **2.5a-c** followed by a rapid isomerization via a H-shift to re-aromatize the fused ring was proposed to account for formation of the observed 1,2-dihydrophosphinines **2.4a-c** (Scheme 2.4).



Scheme 2.4 Formation of cycloadducts **2.4a-c**.

Several attempts were made to crystallize 1,2-dihydrophosphinines **2.4a-c**, but suitable crystals for X-ray analysis were not obtained. In an attempt to obtain suitable crystals, compounds **2.4a-c** were oxidized with elemental sulfur to give the phosphorus(V) analogues, **2.6a-c** (Scheme 2.5).



Scheme 2.5 Oxidation of **2.4a-c** with sulfur.

Oxidized products **2.6a-c** were identified by IR, ¹H, ¹³C, ³¹P, gCOSY, ¹H-¹³C gHSQC and gHMBC NMR spectroscopy, mass spectrometry, and X-ray crystallography. As expected, the ¹H and ¹³C NMR data of **2.6a-c** were very similar to those of **2.4a-c**. Noticably, the chemical shift of the ³¹P signal of the oxidized structures was shifted downfield to ~ 30 ppm (from - 26 ppm). Both the IR and mass spectra were consistent

with the incorporation of sulfur into the structure. Crystals of **2.6a-c** were grown by slow diffusion of hexanes into a concentrated benzene/Et₂O solution. The molecular structures of **2.6a-c** were determined by X-ray crystallography; a thermal ellipsoid plot of **2.6b** is shown in Figure 2.2. Selected bond lengths and angles of **2.6a-c** are given in Table 2.1. The phosphorus atom lies out of the plane made by the remaining carbon atoms of the six-membered ring, which gives the ring a puckered conformation. The intracyclic bond angles at phosphorus are close to 98° and the intracyclic P-C bond lengths are between 1.79 – 1.86 Å. The metrics of **2.6a-c** are comparable to those of other crystallographically characterized 1,2-dihydrophosphines.¹⁹

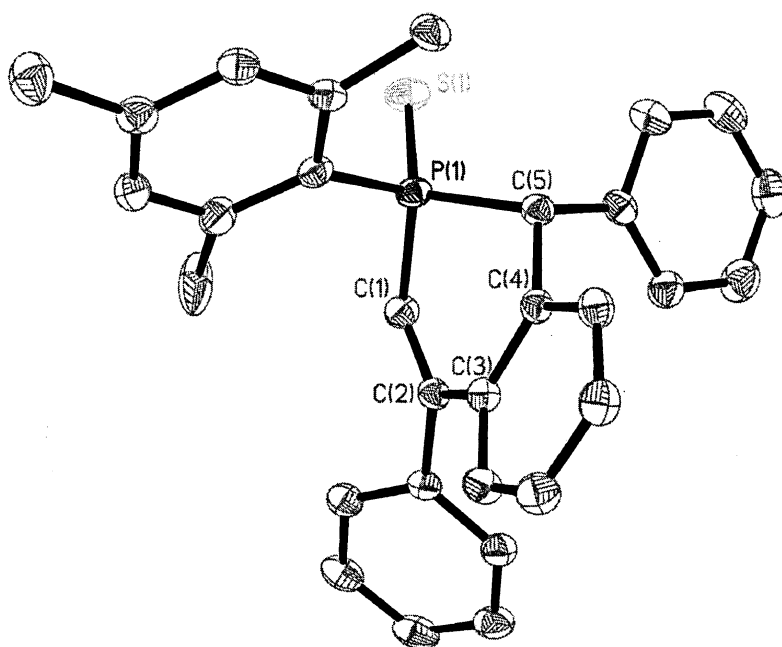
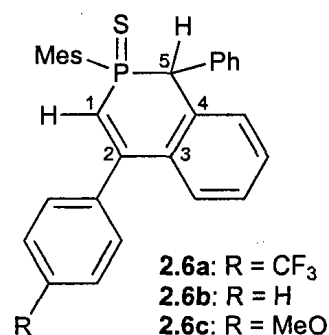


Figure 2.2 Thermal ellipsoid plot (50% probability surface) of **2.6b**. Hydrogen atoms are omitted for clarity. Selected bond lengths (Å) and angles (deg) for **2.6a-c** are given in Table 2.1.

Table 2.1 Selected bond lengths (Å) and angles (degrees) for **2.6a-c**.

	2.6a	2.6b^a	2.6c
Bond Lengths (Å)			
P–C1	1.781(3)	1.795(2)	1.787(2)
P–C5	1.861(3)	1.853(2)	1.864(2)
C1–C2	1.359(4)	1.345(3)	1.342(3)
C2–C3	1.477(4)	1.483(3)	1.487(3)
C3–C4	1.393(4)	1.411(3)	1.404(3)
C4–C5	1.515(4)	1.515(3)	1.521(3)
Bond Angles (degrees)			
P–C1–C2	123.7(2)	122.21(15)	122.49(17)
C1–C2–C3	121.9(3)	121.65(18)	119.02(19)
C2–C3–C4	121.6(2)	119.49(17)	121.12(18)
C3–C4–C5	123.7(2)	122.69(17)	119.87(19)
C4–C5–P	109.43(18)	108.82(13)	105.93(13)
C5–P–C1	99.24(13)	97.69(10)	97.85(10)

^a Two molecules of **2.6b** were present in the asymmetric unit: parameters are given for one of the two molecules.

Adducts **2.4a-c** are bright green solids whereas the oxidized phosphorus(V) analogues, **2.6a-c**, are colourless. 1,2-Dihydrophosphinines **2.4a-c** were analyzed by UV-vis spectroscopy (Figure 2.3). In addition to the absorption attributed to the aromatic substituents at ~250 nm in the UV-vis spectra of **2.4a-c**, a second, lower energy absorption was observed at ~345 nm, which was assigned to the n to π^* transition (Table 2.2). There was no absorption present in the visible range.

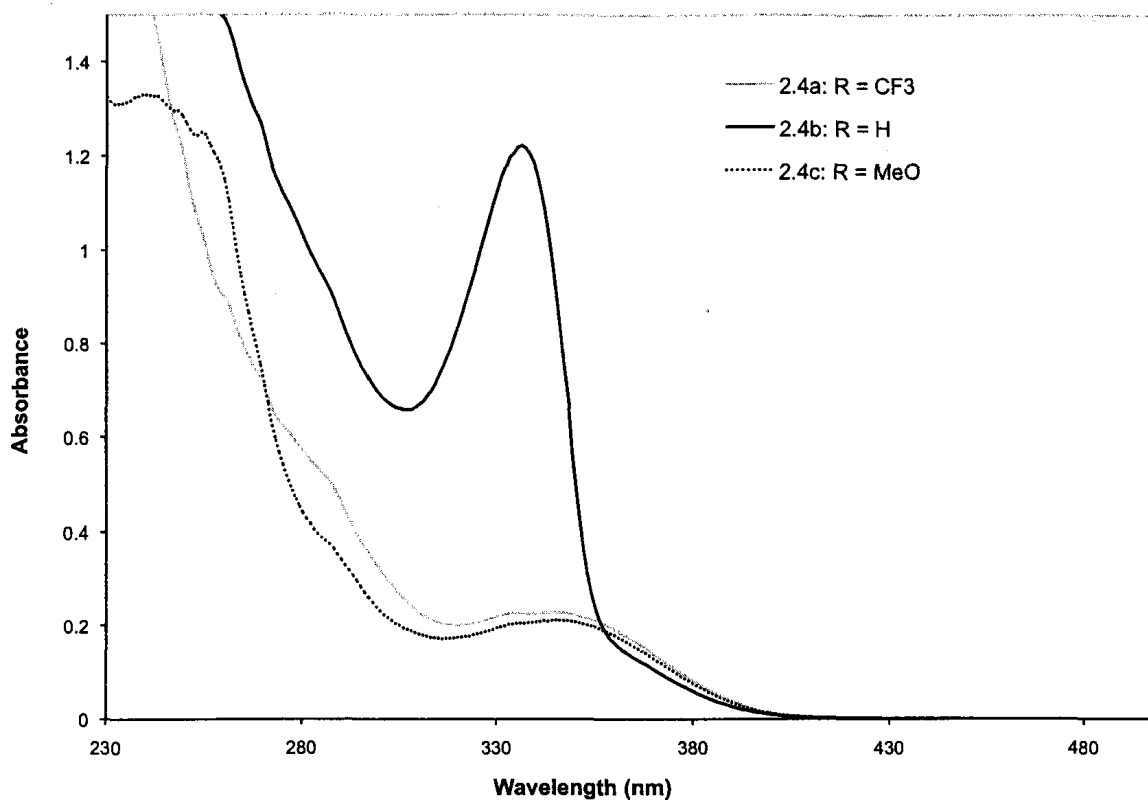


Figure 2.3 UV-vis spectra of **2.4a-c** in THF. The spectra were recorded at 6.0×10^{-5} M (**2.4a**), 7.5×10^{-5} M (**2.4b**), and 5.3×10^{-5} M (**2.4c**).

Compounds **2.4a-c** were also analyzed by fluorescence spectroscopy. Excitation at the lower energy absorption (~ 340 nm) gave rise to a broad emission band for each compound between 450 and 500 nm (Figure 2.4; Table 2.2), which is consistent with the observed colour of these phosphines.

Table 2.2 Absorption and fluorescence data for **2.4a-c** in THF.

	λ_{\max} (nm)	$\log \epsilon$	λ_{em} (nm)
2.4a	344	3.6	449, 476
2.4b	336	4.2	449, 478
2.4c	344	3.6	467

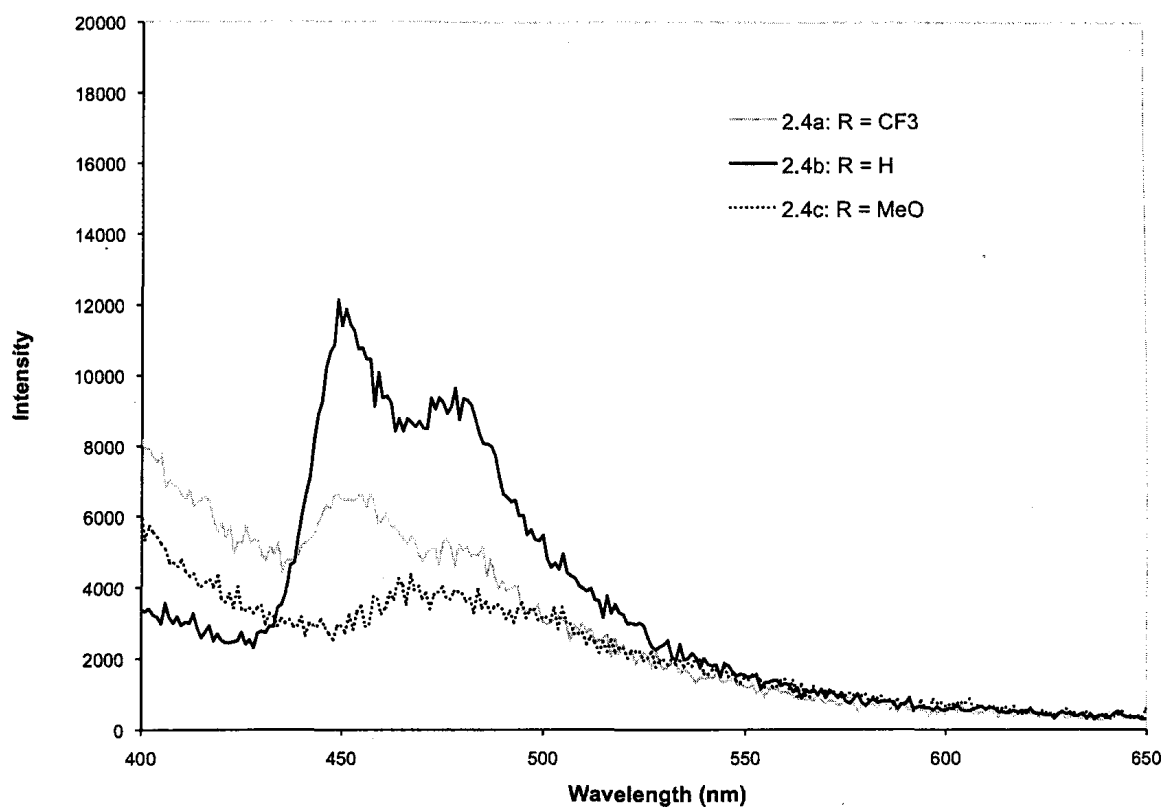
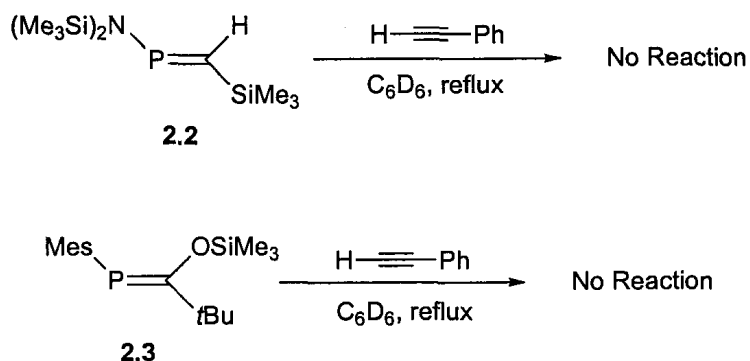


Figure 2.4 Emission spectra of 2.4a-c in THF.

2.2.2 Addition of Aromatic Alkynes to Phosphaalkenes 2.2 and 2.3

The reaction of phosphaalkenes P-bis(trimethylsilyl)amino(trimethylsilyl)methylenephosphine, **2.2**, and P-mesityl[(*t*-butyl)(trimethylsiloxy)]methylenephosphine, **2.3**, with phenylacetylene was studied. Unlike phosphaalkene **2.1**, neither phosphaalkene **2.2** or **2.3** has aromatic substituents on carbon, and thus, the [4+2] cycloaddition pathway is not possible. When **2.2** and **2.3** were both treated with phenylacetylene, there was no reaction observed even after the reaction mixture was refluxed in C₆D₆ (Scheme 2.6), consistent with a previous report on the reactivity of **2.2** towards phenylacetylene.²⁰ Since

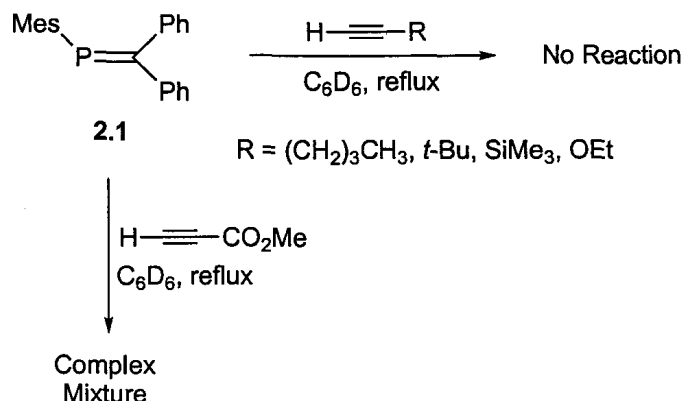
phenylacetylene did not react with **2.2** or **2.3**, the addition of other aromatic alkynes to these phosphalkenes was not investigated.



Scheme 2.6 Attempted addition of phenylacetylene to phosphalkenes **2.2** and **2.3**.

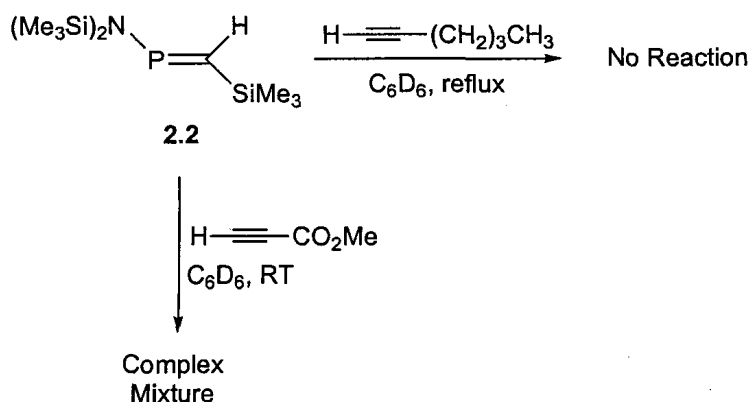
2.2.3 Addition of Non-Aromatic Alkynes to Phosphalkenes **2.1**, **2.2**, **2.3**

As with the addition of aromatic alkynes, a solution of phosphalkene **2.1** in C_6D_6 was treated with excess alkyne ($\text{R}-\text{C}\equiv\text{H}$; $\text{R} = (\text{CH}_2)_3\text{CH}_3$, *t*Bu, SiMe_3 , OEt, $\text{C}(\text{O})\text{OMe}$) and heated to reflux (Scheme 2.7). The reactions were heated for at least 20 h, and in some cases, up to 6 days. The reactions were monitored by ^1H and ^{31}P NMR spectroscopy. With the electron rich alkynes ($\text{R} = (\text{CH}_2)_3\text{CH}_3$, *t*Bu, SiMe_3), there was no reaction observed. Upon addition of methyl propiolate ($\text{H}-\text{C}\equiv\text{C}(\text{O})\text{OMe}$), an electron deficient non-aromatic alkyne, phosphalkene **2.1** was entirely consumed; however, a complex mixture of products was formed, from which no single addition product could be separated.

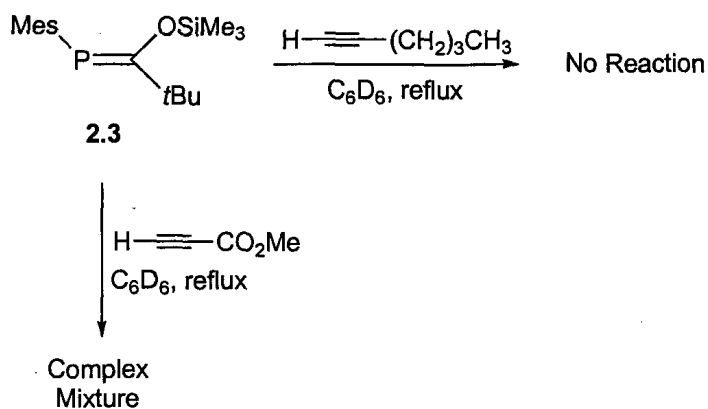


Scheme 2.7 Addition of non-aromatic alkynes to phosphalkene **2.1**.

Phosphaalkenes **2.2** and **2.3** were treated with hexyne and methyl propiolate as representative electron rich and electron deficient non-aromatic alkynes, respectively. No reaction was observed between hexyne and either phosphalkene **2.2** (Scheme 2.8) or **2.3** (Scheme 2.9) in refluxing C_6D_6 . Methyl propiolate reacted with **2.2** at room temperature; the phosphalkene was entirely consumed after 2 days (Scheme 2.8). Unfortunately, like the reaction of methyl propiolate with **2.1**, an intractable mixture was obtained and no single product could be isolated. Phosphalkene **2.3** did not react with methyl propiolate at room temperature; a complex mixture was obtained after 5 days in refluxing C_6D_6 (Scheme 2.9).



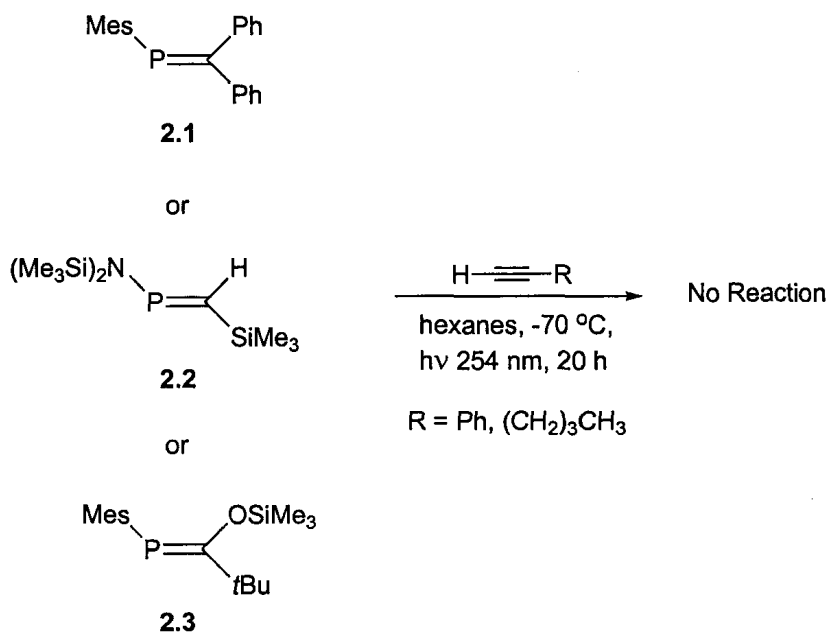
Scheme 2.8 Addition of non-aromatic alkynes to phosphalkene **2.2**.



Scheme 2.9 Addition of non-aromatic alkynes to **2.3**.

2.2.4 Addition of Alkynes to Phosphaalkenes **2.1**, **2.2**, and **2.3** under Photochemical Conditions

Since phosphaalkenes **2.1**, **2.2**, and **2.3** did not appear to react with several alkynes under thermal conditions, photochemical conditions were explored. Hexane solutions of phosphaalkenes **2.1**, **2.2**, or **2.3** were irradiated in the cold ($-70\text{ }^\circ\text{C}$) at 254 nm^{21} in the presence of either phenylacetylene or hexyne. The reactions were monitored by ^{31}P NMR spectroscopy. After 20 h of irradiation, no ^{31}P -containing products were observed in any of the reactions (Scheme 2.10). In the case of phosphaalkene **2.3**, a small amount of isomerization from the *E*-phosphaalkene to the *Z*-isomer was observed.



Scheme 2.10 Irradiation of phosphalkenes **2.1**, **2.2**, and **2.3** with alkynes.

2.3 Discussion

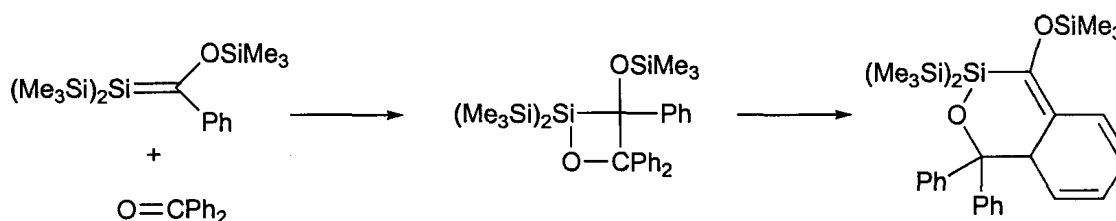
Discussions of the reactivity of phosphalkenes **2.1**, **2.2**, and **2.3** and the properties of 1,2-dihydrophosphinines **2.4a-c** are presented in sections 2.3.1 and 2.3.2, respectively. A comparison of phosphalkene reactivity to alkene and silene chemistry is presented in section 2.3.3.

2.3.1 Reactivity of Phosphalkenes towards Alkynes

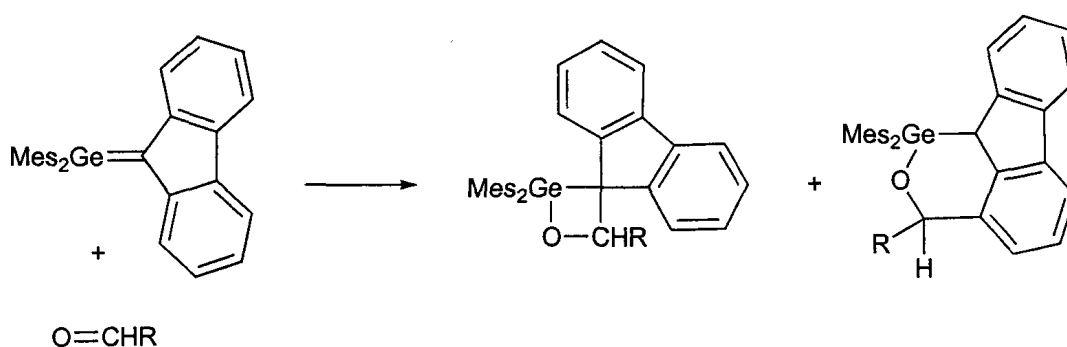
1,2-Dihydrophosphinines **2.4a-c**, formed in the reaction between aromatic alkynes and phosphalkene **2.1**, are likely derived from a formal [4+2] cycloaddition followed by a H-shift; the C-phenyl substituted phosphalkene acts as the 4π component and the alkyne as the 2π component in the cycloaddition. For a phosphalkene to behave as the 4π component, there must be a significant amount of delocalization between the P=C

bond and at least one of the aromatic rings on carbon. A degree of conjugation between P=C bonds and phenyl rings has indeed been noted for phosphalkene **2.1**,^{22a} as well as for the related phosphalkene, (Mes*P=C(H)Ar).^{22b}

Analogous chemistry has been reported in related systems. For example, upon addition of benzophenone, a C-phenyl substituted Brook silene yields the bicyclic[4.4.0] ring system, exclusively (Scheme 2.11),²³ and the addition of an aldehyde to an aryl substituted germene gave a 1,2-oxagermin (Scheme 2.12).²⁴ however, there are no reported examples involving an alkyne.



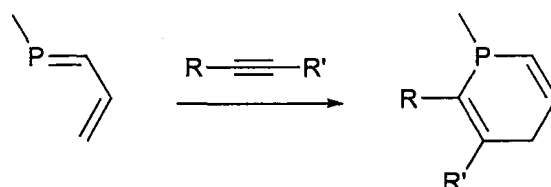
Scheme 2.11 Addition of benzophenone to a Brook silene.



Scheme 2.12 Addition of an aldehyde to dimesitylfluorenylidengermane.

Simple, non-aromatic 1-phosphabutadienes also undergo [4+2] cycloaddition reactions upon treatment with dienophiles.⁵ Examples of cycloadditions between 1-phosphabutadienes and alkynes have been reported; however, the addition products are

generally 1,4-dihydrophosphinines, rather than 1,2-dihydrophosphinines (Scheme 2.13).^{5,25} Re-aromatization of the fused ring system likely promotes the isomerization of 1,4-dihydrophosphinines **2.5a-c** to 1,2-dihydrophosphinines **2.4a-c** (Scheme 2.4) in the reactions between phosphalkene **2.1** and the aromatic alkynes.

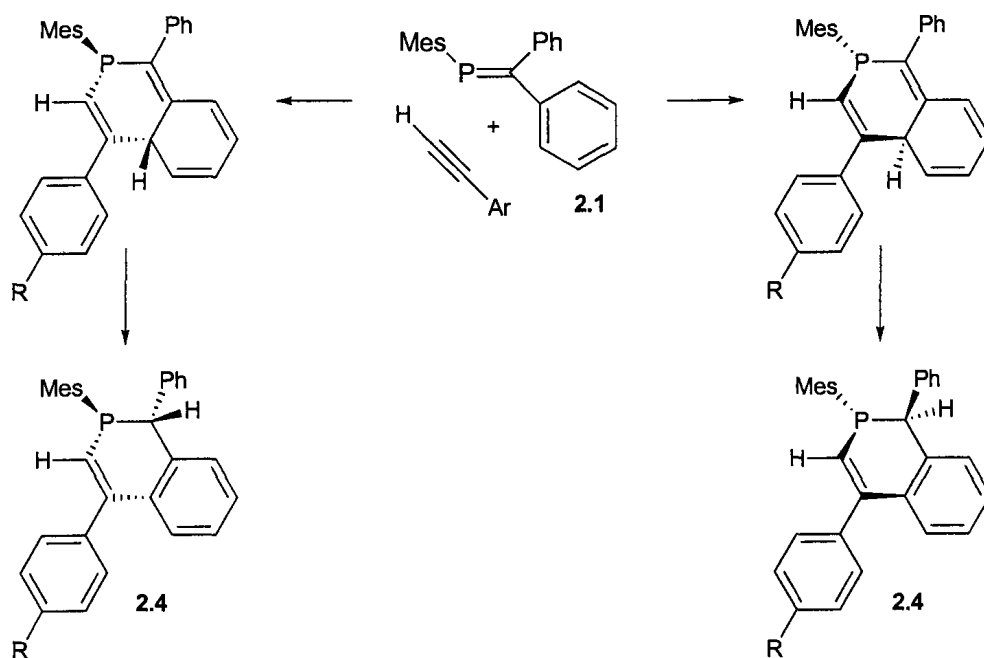


Scheme 2.13 Cycloaddition reactions of non-aromatic 1-phosphabutadienes with alkynes.

Cycloadducts **2.4a-c** were formed regio- and stereospecifically; only a single diastereomer was obtained for each compound. The regiochemistry of alkyne addition to phosphalkene **2.1** was likely governed by sterics; however, the dipoles of the phosphalkene and the alkyne are aligned when the terminal alkynyl carbon approaches the phosphorus centre. The stereochemistry of **2.4a-c** was determined from the molecular structures of **2.6a-c**; the P-mesityl and remaining C-phenyl group were on opposite sides of the central six-membered ring. The stereoselectivity of the reaction is consistent with a concerted [4+2] cycloaddition followed by a suprafacial H-shift (Scheme 2.14). Since stepwise cycloaddition mechanism would potentially lead to a mixture of diastereomers, the formation of one diastereomer was taken as evidence for a concerted reaction pathway.

In carbon chemistry, a concerted [4+2] cycloaddition is typically favoured when an electron rich diene interacts with an electron deficient dienophile. Phosphalkene **2.1** is substituted with a π -donating mesityl group, and thus, behaves as an electron rich

diene. Furthermore, the aromatic alkynes are relatively electron deficient, as compared to the aliphatic alkynes. Not surprisingly, there was no cycloaddition observed with the electron rich aliphatic alkynes. The reaction between phosphalkene **2.1** and 4-trifluoromethyl-1-ethynylbenzene, the most electron deficient alkyne, took the least amount of time (16 h), compared to the time required to react with the more electron rich phenylacetylene (4 days) or 4-ethynylanisole (6 days), as expected. Methyl propiolate, another electron deficient alkyne, reacted with phosphalkene **2.1**; however, the reaction was not clean. The presence of the ester functional group in methyl propiolate, in addition to the C≡C triple bond, likely leads to side reactions between the phosphalkene and the carbonyl group.



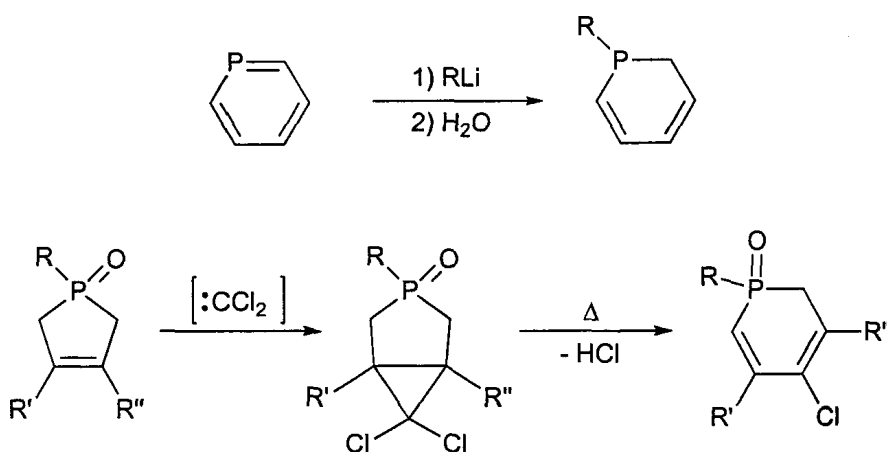
Scheme 2.14 Proposed mechanism of **2.4a-c** formation.

Phosphalkenes **2.2** and **2.3** showed limited reactivity towards alkynes. Neither phosphalkene reacted with phenylacetylene or hexyne and only complex product

mixtures were formed upon treatment with methyl propiolate. In the absence of an C-aryl substituent, the [4+2] cycloaddition pathway is unavailable and, without this reaction pathway, it appears that phosphalkenes do not react with alkynes, which is consistent with a thermally forbidden [2+2] cycloaddition. The electronic nature of the substituents did not have any significant influence on the [2+2] cycloaddition reactivity of these phosphalkenes.

2.3.2 Properties of 1,2-Dihydrophosphinines 2.4a-c

1,2-Dihydrophosphinines, such as 2.4a-c, in general, are well-known phosphorus heterocycles;²⁶ however, the synthesis of 1,2-dihydrophosphinines via cycloaddition between a phosphalkene and an alkyne has not previously been reported. Typically, 1,2-dihydrophosphinines are synthesized from either the addition of an organometallic reagent to the parent phosphinine or the ring-expansion of a dihydrophosphole (Scheme 2.15).^{6,26}



Scheme 2.15 Typical routes to 1,2-dihydrophosphinines.

1,2-Dihydrophosphinines **2.4a-c** contain a significant amount of π -conjugation between the central six-membered ring and the fused aromatic ring. π -Conjugated organophosphorus derivatives are of current interest due to their interesting optical and electronic properties. Phospholes, in particular, have been investigated extensively for the development of new materials for solar cells and organic light emitting diodes.²⁷ In contrast to pyrroles, phospholes do not exhibit a high degree of aromaticity. The lone pair does not interact with the π -system very efficiently since phosphorus has a much higher barrier for planarization than nitrogen. The small amount of aromatic character that is present in phospholes actually arises from hyperconjugation between the exocyclic P-R σ -bond and the π -system. Phospholes also have a high electron affinity, similar to that of siloles. The combination of low aromaticity, σ - π hyperconjugation, and high electron affinity separates phospholes from both pyrroles and thiophenes in terms of optical and electronic properties, which makes them desirable as materials in various photonic applications.

Other types of phosphorus-containing ring systems, such as phosphinines and 1,2-dihydrophosphinines, have not been studied to the same extent as phospholes with respect to their potential for use in π -conjugated materials. Like phospholes, 1,2-dihydrophosphinines **2.4a-c** were shown to be photoluminescent; absorption of light in the UV range gives rise to emission in the visible range at ~ 450 nm. In general, 1,2-dihydrophosphinines have not been reported to be photoluminescent; however, the additional π -conjugation from the fused aromatic ring likely promotes this behaviour in **2.4a-c**. The phosphorus(III) centre, in addition to the extended conjugated π -system, plays an important role in the photoluminescence of **2.4a-c**; the corresponding phosphine

sulfides **2.6a-c** are colourless. It has not been determined whether there is any σ - π hyperconjugation between the exocyclic P-Mes bond and the cyclic diene moiety; however, it seems likely that σ - π hyperconjugation is present in **2.4a-c** since modification of the geometry at P, through oxidation, affects the emission. Although a detailed investigation of the optical properties of **2.4a-c** was not performed, as it was not the focus of this project, the unique behaviour of these systems is quite interesting. The preparation of **2.4a-c** was simple and could easily be performed on a large scale, which may promote future interest in these systems.

2.3.3 Comparison of Phosphaalkene Reactivity to Silenes and Alkenes

This work shows that phosphaalkenes seem to mimic alkenes more so than silenes in terms of their reactivity towards alkynes. In alkene chemistry, $[2\pi s+2\pi s]$ cycloaddition reactions are thermally forbidden,²⁸ the same reaction appears to be thermally forbidden in phosphaalkene chemistry as evidenced by the lack of reactivity between phosphaalkenes **2.1** – **2.3** and terminal alkynes. The previously reported examples of formal $[2+2]$ cycloadditions between phosphaalkenes and alkynes all involved electron rich – electron poor combinations of reagents,^{13,14} which likely promoted stepwise addition mechanisms. The addition of alkynes to Brook silenes has been shown to proceed via a stepwise pathway;²⁹ however, silenes are more reactive than phosphaalkenes, and thus, the stepwise cycloaddition pathways may be more accessible.

On the other hand, $[4\pi s+2\pi s]$ cycloaddition reactions are thermally allowed in carbon chemistry. Thus, this pathway is also likely available to phosphaalkenes. The preference for phosphaalkenes to undergo $[4+2]$ rather than $[2+2]$ cycloaddition reactions

suggests that the [4+2] pathway is lower in energy than a stepwise [2+2] pathway. The observed reactivity of phosphalkenes **2.1** – **2.3** with alkynes provides further support for the diagonal relationship between the chemistry of low valent phosphorus and carbon compounds.^{1,2}

Under photochemical conditions, a [2 π s+2 π s] cycloaddition of alkenes is symmetry allowed. Since phosphalkenes **2.1** – **2.3** appear to behave in a similar manner to alkenes, alkyne cycloaddition may be achieved through excitation of the P=C bond. Unfortunately, this was not observed. *E/Z* isomerization of the P=C bond in phosphalkene **2.3** was observed providing evidence that the P=C bond was indeed being excited; however, the excited state may have an extremely short lifetime making reaction with the alkyne unlikely. Under the conditions examined, an excited state may not have been achieved with phosphalkenes **2.1** and **2.2**.

2.4 Conclusions

We have examined the addition of simple alkynes to three different phosphalkenes (**2.1**, **2.2**, **2.3**) under thermal and photochemical conditions. 1,2-Dihydrophosphinines **2.4a-c** were formed when 1-trifluoromethyl-4-ethynyl-benzene, phenylacetylene, or 4-ethynylanisole was added to MesP=CPh₂ (**2.1**), respectively. Phosphalkene **2.1** acted as the 4 π component in the cycloadditions, through use of the phenyl substituent, to yield these new phosphorus heterocycles. The addition of a number of aliphatic alkynes was also attempted; no products were observed for most cases. A reaction was observed between **2.1** and methyl propiolate; however, no one product could be isolated from the complex mixture formed. Phosphalkenes **2.2** and **2.3** showed very

little reactivity towards terminal alkynes. Neither reacted with phenylacetylene or hexyne upon heating and, again, intractable mixtures were produced upon treatment with methyl propiolate. No reaction was observed upon irradiation of any of the phosphalkenes (**2.1**, **2.2**, or **2.3**) with phenylacetylene or hexyne.

Although there were no new 1,2-dihydrophosphetes (or phosphacyclobutenes) formed from [2+2] cycloaddition, three new 1,2-dihydrophosphinines, **2.4a-c**, were produced from [4+2] cycloaddition providing a new synthetic approach to these phosphorus heterocycles. The H-shift to re-aromatize the fused aromatic ring leads to the formation of 1,2-dihydrophosphinine **2.4a-c** from the initial cycloadduct, 1,4-dihydrophosphinine **2.5a-c**. Other cycloadditions between simple 1-phosphabutadienes and alkynes generally give 1,4-dihydrophosphinines.

The overall lack of reactivity with terminal alkynes emphasizes that phosphalkenes do indeed mimic alkenes in terms of their cycloaddition chemistry. Regardless of the polarity of the phosphalkene examined, [2+2] cycloaddition with aromatic/aliphatic terminal alkynes does not appear to be a favoured reaction.

2.5 Experimental

2.5.1 General Experimental Details

All reactions were carried out under an inert atmosphere (argon) in flame-dried NMR tubes. The C_6D_6 was distilled from $LiAlH_4$, degassed prior to use, and then stored over 4 Å molecular sieves. Hexanes and dichloromethane were dried using a solvent purification system (Innovative Technologies Inc., Newburyport, Massachusetts) in which the solvent was passed through an alumina-packed column. Phenylacetylene, 1-

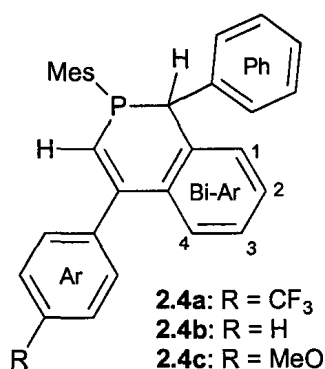
trifluoromethyl-1-ethynylbenzene, 4-ethynylanisole, hexyne, *t*-butylacetylene, trimethylsilylacetylene, ethoxyacetylene, and methyl propiolate were purchased from the Aldrich Chemical Co. and stored over 4 Å molecular sieves. P-Mesityldiphenylmethylenephosphine, **2.1**,^{15b} P-[bis(trimethylsilyl)amino][(trimethylsilyl)methylene]phosphine, **2.2**,¹⁶ and P-mesityl[(*t*-butyl)(trimethylsiloxy)methylene]phosphine, **2.3**,¹⁷ were prepared according to reported procedures.

The NMR spectra were recorded on a Varian Mercury 400, Inova 400 or Inova 600 spectrometer. The internal NMR standards used were residual C₆D₅H (7.15 ppm) for ¹H NMR spectra and the central signal of C₆D₆ (128.0 ppm) for ¹³C NMR spectra. An external standard of 85% H₃PO₄ (0 ppm) was used for the ³¹P NMR spectra and C₆F₆ (-164.9 ppm) was used for the ¹⁹F NMR spectra. Electron impact mass spectra were obtained using a MAT model 8400 mass spectrometer using an ionizing voltage of 70 eV. Mass spectral data are reported in mass-to-charge units, *m/z*. IR spectra were recorded (cm⁻¹) from thin films on a Bruker Tensor 27 FT-IR spectrometer.

2.5.2 General Procedure for the Addition of Aromatic Alkynes to Phosphaalkene 2.1

A solution of phosphaalkene (100 mg, 0.3 mmol) and excess alkyne in C₆D₆ (1.5 mL) was heated to reflux. The reaction was monitored by ¹H and ³¹P NMR spectroscopy. Phosphaalkene **2.1** was completely consumed after 20 h, 4 days, or 6 days of heating with 1-trifluoromethyl-1-ethynylbenzene, phenylacetylene, or 4-ethynyl-anisole, respectively. Upon completion of the reaction, the solvent and excess alkyne were removed under vacuum. The crude products were sticky yellow solids. Preparative thin-layer chromatography was performed to purify the crude products (silica gel, 1:1 CH₂Cl₂

/hexanes) yielding 1,2-dihydrophosphinine **2.4a-c** (23 - 33% isolated yields) as bright green waxy solids. Compounds **2.4a-c** oxidized slowly in air and upon adsorption to silica, and thus, IR spectra of **2.4a-c** were not recorded due to the inability to obtain samples of high purity (>95 %). The products were stored under nitrogen to prevent further oxidation.



2.4a: green waxy solid; UV-vis (THF): $\lambda_{\max} = 344$ nm, $\lambda_{\text{em}} = 449, 476$ nm; ¹H NMR (C₆D₆) δ 1.93 (s, 3 H, Mes *p*-CH₃), 2.47 (s, 6 H, Mes *o*-CH₃), 5.53 (br s, 1 H, P-CHPh), 6.43 (d, $J_{\text{PC}} = 17$ Hz, 1 H, P-CH=CAr), 6.58 (br s, 2 H, Mes-H), 6.87 – 6.90 (m, 3 H, Bi-Ar 2/3/4-H), 6.95 – 6.97 (m, 1 H, Ph *p*-H), 7.02 – 7.06 (m, 3 H, Ph *m*-H/Bi-Ar 1-H), 7.11 – 7.12 (m, 2 H, Ar *o*-H), 7.33 – 7.35 (m, 4 H, Ph *o*-H/Ar *m*-H); ¹³C NMR (C₆D₆) δ 20.85 (Mes *p*-CH₃), 24.14 (d, $J_{\text{PC}} = 16$ Hz, Mes *o*-CH₃), 45.90 (d, $J_{\text{PC}} = 12$ Hz, P-CHPh), 125.07 (q, $J_{\text{FC}} = 270$ Hz, CF₃), 125.61 (q, $J_{\text{FC}} = 4.0$ Hz, Ar *m*-C), 126.63 (d, $J_{\text{PC}} = 21$ Hz, Mes *i*-C), 126.91 (Bi-Ar 3-C), 126.96 (d, $J_{\text{PC}} = 2.9$ Hz, Ph *p*-C), 128.1³⁰ (Bi-Ar 4-C), 128.53 (Bi-Ar 2-C), 128.65 (d, $J_{\text{PC}} = 5.7$ Hz, Bi-Ar 1-C), 128.79 (Ph *m*-C), 128.89 (d, $J_{\text{PC}} = 2.9$ Hz, Ar *o*-C), 129.30 (q, $J_{\text{FC}} = 18$ Hz, Ar *p*-C), 130.21 (d, $J_{\text{PC}} = 3.9$ Hz, Mes *m*-C), 130.40 (d, $J_{\text{PC}} = 8.6$ Hz, Ph *o*-C), 132.78 (d, $J_{\text{PC}} = 19$ Hz, P-CH=CAr), 136.20 (d, $J_{\text{PC}} = 2.9$ Hz, PCH-C=CAr), 138.33 (d, $J_{\text{PC}} = 13$ Hz, PCHPh-C=C), 139.90 (Mes *p*-C), 140.42

(d, $J_{PC} = 12$ Hz, Ph *i*-C), 142.90 (d, $J_{PC} = 12$ Hz, P-CH=CAr), 145.66 (d, $J_{PC} = 15$ Hz, Mes *o*-C), 146.65 (Ar *i*-C); ^{31}P NMR (C_6D_6) δ -26.0; ^{19}F NMR (C_6D_6) δ -62.1; High-Resolution EI-MS for $\text{C}_{31}\text{H}_{26}\text{PF}_3$ m/z calcd 486.1724, found 486.1716.

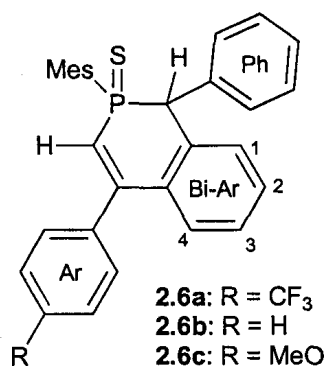
2.4b: green waxy solid; UV-vis (THF): $\lambda_{\text{max}} = 336$ nm, $\lambda_{\text{em}} = 449, 478$ nm; ^1H NMR (C_6D_6) δ 1.92 (s, 3 H, Mes *p*-CH₃), 2.48 (s, 6 H, Mes *o*-CH₃), 5.56 (br s, 1 H, P-CHPh), 6.52 (d, $J_{\text{PH}} = 19$ Hz, 1 H, P-CH=CAr), 6.57 (br s, 2 H, Mes-H), 6.87 – 6.88 (m, 2 H, Bi-Ar 2/4-H), 6.95 (t, $J = 7.5$ Hz, 1 H, Ph *p*-H), 7.02 – 7.05 (m, 3 H, Ph *m*-H/Bi-Ar 1-H), 7.10 – 7.13 (m, 1 H, Ar *p*-H), 7.15 – 7.18 (m, 3 H, Bi-Ar 3-H/Ar *m*-H), 7.32 – 7.34 (m, 2 H, Ar *m*-H), 7.36 (d, $J = 8.4$ Hz, 2 H, Ph *o*-H); ^{13}C NMR (C_6D_6) δ 20.86 (Mes *p*-C), 24.16 (d, $J_{PC} = 17$ Hz, Mes *o*-C), 45.99 (d, $J_{PC} = 11$ Hz, P-CHPh), 126.77 (Ph *p*-C), 126.80 (Bi-Ar 4 or 2-C), 127.18 (d, $J_{PC} = 22$ Hz, Mes *i*-C), 127.43 (Ar *p*-C), 128.30, 128.50, 128.53, 128.66, 128.68, 128.70 (Ph *m*-C/Bi-Ar 1 and 3-C/Bi-Ar 2 or 4-C/Ar *o*- and *m*-C), 130.13 (d, $J_{PC} = 3.5$ Hz, Mes *m*-C), 130.42 (d, $J_{PC} = 8.0$ Hz, Ph *o*-C), 130.69 (d, $J_{PC} = 18$ Hz, P-CH=CAr), 136.89 (d, $J_{PC} = 3.5$ Hz, PCHPh-C=C), 138.38 (d, $J_{PC} = 13$ Hz, PCHPh-C=C), 139.56 (Mes *p*-C), 140.82 (d, $J_{PC} = 11$ Hz, Ph *i*-C), 143.32 (d, $J_{PC} = 2.3$ Hz, Ar *i*-C), 144.43 (d, $J_{PC} = 10$ Hz, P-CH=CAr), 145.68 (d, $J_{PC} = 16$ Hz, Mes *o*-C); ^{31}P NMR (C_6D_6) δ -27.0; High-Resolution EI-MS for $\text{C}_{30}\text{H}_{27}\text{P}$ m/z calcd 418.1850, found 418.1844.

2.4c: green waxy solid; UV-vis (THF): $\lambda_{\text{max}} = 344$ nm, $\lambda_{\text{em}} = 467$ nm; ^1H NMR (C_6D_6) δ 1.93 (s, 3 H, Mes *p*-CH₃), 2.52 (s, 6 H, Mes *o*-CH₃), 3.33 (s, 3 H, OCH₃), 5.58 (br s, 1 H, P-CHPh), 6.53 (d, $J_{\text{PH}} = 18$ Hz, 1 H, P-CH=CAr), 6.58 (br s, 2 H, Mes-H), 6.78 – 6.80 (m, 2 H, Ar *m*-H), 6.89 – 7.00 (m, 3 H, Ph *p*-H/Bi-Ar 2- and 3-H), 7.03 – 7.06 (m, 3 H, Ph *m*-H/Bi-Ar 1-H), 7.26 – 7.28 (m, 3 H, Bi-Ar 4-H/Ar *o*-H), 7.38 (d, $J = 7.8$ Hz, 2 H, Ph

o-H); ^{13}C NMR (C_6D_6) δ 20.85 (Mes *p*- $\underline{\text{C}}\text{H}_3$), 24.18 (d, $J_{\text{PC}} = 17$ Hz, Mes *o*- $\underline{\text{C}}\text{H}_3$), 46.04 (d, $J_{\text{PC}} = 13$ Hz, P- $\underline{\text{C}}\text{HPh}$), 54.82 ($\text{O}\underline{\text{C}}\text{H}_3$), 114.18 (Ar *m*- $\underline{\text{C}}$), 126.76 (Ph *p*- $\underline{\text{C}}$), 127.38 (d, $J_{\text{PC}} = 23$ Hz, Mes *i*- $\underline{\text{C}}$), 128.27 – 128.29 (Bi-Ar 2/3- $\underline{\text{C}}$), 128.50 – 128.54 (Bi-Ar 1/4- $\underline{\text{C}}$), 128.68 (Ph *m*- $\underline{\text{C}}$), 129.50 (d, $J_{\text{PC}} = 18$ Hz, P- $\underline{\text{C}}\text{H}=\text{CAr}$), 129.81 (d, $J_{\text{PC}} = 3.5$ Hz, Ar *o*- $\underline{\text{C}}$), 130.15 (d, $J_{\text{PC}} = 4.7$ Hz, Mes *m*- $\underline{\text{C}}$), 130.43 (d, $J_{\text{PC}} = 9.2$ Hz, Ph *o*- $\underline{\text{C}}$), 135.64 (d, $J_{\text{PC}} = 3.5$ Hz, Ar *i*- $\underline{\text{C}}$), 137.12 (d, $J_{\text{PC}} = 3.5$ Hz, PCHPh- $\underline{\text{C}}=\underline{\text{C}}$), 138.55 (d, $J_{\text{PC}} = 12$ Hz, PCHPh- $\underline{\text{C}}=\underline{\text{C}}$), 139.50 (Mes *p*- $\underline{\text{C}}$), 140.89 (d, $J_{\text{PC}} = 11$ Hz, Ph *i*- $\underline{\text{C}}$), 144.10 (d, $J_{\text{PC}} = 10$ Hz, P- $\underline{\text{C}}\text{H}=\underline{\text{C}}\text{Ar}$), 145.69 (d, $J_{\text{PC}} = 15$ Hz, Mes *o*- $\underline{\text{C}}$), 159.59 (Ar *p*- $\underline{\text{C}}$); ^{31}P NMR (C_6D_6) δ -27.3; High-Resolution EI-MS for $\text{C}_{31}\text{H}_{29}\text{PO}$ m/z calcd 448.1956, found 448.1966.

2.5.3 Oxidation of 1,2-dihydrophosphinine 2.4a-c with Sulfur

Sulfur powder (25 mg, 0.75 mmol) was added to a solution of **2.4a-c**³¹ (0.3 mmol)³² in dichloromethane (3 mL) at room temperature. The reaction mixture was allowed to stir overnight. The excess sulfur powder was removed by filtration and the product mixture was purified by preparative thin-layer chromatography (silica gel, 9:1 hexanes/acetone). 1,2-Dihydrophosphinine sulfides **2.6a-c** were obtained as white solids (20 - 23% isolated yields). Since 1,2-dihydrophosphinines **2.4a-c** oxidized slowly in air and upon adsorption to silica, compounds **2.6a-c** were contaminated with a small amount of the corresponding phosphinine oxides. Colourless crystals were grown by the slow diffusion of hexanes into an ether/benzene solution of **2.6a-c** and the molecular structures were determined by X-ray crystallography.



2.6a: colourless solid; IR cm⁻¹ 701 (m), 739 (s, P=S), 824 (w), 1018 (w), 1067 (m), 1128 (m), 1168 (m), 1265 (m), 1323 (s), 1407 (w), 1451 (w), 1605 (w), 2850 (w), 2919 (w), 3052 (w); ¹H NMR (C₆D₆) δ 1.79 (s, 3 H, Mes *p*-CH₃), 2.64 (br s, 6 H, Mes *o*-CH₃), 5.17 (d, *J*_{PH} = 14 Hz, 1 H, P-CHPh), 6.03 (d, *J*_{PH} = 15 Hz, 1 H, P-CH=CAr), 6.43 (d, *J*_{PH} = 3.6 Hz, 2 H, Mes-H), 6.63 – 6.69 (m, 3 H, Bi-Ar 2/3/4-H), 6.74 – 6.75 (m, 1 H, Bi-Ar 1-H), 7.07 – 7.10 (m, 3 H, Ar *o*-H/Ph *p*-H), 7.22 (t, *J* = 7.5 Hz, 2 H, Ph *m*-H), 7.29 – 7.31 (m, 2 H, Ar *m*-H), 7.56 (d, *J* = 7.8 Hz, 2 H, Ph *o*-H); ¹³C NMR (C₆D₆) δ 20.54 (Mes *p*-CH₃), 24.73 (Mes *o*-CH₃), 50.10 (d, *J*_{PC} = 47 Hz, P-CHPh), 124.75 (q, *J*_{FC} = 270 Hz, CF₃), 125.54 (d, *J*_{PC} = 73 Hz, P-CH=CAr), 125.86 (q, *J*_{FC} = 3.5 Hz, Ar *m*-C), 127.62 (d, *J*_{PC} = 3.5 Hz, Ph *p*-C), 128.1³⁰ (Ph *m*-C), 128.2³⁰ (Bi-Ar 3-C), 128.52 (d, *J*_{PC} = 3.3 Hz, Bi-Ar 4-C), 128.6³⁰ (d, *J*_{PC} = 90 Hz³³, Mes *i*-C), 128.84 (Ar *o*-C), 129.72 (Bi-Ar 2-C), 130.44 (d, *J*_{PC} = 4.7 Hz, Ph *o*-C), 130.75 (q, *J*_{FC} = 32 Hz, Ar *p*-C), 130.87 (d, *J*_{PC} = 8.1 Hz, Bi-Ar 1-C), 131.49 (d, *J*_{PC} = 12 Hz, Mes *m*-C), 133.97 (d, *J*_{PC} = 4.7 Hz, Ph *i*-C), 134.46 (d, *J*_{PC} = 14 Hz, PCHPh-C=C), 136.03 (d, *J*_{PC} = 5.7 Hz, PCHPh-C=C), 140.09 (d, *J*_{PC} = 2.4 Hz, Mes *p*-C), 140.63 (d, *J*_{PC} = 9.2 Hz, Mes *o*-C), 143.28 (d, *J*_{PC} = 15 Hz, Ar *i*-C), 147.04 (P-CH=CAr); ³¹P NMR (C₆D₆) δ 30.0; ¹⁹F NMR (C₆D₆) δ -62.4; High-Resolution EI-MS for C₃₁H₂₆F₃PS *m/z* calcd 518.1445, found 518.1435.

2.6b: colourless solid; IR cm^{-1} 685 (m), 698 (s, P=S), 735 (m), 780 (m), 850 (w), 1031 (w), 1076 (w), 1266 (w), 1444 (m), 1494 (m), 1556 (w), 1603 (m), 2922 (w), 3028 (w), 3058 (w); ^1H NMR (C_6D_6) δ 1.78 (s, 3 H, Mes p - CH_3), 2.69 (br s, 6 H, Mes o - CH_3), 5.19 (d, $J_{\text{PH}} = 15$ Hz, 1 H, P- CHPh), 6.11 (d, $J_{\text{PH}} = 17$ Hz, 1 H, P- $\text{CH}=\text{CAr}$), 6.42 (d, $J_{\text{PH}} = 3.0$ Hz, 2 H, Mes- H), 6.62 – 6.66 (m, 2 H, Bi-Ar 2/3- H), 6.76 (d, $J = 6.0$ Hz, 1 H, Bi-Ar 1- H), 6.93 (d, $J = 9.0$ Hz, 1 H, Bi-Ar 4- H), 7.05 (t, $J = 7.2$ Hz, 1 H, Ph p - H), 7.10 – 7.14 (m, 3 H, Ar m,p - H), 7.19 (t, $J = 7.2$ Hz, 2 H, Ph m - H), 7.28 (d, $J = 6.6$ Hz, 2 H, Ar o - H), 7.64 (d, $J = 7.2$ Hz, 2 H, Ph o - H); ^{13}C NMR (C_6D_6) δ 20.53 (Mes p - CH_3), 24.68 (Mes o - CH_3), 50.18 (d, $J_{\text{PC}} = 48$ Hz, P- CHPh), 123.80 (d, $J_{\text{PC}} = 75$ Hz, P- $\text{CH}=\text{CAr}$), 127.45 (d, $J_{\text{PC}} = 2.9$ Hz, Ph p - C), 128.0³⁰ (Bi-Ar 3- C), 128.1³⁰ (Ph m - C), 128.64 (Ar o - C), 128.91 (Bi-Ar 4- C), 128.94 (Ar m - C), 129.01 (Ar p - C), 129.10 (d, $J_{\text{PC}} = 81$ Hz, Mes i - C), 129.41 (Bi-Ar 2- C), 130.51 (d, $J_{\text{PC}} = 5.0$ Hz, Ph o - C), 130.75 (d, $J_{\text{PC}} = 8.7$ Hz, Bi-Ar 1- C), 131.43 (d, $J_{\text{PC}} = 11$ Hz, Mes m - C), 134.25 (d, $J_{\text{PC}} = 3.9$ Hz, Ph i - C), 135.21 (d, $J_{\text{PC}} = 14$ Hz, PCHPh- $\text{C}=\text{C}$), 136.19 (d, $J_{\text{PC}} = 5.7$ Hz, PCHPh- $\text{C}=\text{C}$), 139.78 (d, $J_{\text{PC}} = 3.0$ Hz, Mes p - C), 139.96 (d, $J_{\text{PC}} = 14$ Hz, Ar i - C), 140.63 (d, $J_{\text{PC}} = 9.6$ Hz, Mes o - C), 148.78 (P- $\text{CH}=\text{CAr}$); ^{31}P NMR (C_6D_6) δ 30.3; High-resolution EI-MS for $\text{C}_{30}\text{H}_{27}\text{PS}$ m/z , calcd 450.1571, found 450.1560.

2.6c: colourless solid; IR cm^{-1} 670 (s), 695 (s), 735 (s), 778 (m), 812 (m), 933 (w) 1031 (s), 1178 (s), 1253 (s), 1292 (m), 1331 (m), 1376 (w), 1411 (w), 1451 (m), 1510 (s), 1552 (w), 1606 (s), 2837 (w), 2929 (w), 2964 (w), 3033 (w); ^1H NMR (C_6D_6) δ 1.79 (s, 3 H, Mes p - CH_3), 2.72 (br s, 6 H, Mes o - CH_3), 3.32 (s, 3 H, OCH_3), 5.20 (d, $J_{\text{PH}} = 14$ Hz, 1 H, P- CHPh), 6.09 (dd, $J_{\text{PH}} = 16$ Hz, $J = 1.8$ Hz, 1 H, P- $\text{CH}=\text{CAr}$), 6.44 (d, $J_{\text{PH}} = 3.6$ Hz, 2 H, Mes- H), 6.65 (t, $J = 7.5$ Hz, 1 H, Bi-Ar 2- H), 6.70 (t, $J = 7.5$ Hz, 1 H, Bi-Ar 3- H), 6.72 –

6.75 (m, 2 H, Ar *m*-H), 6.76 – 6.78 (m, 1 H, Bi-Ar 1-H), 7.03 – 7.07 (m, 2 H, Bi-Ar 4-H/Ph *p*-H) 7.20 – 7.24 (m, 4 H, Ph *m*-H/Ar *o*-H), 7.66 (d, $J = 7.8$ Hz, 2 H, Ph *o*-H); ^{13}C NMR (C_6D_6) δ 20.54 (Mes *p*-CH₃), 24.69 (Mes *o*-CH₃), 50.19 (d, $J_{\text{PC}} = 48$ Hz, P-CHPh), 54.92 (OCH₃), 114.50 (Ar *m*-C), 122.09 (d, $J_{\text{PC}} = 76$ Hz, P-CH=CAr), 127.41 (d, $J_{\text{PC}} = 3.5$ Hz, Ph *p*-C), 127.92 (Bi-Ar 3-C), 128.0³⁰ (Ph *m*-C), 128.97 (d, $J_{\text{PC}} = 2.4$ Hz, Bi-Ar 4-C), 129.31 (d, $J_{\text{PC}} = 79$ Hz, Mes *i*-C), 129.37 (Bi-Ar 2-C), 130.01 (Ar *o*-C), 130.53 (d, $J_{\text{PC}} = 4.5$ Hz, Ph *o*-C), 130.77 (d, $J_{\text{PC}} = 9.2$ Hz, Bi-Ar 1-C), 131.43 (d, $J_{\text{PC}} = 10$ Hz, Mes *m*-C), 132.00 (d, $J_{\text{PC}} = 15$ Hz, Ar *i*-C), 134.33 (d, $J_{\text{PC}} = 4.7$ Hz, Ph *i*-C), 135.41 (d, $J_{\text{PC}} = 14$ Hz, PCHPh-C=C), 136.35, (d, $J_{\text{PC}} = 5.7$ Hz, PCHPh-C=C), 139.71 (d, $J_{\text{PC}} = 2.3$ Hz, Mes *p*-C), 140.59 (d, $J_{\text{PC}} = 10$ Hz, Mes *o*-C), 148.65 (P-CH=CAr), 160.87 (Ar *p*-C); ^{31}P NMR (C_6D_6) δ 30.4; High-resolution EI-MS for $\text{C}_{31}\text{H}_{29}\text{OPS}$ m/z calcd 480.1677, found 480.1666.

2.5.4 General Procedure for the Addition of Other Alkynes to Phosphaalkenes 2.1, 2.2, and 2.3

A solution of phosphaalkene (0.3 mmol) and excess alkyne in C_6D_6 (1.5 mL) was heated to reflux. The reaction was monitored by ^1H and ^{31}P NMR spectroscopy. There was never any indication of reaction, except for when methyl propiolate was used. In that case, the solvent was removed by rotary evaporation yielding a yellow residue. Chromatographic separation of the crude product was attempted; however, no single compound was isolated.

2.5.5 General Procedure for the Addition of Alkynes to Phosphaalkenes 2.1, 2.2, and 2.3 under Photochemical Conditions

A solution of phosphaalkene (0.3 mmol) and excess alkyne in hexanes (1.5 mL) was irradiated at 254 nm in the cold (-70 °C) for 20 h. The reaction was monitored by ^{31}P NMR spectroscopy. The ^{31}P signal for the phosphaalkene (2.1 – 2.3) was unchanged and no new signals were observed.

2.6 References

1. (a) Mathey, F. *Acc. Chem. Res.* **1992**, *25*, 90; (b) Dillon, K. B.; Mathey, F.; Nixon, J. F. *Phosphorus: The Carbon Copy*; John Wiley & Sons: New York, 1998; (c) Mathey, F. *Angew. Chem. Int. Ed.* **2003**, *42*, 1578; (d) Gates, D. *Top. Curr. Chem.* **2005**, *250*, 107.
2. For additional reviews on phosphaalkene reactivity see: (a) Appel, R.; Knoll, F.; Ruppert, I. *Angew. Chem. Int. Ed. Engl.* **1981**, *20*, 731; (b) Scherer, O. J. *Angew. Chem. Int. Ed. Engl.* **1985**, *24*, 924; (c) Markovskii, L. N.; Romanenko, V. D. *Tetrahedron* **1989**, *45*, 6019; (d) Nixon, J. F. *Chem. Rev.* **1988**, *88*, 1327; (e) Appel, R.; Knoll, F.; *Adv. Inorg. Chem.* **1989**, *33*, 259; (f) Appel, R. In *Multiple Bonds and Low Coordination in Phosphorus Chemistry*; Regitz, M., Scherer, O. J., Eds.; Thieme: Stuttgart, 1990; p157-269; (g) Gaumont, A.C.; Denis, J. M. *Chem. Rev.* **1994**, *94*, 1413; (h) Weber, L. *Angew. Chem. Int. Ed. Engl.* **1996**, *35*, 271; (i) Yoshifuji, M. *J. Chem. Soc. Dalton Trans.* **1998**, 3343; (j) Weber, L. *Eur. J. Inorg. Chem.* **2000**, 2425.
3. For reviews on silene reactivity see: (a) Gusel'nikov, L. E.; Nametkin, N. S. *Chem. Rev.* **1979**, *79*, 529; (b) Wiberg, N. *J. Organomet. Chem.* **1984**, *273*, 141; (c) Raabe, G.; Michl, J. *Chem. Rev.* **1985**, *85*, 419; (d) Brook, A. G.; Baines, K. M. *Adv. Organomet. Chem.* **1986**, *25*, 1; (e) Brook, A. G.; Brook, M. A. *Adv. Organomet. Chem.* **1996**, *39*, 71; (f) Müller, T.; Ziche, W.; Auner, N. In *The Chemistry of Organosilicon Compounds*; Rappoport, Z., Apeloig, Y., Eds.; Wiley & Sons: New York, 1998; Vol. 2, Chapter 16; (h) Morkin, T. L.; Owens, T. R.; Leigh, W. J. In *The Chemistry of Organic Silicon*

- Compounds*; Rappoport, Z., Apeloig, Y., Eds.; Wiley & Sons: New York, 2001; Vol. 3, Chapter 17; (i) Morkin, T. L.; Leigh, W. J. *Acc. Chem. Res.* **2001**, *34*, 129.
4. Mathey, F.; Charrier, C.; Maigrot, N.; Marinetti, A.; Ricard, L.; Tran Huy, N.-H. *Comment. Inorg. Chem.* **1992**, *12*, 61.
5. Bansal, R. K.; Kumawat, S. K. *Tetrahedron* **2008**, *64*, 10945.
6. Keglevich, G. *Curr. Org. Chem.* **2006**, *10*, 93.
7. (a) Mark, J. E.; Allcock, H. R.; West, R. *Inorganic Polymers*; Oxford University Press: Oxford, 2005; (b) Manners, I. *Angew. Chem. Int., Ed. Engl.* **1996**, *35*, 1602; (c) Manners, I. *Angew. Chem. Int. Ed.* **2006**, *46*, 1565.
8. Boyd, B. A.; Thoma, R. J.; Neilson, R. H. *Tetrahedron Lett.* **1987**, *28*, 6121.
9. (a) Tran Huy, N.-H.; Ricard, L.; Mathey, F. *Organometallics* **1988**, *7*, 1791; (b) Marinetti, A.; Ricard, L.; Mathey, F. *Organometallics* **1990**, *9*, 788; (c) Le Floch, P.; Mathey, F. *Synlett* **1990**, 171.
10. (a) Neilson, R. H.; Boyd, B. A.; Dubois, D. A.; Hani, R.; Scheide, G. M.; Shore, J. T.; Wettermark, U. G.; *Phosphorus, Sulfur, Silicon Relat. Elem.* **1987**, *30*, 463; (b) Boyd, B. A.; Thoma, R. J.; Watson, W. H.; Neilson, R. H. *Organometallics* **1988**, *7*, 572.
11. Marinetti, A.; Fischer, J.; Mathey, F. *J. Am. Chem. Soc.* **1985**, *107*, 5001.
12. Doxsee, K. M.; Shen, G. S. *J. Am. Chem. Soc.* **1989**, *111*, 9129.
13. (a) Weber, L.; Rühlicke, A. *J. Organomet. Chem.* **1994**, *470*, C1; (b) Weber, L.; Kaminski, O.; Stammler, H.-G.; Neumann, B.; Boese, R. *Z. Naturforsch. B* **1994**, *49*, 1693; (c) Weber, L.; Kaminski, O.; Rühlicke, A.; Quasdorff, B.; Stammler, H.-G.; Neumann, B. *Organometallics* **1996**, *15*, 123.
14. (a) (b) Marinetti, A.; Mathey, F. *J. Chem. Soc., Chem. Commun.* **1990**, 153; (c) Dietz, J.; Renner, J.; Bergsträßer, U.; Binger, P.; Regitz, M. *Eur. J. Org. Chem.* **2003**, 512; (d) Grobe, J.; LeVan, D. *J. Fluorine Chem.* **2004**, *125*, 801.

15. (a) Klebach, Th. C.; Lourens, R.; Bickelhaupt, F. *J. Am. Chem. Soc.* **1978**, *100*, 4886; (b) Yam, M.; Chong, J. H.; Tsang, C.-W.; Patrick, B. O.; Lam, A. E.; Gates, D. P. *Inorg. Chem.* **2006**, *45*, 5225.
16. Neilson, R. H. *Inorg. Chem.* **1981**, *20*, 1679.
17. Becker, G. Z. *Anorg. Allgem. Chem.* **1976**, *423*, 242.
18. Quin, L. D. *A Guide to Organophosphorus Chemistry*; Wiley & Sons: New York, 2000.
19. Fuchs, E.; Breit, B.; Bergsträber, U.; Hoffmann, J.; Heydt, H.; Regitz, M. *Synthesis* **1991**, 1099.
20. Angelov, C. M.; Neilson, R. H. *Inorg. Chem.* **1993**, *32*, 334.
21. Phosphaalkenes were irradiated at 254 nm using a Rayonet Photochemical Reactor. The choice of irradiation wavelength was made upon examination of the UV-vis absorption data of the phosphaalkenes. The lowest energy absorptions were assigned to π to π^* transitions: **2.1** 324 nm, ^{15b} **2.2** 280 nm (this work), **2.3** 310 nm (Wright, V. A.; Patrick, B. O.; Schneider, C.; Gates, D. P. *J. Am. Chem. Soc.* **2006**, *128*, 8836).
22. (a) van der Knaap, Th. A.; Klebach, Th. C.; Visser, F.; Bickelhaupt, F.; Ros, P.; Baerends, E. J.; Stam, C. H.; Konun, M. *Tetrahedron* **1984**, *40*, 765. (b) Termaten, A.; van der Sluis, M.; Bickelhaupt, F. *Eur. J. Org. Chem.* **2003**, 2049.
23. Brook, A. G.; Chatterton, W. J.; Sawyer, J. F.; Hughes, D. W.; Vorspohl, K. *Organometallics* **1987**, *6*, 1246.
24. Allan, C. J.; Pavelka, L. C.; Baines, K. M. *manuscript in preparation*.
25. (a) Mathey, F.; Mercier, F.; Charrier, C. *J. Am. Chem. Soc.* **1981**, *103*, 4595; (b) Tran Huy, N. H.; Mathey, F. *Tetrahedron Lett.* **1988**, *29*, 3077; (c) Trauner, H.; de la Cuesta, E.; Marinetti, A.; Mathey, F. *Bull. Soc. Chim. Fr.* **1995**, *132*, 384.

26. Gallagher, M. J. *Phosphorus-Carbon Heterocyclic Chemistry: The Rise of a New Domain*; Mathey, F., Ed.; Pergamon/Elsevier: Amsterdam, 2001; p 463.
27. Crassous, J.; Réau, R. *Dalton Trans.* **2008**, 6865.
28. (a) Woodward, R. B.; Hoffman, R. *J. Am. Chem. Soc.* **1965**, *87*, 395. (b) Woodward, R. B.; Hoffman, R. *Conservation of Orbital Symmetry*; Academic: New York, 1970.
29. Milnes, K. K.; Jennings, M. C.; Baines, K. M. *J. Am. Chem. Soc.* **2006**, *128*, 2491.
30. Chemical shift estimated from ^1H - ^{13}C gHMBC spectrum.
31. Addition product **2.4** was not isolated before oxidation.
32. Theoretical yield of **2.4** based on mmol of phosphalkene **2.1**.
33. Coupling constant (J) estimated from ^1H - ^{13}C gHMBC spectrum.

Chapter 3

Reactivity of a Germene towards Terminal Alkynes: Competition between Cycloaddition, Ene-Addition and CH-Insertion

3.1 Introduction

The isolation of the first stable silene,¹ $R_2Si=CR_2$, and disilene,² $R_2Si=SiR_2$, in 1981 were major breakthroughs in the chemistry of unsaturated main group compounds and led to the accelerated development of this field. The most widely studied of these unsaturated species continues to be those containing silicon;³ however, the study of doubly bonded species containing the heavier group 14 elements (Ge, Sn, Pb) has been gaining interest.^{4,5}

The cycloaddition reactions of silenes have begun to attract the attention of the synthetic organic community.⁶ The regio- and stereospecificity of the reactions and the presence of the main group atom, which remains available for further functionalization of the primary product, are the key features that make the cycloaddition reactions of silenes appealing. Given the importance of the cycloaddition reactions of silenes, not only as a fundamental reaction in silicon chemistry but also in organic synthesis, our group has explored the mechanism of the cycloaddition reactions of silenes, particularly with alkynes.⁷

The reactivity of silenes towards alkynes has been well-studied, especially for the relatively non-polar Brook silenes, $(Me_3Si)_2Si=C(R)(OSiMe_3)$; typically, alkyne addition yields silacyclobutenes regioselectively and in high yield.³ Through the use of a

molecular probe, cyclopropyl alkyne **3.1a-c** (Figure 3.1),⁸ the cycloaddition of alkynes to Brook silenes was determined to proceed via a diradical intermediate (Scheme 3.1).⁷

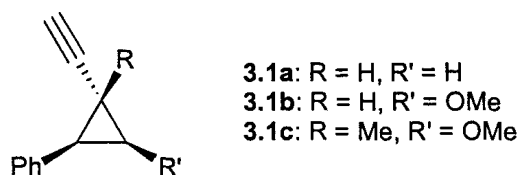
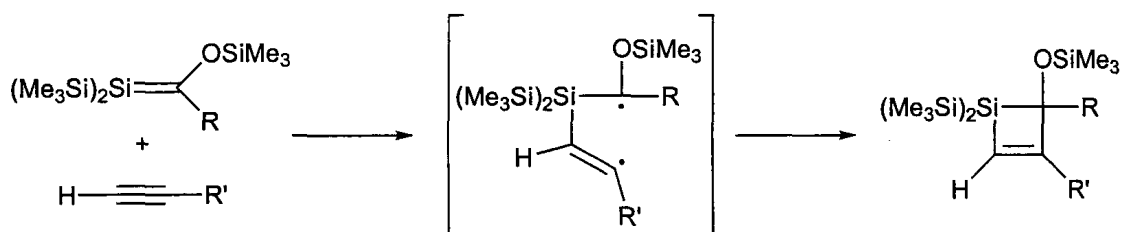


Figure 3.1 Alkynyl mechanistic probes.

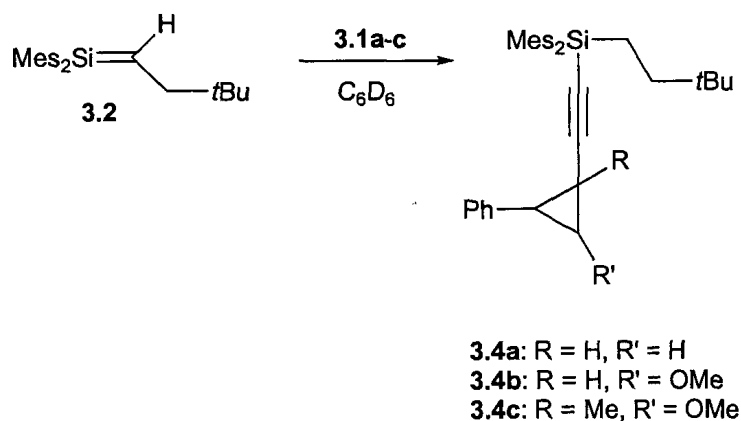


Scheme 3.1 Mechanism of alkyne addition to Brook silenes.

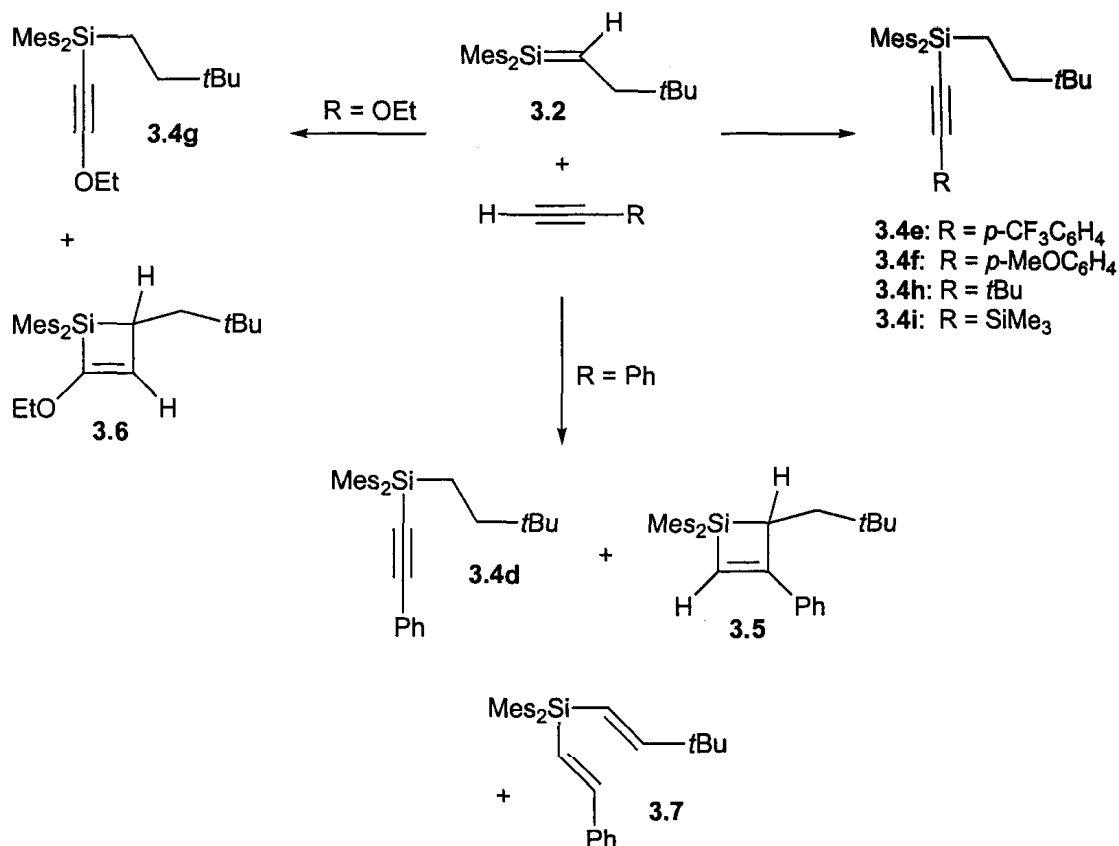
Surprisingly, the addition of alkynes to polar silenes, as well as germenes, has not been examined to the same extent as the Brook silenes. Although Brook silenes are a specialized class of silenes, they are by far the most widely studied. Given the known dependence of metallene reactivity on the polarity of the M=C bond, it was of interest to examine the reactivity and mechanistic chemistry of the naturally polarized systems. Silene $\text{Mes}_2\text{Si}=\text{C}(\text{H})\text{CH}_2t\text{Bu}$, **3.2**,⁹ and the analogous germene, $\text{Mes}_2\text{Ge}=\text{C}(\text{H})\text{CH}_2t\text{Bu}$, **3.3**,¹⁰ were chosen as substrates to explore the scope of alkyne reactivity.

When cyclopropyl alkynes **3.1a-c**, as well as a variety of other terminal alkynes, were added to neopentylsilene **3.2**, the major products isolated were silylacetylenes **3.4a-i**, from insertion of the terminal C-H bond of the alkyne across the Si=C bond, rather than the expected cycloadducts (Scheme 3.2, 3.3).¹¹ Of the numerous terminal alkynes

investigated, only phenylacetylene and ethoxyacetylene yielded cycloadducts upon addition to **3.2**, silacyclobutenes **3.5** and **3.6**, respectively, in addition to the corresponding silylacetylenes **3.4d** and **g** (Scheme 3.3). A minor amount of vinylsilane **3.7**, from formal ene-addition, was also observed in the reaction between silene **3.2** and phenylacetylene (Scheme 3.3). Since **3.2** did not react with the C≡C triple bond of cyclopropyl alkynes **3.1a-c**, no information could be discerned regarding the mechanism of alkyne addition. Furthermore, it appears that silene **3.2** is not an appropriate reagent for use in the synthesis of organic ring systems. The general preference for CH-insertion over cycloaddition was attributed to the polarity of silene **3.2** and provided an interesting example of how the polarity of the Si=C bond can directly influence the type of products formed in a given reaction.



Scheme 3.2 Addition of alkynyl probes to silene **3.2**.



Scheme 3.3 Addition of simple alkynes to silene 3.2.

On the other hand, germenes are inherently less polar than silenes; naturally polarized germenes have intermediate polarity between Brook silenes and naturally polarized silenes. Thus, the use of a naturally polarized germene, such as $\text{Mes}_2\text{Ge}=\text{C}(\text{H})\text{CH}_2\text{tBu}$, 3.3, may lead to alkyne cycloadducts in higher yields compared to the analogous silene. Thus, we were eager to explore the reactivity of neopentylgermene 3.3 towards terminal alkynes and compare the results with those obtained from neopentylsilene 3.2 as well as the non-polar Brook silenes.

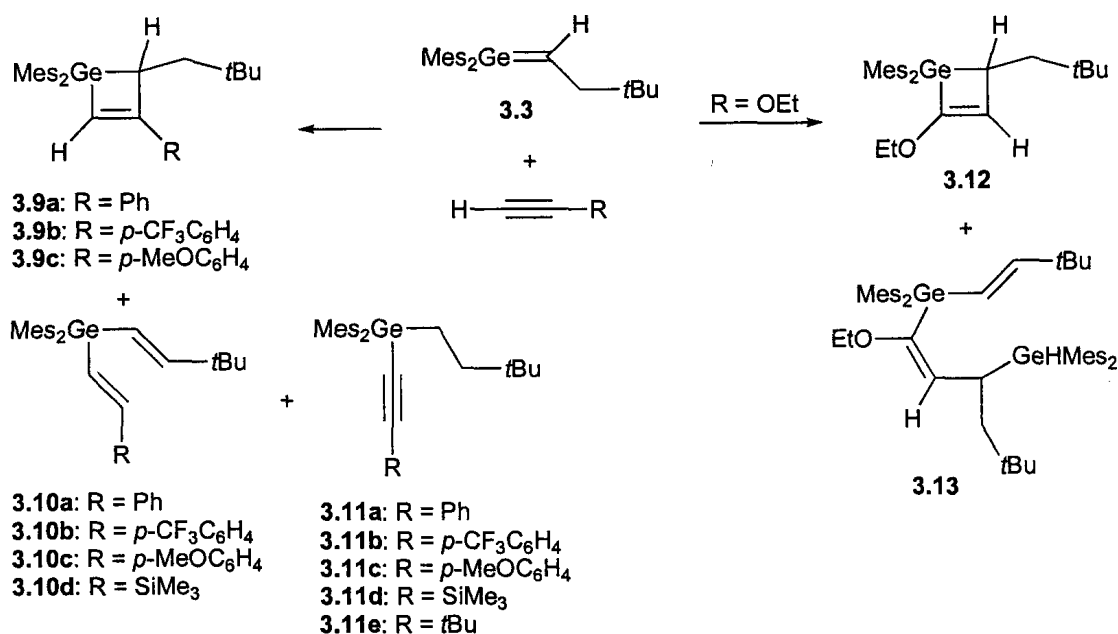
3.2 Results: Addition of Alkynes to Germene 3.3

Germene 3.3¹⁰ was synthesized prior to each reaction and used *in situ* without purification. A colourless pentane solution of fluorovinylgermane 3.8 was cooled to -78 °C and then treated with *t*BuLi. Upon warming to room temperature, the solution became pale yellow in colour and a fine precipitate appeared (LiF) indicating the formation of germene 3.3. It was necessary to add slightly less than 1 equivalent of *t*BuLi to fluorovinylgermane 3.8 when forming 3.3 to prevent polymerization of the germene.¹² As such, germene 3.3 was always contaminated with residual fluorogermane 3.8. The pentane was removed and the residue was dissolved in C₆D₆ before the alkyne was added; the presence of 3.3 was confirmed by ¹H NMR spectroscopy. The reactions were kept at room temperature for up to 6 days¹² and monitored regularly by ¹H NMR spectroscopy.

A mixture of germacyclobutene 3.9a, vinylgermane 3.10a, and germylacetylene 3.11a, was produced after 2 – 3 days upon reaction of germene 3.3 with phenylacetylene (Scheme 3.4). Similar product mixtures were obtained with 1-ethynyl-4-(trifluoromethyl)benzene (3.9b, 3.10b, and 3.11b; ~ 24 h) and 4-ethynylanisole (3.9c, 3.10c, and 3.11c; 4 – 5 days) (Scheme 3.4). In contrast, only vinylgermane 3.10d and germylacetylene 3.11d were formed when germene 3.3 was allowed to react with trimethylsilylacetylene and only germylacetylene 3.11e was formed upon reaction with *t*-butylacetylene, each after 6 days (Scheme 3.4). A significant amount of variation was noted in the product ratios obtained from reaction with each alkyne (3.9:3.10:3.11). Representative results are presented in Table 3.1 and a detailed description of the variability follows. Vinylgermanes 3.10a-d and germylacetylenes 3.11a-e were isolated

from residual fluorogermane **3.8** by chromatography; however, vinylgermanes **3.10a-d** could not be separated from the corresponding germylacetylenes **3.11a-d**. Germacyclobutenes **3.9a-c** decomposed upon prolonged exposure to the atmosphere or upon adsorption to silica gel, and thus, were not isolated.

The addition of ethoxyacetylene to germene **3.3** yielded a complex mixture of compounds within a few hours. Germacyclobutene **3.12** and vinylgermane **3.13** were identified as the major products by ^1H NMR spectroscopy (Scheme 3.4). The ratio of germacyclobutene **3.12** to vinylgermane **3.13** was variable; **3.12** ranged from 5 to 38% of the product mixture. The relative amount of **3.13** increased as the concentration of **3.3** increased. Unlike aryl-substituted germacyclobutenes **3.9a-c**, **3.12** did not decompose to any significant degree upon adsorption to silica, but did decompose after prolonged exposure to the atmosphere. Despite many attempts, **3.12** and **3.13** could not be separated from each other by chromatography; however, after the eventual decomposition of **3.12**, a sample of **3.13** was isolated.



Scheme 3.4 Reactions of terminal alkynes with germene **3.3**.

Table 3.1 Product ratios from the reactions of terminal alkynes with germene 3.3.

Entry	R-≡H	Scale ^a (mmol 3.3)	Alkyne Conc. ^b (M)	Order ^c	Initial Ratio ^d (3.8:3.3:3.11)	Product Ratio ^e (3.9:3.10:3.11)	Reaction Time	Adduct ^f (%)
1			0.30	germene	11:86:3	26:70:4	3 days	73
2		0.13	0.30	alkyne	9:54:37	7:23:70	3 days	90
3	Ph		0.60	alkyne	5:48:47	11:27:62	2 days	95
4	(a)		0.60	alkyne	13:67:20	18:48:34	2 days	90
5		0.26	0.30	germene	6:80:14	14:43:43	3 days	81
6			0.30	alkyne	9:41:50	2:14:84	2 days	> 99
7			0.30	germene	9:83:8	28:60:12	24 h	90
8		0.13	0.30	alkyne	8:79:13	26:50:24	24 h	94
9	CF ₃ C ₆ H ₄		0.60	alkyne	5:83:12	25:59:16	< 24 h	95
10	(b)		0.60	alkyne	12:82:6	29:62:9	< 24 h	93
11		0.26	0.30	alkyne	6:21:73	1:2:97	< 24 h	> 99
12			0.30	germene	10:85:5	12:61:27	4 days	64
13	MeOC ₆ H ₄	0.13	0.30	alkyne	11:83:6	11:52:37	5 days	67
14	(c)		0.60	alkyne	11:70:19	8:44:48	2 days	86
15		0.26	0.30	alkyne	9:74:17	4:34:62	3 days	76
16			0.30	germene	5:93:2	0:44:56	6 days	16
17	SiMe ₃	0.13	0.30	alkyne	10:74:16	0:8:92	6 days	39
18	(d)		0.60	alkyne	10:35:55	0:6:94	3 days	85
19			0.30	germene	4:93:3	0:0:100	5 days	28
20	<i>t</i> Bu	0.13	0.30	alkyne	10:68:21	0:0:100	6 days	49
21	(e)		0.60	alkyne	12:49:39	0:0:100	4 days	72

^a Germene 3.3 concentration remained constant: 0.24 – 0.26 M (C₆D₆); ^b Alkyne concentration of 0.3 M and 0.6 M correlate to 1.3 and 2.5 equiv, respectively, relative to germene 3.3; ^c Reagent listed was added to NMR tube first; ^d Initial ratio measured within the first 30 minutes of mixing. Reactions were then monitored daily until germene was consumed; ^e Product ratios calculated from integration of the appropriate signals in the ¹H NMR spectra of the reaction mixture (after removal of the polymeric material); ^f Alkyne adduct % calculated from integration of the appropriate signals in the ¹H NMR spectra of the reaction mixture (after removal of the polymeric material) relative to the total amount of molecular products formed from germene 3.3 including head-to-tail dimer 3.14, rearrangement product 3.15, and water adduct 3.16.

The product ratios (3.9:3.10:3.11) observed in the reactions between germene 3.3 and phenylacetylene, 1-ethynyl-4-(trifluoromethyl)benzene, 4-ethynylanisole, trimethylsilylacetylene or *t*-butylacetylene varied considerably depending on the reaction conditions (Table 3.1); the scale of the reaction, the order of addition, and the alkyne concentration all influenced the ratios. The concentration of germene 3.3 was kept constant in all reactions (0.24 – 0.26 M).

Reaction of **3.3** with each of the aromatic alkynes gave a mixture containing germacyclobutene **3.9**, vinylgermane **3.10**, and germylacetylene **3.11**. The relative amount of germylacetylene **3.11** varied the most, ranging from 4 – 84 % (**3.11a**; Table 3.1, Entries 1 – 6), 9 – 97 % (**3.11b**; Table 3.1, Entries 7 – 11), and 27 – 62 % (**3.11c**; Table 3.1, Entries 12 – 15) of the product mixture depending on the conditions. Interestingly, regardless of the percentage of **3.11a-c**, the ratio of germacyclobutene **3.9** to vinylgermane **3.10** remained fairly constant (**3.9a**: **3.10a** = 1:3, **3.9b**: **3.10b** = 1:2, **3.9c**: **3.10c** = 1:5), even as the absolute amounts fluctuated.

Doubling the scale of the reaction, from 0.13 to 0.26 mmol of germene **3.3**, while keeping the remaining variables constant, lead to a significant increase in the relative amount of **3.11a-c** (Table 3.1, Entries 5, 6, 11, 15), and consequently, a relative decrease in the amounts of **3.9a-c** and **3.10a-c**. The order of addition also had an influence on the relative amount of germylacetylene **3.11a-c**; an increase in the relative amount of **3.11a-c** was consistently observed when the germene was added to the alkyne as opposed to when the alkyne was added to the germene, given the same scale and alkyne concentration (Table 3.1, Entries 2 – 4, 6, 8 – 11, 13 - 15). In contrast, there was no consistent trend associated with an increase in the alkyne concentration: the relative amount of **3.11a** and **b** decreased slightly, while that of **3.11c** increased slightly (Table 3.1, Entries 3, 4, 9, 10, 14). A higher concentration of alkyne did, however, lead to a sharp decrease in the reaction time and an increase in the percentage of alkyne adducts produced with all the aromatic alkynes. These changes were most apparent in the reaction with 4-ethynylanisole, which was the slowest of the aromatic alkynes to react with germene **3.3**.

There was no germacyclobutene formed in the reaction between germene **3.3** and trimethylsilylacetylene; however, the ratio of vinylgermane **3.10d** to germylacetylene **3.11d** was affected by the order of addition and the alkyne concentration. The reaction was not performed on a larger scale. When the germene was added to trimethylsilylacetylene, a higher portion of **3.11d** was obtained as compared to when trimethylsilylacetylene was added to the germene (Table 3:1, Entry 17). The same trend was observed with the aromatic alkynes. In addition, an increase in the concentration of trimethylsilylacetylene lead to a notably shorter reaction time and higher yield of alkyne adducts (Table 3:1, Entry 18).

Germylacetylene **3.11e** was the only product isolated from the reaction of germene **3.3** with *t*-butylacetylene. Although product ratios are irrelevant, the order of addition and alkyne concentration both influenced the reaction time and the percentage of alkyne adduct that formed. An increase in the relative amount of alkyne adduct was observed when the germene was added to *t*-butylacetylene as compared to when the alkyne was added to the germene (Table 3:1, Entry 20). A further increase in the amount of alkyne adduct, as well as a decrease in reaction time, was observed with the concentration of *t*-butylacetylene was doubled (Table 3:1, Entry 21).

In addition to affecting the product ratio (**3.9:3.10:3.11**), the scale, order of addition, and alkyne concentration also had an influence on the initial amount of germylacetylene **3.11** produced. Unlike germacyclobutene **3.9** or vinylgermane **3.10**, there was evidence for **3.11** formation in the ¹H NMR spectra of the reaction solution directly after mixing. The initial amount of **3.11** was quantified relative to the amount of germene **3.3** and residual fluorovinylgermane **3.8** present (Table 3.1). Similar trends were

observed between the initial amounts of **3.11** and the scale, order of addition, and alkyne concentration as those noted for the final amount of **3.11**. In general, when a higher portion of germylacetylene **3.11** was produced directly after mixing, a greater portion of **3.11** was present in the product mixture.

The relative yield of alkyne addition products decreased significantly with increased reaction times. When left in solution for extended periods, germene **3.3** can dimerize and rearrange to give digermacyclobutane **3.14** and vinylgermane **3.15**, respectively (Figure 3.2).¹² Also, minor amounts of digermoxane **3.16** can form from the addition of adventitious water (Figure 3.2). These side reactions became more significant, contributing to lower yields of alkyne adducts, the longer **3.3** was left in solution (Table 3.1). Furthermore, a minor amount of polymeric material, from the uninitiated polymerization of germene **3.3**, was produced in each reaction;¹² however, the amount of polymer remained relatively constant, and thus, was not included in the adduct yield calculations.

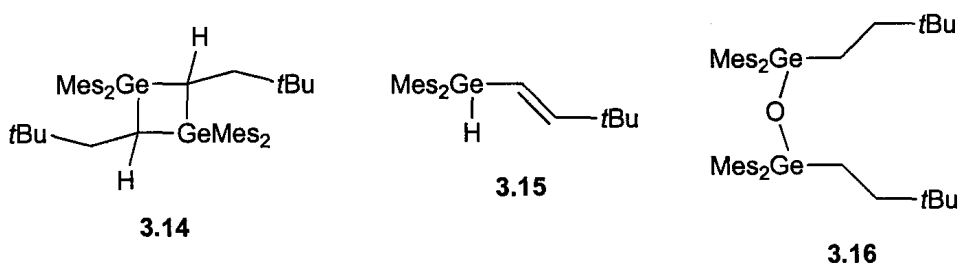


Figure 3.2 Digermacyclobutane **3.14**, vinylgermane **3.15**, and digermoxane **3.16**.

Germacyclobutenes **3.9a-c** were identified as part of the crude product mixtures by ¹H, ¹³C, gCOSY, ¹H-¹³C gHSQC and gHMBC NMR spectroscopy due to their sensitivity to moisture, which made isolation extremely difficult. Vinylgermanes **3.10a-d**

and germylacetylenes **3.11a-e** as well as germacyclobutene **3.12** and vinylgermane **3.13** were identified by IR, ^1H , ^{13}C , gCOSY, ^1H - ^{13}C gHSQC and gHMBC NMR spectroscopy, and mass spectrometry after purification.

The ^1H NMR spectra of germacyclobutenes **3.9a-c** and **3.12** were similar to those of silacyclobutenes **3.5** and **3.6** and were consistent with the proposed structures. A multiplet assigned to the saturated CH in the ring (~ 3.7 ppm (**3.9a-c**) or 2.99 ppm (**3.12**)) and a signal assigned to the vinylic hydrogen (~ 6.9 ppm (**3.9a-c**) or 5.81 ppm (**3.12**)) were observed in the ^1H NMR spectra of **3.9a-c** and **3.12**. The alkene functional group was confirmed by the presence of two signals in the ^{13}C NMR spectra of germacyclobutenes **3.9a-c** and **3.12** consistent with the expected chemical shift of alkenyl carbons. Unfortunately, the regiochemistry of the germacyclobutenes could not be determined based on these NMR spectroscopic data. Evidence for the assigned regiochemistry of **3.9a-c** and **3.12** is presented in section 3.3.

Due to the similarities between the spectroscopic data of vinylgermanes **3.10a-d**, only the spectral features of **3.10b** will be discussed. As with analogous vinylsilane **3.7**, there were two pairs of doublets (6.15 and 6.38 ppm, $J = 18$ Hz; 6.87 and 7.28 ppm, $J = 19$ Hz) in the ^1H NMR spectrum of **3.10b** assigned to the vinylic hydrogens on the two *trans*-oriented Ge-CH=CH-R double bonds. The upfield pair of doublets was assigned to the Ge-CH=CH-*t*Bu moiety; both vinylic signals showed a correlation to the signal assigned to the quaternary ^{13}C of the *t*Bu substituent in the ^1H - ^{13}C gHMBC NMR spectrum of **3.10b**. The downfield pair of doublets was assigned to the hydrogens on the Ge-CH=CH-Ar double bond. The existence of the two alkene functional groups in **3.10b** was confirmed by the presence of four signals in the ^{13}C NMR spectra of **3.10b** that fell

within the typical chemical shift range for alkenic carbons: 123.83 (Ge-CH=CH-*t*Bu), 135.43 (Ge-CH=CH-Ph), 141.09 (Ge-CH=CH-Ph), 156.52 ppm (Ge-CH=CH-*t*Bu).

As with vinylgermanes **3.10a-d**, the spectral features of germylacetylenes **3.11a-e** were very similar, and thus, only those of **3.11b** will be discussed in detail. Two multiplets in the ^1H NMR spectrum of germylacetylenes **3.11b** at 1.71-1.74 and 1.75-1.78 ppm were assigned to an AA'XX' spin system attributable to a X-CH₂CH₂-Y moiety. One of the substituents on the CH₂CH₂ moiety was determined to be a *t*Bu group; there was a correlation in the ^1H - ^{13}C gHMBC NMR spectrum of **3.11b** between a ^{13}C signal assigned to one of the CH₂ carbons and a signal in the ^1H dimension assigned to the *t*Bu CH₃. The other substituent was determined to be Mes₂RGe as revealed by correlations between one of the multiplets in the ^1H dimension and the ^{13}C signal assigned to the aromatic *ipso* carbon of the mesityl group in the ^1H - ^{13}C gHMBC NMR spectrum of **3.11b**. The alkyne functional group was confirmed by the presence of two signals in the ^{13}C NMR spectrum of **3.11b** at 100.15 and 104.77 ppm, which fall in the typical chemical shift range for alkynyl ^{13}C 's, and by an absorption observed in the IR spectrum of **3.11b** at 2157 cm⁻¹.

Vinylgermane **3.13** was formed from the reaction of two equivalents of germene **3.3** with one equivalent of ethoxyacetylene. The high-resolution ES-TOF mass spectrum of **3.13** revealed a molecular ion at m/z 855.4125, which was in excellent agreement with the calculated value of a 2:1 adduct (C₅₂H₇₃O⁷⁰Ge⁷²Ge (M⁺) m/z calcd 855.4116). In the ^1H NMR spectrum of **3.13**, there are signals consistent with the presence of four different mesityl groups, two *t*Bu groups, and one OCH₂CH₃ group. Also, four doublets were observed in the vinylic region of the ^1H NMR spectrum, two of which were coupled to each other (5.94 and 6.27 ppm, $J = 18$ Hz). In the ^1H - ^{13}C gHMBC NMR spectrum of

3.13, one of the two J coupled vinylic doublets correlated to the quaternary ^{13}C signal of one of the $t\text{Bu}$ substituents. Thus, these two J coupled doublets were assigned to the vinylic hydrogens on the *trans*-oriented $\text{Mes}_2\text{Ge}(\text{R})\text{-CH=CH-}t\text{Bu}$ moiety. Of the other two signals in the vinylic region of the ^1H NMR spectrum, one was assigned to a third vinylic hydrogen (5.40 ppm, 1 H, $J = 10.8$ Hz) and the other to a Ge-H (5.52 ppm, 1 H, $J = 3.6$ Hz). A correlation was observed between the ^1H signal at 5.40 ppm and a ^{13}C signal at 130.42 ppm in the $^1\text{H-}^{13}\text{C}$ gHSQC NMR spectrum of **3.13**, which is consistent with a vinylic hydrogen. There was no correlation from the ^1H signal at 5.52 ppm to any signals in the ^{13}C dimension of the $^1\text{H-}^{13}\text{C}$ gHSQC NMR spectrum of **3.13**, and thus, the ^1H signal was assigned to the $\text{Mes}_2\text{Ge-H}$.

In addition, two doublets of doublets, at 1.59 and 1.77 ppm, as well as a multiplet at 3.98 ppm, each integrating for 1 H, were observed in the ^1H NMR spectrum of **3.13** and were assigned to the hydrogens of a CHCH_2 fragment. The doublets of doublets were assigned to the CHCH_2 hydrogens and the multiplet was assigned to the CHCH_2 hydrogen. Each of the CHCH_2 ^1H signals showed a correlation to the ^{13}C signal assigned to the CH_3 of the second $t\text{Bu}$ substituent in the $^1\text{H-}^{13}\text{C}$ gHMBC NMR spectrum of **3.13**, which is consistent with a CHCH_2tBu moiety. Also, the gCOSY NMR spectrum of **3.13** showed correlations between the multiplet at 3.98 ppm (CHCH_2) and both doublets of doublets (CHCH_2) as well as one of the vinylic doublets (5.40 ppm, $J = 10.8$ Hz) and the $\text{Mes}_2\text{Ge-H}$ signal (5.52 ppm, $J = 3.6$ Hz). The vinylic signal (5.40 ppm) that couples to the multiplet at 3.98 ppm has been assigned to the EtO-C=C-H hydrogen based on the upfield chemical shift and a correlation to the ^{13}C signal assigned to the EtO-C=C-H carbon (156.36 ppm) in the $^1\text{H-}^{13}\text{C}$ gHMBC NMR spectrum of **3.13** as well as the

previously mentioned correlation to the ^{13}C signal at 130.42 ppm in the ^1H - ^{13}C gHSQC NMR spectrum of **3.13**, assigned to the $\text{EtO}-\text{C}=\underline{\text{C}}-\text{H}$ carbon. Thus, the CHCH_2tBu fragment can be elaborated to $\text{Mes}_2\text{Ge}(\text{H})-\text{CH}[\text{CH}=\text{C}(\text{R})\text{OEt}]\text{CH}_2t\text{Bu}$. Given the mass spectral data, it is clear that these two fragments, $\text{Mes}_2\text{Ge}(\text{R})-\text{CH}=\text{CH}-t\text{Bu}$ and $\text{Mes}_2\text{Ge}(\text{H})-\text{CH}[\text{CH}=\text{C}(\text{R})\text{OEt}]\text{CH}_2t\text{Bu}$, must be connected to make one molecule.

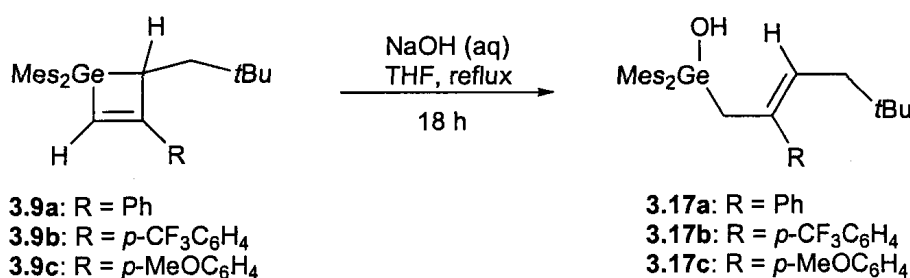
3.3 Determination of Regiochemistry of Germacyclobutenes

The germacyclobutenes (**3.9a-c** and **3.12**) were examined by ^1H 1-D ROE spectroscopy to determine the regiochemistry of the ring. Unfortunately, since aryl-substituted germacyclobutenes **3.9a-c** could not be isolated, the spectra were recorded on the crude product mixture where few signals could be cleanly irradiated. Irradiation of the signal assigned to the saturated ring GeCH (3.75 ppm) in **3.9a** lead to enhancement of the signal at 7.55 ppm, assigned to the ortho hydrogen of the phenyl substituent. A similar response was observed when the signal assigned to the saturated ring GeCH of **3.9b** or **3.9c** was irradiated. There was no enhancement of the vinylic ^1H signals observed when the GeCH signals were irradiated. Also, enhancement of the mesityl $o\text{-CH}_3$ signals was observed after irradiation of the signal assigned to the vinylic ^1H signal (6.91 ppm) of **3.9b**. The vinylic ^1H signals of **3.9a** and **c** could not be irradiated due the presence of overlapping signals. These results suggest that the vinylic ^1H is attached to the unsaturated ring carbon adjacent to germanium.

Some key differences were noted in the ^1H 1-D ROE spectroscopic data for ethoxy-substituted germacyclobutene **3.12** compared to **3.9a-c**. Most notably, enhancement of the signal assigned to the vinylic ^1H signal was observed after irradiation

of the signal at 2.99 ppm assigned to the saturated ring GeCH_2 . Irradiation of the signal at 0.96 ppm assigned to the $\text{C}(\text{CH}_3)_3$ group also lead to enhancement of the vinylic ^1H signal. There was no enhancement of the mesityl $o\text{-CH}_3$ signals after irradiation of the signal at 5.81 ppm assigned to the vinylic ^1H ; however, there was enhancement of the mesityl $o\text{-CH}_3$ signals after irradiation of the signal assigned to the OCH_2CH_3 hydrogens. Thus, the regiochemistry of **3.12** was determined to be opposite to that of **3.9a-c**; the vinyl ^1H is attached to the unsaturated ring carbon two bonds from germanium.

The regiochemistry of the ring systems was also determined by chemical degradation. Compounds **3.9a-c** and **3.12** were treated with aqueous NaOH (15%) in refluxing THF (Scheme 5). Only germacyclobutenes **3.9a-c** were observed to react with NaOH; the ethoxy-substituted ring, **3.12**, was unreactive towards NaOH under these conditions.



Scheme 3.5 Ring-opening of germacyclobutenes **3.9a-c**.

The ring-opened products, **3.17a-c** were identified by IR, ^1H , ^{13}C , gCOSY, ^1H - ^{13}C gHSQC and gHMBC NMR spectroscopy. There are several features in the NMR spectral data of **3.17a-c** that provide unambiguous evidence for the structure of the products. The spectral features of **3.17a-c** are very similar, and thus, only the spectral data of **3.17a** will be discussed. A triplet assigned to the vinylic ^1H (5.60 ppm, 1 H), a doublet assigned to

the CH_2tBu (1.96 ppm, 2 H), and a singlet assigned to the GeCH_2 (2.87 ppm, 2 H) were present in the ^1H NMR spectrum of **3.17a**. The triplet at 5.60 ppm showed a correlation to the doublet at 1.96 ppm in the gCOSY NMR spectrum of **3.17a**, and hence, the vinylic ^1H is adjacent to the CH_2tBu to give a $\text{C}=\text{C}(\text{H})\text{CH}_2t\text{Bu}$ moiety. The singlet at 2.87 ppm assigned to the GeCH_2 showed correlations to the ^{13}C signals at 125.29, 138.32, and 142.32 ppm in the ^1H - ^{13}C gHMBC NMR spectrum, which correspond to the two alkenic carbons and the *ipso* carbon of the phenyl substituent, respectively. The two alkenic carbon signals (125.29 and 138.32 ppm) also correlated to the doublet at 1.96 ppm in the ^1H dimension, assigned to the CH_2tBu hydrogens. Thus, the GeCH_2 must be connected to a $\text{C}(\text{Ph})=\text{C}(\text{H})\text{CH}_2t\text{Bu}$ moiety. The spectral features of **3.17a-c** were very similar to those of **3.18**, the ring-opened product of silacyclobutene **3.5** after treatment with NaOMe.

The structure assigned to **3.17a-c**, where the aryl substituent is attached to the carbon two bonds from germanium, is entirely consistent with the NMR spectroscopic data of **3.17a-c**. Thus, the aryl-substituted germacyclobutenes **3.9a-c** are derived from the addition of the terminal alkynyl carbon to the germanium of germene **3.3**. The original regiochemistry, with respect to alkyne addition to germene **3.3**, should be retained in the ring-opened product. The hydroxide anion selectively attacks the germanium, which leads to cleavage of the former germeric $\text{Ge}=\text{C}$ bond; similar behaviour has been observed when silacyclobutenes were treated with base.^{11,13} Alternative ring-opened products derived from a germacyclobutene with the phenyl substituent on the carbon adjacent to the germanium were considered; however, none of the structures were consistent with the spectroscopic data obtained.

The reduced reactivity of **3.12** towards NaOH in comparison to **3.9a-c** is consistent with the ethoxy substituent being located on the carbon adjacent to germanium. Presumably, the intermediate anion would be much less stable with the ethoxy substituent in this position; the added instability may be sufficient to make NaOH addition unfavourable (Figure 3.3).

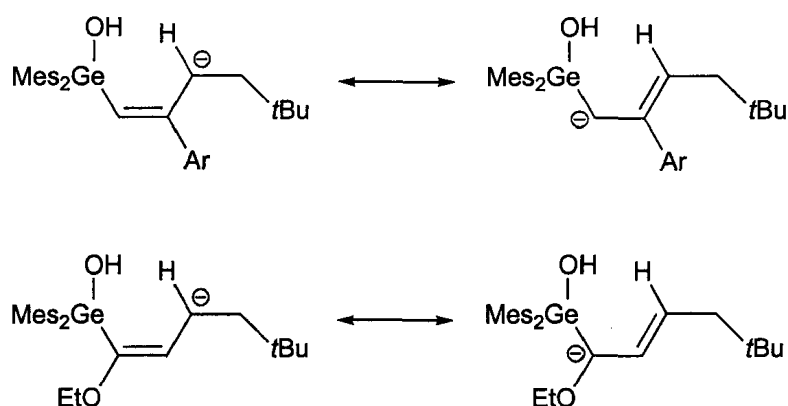


Figure 3.3 Resonance structures of ring-opened anions.

3.4 Discussion of Germene 3.3 Reactivity

Cycloadducts, ene-addition products, and CH-insertion products were obtained upon reaction of germene **3.3** with terminal alkynes. A discussion of cycloadduct formation is presented in section 3.4.1, followed by a discussion on the ene-addition and CH-insertion products in sections 3.4.2 and 3.4.3, respectively. A summary of the three alkyne addition pathways is presented in section 3.4.4.

3.4.1 Cycloaddition

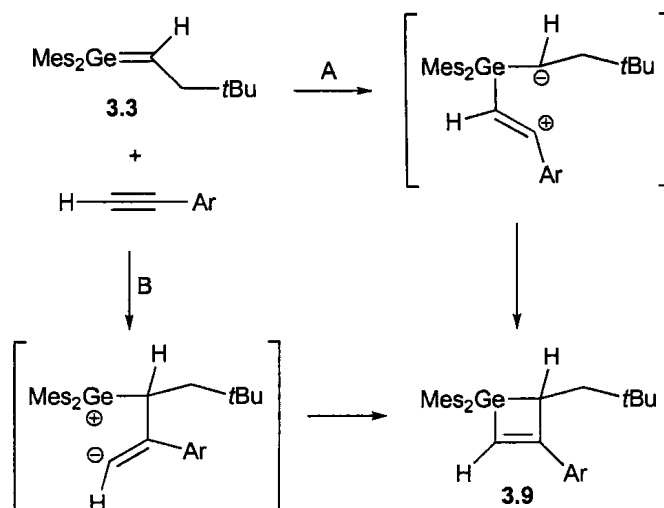
Germacyclobutenes **3.9a-c** and **3.12** are derived from cycloaddition between germene **3.3** and phenylacetylene, 1-ethynyl-4-(trifluoromethyl)benzene, 4-ethynylanisole,

or ethoxyacetylene, respectively. The aryl substituted alkynes cycloadd to **3.3** with the same orientation that is typically observed in the addition of terminal alkynes to silenes.^{14,15,16} Furthermore, the regiochemistry of germacyclobutenes **3.9a-c** is analogous to silacyclobutene **3.5**, formed in the reaction between phenylacetylene and neopentylsilene **3.2**.¹¹ Germacyclobutene **3.12**, however, has the opposite regiochemistry to **3.9a-c**. Thus, ethoxy-substituted germacyclobutene **3.12** is derived from the addition of the terminal alkynyl carbon to the germeric carbon of **3.3**, rather than to the germanium.

Whereas phenylacetylene, 1-ethynyl-4-(trifluoromethyl)benzene, 4-ethynylanisole, and ethoxyacetylene yielded cycloadducts upon reaction with germene **3.3**, trimethylsilylacetylene and *t*-butylacetylene did not. The aromatic and ethoxy substituents polarize the alkyne thereby making the carbon-carbon triple bond more reactive than that of the other alkynes. Based on reaction times, 1-ethynyl-4-(trifluoromethyl)benzene was the most reactive aromatic alkyne towards cycloaddition with **3.3**, followed by phenylacetylene and 4-ethynylanisole. Trifluoromethylbenzene is the most electron-withdrawing aryl substituent ($\sigma_p(\text{CF}_3) = 0.551$, $\sigma_p(\text{MeO}) = -0.268$),¹⁷ which would lead to the greatest polarization of the alkyne. Thus, it is apparent that a significantly polarized $\text{C}\equiv\text{C}$ triple bond is required to favour cycloaddition with germene **3.3**.

Due to the preference for cycloaddition with polarized alkynes, the formation of germacyclobutenes **3.9a-c** likely proceeds via a stepwise mechanism involving a 1,4-zwitterionic intermediate. A zwitterionic pathway was also proposed for the addition of phenylacetylene to the analogous neopentylsilene **3.2**.¹¹ Nucleophilic addition of the alkyne on the silene was thought to be the most probable pathway; the polar $\text{Si}=\text{C}$ bond

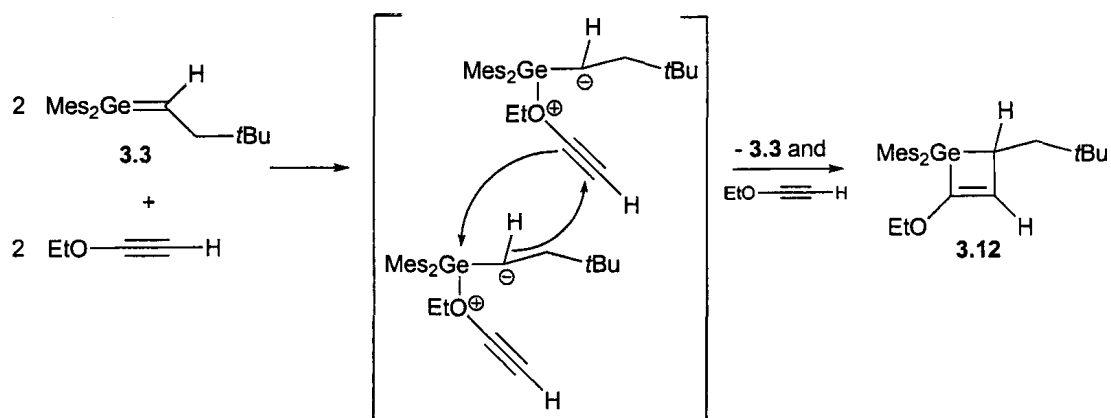
makes the silicon particularly electrophilic.^{3g} In contrast, naturally polarized germenes, such as **3.3**, are known to be much less polar, and thus, much less susceptible towards nucleophilic attack, than corresponding silenes.¹⁸ Although a comparable mechanism involving nucleophilic addition of the aromatic alkynes on germanium may be possible (Pathway A, Scheme 3.6), it is more likely that the germenic carbon of **3.3** behaves as the nucleophile (Pathway B, Scheme 3.6) since the largest portion of cycloadduct was observed with 1-ethynyl-4-(trifluoromethylbenzene), the most electron deficient aromatic alkyne.¹⁹



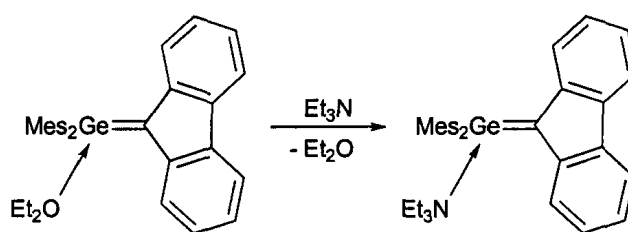
Scheme 3.6 Proposed mechanism of cycloaddition with aromatic alkynes.

A zwitterionic pathway is also likely for the addition of ethoxyacetylene to germene **3.3**; however, the structure of the intermediate must differ from either of those proposed for the addition of the aromatic alkynes, to obtain a germacyclobutene with the opposite regiochemistry. As with silene **3.2**,¹¹ the proposed intermediate is an oxonium complex where the oxygen is coordinated to the germanium of **3.3** (Scheme 3.7). The nucleophilicity of oxygen compared to the C≡C triple bond, in addition to the

oxophilicity of germanium, could promote the initial complexation of oxygen to the germanium atom of the germene. The Lewis acidity of the related naturally polarized germene, dimesitylfluorenylidene-germane, $\text{Mes}_2\text{Ge}=\text{CR}_2$, has been noted; isolable adducts with diethyl ether and triethylamine have been reported (Scheme 3.8),²⁰ and recently, evidence for complexation to THF has been obtained.²¹ This behaviour is also quite common for silenes. The THF adduct of $\text{Me}_2\text{Si}=\text{C}(\text{SiMe}_3)(\text{SiMe}_t\text{Bu}_2)$, a very polar silene, has been synthesized and characterized by X-ray crystallography.²² Given the precedent for oxygen coordination, the initial formation of a complex between ethoxyacetylene and germene **3.3** is quite probable. After complexation, ring formation likely occurs via nucleophilic attack of the germeric carbon on the terminal alkynyl carbon of a second ethoxyacetylene-germene complex followed by attack of the substituted alkynyl carbon on germanium, thereby forming germacyclobutene **3.12** and releasing an equivalent of ethoxyacetylene and **3.3** (Scheme 3.7). An intramolecular cyclization was also considered; however, this type of ring closure seems unlikely due to the geometry of the complex. The proposed mechanism, beginning with the formation of an oxonium complex, would lead to a germacyclobutene with the opposite regiochemistry compared to the aryl-substituted germacyclobutenes **3.9a-c**.



Scheme 3.7 Proposed mechanism of cycloaddition with ethoxyacetylene.



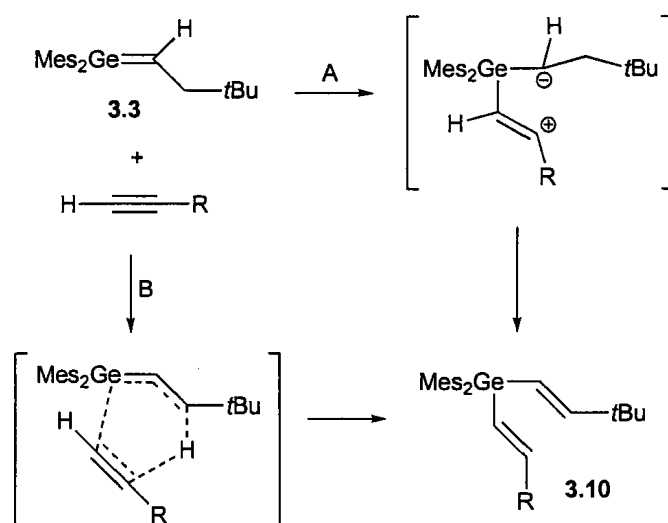
Scheme 3.8 Lewis acid-base complexes of $\text{Mes}_2\text{Ge}=\text{CR}_2$.

3.4.2 Ene-Addition

Vinylgermanes **3.10a-d** are the formal ene-addition products from germene **3.3** and phenylacetylene, 1-ethynyl-4-(trifluoromethyl)benzene, 4-ethynylanisole, or trimethylsilylacetylene, respectively. The alkyne acts exclusively as the enophile and germene **3.3** as the ene-component. Similar reactivity has previously been observed between **3.3** and non-enolizable aldehydes and ketones.²³ In contrast, germene **3.3** has been reported to act exclusively as the enophile upon addition of enolizable aldehydes and ketones.²³ Thus, the addition of terminal alkynes with an α -H may lead to different behaviour of the germene. Interestingly, the ene-addition pathway predominates over cycloaddition in the reaction between germene **3.3** and carbonyl compounds as it does in

the reaction between **3.3** and terminal alkynes. Although, the alkynes are undoubtedly poorer enophiles compared to carbonyl compounds, which evidently allows cycloaddition to compete to some extent with ene-addition.

Mechanistically, either a concerted ene-addition or a [1,6]-hydride shift from a 1,4-zwitterionic intermediate could lead to vinylgermanes **3.10a-d** (Scheme 3.9); however, given that the necessary 1,4-zwitterionic intermediate was deemed unlikely (*cf.* section 3.4.1), a concerted pathway seems more probable. Interestingly, the same relative regiochemistry was observed in **3.10a-c** as in the aryl-substituted germacyclobutenes **3.9a-c**. Ene-addition was not observed upon reaction of germene **3.3** with *t*-butylacetylene; evidently, the alkyne is too electron rich to function as a viable enophile.



Scheme 3.9 Proposed mechanism for vinylgermanes **3.10a-d** formation.

The formation of vinylgermane **3.13** was unexpected. This unusual adduct was derived from the reaction of ethoxyacetylene with two equivalents of germene **3.3**. An increase in the relative amount of vinylgermane **3.13** was observed with an increase in the concentration of **3.3**, which is consistent with a 2:1/germene:alkyne adduct. This type

of product was not observed in the reaction between neopentylsilene **3.2** and ethoxyacetylene; only silylacetylene **3.4g** and silacyclobutene **3.6** were formed.¹¹

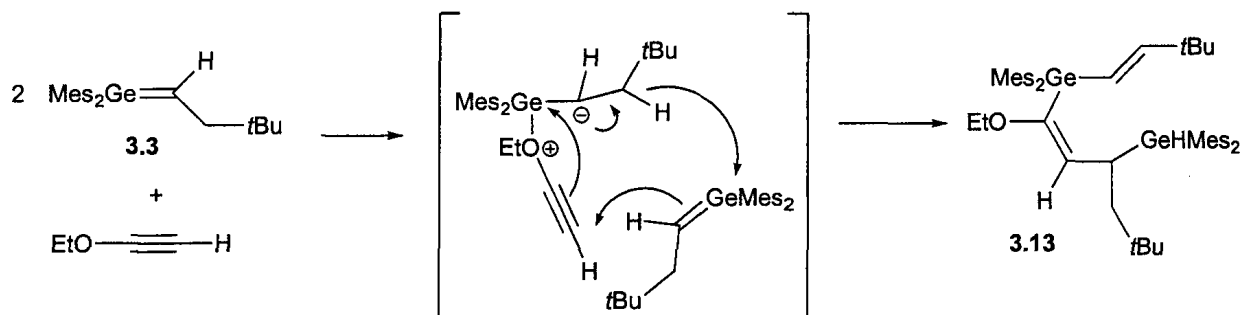
Vinylgermane **3.13** most likely arises from an ene-reaction between germene **3.3** and the ethoxyacetylene-germene zwitterionic complex, first proposed as an intermediate in the cycloaddition between **3.3** and ethoxyacetylene (Scheme 3.7). This Lewis acid-base complex must have a significant lifetime in solution to enable the formation of vinylgermane **3.13**. The persistence of similar Lewis acid-base complexes of a naturally polarized germene, $\text{Mes}_2\text{Ge}=\text{CR}_2$, with ethers was discussed previously in section 3.4.1.^{20,21,22} Since it appears as though the ethoxyacetylene-germene complex participates in the formation of both germacyclobutene **3.12** and vinylgermane **3.13**, there must be a competition between ring formation, via reaction with a second complex, and the addition of a second equivalent of germene **3.3**.

A similar ethoxyacetylene complex was also proposed with silene **3.2**,¹¹ as an intermediate in silacyclobutene **3.6** formation; however, an analogous vinylsilane was not observed. Thus, the addition of a second equivalent of silene **3.2** to the ethoxyacetylene complex must not be competitive with ring formation for the silene. Due to the greater electrophilicity of silicon, in comparison to germanium, the silene acid-base complex likely has a higher degree of zwitterionic character, which would increase the nucleophilicity of the silenic carbon. As a result, the rate of silacyclobutene formation, from nucleophilic attack of the silenic carbon on the alkyne, is likely much faster than the ene reaction with a second equivalent of silene **3.2**. Alternatively, there may not be any free silene present in solution to participate in such an ene-reaction. The equilibrium between free and complexed silene presumably lies heavily towards the complex.

In contrast, coordination of ethoxyacetylene to the less polar germene may form a weaker, less polarized, and thus, less reactive complex, which may allow the ene-reaction to be competitive with cyclization. Furthermore, the equilibrium between free and complexed germene may not favour the complex as strongly as that of the silene, and thus, free germene would be available for reaction. These explanations are consistent with germene reactivity, in general, where it has been shown that germenes are substantially less reactive toward nucleophilic reagents, such as alcohols and amines, than analogous silenes.¹⁸

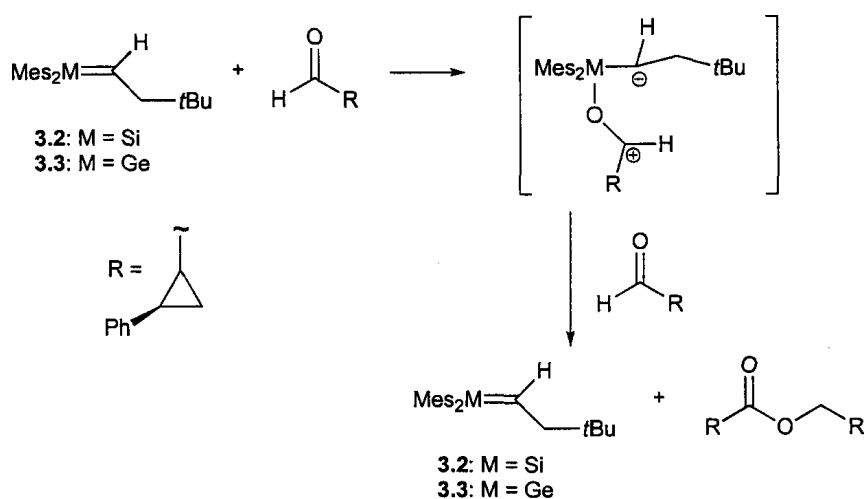
Vinylgermane **3.13** formation likely involves a stepwise ene-addition where the complex acts as the ene-component and the additional germene molecule as the enophile. Ene-addition does not occur between two molecules of germene **3.3** in the absence of ethoxyacetylene. The only reaction observed between two molecules of germene **3.3** is slow head-to-tail dimerization (days);¹² vinylgermane **3.13** formation was much faster (hours). The complexation of ethoxyacetylene increases the electron density on the germenic carbon and, apparently, promotes the observed ene-addition. The addition of nucleophiles to enhance reactivity is a common strategy in organic chemistry; however, the nucleophile usually behaves as a catalyst and is not incorporated into the product. In fact, an example of nucleophilic catalysis has been observed with germene **3.3**; the addition of an N-heterocyclic carbene promotes dimerization of the germene in 2 h.²⁴ In the formation of vinylgermane **3.13**, however, the nucleophile does not act as a catalyst. The incorporation of ethoxyacetylene into the product may be due to the presence of an accessible reactive site on the complexed molecule (a C≡C bond). Furthermore, steric

crowding may prevent the complex and germene **3.3** from approaching one another in the necessary orientation to react and subsequently release ethoxyacetylene.



Scheme 3.10 Proposed mechanism for vinylgermane **3.13** formation.

In contrast the addition of a nucleophile to activate germene **3.3**, the germene can have also act as a Lewis-acid catalyst to activate a substrate. An acid-base complex of germene **3.3** (or silene **3.2**) with *trans*-2-phenylcyclopropanecarbaldehyde was shown to react with a second equivalent of aldehyde to form an ester; the metallene was regenerated during the course of the reaction (Scheme 3.11).^{25,26} The Lewis-acid catalyzed dimerization of an aldehyde is a well-known reaction, the Tischenko reaction.²⁷



Scheme 3.11 Metallene-catalyzed aldehyde dimerization.

3.4.3 CH-insertion

Germylacetylenes **3.11a-e** are derived from addition of the acetylenic C-H bond across the Ge=C bond of germene **3.3**. Similar insertion products, silylacetylenes **3.4**, were observed when terminal alkynes were added to neopentylsilene **3.2**. The acetylenic hydrogen becomes bound to the former silenic carbon as determined by the addition of a deuterated terminal alkyne. Presumably, the acetylenic hydrogen also becomes bound to the former germeric carbon during addition of terminal alkynes to germene **3.3**. The possibility that germylacetylenes **3.11a-e** were formed by reaction of the germene precursor, an α -germyl anion, with the alkyne was considered; however, the spectroscopic evidence clearly indicated that germene **3.3** is formed *prior* to reaction with the alkyne, and thus, this possibility was ruled out.

Analogous products have been isolated from the addition of phenylacetylene to a germanimine (Ge=N) and a germaphosphene (Ge=P).^{28,29} The formation of the σ -addition products to the germaphosphene and germanimine were attributed to the highly polar nature of the double bond, i.e. $\text{Ge}^+ \text{-E}^-$ (E = N, P).

Since the polarity of the Ge=C bond of germene **3.3** is comparable to that of the Ge=P bond in a germaphosphene, it seems reasonable that the germylacetylenes **3.11a-e** are formed by the polarized germene **3.3** acting as a Bronsted base, abstracting the terminal alkynyl proton. Whether this proceeds via a stepwise or concerted pathway, however, cannot be determined at this stage.

The formation of germylacetylenes **3.11a-e** indicates that the Ge=C bond of germene **3.3** is quite polar; however, it is not as polar as the Si=C bond of silene **3.2**. The polarity plays an important role in determining pathway selectivity. Cycloaddition and

ene-addition pathways are competitive with CH-insertion in the reactions of germene **3.3** with terminal alkynes, whereas CH-insertion was the dominant reaction pathway with the more polar, and thus, more basic silene **3.2**.

3.4.4 Summary of Alkyne Addition Pathways

A mixture of products was obtained when germene **3.3** was treated with a terminal alkyne. Three modes of addition were consistently observed: cycloaddition, ene-addition, and CH-insertion. The relative amount of each type of product depended on the nature of the alkyne as well as the reaction conditions.

Cycloaddition was observed with aromatic alkynes and ethoxyacetylene, to form germacyclobutenes **3.9a-c** and **3.12**, respectively; however, different regiochemistry of addition was observed for the different types of alkynes. Two different mechanisms were proposed to account for the variation in regiochemistry; complexation of the oxygen in ethoxyacetylene to the germanium of germene **3.3** is key in directing the regiochemistry of the reaction with this substrate. There were no cycloadducts formed upon reaction of **3.3** with trimethylsilylacetylene or *t*-butylacetylene. An electron withdrawing substituent on the alkyne appears to be required to promote cycloaddition; 1-ethynyl-4-(trifluoromethylbenzene) gave the highest amount of cycloadduct with **3.3**. A stepwise, zwitterionic mechanism was proposed to account for the formation of cycloadducts with the aromatic alkynes.

Ene-addition was a prominent reaction between terminal alkynes and germene **3.3**; reaction with all of the alkynes, except *t*-butylacetylene, gave an ene-product. Reaction between **3.3** and the aromatic alkynes or trimethylsilylacetylene gave

vinylgermanes **3.10a-d**, where the germene behaved as the ene-component and the alkyne as the enophile. As with the cycloadducts, an anomalous ene-adduct was observed from the reaction with ethoxyacetylene. Again, the difference likely arises from the initial complexation of ethoxyacetylene to the germene. The germene-ethoxyacetylene complex then behaves as the ene-component and a second equivalent of germene **3.3** as the enophile. The same trend in reactivity was observed for the ene pathway that was observed for the cycloaddition pathway: a greater fraction of ene-adduct was isolated with the use of more electron deficient alkynes. Ene-addition likely proceeds via a concerted pathway; however, a stepwise, zwitterionic mechanism cannot be ruled out.

Insertion of the terminal C-H bond across the Ge=C bond on germene **3.3** was observed with the aromatic alkynes, trimethylsilylacetylene, and *t*-butylacetylene, to form germylacetylenes **3.11a-e**. There was no evidence for this mode of addition with ethoxyacetylene. The major products from the reaction of **3.3** with ethoxyacetylene seem to be derived from an initial coordination complex. Due to geometry constraints, intramolecular addition of the terminal C-H bond to the germene from the complex would be extremely difficult. An intermolecular reaction with another equivalent of alkyne could occur; however, this pathway is apparently not favoured. Unlike the cycloaddition and ene-addition pathways, the relative amount of **3.11a-e** was less dependent on the alkyne and more dependent on the reaction conditions. A greater portion of **3.11a-e** was obtained when the germene solution was added to the alkyne and when the reactions were performed on a larger scale. Also, under these conditions, a significant amount of **3.11a-e** was present immediately after mixing, followed by slow growth over the course of the reaction. Thus, the variability in the relative amount of

3.11a-e may be tied to the entropy of mixing. Presumably, the transition state for the deprotonation of a terminal alkyne does not require a high degree of order, while cycloaddition and ene-addition require a highly ordered transition state. Under mixing conditions, germylacetylene **3.11a-e** formation may be favoured over other competing pathways.

3.5 Conclusions

The variable reactivity of germene **3.3** with alkynes was in contrast to that of silene **3.2**, which consistently preferred to insert into the C-H bond of the terminal alkynes. The preference for CH-insertion was attributed to the polarity of the Si=C bond. Evidently, the Ge=C bond of germene **3.3** is less polar than the Si=C bond of silene **3.2** since CH-insertion was less prominent.

The formation of germacyclobutenes **3.9a-c** and **3.12** is best explained from zwitterionic intermediates. The nature of the zwitterionic intermediate, however, changes depending on the alkyne examined. Further study using computational methods may give us insight into the mechanistic details of alkyne addition to both polar silenes and germenes to aid in the understanding of the observed reactivity.³⁰

The reactivity of naturally polarized germene **3.3** towards terminal alkynes is very different in comparison to its silicon analogue, silene **3.2**, which, in turn, is different from the reactivity of the relatively non-polar Brook silenes. Brook silenes predominantly give cycloadducts with alkynes, while neopentyl silene **3.2** predominantly gives CH-insertion adducts. The reactivity of germene **3.3** is intermediate; both cycloadducts and CH-insertion adducts, as well as ene-adducts, were observed upon reaction with alkynes.

Unfortunately, the diverse reactivity of germene **3.3** towards alkynes makes this reaction of little use for the synthesis of organic ring systems.

3.6 Experimental

3.6.1 General Experimental Details

All reactions were performed in flame-dried Schlenk tubes, or NMR tubes sealed with a septum, under an inert atmosphere of argon. Benzene- d_6 was distilled from $LiAlH_4$, stored over 4 Å molecular sieves, and degassed prior to use. Pentane was purged with N_2 and passed through alumina prior to use. $tBuLi$ was purchased from the Aldrich Chemical Co.. 1,1-Dimesitylneopentylgermene, **3.3**,¹⁰ was prepared according to the previously reported procedures. The NMR standards used are as follows: residual C_6D_5H (7.15 ppm) for 1H NMR spectra, C_6D_6 central transition (128.0 ppm) for ^{13}C NMR spectra, and Me_4Si as an external standard, 0 ppm, for 1H - ^{29}Si gHMBC spectra. IR spectra were recorded (cm^{-1}) from thin films on a Bruker Tensor 27 FT-IR spectrometer. Electron impact mass spectra were obtained using a MAT model 8400 mass spectrometer using an ionizing voltage of 70 eV. Mass spectral data are reported in mass-to-charge units, m/z .

3.6.2 General Procedure for the Reaction of Alkynes with Germene **3.3**

A pentane solution of fluorodimesitylvinylgermane, **3.8**, (100 mg, 0.28 mmol) was converted to 1,1-dimesitylneopentylgermene, **3.3**. The pentane was removed *in vacuo* yielding a pale yellow residue. The residue was dissolved in C_6D_6 (1.1 mL). An aliquot (0.1 mL) was removed and the ratio of germene **3.3** to fluorogermene **3.8** was

determined by ^1H NMR spectroscopy. A portion of the germene solution (0.5 or 1.0 mL) was then added to an NMR tube. For reactions where the germene was added to the alkyne, the NMR tube already contained the alkyne (1.2 or 2.3 equiv) upon addition of the germene solution. For reactions where the alkyne was added to the germene, alkyne (1.2 equiv) was then added to the germene solution. The progress of the reaction was monitored by ^1H NMR spectroscopy for up to 6 days. The solvent was removed by rotary evaporation yielding a yellow residue. Polymeric material, from the uninitiated polymerization of germene **3.3**,¹² was removed from the crude product mixture by precipitation from a dichloromethane solution with acetonitrile. The ratio of products in the crude reaction mixture was determined by ^1H NMR spectroscopy. The product mixture was usually contaminated with residual alkyne and fluorogermene **3.8**. The products were separated from fluorogermene **3.8** and residual alkyne by chromatography.

3.9a: ^1H NMR (C_6D_6) δ 0.90 (s, 9 H, $\text{C}(\underline{\text{C}}\text{H}_3)_3$), 1.85 (dd, $J = 10, 14$ Hz, 1 H, CHCH_2tBu), 2.01 (dd, $J = 1.5, 15$ Hz, 1 H, CHCH_2tBu), 2.11 (s, 3 H, Mes p - $\underline{\text{C}}\text{H}_3$), 2.14 (s, 3 H, Mes p - $\underline{\text{C}}\text{H}_3$), 2.47 (s, 6 H, Mes o - $\underline{\text{C}}\text{H}_3$), 2.55 (s, 6 H, Mes o - $\underline{\text{C}}\text{H}_3$), 3.75 (d, $J = 10$ Hz, 1 H, CHCH_2tBu), 6.70 (Mes- $\underline{\text{H}}$), 6.74 (Mes- $\underline{\text{H}}$), 6.93 (s, 1 H, Ge- $\underline{\text{C}}\text{H}=\text{CPh}$), 7.10 – 7.13 (m, 1 H, Ph p - $\underline{\text{H}}$), 7.20 – 7.23 (m, 2 H, Ph m - $\underline{\text{H}}$), 7.55 – 7.56 (m, 2 H, Ph o - $\underline{\text{H}}$); ^{13}C NMR (C_6D_6) δ 20.91 – 21.04 (Mes p - $\underline{\text{C}}\text{H}_3$), 23.98 (Mes o - $\underline{\text{C}}\text{H}_3$), 25.02 (Mes o - $\underline{\text{C}}\text{H}_3$), 29.78 ($\text{C}(\underline{\text{C}}\text{H}_3)_3$), 43.07 (CHCH_2tBu), 44.35 20 (CHCH_2tBu), 126.22 (Ph o - $\underline{\text{C}}$), 127.89 (Ph p - $\underline{\text{C}}$), 128.60 (Ph m - $\underline{\text{C}}$), 128.98 (Mes m - $\underline{\text{C}}$), 129.39 (Mes m - $\underline{\text{C}}$), 133.85 (Mes i - $\underline{\text{C}}$), 137.35 (Ge- $\underline{\text{C}}\text{H}=\text{CPh}$), 137.73 (Ph i - $\underline{\text{C}}$), 138.57 (Mes i - $\underline{\text{C}}$), 142.16 (Mes o - $\underline{\text{C}}$), 144.01 (Mes o - $\underline{\text{C}}$), 158.94 (Ge- $\underline{\text{C}}\text{H}=\text{CPh}$).

3.9b: ^1H NMR (C_6D_6) δ 0.89 (s, 9 H, $\text{C}(\underline{\text{CH}}_3)_3$), 1.81 (dd, $J = 9.3, 15$ Hz, 1 H, CHCH_2tBu), 1.84 (dd, $J = 3.0, 15$ Hz, 1 H, CHCH_2tBu), 2.08 (s, 3 H, Mes $p\text{-CH}_3$), 2.13 (s, 3 H, Mes $p\text{-CH}_3$), 2.44 (s, 6 H, Mes $o\text{-CH}_3$), 2.58 (s, 6 H, Mes $o\text{-CH}_3$), 3.64 (dd, $J = 2.4, 9.6$ Hz, 1 H, CHCH_2tBu), 6.75 (s, 2 H, Mes- $\underline{\text{H}}$), 6.76 (s, 2 H, Mes- $\underline{\text{H}}$), 6.92 (s, 1 H, Ge- $\underline{\text{CH}}=\text{CAr}$), 7.33 – 7.35 (m, 2 H, Ar $o\text{-H}$), 7.40 – 7.41 (m, 2 H, Ar $m\text{-H}$); ^{13}C NMR (C_6D_6) δ 21.00 (Mes $p\text{-CH}_3$), 23.95 (Mes $o\text{-CH}_3$), 25.17 (Mes $o\text{-CH}_3$), 29.70 ($\text{C}(\underline{\text{CH}}_3)_3$), 31.08 ($\underline{\text{C}}(\text{CH}_3)_3$), 42.74 ($\underline{\text{C}}\text{HCH}_2t\text{Bu}$), 44.20 ($\text{CH}\underline{\text{C}}\text{H}_2t\text{Bu}$), 125.5 – 125.7 (Ar $m\text{-C}$), 126.31 (Ar $o\text{-C}$), 129.08 (Mes $m\text{-C}$), 129.4 – 129.6 (Ar $p\text{-C}$), 129.58 (Mes $m\text{-C}$), 133.38 (Mes $i\text{-C}$), 137.96 (Mes $i\text{-C}$), 138.55 (Mes $p\text{-C}$), 139.13 (Mes $p\text{-C}$), 140.60 (Ge- $\underline{\text{CH}}=\text{CAr}$), 140.80 (Ar $i\text{-C}$), 142.08 (Mes $o\text{-C}$), 143.89 (Mes $o\text{-C}$), 157.2 (Ge- $\underline{\text{CH}}=\text{CAr}$); ^{19}F NMR (C_6D_6) δ -62.2.

3.9c: ^1H NMR (C_6D_6) δ 0.94 (s, 9 H, $\text{C}(\underline{\text{CH}}_3)_3$), 1.89 (dd, $J = 11, 15$ Hz, 1 H, CHCH_2tBu), 1.97 (d, $J = 15$ Hz, 1 H, CHCH_2tBu), 2.49 (s, 6 H, Mes $o\text{-CH}_3$), 2.56 (s, 6 H, Mes $o\text{-CH}_3$), 3.32 (s, 3 H, OCH_3), 3.74 (d, $J = 10$ Hz, 1 H, CHCH_2tBu), 6.84 (s, 1 H, Ge- $\underline{\text{CH}}=\text{CAr}$), 6.84 – 6.85 (m, 2 H, Ar $m\text{-H}$), 7.51 – 7.53 (m, 2 H, Ar $o\text{-H}$); ^{13}C NMR (C_6D_6) δ 43.24 ($\underline{\text{C}}\text{HCH}_2t\text{Bu}$), 44.41 ($\text{CH}\underline{\text{C}}\text{H}_2t\text{Bu}$), 134.75 (Ge- $\underline{\text{CH}}=\text{CAr}$), 158.56 (Ge- $\underline{\text{CH}}=\text{CAr}$).

3.10a: colourless waxy solid, contaminated with **3.14**, and **3.16**; ^{31}P NMR (C_6D_6) δ 0.96 (s, 9 H, $\text{C}(\underline{\text{CH}}_3)_3$), 2.12 (s, 6 H, Mes $p\text{-CH}_3$), 2.43 (s, 12 H, Mes $o\text{-CH}_3$), 6.16 (d, $J = 18$ Hz, 1 H, Ge- $\underline{\text{CH}}=\underline{\text{CH}}-t\text{Bu}$), 6.41 (d, $J = 18$ Hz, 1 H, Ge- $\underline{\text{CH}}=\underline{\text{CH}}-t\text{Bu}$), 6.78 (s, 4 H, Mes- $\underline{\text{H}}$), 6.98 – 7.05 (m, 3 H, Ph $m/p\text{-H}$), 7.03 (d, $J = 18$ Hz, 1 H, Ge- $\underline{\text{CH}}=\underline{\text{CH}}\text{-Ph}$), 7.23 – 7.24 (m, 2 H, Ph $o\text{-H}$), 7.29 (d, $J = 18$ Hz, 1 H, Ge- $\underline{\text{CH}}=\underline{\text{CH}}\text{-Ph}$); ^{13}C NMR (C_6D_6) δ 21.0 (Mes $p\text{-CH}_3$), 24.86 (Mes $o\text{-CH}_3$), 29.03 ($\text{C}(\underline{\text{CH}}_3)_3$), 35.18 ($\underline{\text{C}}(\text{CH}_3)_3$), 124.26 (Ge-

$\underline{\text{C}}\text{H}=\underline{\text{C}}\text{H}-t\text{Bu}$), 126.92 (Ph *o*- $\underline{\text{C}}$), 128.0 (Ph *p*- $\underline{\text{C}}$),³² 128.76 (Ph *m*- $\underline{\text{C}}$), 129.51 (Mes *m*- $\underline{\text{C}}$), 131.60 (Ge- $\underline{\text{C}}\text{H}=\underline{\text{C}}\text{H}$ -Ph), 135.32 (Mes *i*- $\underline{\text{C}}$), 138.25 (Mes *p*- $\underline{\text{C}}$), 138.75 (Ge- $\underline{\text{C}}\text{H}=\underline{\text{C}}\text{H}$ -Ph), 142.86 (Ph *i*- $\underline{\text{C}}$), 143.50 (Mes *o*- $\underline{\text{C}}$), 156.17 (Ge- $\underline{\text{C}}\text{H}=\underline{\text{C}}\text{H}$ -*t*Bu); High-Resolution EI-MS for $\text{C}_{32}\text{H}_{40}^{70}\text{Ge}$ (M^+) m/z calcd 494.2372, found 494.2384.

3.10b: colourless waxy solid; IR cm^{-1} 797 (w), 849 (m), 992 (w), 1016 (w), 1068 (s), 1128 (s), 1166 (s), 1325 (s), 1363 (w), 1410 (w), 1467 (m), 1604 (m), 2866 (m), 2958 (s); ^1H NMR (C_6D_6) δ ^1H NMR (C_6D_6) δ 0.97 (s, 9 H, $\text{C}(\underline{\text{C}}\text{H}_3)_3$), 2.13 (s, 6 H, Mes *p*- $\underline{\text{C}}\text{H}_3$), 2.41 (s, 12 H, Mes *o*- $\underline{\text{C}}\text{H}_3$), 6.15 (d, $J = 18$ Hz, 1 H, Ge- $\underline{\text{C}}\text{H}=\underline{\text{C}}\text{H}$ -*t*Bu), 6.38 (d, $J = 18$ Hz, 1 H, Ge- $\underline{\text{C}}\text{H}=\underline{\text{C}}\text{H}$ -*t*Bu), 6.79 (s, 4 H, Mes- $\underline{\text{H}}$), 6.87 (d, $J = 19$ Hz, 1 H, Ge- $\underline{\text{C}}\text{H}=\underline{\text{C}}\text{H}$ -Ar), 6.95 – 6.96 (m, 2 H, Ar *o*- $\underline{\text{H}}$), 7.23 – 7.25 (m, 2 H, Ar *m*- $\underline{\text{H}}$), 7.28 (d, 1 H, Ge- $\underline{\text{C}}\text{H}=\underline{\text{C}}\text{H}$ -Ar, $J = 19$ Hz); ^{13}C NMR (C_6D_6) δ 20.99 (Mes *p*- $\underline{\text{C}}\text{H}_3$), 24.83 (Mes *o*- $\underline{\text{C}}\text{H}_3$), 28.99 ($\text{C}(\underline{\text{C}}\text{H}_3)_3$), 35.22 ($\underline{\text{C}}(\text{CH}_3)_3$), 123.83 (Ge- $\underline{\text{C}}\text{H}=\underline{\text{C}}\text{H}$ -*t*Bu), 124.97 (q, $J_{\text{CF}} = 270$ Hz, $\underline{\text{C}}\text{F}_3$), 125.63 (q, $J_{\text{CF}} = 4.5$ Hz, Ar *m*- $\underline{\text{C}}$), 126.96 (Ar *o*- $\underline{\text{C}}$), 129.41 (q, $J = 9.2$ Hz, Ar *p*- $\underline{\text{C}}$), 129.60 (Mes *m*- $\underline{\text{C}}$), 134.87 (Mes *i*- $\underline{\text{C}}$), 135.43 (Ge- $\underline{\text{C}}\text{H}=\underline{\text{C}}\text{H}$ -Ar), 138.53 (Mes *p*- $\underline{\text{C}}\text{H}_3$), 141.09 (Ge- $\underline{\text{C}}\text{H}=\underline{\text{C}}\text{H}$ -Ar), 141.84 (Ar *i*- $\underline{\text{C}}$), 143.44 (Mes *o*- $\underline{\text{C}}$), 156.52 (Ge- $\underline{\text{C}}\text{H}=\underline{\text{C}}\text{H}$ -*t*Bu); ^{19}F NMR (C_6D_6) δ -62.5; High-Resolution EI-MS for $\text{C}_{33}\text{H}_{39}^{74}\text{Ge}$ (M^+) m/z calcd 566.2224, found 566.2098.

3.10c: colourless waxy solid, contaminated with **3.11c**;³¹ ^1H NMR (C_6D_6) δ 0.97 (s, 9 H, $\text{C}(\underline{\text{C}}\text{H}_3)_3$), 2.13 (s, 6 H, Mes *p*- $\underline{\text{C}}\text{H}_3$), 2.46 (s, 12 H, Mes *o*- $\underline{\text{C}}\text{H}_3$), 3.22 (s, 3 H, $\text{O}\underline{\text{C}}\text{H}_3$), 6.18 (d, $J = 18$ Hz, 1 H, Ge- $\underline{\text{C}}\text{H}=\underline{\text{C}}\text{H}$ -*t*Bu), 6.43 (d, $J = 18$ Hz, 1 H, Ge- $\underline{\text{C}}\text{H}=\underline{\text{C}}\text{H}$ -*t*Bu), 6.67 – 6.69 (m, 2 H, Ar *m*- $\underline{\text{H}}$), 6.79 (s, 4 H, Mes- $\underline{\text{H}}$), 7.03 (d, $J = 19$ Hz, 1 H, Ge- $\underline{\text{C}}\text{H}=\underline{\text{C}}\text{H}$ -Ar), 7.15 (d, $J = 19$ Hz, 1 H, Ge- $\underline{\text{C}}\text{H}=\underline{\text{C}}\text{H}$ -Ar), 7.21 – 7.23 (m, 2 H, Ar *o*- $\underline{\text{H}}$); ^{13}C NMR (C_6D_6) δ 21.01 (Mes *p*- $\underline{\text{C}}\text{H}_3$), 24.88 (Mes *o*- $\underline{\text{C}}\text{H}_3$), 29.07 ($\text{C}(\underline{\text{C}}\text{H}_3)_3$), 35.16 ($\underline{\text{C}}(\text{CH}_3)_3$),

54.70 (OCH_3), 114.25 (Ar $m\text{-C}$), 124.56 (Ge- $\text{CH}=\text{CH}\text{-}t\text{Bu}$), 128.65 (Ge- $\text{CH}=\text{CH}\text{-Ar}$), 129.29 (Ar $o\text{-C}$), 129.51 (Mes $m\text{-C}$), 131.80 (Ar $i\text{-C}$), 135.56 (Mes $i\text{-C}$), 138.18 (Mes $p\text{-C}$), 142.41 (Ge- $\text{CH}=\text{CH}\text{-Ar}$), 143.55 (Mes $o\text{-C}$), 156.06 (Ge- $\text{CH}=\text{CH}\text{-}t\text{Bu}$), 160.08 (Ar $p\text{-C}$); High-Resolution EI-MS for $\text{C}_{33}\text{H}_{42}^{74}\text{GeO}$ (M^+) m/z calcd 528.2455, found 528.2458.

3.11a: colourless waxy solid; IR cm^{-1} 691 (s), 756 (s), 809 (m), 848 (s), 885 (w), 1026 (s), 1215 (m), 1243 (m), 1263 (m), 1290 (w), 1363 (m), 1410 (m), 1447 (s), 1467 (s), 1556 (m), 1603 (s), 2155 (m, $\text{C}\equiv\text{C}$), 2865 (m), 2956 (s); ^1H NMR (C_6D_6) δ 0.88 (s, 9 H, $\text{C}(\text{CH}_3)_3$), 1.76 (s, 4 H, $\text{GeCH}_2\text{CH}_2t\text{Bu}$), 2.09 (s, 6 H, Mes $p\text{-CH}_3$), 2.60 (s, 12 H, Mes $o\text{-CH}_3$), 6.74 (s, 4 H, Mes- H), 6.89 – 6.92 (m, 3 H, Ph $m/p\text{-H}$), 7.40 – 7.43 (m, 2 H, Ph $o\text{-H}$); ^{13}C NMR (C_6D_6) δ 18.42 (GeCH_2), 20.95 (Mes $p\text{-CH}_3$), 24.21 (Mes $o\text{-CH}_3$), 29.00 ($\text{C}(\text{CH}_3)_3$), 31.34 ($\text{C}(\text{CH}_3)_3$), 39.91 (CH_2tBu), 96.77 (Ge- $\text{C}\equiv\text{C}\text{-Ph}$), 106.45 (Ge- $\text{C}\equiv\text{C}\text{-Ph}$), 124.50 (Ph $i\text{-C}$), 128.20 (Ph $p\text{-C}$), 128.44 (Ph $m\text{-C}$), 129.70 (Mes $m\text{-C}$), 131.877 (Ph $o\text{-C}$), 134.59 (Mes $i\text{-C}$), 138.48 (Mes $p\text{-C}$), 143.24 (Mes $o\text{-C}$); High-Resolution EI-MS for $\text{C}_{32}\text{H}_{40}^{70}\text{Ge}$ (M^+) m/z calcd 494.2373, 494.2369.

3.11b: colourless waxy solid; IR cm^{-1} 703 (m), 740 (m), 843 (s), 885 (w), 1017 (m), 1067 (s), 1105 (m), 1130 (s), 1167 (s), 1220 (w), 1263 (w), 1322 (s), 1364 (m), 1405 (m), 1468 (m), 1556 (w), 1614 (m), 2157 (w, $\text{C}\equiv\text{C}$), 2866 (m), 2957 (s); ^1H NMR (C_6D_6) δ 0.89 (s, 9 H, $\text{C}(\text{CH}_3)_3$), 1.71 – 1.74 (XX' portion of an AA'XX' spin system, 2 H, CH_2tBu), 1.75 – 1.78 (AA' portion of an AA'XX' spin system, 2 H, GeCH_2), 2.10 (s, 6 H, Mes $p\text{-CH}_3$), 2.57 (s, 12 H, Mes $o\text{-CH}_3$), 6.75 (s, 4 H, Mes- H), 7.06 – 7.08 (m, 2 H, Ar $m\text{-H}$), 7.15 – 7.17 (m, 2 H, Ar $o\text{-H}$); ^{13}C NMR (C_6D_6) δ 18.38 (GeCH_2), 20.93 (Mes $p\text{-CH}_3$), 24.18 (Mes $o\text{-CH}_3$), 28.98 ($\text{C}(\text{CH}_3)_3$), 31.34 ($\text{C}(\text{CH}_3)_3$), 39.94 (CH_2tBu), 100.15 (Ge- $\text{C}\equiv\text{C}\text{-Ar}$), 104.77 (Ge- $\text{C}\equiv\text{C}\text{-Ar}$), 124.57 (q, $J_{\text{CF}} = 270$ Hz, Ar- CF_3), 125.33 (q, $J_{\text{CF}} = 3.5$ Hz, Ar $m\text{-}$

$\underline{\text{C}}$), 127.88 (Ar i - $\underline{\text{C}}$), 129.75 (q, $J_{\text{CF}} = 32$ Hz, Ar p - $\underline{\text{C}}$), 129.78 (Mes m - $\underline{\text{C}}$), 131.98 (Ar o - $\underline{\text{C}}$), 134.17 (Mes i - $\underline{\text{C}}$), 138.75 (Mes p - $\underline{\text{C}}$), 143.15 (Mes o - $\underline{\text{C}}$); High-Resolution EI-MS for $\text{C}_{33}\text{H}_{39}\text{F}_3$ ^{70}Ge (M^+) m/z calcd 562.2246, 562.2235.

3.11c: colourless waxy solid, contaminated with **3.10c**; IR cm^{-1} 2153 (w, $\text{C}\equiv\text{C}$); ^1H NMR (C_6D_6) δ 0.89 (s, 9 H, $\text{C}(\underline{\text{C}}\text{H}_3)_3$), 1.78 (s, 4 H, $\text{Ge}\underline{\text{C}}\text{H}_2\underline{\text{C}}\text{H}_2t\text{Bu}$), 2.10 (s, 6 H, Mes p - $\underline{\text{C}}\text{H}_3$), 2.62 (s, 12 H, Mes o - $\underline{\text{C}}\text{H}_3$), 3.11 (s, 3 H, Ar- $\text{O}\underline{\text{C}}\text{H}_3$), 6.51 – 6.53 (m, 2 H, Ar m - $\underline{\text{H}}$), 6.75 (s, 4 H, Mes- $\underline{\text{H}}$), 7.38 – 7.40 (m, 2 H, Ar o - $\underline{\text{H}}$); ^{13}C NMR (C_6D_6) δ 18.49 ($\text{Ge}\underline{\text{C}}\text{H}_2$), 20.94 (Mes p - $\underline{\text{C}}\text{H}_3$), 24.23 (Mes o - $\underline{\text{C}}\text{H}_3$), 29.02 ($\text{C}(\underline{\text{C}}\text{H}_3)_3$), 31.35 ($\underline{\text{C}}(\text{CH}_3)_3$), 39.93 ($\underline{\text{C}}\text{H}_2t\text{Bu}$), 54.62 ($\text{O}\underline{\text{C}}\text{H}_3$), 94.82 ($\text{Ge}-\underline{\text{C}}\equiv\text{C}-\text{Ar}$), 106.57 ($\text{Ge}-\underline{\text{C}}\equiv\text{C}-\text{Ar}$), 114.19 (Ar m - $\underline{\text{C}}$), 116.72 (Ar i - $\underline{\text{C}}$), 129.69 (Mes m - $\underline{\text{C}}$), 133.36 (Ar o - $\underline{\text{C}}$), 134.82 (Mes i - $\underline{\text{C}}$), 138.40 (Mes p - $\underline{\text{C}}$), 143.28 (Mes o - $\underline{\text{C}}$), 159.96 (Ar p - $\underline{\text{C}}$); High-Resolution EI-MS for $\text{C}_{33}\text{H}_{42}$ ^{74}GeO (M^+) m/z calcd 528.2455, found 528.2458.

3.11d: colourless oil, contaminated with minor amounts of **3.14** and **3.16**; IR cm^{-1} 2089 (w, $\text{C}\equiv\text{C}$); ^1H NMR (C_6D_6) δ 0.14 (s, 9 H, $\text{Si}(\underline{\text{C}}\text{H}_3)_3$), 0.89 (s, 9 H, $\text{C}(\underline{\text{C}}\text{H}_3)_3$), 1.66 – 1.69 (XX' portion of an AA'XX' spin system, 2 H, $\text{Ge}\underline{\text{C}}\text{H}_2$), 1.70 – 1.74 (AA' portion of an AA'XX' spin system, 2 H, $\underline{\text{C}}\text{H}_2t\text{Bu}$), 2.07 (s, 6 H, Mes p - $\underline{\text{C}}\text{H}_3$), 2.55 (s, 12 H, Mes o - $\underline{\text{C}}\text{H}_3$), 6.71 (s, 4 H, Mes- $\underline{\text{H}}$); ^{13}C NMR (C_6D_6) δ -0.20 ($\text{Si}(\underline{\text{C}}\text{H}_3)_3$), 18.29 ($\text{Ge}\underline{\text{C}}\text{H}_2$), 20.91 (Mes p - $\underline{\text{C}}\text{H}_3$), 24.20 (Mes o - $\underline{\text{C}}\text{H}_3$), 29.00 ($\text{C}(\underline{\text{C}}\text{H}_3)_3$), 31.28 ($\underline{\text{C}}(\text{CH}_3)_3$), 39.83 ($\underline{\text{C}}\text{H}_2t\text{Bu}$), 114.54 ($\text{Ge}-\underline{\text{C}}\equiv\text{C}-\text{SiMe}_3$), 116.60 ($\text{Ge}-\underline{\text{C}}\equiv\text{C}-\text{SiMe}_3$), 129.66 (Mes m - $\underline{\text{C}}$), 134.45 (Mes i - $\underline{\text{C}}$), 138.44 (Mes p - $\underline{\text{C}}$), 143.23 (Mes o - $\underline{\text{C}}$); High-Resolution EI-MS for $\text{C}_{29}\text{H}_{44}$ $^{74}\text{GeSi}$ (M^+) m/z calcd 494.2428, found 494.2403.

3.11e: colourless oil, contaminated with minor amounts of **3.14** and **3.16**; IR cm^{-1} 2148 – 2181 (w, $\text{C}\equiv\text{C}$); ^1H NMR (C_6D_6) δ 0.91 (s, 9 H, $\text{CH}_2-\text{C}(\underline{\text{C}}\text{H}_3)_3$), 1.16 (s, 9 H, $\text{C}\equiv\text{C}$ -

C(CH₃)₃), 1.64 – 1.67 (XX' portion of an AA'XX' spin system, 2 H, GeCH₂), 1.69 – 1.73 (AA' portion of an AA'XX' spin system, 2 H, CH₂*t*Bu), 2.08 (s, 6 H, Mes *p*-CH₃), 2.56 (s, 12 H, Mes *o*-CH₃), 6.73 (s, 4 H, Mes-H); ¹³C NMR (C₆D₆) δ 18.40 (GeCH₂), 20.93 (Mes *p*-CH₃), 24.18 (Mes *o*-CH₃), 28.56 (C≡C-C(CH₃)₃), 29.07 (CH₂-C(CH₃)₃), 30.77 (C≡C-C(CH₃)₃), 31.30 (CH₂-C(CH₃)₃), 39.91 (CH₂*t*Bu), 84.08 (Ge-C≡C-*t*Bu), 115.78 (Ge-C≡C-*t*Bu), 129.62 (Mes *m*-C), 135.07 (Mes *i*-C), 138.22 (Mes *p*-C), 143.25 (Mes *o*-C); High-Resolution EI-MS for C₃₀H₄₄⁷⁴Ge (M⁺) *m/z* calcd 478.2661, found 478.2644.

3.12: colourless oil, contaminated with **3.13**; ³¹P NMR (C₆D₆) δ 0.96 (s, 9 H, C(CH₃)₃), 1.08 (t, *J* = 7.2 Hz, 3 H, OCH₂CH₃), 1.47 (dd, *J* = 10, 14 Hz, 1 H, CHCH₂*t*Bu), 1.82 (dd, *J* = 3, 14 Hz, 1 H, CHCH₂*t*Bu), 2.07 (s, 3 H, Mes *p*-CH₃), 2.08 (s, 3 H, Mes *p*-CH₃), 2.57 (s, 6 H, Mes *o*-CH₃), 2.60 (s, 6 H, Mes *o*-CH₃), 2.99 (ddd, *J* = 2.4, 3.0, 10 Hz, 1 H, CHCH₂*t*Bu), 3.55 – 3.63 (m, 2 H, OCH₂CH₃), 5.81 (d, *J* = 1.8 Hz, 1 H, CH=C(OEt)), 6.71 (s, 2 H, Mes-H), 6.75 (s, 2 H, Mes-H); ¹³C NMR (C₆D₆) δ 14.54 (OCH₂CH₃), 20.96 – 20.98 (Mes *p*-CH₃), 24.85 (Mes *o*-CH₃), 25.63 (Mes *o*-CH₃), 29.98 (C(CH₃)₃), 32.25 (C(CH₃)₃), 32.57 (CHCH₂*t*Bu), 48.00 (CHCH₂*t*Bu), 64.50 (OCH₂CH₃), 116.33 (CH=C(OEt)), 128.92 (Mes *m*-C), 129.16 (Mes *m*-C), 134.82 (Mes *i*-C), 136.71 (Mes *i*-C), 138.20 – 138.65 (Mes *p*-C), 142.83 (Mes *o*-C), 143.28 (Mes *o*-C), 164.95 (CH=C(OEt)); High-Resolution EI-MS for C₂₈H₄₀⁷⁴GeO (M⁺) *m/z* calcd 466.2295, found 466.2310.

3.13: colourless oil, contaminated with a minor amount of **3.12**; IR cm⁻¹ 693 (m), 741 (m), 800 (s), 848 (s), 1080 (m), 1260 (s), 1362 (m), 1409 (m), 1450 (s), 1556 (m), 1603 (s), 2732 (w), 2864 (m), 2957 (s); ¹H NMR (C₆D₆) δ 0.90 (s, 9 H, C(CH₃)₃), 0.99 (s, 9 H, C(CH₃)₃), 1.16 (t, *J* = 6.9 Hz, 3 H, OCH₂CH₃), 1.59 (dd, *J* = 11, 14 Hz, 1 H,

CHCH₂*t*Bu), 1.77 (dd, $J = 1.2, 14$ Hz, 1 H, CHCH₂*t*Bu), 2.10 (s, 3 H, Mes *p*-CH₃), 2.11 (s, 3 H, Mes *p*-CH₃), 2.12 (s, 3 H, Mes *p*-CH₃), 2.14 (s, 3 H, Mes *p*-CH₃), 2.37 (s, 6 H, Mes *o*-CH₃), 2.43 (s, 6 H, Mes *o*-CH₃), 2.46 (s, 6 H, Mes *o*-CH₃), 2.49 (s, 6 H, Mes *o*-CH₃), 3.66 (dq, $J = 6.9, 9.3$ Hz, 1 H, OCH₂CH₃), 3.92 (dq, $J = 6.9, 9.3$ Hz, 1 H, OCH₂CH₃), 3.98 (dddd, $J = 1.2, 3.6, 10, 11$ Hz, 1 H, CHCH₂*t*Bu), 5.41 (d, $J = 10$ Hz, 1 H, CH=C(OEt)), 5.53 (d, $J = 3.6$ Hz, 1 H, Ge-H), 5.94 (d, $J = 19$ Hz, 1 H, Ge-CH=CH-*t*Bu), 6.27 (d, $J = 19$ Hz, 1 H, Ge-CH=CH-*t*Bu), 6.76 (s, 2 H, Mes-H), 6.77 (s, 2 H, Mes-H), 6.78 (s, 4 H, Mes-H); ¹³C NMR (C₆D₆) δ 15.96 (OCH₂CH₃), 20.96 (Mes *p*-CH₃), 20.98 (Mes *p*-CH₃), 21.08 (Mes *p*-CH₃), 24.41 (Mes *o*-CH₃), 24.53 (Mes *o*-CH₃), 24.97 (Mes *o*-CH₃), 26.53 (CHCH₂), 28.75 (C(CH₃)₃), 30.24 (C(CH₃)₃), 32.57 (C(CH₃)₃), 34.96 (C(CH₃)₃), 46.98 (CHCH₂*t*Bu), 67.56 (OCH₂CH₃), 126.59 (Ge-CH=CH-*t*Bu), 129.08 (Mes *m*-C), 129.16 (Mes *m*-C), 129.50 (Mes *m*-C), 129.55 (Mes *m*-C), 130.42 (CH=C(OEt)), 135.00 (Mes *i*-C), 135.42 (Mes *i*-C), 135.93 (Mes *i*-C), 135.98 (Mes *i*-C), 137.98 (Mes *p*-C), 138.01 (Mes *p*-C), 138.10 (Mes *p*-C), 143.62 (Mes *o*-C), 143.65 (Mes *o*-C), 143.79 (Mes *o*-C), 143.81 (Mes *o*-C), 154.81 (Ge-CH=CH-*t*Bu), 156.36 (CH=C(OEt)); High-Resolution ES TOF-MS for C₅₂H₇₃O⁷⁰Ge⁷²Ge (M⁺) m/z calcd 855.4116, found 855.4125.

3.6.3 General Reaction of Germacyclobutenes 3.9a-c with Sodium Hydroxide

Excess sodium hydroxide solution (5 mL, 15%) was added to the crude product mixture from the addition of aromatic alkyne to germene 3.3 consisting of germacyclobutene 3.9a, b, or c, along with vinylgermane 3.10a, b, or c, germylacetylene 3.11a, b, or c, and fluorovinylgermane 3.8 (~40 mg), dissolved in THF (5 mL). The

solution was refluxed for 18 h. The mixture was extracted with diethyl ether. The organic layer was dried over MgSO₄ and filtered. The solvents were removed under vacuum to yield a light yellow oil (~35 mg), which was purified by preparative thin-layer chromatography (9:1/hexanes:EtOAc). Compounds **3.17a-c** were isolated as colourless oils (2 – 5 mg).

3.17a: colourless oil; IR cm⁻¹ 645 (m), 702 (m), 763 (w), 848 (m), 912 (w), 1027 (w), 1264(w), 1364 (w), 1377 (w), 1409 (w), 1451 (m), 1557 (w), 1603 (m), 1727 (m), 2865 (m), 2927 (s), 2955 (s), 3300 – 3600 (br w, OH); ¹H NMR (C₆D₆) δ 0.78 (s, 9 H, C(CH₃)₃), 1.96 (d, *J* = 7.2 Hz, 2 H, C=CH-CH₂), 2.09 (s, 6 H, Mes *p*-CH₃), 2.38 (s, 12 H, Mes *o*-CH₃), 2.87 (s, 2 H, GeCH₂), 5.60 (t, *J* = 7.5 Hz, 1 H, C=CH-CH₂), 6.66 (s, 4 H, Mes-H), 6.96 – 6.98 (m, 1 H, Ph-H), 7.02 – 7.05 (m, 4 H, Ph-H); ¹³C NMR (C₆D₆) δ 20.94 (Mes *p*-CH₃), 23.55 (Mes *o*-CH₃), 29.39 (C(CH₃)₃), 31.21 (C(CH₃)₃), 32.85 (GeCH₂), 43.23 (CH₂*t*Bu), 125.29 (C=CH-CH₂*t*Bu), 126.56 (Ph *p*-C), 127.89 (Ph *m*-C), 129.05 (Ph *o*-C), 129.45 (Mes *m*-C), 136.42 (Mes *i*-C), 138.32 (C=CH-CH₂*t*Bu), 138.67 (Mes *p*-C), 142.32 (Ph *i*-C), 143.01 (Mes *o*-C).

3.17b: colourless oil; IR cm⁻¹ 848 (m), 1018 (w), 1070 (m), 1125 (m), 1164 (m), 1325 (s), 1452 (w), 1603 (w), 1734 (w), 2868 (m), 2957 (s), 3300 – 3600 (br w, OH); ¹H NMR (C₆D₆) δ 0.79 (s, 9 H, C(CH₃)₃), 1.88 (d, *J* = 7.2 Hz, 2 H, C=CH-CH₂), 2.08 (s, 6 H, Mes *p*-CH₃), 2.31 (s, 12 H, Mes *o*-CH₃), 2.74 (s, 2 H, GeCH₂), 5.65 (t, *J* = 7.2 Hz, 1 H, C=CH-CH₂), 6.60 (Mes-H), 6.84 – 6.86 (m, 2 H, Ar-H), 7.16 – 7.18 (m, 2 H, Ar-H); ¹³C NMR (C₆D₆) δ 20.85 (Mes *p*-CH₃), 23.47 (Mes *o*-CH₃), 29.36 (C(CH₃)₃), 31.29 (C(CH₃)₃), 36.33 (GeCH₂), 43.11 (CH₂*t*Bu), 124.57 (q, *J*_{CF} = 3.5 Hz, Ar *m*-C), 125.1³² (q, *J* = 270 Hz, CF₃), 126.31 (C=CH-CH₂*t*Bu), 128.42 (Ar *p*-C), 129.31 (Ar *o*-C), 129.47

(Mes *m*-C), 136.04 (Mes *i*-C), 137.22 (C=CH-CH₂*t*Bu), 138.95 (Mes *p*-C), 142.77 (Mes *o*-C), 145.58 (Ar *i*-C).

3.17c: colourless oil, contaminated with **3.11c** and Mes₂Ge(OH)CH₂CH₂*t*Bu; IR cm⁻¹ 3100 – 3600 (br w, OH); ¹H NMR (C₆D₆) δ 0.82 (s, 9 H, C(CH₃)₃), 2.00 (d, *J* = 7.8 Hz, 2 H, C=CH-CH₂), 2.09 (s, 6 H, Mes *p*-CH₃), 2.40 (s, 12 H, Mes *o*-CH₃), 2.88 (s, 2 H, GeCH₂), 3.27 (OCH₃), 5.58 (t, *J* = 7.2 Hz, 1 H, C=CH-CH₂), 6.64 – 6.66 (m, 2 H, Ar-H), 6.66 (Mes-H), 6.96 – 6.98 (m, 2 H, Ar-H).

3.7 References

1. (a) Brook, A. G.; Abdesaken, F.; Gutekunst, B.; Gutekunst, G.; Kallury, R. K. M. R. *J. Chem. Soc., Chem. Commun.* **1981**, 191; (b) Brook, A. G.; Nyburg, S. C.; Abdesaken, F.; Gutekunst, B.; Gutekunst, G.; Kallury, R. K. M. R.; Poon, Y. C.; Chang, Y. M.; Wong-Na, W. *J. Am. Chem. Soc.* **1982**, *104*, 5667.
2. West, R.; Fink, M. J.; Michl, J. *Science* **1981**, *214*, 1343.
3. For reviews on silenes see: (a) Gusel'nikov, L. E.; Nametkin, N. S. *Chem. Rev.* **1979**, *79*, 529; (b) Raabe, G.; Michl, J. *Chem. Rev.* **1985**, *85*, 419; (c) Brook, A. G.; Baines, K. M. *Adv. Organomet. Chem.* **1986**, *25*, 1; (d) Brook, A. G.; Brook, M. A. *Adv. Organomet. Chem.* **1996**, *39*, 71; (e) Müller, T.; Ziche, W.; Auner, N. *The Chemistry of Organic Silicon Compounds*; Rappoport, Z.; Apeloig, Y., Eds.; Wiley & Sons: New York, 1998; Vol. 2, Chapter 16; (f) Morkin, T. L.; Owens, T. R.; Leigh, W. J. *The Chemistry of Organic Silicon Compounds*; Rappoport, Z.; Apeloig, Y., Eds.; Wiley & Sons: New York, 2001; Vol. 3, Chapter 17; (g) Ottosson, H.; Eklöf, A. M. *Coord. Chem. Rev.* **2008**, *252*, 1287.
4. For reviews on multiply bonded species containing Ge, Sn, and Pb see: (a) Power, P. P.; *Chem. Rev.* **1999**, *99*, 3463; (b) Tokitoh, N.; Okazaki, R. *Adv. Organomet. Chem.* **2001**, *47*, 121; (c) Tokitoh, N.; Okazaki, R. Rappoport, Z. *The Chemistry of Organic*

Germanium, Tin and Lead Compounds; Rappoport, Z., Eds.; Wiley & Sons: New York, 2002; Vol. 2, Part 1, pp 843 – 901.

5. For reviews on germenes see: (a) Wiberg, N. *J. Organomet. Chem.* **1984**, *273*, 141; (b) Barrau, J.; Escudié, J.; Satgé, J. *Chem Rev.* **1990**, *90*, 283; (c) Escudie, J.; Couret, C.; Ranaivonjatovo, J. *Coord. Chem. Rev.* **1998**, *180*, 565.

6. Ottoson, H.; Steel, P. G. *Chem. Eur. J.* **2006**, *12*, 1576.

7. (a) Milnes, K. K.; Jennings, M. C.; Baines, K. M. *J. Am. Chem. Soc.* **2006**, *128*, 2491; (b) Milnes, K. K.; Baines, K. M. *Can. J. Chem.* **2009**, *87*, 307.

8 (a) Milnes, K. K.; Gottschling, S. E.; Baines, K. M. *Org. Biomol. Chem.* **2004**, *2*, 3530; (b) Gottschling, S. E.; Grant, T. N.; Milnes, K. K.; Jennings, M. C.; Baines, K. M. *J. Org. Chem.* **2005**, *70*, 2686.

9. (a) Delpon-Lacaze, G.; Couret, C. *J. Organomet. Chem.* **1994**, *480*, C14; (b) Delpon-Lacaze, G.; de Battisti, C.; Couret, C. *J. Organomet. Chem.* **1996**, *514*, 59.

10. Couret, C.; Escudié, J.; Delpon-Lacaze, G.; Satgé, J. *Organometallics*, **1992**, *11*, 3176.

11. Milnes, K. K.; Pavelka, L. C.; Baines, K. M. *manuscript in preparation*.

12. Pavelka, L. C.; Holder, S. J.; Baines, K. M. *Chem. Commun.* **2008**, 2346.

13. Mohseni-Ala, J.; Auner, N. *Inorg. Chim. Acta* **2006**, *359*, 4677.

14. Conlin, R. T.; Kwak, Y.-W.; Huffaker, H. B. *Organometallics* **1983**, *2*, 343.

15. Apeloig, Y.; Bravo-Zhivotovskii, D.; Zharov, I.; Panov, V.; Leigh, W. J.; Sluggett, G. *W. J. Am. Chem. Soc.* **1998**, *120*, 1398.

16. (a) Brook, A. G.; Harris, J. W.; Lennon, J.; El Sheikh, M. *J. Am. Chem. Soc.* **1979**, *101*, 83; (b) Brook, A. G.; Baumegger, A.; Lough, A. J. *Organometallics* **1992**, *11*, 3088; (c) Lassacher, P.; Brook, A. G.; Lough, A. J. *Organometallics* **1995**, *14*, 4359.

17. Jaffé, H. H. *Chem. Rev.* **1953**, *53*, 191.
18. (a) Toltl, N. P.; Leigh, W. J. *J. Am. Chem. Soc.* **1998**, *120*, 1172; (b) Leigh, W. J. *Pure Appl. Chem.* **1999**, *71*, 453; (c) Leigh, W. J.; Potter, G. D.; Huck, L. A.; Bhattacharya, A. *Organometallics* **2008**, *27*, 5948.
19. Although cycloadduct were only observed with polarized alkynes and a zwitterionic pathway seems most probable, a diradical pathway cannot be ruled out.
20. (a) Couret, C.; Escudié, J.; Satgé, J.; Lazraq, M. *J. Am. Chem. Soc.* **1987**, *109*, 4411; (b) Lazraq, M.; Escudié, J.; Couret, C.; Satgé, J. *Angew. Chem. Int. Ed.* **1988**, *27*, 828.
21. Allan, C. J.; Pavelka, L. C.; Baines, K. M. *manuscript in preparation*.
22. (a) Wiberg, N.; Wagner, G.; Müller, G.; Riede, J. *J. Organomet. Chem.* **1984**, *271*, 381; (b) Wiberg, N.; Wagner, G.; Müller, G. *Angew. Chem. Int. Ed. Engl.* **1985**, *24*, 229; (c) Wiberg, N.; Wagner, G.; Reber, G.; Riede, J.; Müller, G. *Organometallics* **1987**, *6*, 35.
23. Delpon-Lacaze, G.; Couret, C.; Escudié, J.; Satgé, J. *Main Group Metal Chemistry* **1993**, *16*, 419.
24. Rugar, P. A. PhD Thesis, UWO, 2009.
25. Milnes, K. K.; Baines, K. M. *Organometallics* **2007**, *26*, 2392.
26. Pavelka, L. C.; Baines, K. M. *Unpublished results*.
27. Seki, T.; Nakajo, T.; Onaka, M. *Chem. Lett.* **2006**, *35*, 824.
28. (a) Rivière-Baudet, M.; Khallaayoun, A.; Satgé, J. *J. Organomet. Chem.* **1993**, *462*, 89. (b) Rivière-Baudet, M.; Khallaayoun, A.; Satgé, J. *Organometallics* **1993**, *12*, 1003.
29. Escudié, J.; Couret, C.; Andrianarison, M.; Satgé, J. *J. Am. Chem. Soc.* **1987**, *109*, 386.
30. For information on the computational study see Chapter 4 of this thesis.

31. IR data is not listed due to the inability to obtain a sample in high purity (> 95 %).

32. Chemical shift estimated from gHMBC.

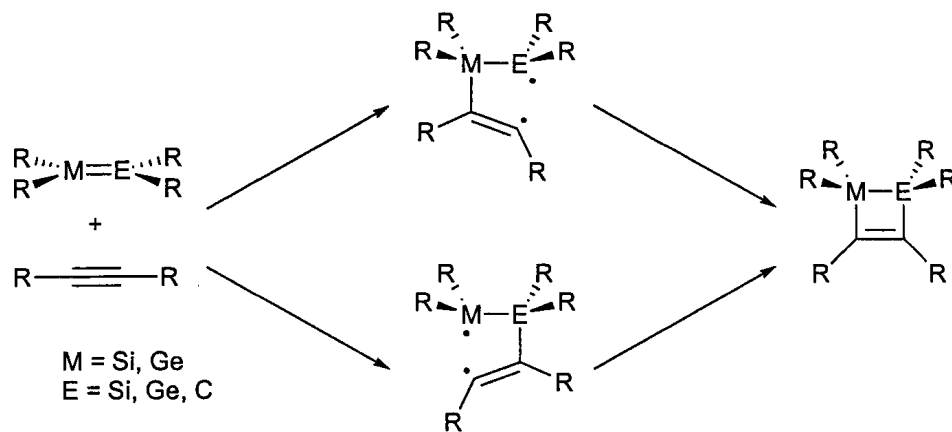
Chapter 4

Mechanism of the Addition of Alkynes to Polar Metallenes ($R_2M=CR_2$; M = Si, Ge): A Density Functional Theory Study

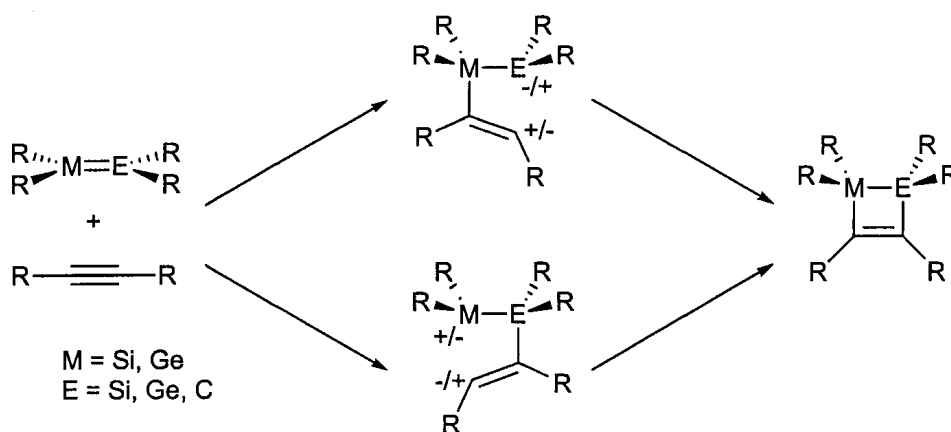
4.1 Introduction

Compounds that contain multiple bonds to heavy group 14 elements have long been an interest in inorganic chemistry; however, it was not until the synthesis of stable compounds of this type, including those involving silicon^{1,2} and germanium^{3,4,5}, that more detailed studies into their chemistry could be undertaken. The reactivity of the dimetallenes^{6,7} ($R_2M=MR_2$) and metallenes^{8,9} ($R_2M=CR_2$) is often compared to that of their carbon analogues, the alkenes, to aid in the interpretation of their chemistry and to examine periodic trends. Although several similarities in the types of products formed exist,⁶⁻⁹ the reactivity of (di)metallenes is generally much greater than that of alkenes. To gain a better understanding of their reactivity, it is necessary to examine the mechanisms of the reactions in which the (di)metallenes participate. The mechanistic chemistry of (di)metallenes is relatively under-developed; there are only a few classes of reactions that have been well studied, such as the addition of alcohols^{10,11,12} and carbonyl compounds^{11a,13,14}. Both reactions are believed to proceed via stepwise mechanisms, through initial nucleophilic attack of the oxygen on the (di)metallene.

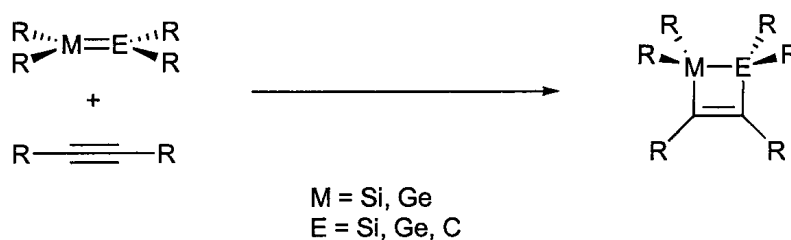
One of the most important reactions of silenes ($R_2Si=CR_2$), disilenes ($R_2Si=SiR_2$), and digermenes ($R_2Ge=GeR_2$) is the addition of alkynes to give (di)metallacyclobutenes (Scheme 4.1). Alkynes have often been used as effective trapping reagents for transient



a. Possible diradical pathways



b. Possible zwitterionic pathways



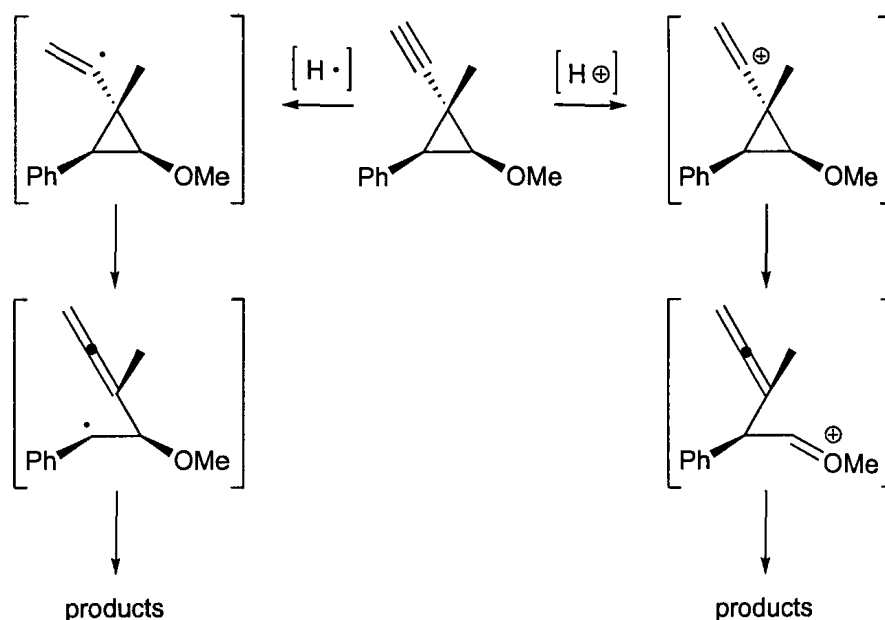
c. Possible concerted pathway

Scheme 4.1 Overview of possible mechanisms for the addition of alkynes to (di)metallenes to form (di)metallocyclobutenes.

(di)metallenes because the addition occurs cleanly and in high yield. Furthermore, silacyclobutenes are useful for the synthesis of more elaborate organic and organosilicon compounds^{15,16} as well as for use as precursors in polymer chemistry.¹⁷ The high

regiospecificity of the cycloaddition reaction between silenes and alkynes makes this method for the synthesis of silacyclobutenes advantageous. Given the prominent role of alkyne addition, the mechanism of (di)metallacyclobutene formation is of significant interest. A variety of pathways have been proposed including both concerted and stepwise mechanisms (Scheme 4.1).

The reported mechanistic studies on alkyne addition have focused primarily on disilenes, digermenes, and Brook silenes. A brief summary of the work is presented here. The addition of diphenylacetylene to either *trans*- or *cis*-1,2-dimethyl-1,2-diphenyldisilene led to scrambling of the stereochemistry in the disilacyclobutene products. This result provided clear evidence for the formation of an intermediate along the reaction pathway and, in this case, a diradical intermediate was proposed, although there was no experimental evidence to support this conclusion.¹⁸ The addition of alkynes to tetramesityldisilene has also been examined experimentally; cycloaddition was only observed with polar alkynes. Furthermore, when *trans*-1,2-di-*tert*-butyl-1,2-dimesityldisilene was allowed to react with alkynes, scrambling of the stereochemistry was observed in the cyclic products. A zwitterionic intermediate was proposed to explain the increased reactivity of disilenes with polar alkynes, in addition to the stereochemical scrambling.¹⁹ Recently, the nature of the alkyne addition pathway to disilenes was unambiguously determined by Baines and coworkers through the use of an alkynyl mechanistic probe designed to differentiate between radical and ionic intermediates (Scheme 4.2).²⁰ The products derived from the addition of the probe to tetramesityldisilene²¹ as well as tetra(*tert*-butyldimethylsilyl)disilene²² were consistent with the formation of a diradical intermediate.

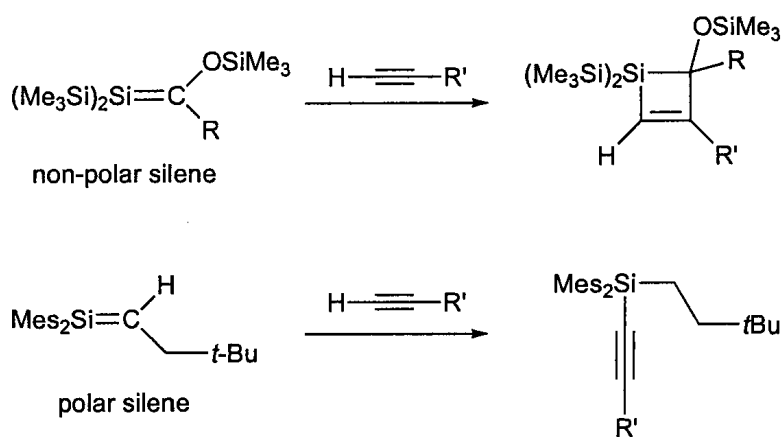


Scheme 4.2 Alkynyl mechanistic probe.

The reaction of digermenes with alkynes has also been examined experimentally.²³ Early reactivity studies made no attempts to elucidate the mechanism of alkyne addition; however, one report alluded to the formation of a zwitterionic intermediate arising from nucleophilic attack of tetramethyldigermene on 1,4-trifluoromethyl-2-butyne.²⁴ In contrast, tetramethyldigermene did not react with non-polar alkynes, and thus, the zwitterionic intermediate was proposed. As with the disilenes, the mechanism of alkyne addition was examined for tetramesityldigermene utilizing the alkynyl mechanistic probe; evidence for a diradical intermediate was obtained.²⁵

The mechanism of alkyne addition to silenes has been studied. The addition of phenylacetylene or trimethylsilylacetylene to an *E/Z* mixture of a Brook silene, $(\text{Me}_3\text{Si})\text{RSi}=\text{C}(\text{OSiMe}_3)(\text{Ad})$, where the *E/Z* ratio was known but not assigned, gave the same ratio of stereoisomers in the silacyclobutene products, and thus, a concerted

pathway was proposed.²⁶ Several other experimental and computational studies into the mechanism of alkyne addition to Brook silenes have been performed and a diradical mechanism was implicated in many instances;²⁷ however, the evidence provided was ambiguous. Recently, unequivocal evidence for a diradical intermediate was obtained experimentally through the use of the alkynyl mechanistic probe.²⁸ However, Brook silenes are a special class of relatively non-polar silenes, and thus, may not be representative of silenes in general. The mechanism of alkyne addition to a polar silene, 1,1-dimesitylneopentylsilene, $\text{Mes}_2\text{Si}=\text{C}(\text{H})\text{CH}_2t\text{Bu}$, using the same alkynyl mechanistic probe, was investigated.²⁹ Unfortunately, cycloaddition between the polar silene and the mechanistic probe was not observed, rather, silylacetylenes, from insertion of the terminal C-H bond across the $\text{Si}=\text{C}$ of the silene, were obtained exclusively (Scheme 4.3).



Scheme 4.3 Addition of the alkynyl mechanistic probe to non-polar and polar silenes.

Far less attention has been devoted to the addition of alkynes to germenes. Only the reactivity of 1,1-dimesitylneopentylgermene towards alkynes has been studied. As with the analogous silene, CH-insertion products were observed; however, several other modes of addition were competitive including ene-addition and cycloaddition.³⁰ The

reaction of 1,1-dimesitylneopentylgermene with the alkynyl mechanistic probe did not give any insight into the mechanism of cycloaddition as only a minor amount of ene-adduct was produced.

In summary, experimental studies have provided insight into the mechanism of alkynes to disilenes, digermenes, and Brook silenes; however, little is known, experimentally or computationally, about the mechanism of alkyne addition to naturally polarized silenes or germenes. Thus, we have examined the addition of acetylene to the parent silene ($\text{H}_2\text{Si}=\text{CH}_2$) and germene ($\text{H}_2\text{Ge}=\text{CH}_2$) using computational methods capable of providing accurate descriptions of both open- and closed-shell systems. A computational investigation of the reaction of propyne with a model Brook silene, $(\text{H}_3\text{Si})_2\text{Si}=\text{C}(\text{OSiH}_3)(\text{CH}_3)$, has been performed,^{27e} but only a concerted addition pathway was examined. A comprehensive study of the potential energy surface for the reaction of alkynes with silenes has not been reported. To our knowledge, no theoretical studies on the addition of alkynes to germenes have been performed.

Since two main modes of addition of alkynes were observed in the experimental studies with polar silenes and germenes, cycloaddition and CH-insertion, this study will focus on the potential energy surfaces leading to the formation of metallacyclobutenes as well as metallylacetylenes. The structures and energies of both intermediate and transition state structures were investigated along possible diradical, zwitterionic, and concerted pathways with the goal of determining the lowest energy reaction pathway for alkyne addition.

4.2 Methods

The addition of carbonyl compounds to polar silenes and germenes was successfully modeled by Mosey *et al.*³¹ using computational methods, and thus, a similar approach was used to study the addition of alkynes to polar silenes and germenes. The parent silene ($\text{H}_2\text{Si}=\text{CH}_2$) and germene ($\text{H}_2\text{Ge}=\text{CH}_2$) were studied as models for naturally polarized silenes and germenes, respectively. Acetylene was used as a model for terminal alkynes. Density functional theory (DFT) calculations were performed with the hybrid B3LYP exchange-correlation functional,³² comprised of Hartree-Fock exchange, Becke's exchange functional,³³ and the correlation functional of Lee, Yang, and Parr,³⁴ using a 6-311++G(d,p) basis set with the Gaussian03³⁵ suite of programs. Geometry optimizations on the reactants, products, closed-shell intermediates and transition states were performed with spin-restricted DFT. Broken-symmetry spin-unrestricted DFT was employed to locate all singlet diradical intermediates and transition-state structures. It should be noted that symmetry breaking results in spin-contamination of the Kohn-Sham determinant. All DFT energies reported include unscaled zero-point energy (ZPE) corrections. Frequency calculations were performed on all B3LYP structures to confirm that the products, reactants, and intermediates had no imaginary frequencies and that the transition states had only one imaginary frequency. Free energies at 298 K and 1 atm were obtained through thermochemical analysis along with the frequency calculations at the B3LYP/6-311++G(d,p) level. Single point energy calculations at the CCSD/6-311++G(d,p) level were performed on the B3LYP optimized geometries. The CCSD energies reported ZPE corrections calculated at the B3LYP/6-311++G(d,p) level. Intrinsic reaction coordinate (IRC) calculations were performed at the B3LYP/6-311++G(d,p) level to confirm that all

reported transition states do indeed lie between the intermediates and the products. Basis set superposition error was not accounted for. Wiberg bond orders³⁶ reported were calculated with the Natural Bond Orbital program³⁷ distributed with Gaussian03 and all spin densities were determined through Mulliken population analysis³⁸ with Gaussian03. Natural population analysis (NPA)³⁹ calculations were performed to determine atomic charges.

4.3 Computational Results

The geometries and energies of the reactants and products will be presented first in sections 4.3.1 and 4.3.2. Descriptions of the various reaction pathways follow in sections 4.3.3 – 4.3.6. The sections have been divided according to the various pathways located, with results from both metallenes being presented within the context of each mechanism to allow for added facility in the comparison of the pathways. The naming system for the structures was adopted to accommodate the two metallenes and the three types of reaction pathways (concerted, diradical, zwitterionic) that we have explored.³¹ The three-component naming system provides a description of the species and the nature of the reaction pathway where it is found. The first part of the name refers to the nature of the pathway (**DR** for diradical, **ZW** for zwitterionic, **CT** for concerted, **CH** for CH-insertion). If more than one unique pathway was located, a numeric character refers to the specific pathway. The second part of the name refers to the metallene involved, **MC** where M = Si or Ge. The third part of the name is an alphabetic character that refers to the stationary point beyond the reactants toward the products. Lastly, the inclusion of a superscript double dagger denotes that the species is a transition state. For example,

DR1-SiC-a[‡] represents a silene transition state that lies on a diradical reaction pathway 1 and the 'a' indicates that this is the first stationary point past the reactants.

4.3.1 Energies and Geometries of the Reactants

The geometries and energies of metallenes have been the focus of several previous studies^{8g,40} including our previous study of the mechanism of formaldehyde addition to (di)metallenes.³¹ Only planar structures are stable for the parent metallenes on the B3LYP potential energy surface. Conversely, both planar and trans-bent structures are possible for the dimetallenes; the trans-bent structures are more stable than the corresponding planar geometry.³¹ In agreement with previous work, no stable trans-bent structures were found for either of the metallenes during geometry optimizations in this study.

4.3.2 Energies and Geometries of the Products

The geometries of the metallacyclobutenes and metallylacetylenes were optimized to compare their energies with those of the reactants, as well as to examine the relative stabilities of the two types of products. The optimized geometries of the four-membered rings of the metallacyclobutenes are planar with C-Si-C-C dihedral angles of 0° (Figure 4.1a). The conformation of the H₂RM-CH₃ single bond is staggered in the metallylacetylenes (Figure 4.1b). Selected geometric values and the energies of the adducts relative to the sum of the energies of the separated reactants are given in Table 4.1.

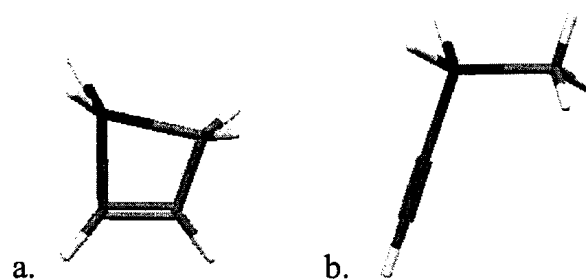
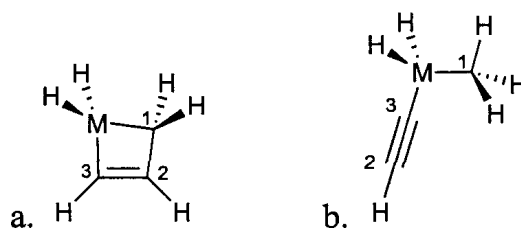


Figure 4.1 Representative optimized geometries: (a) silacyclobutene and (b) silylacetylene. Black = silicon, grey = carbon, white = hydrogen.

For the addition of acetylene to both silene and germene, the products resulting from CH-insertion are more stable (lower energy) than those resulting from cycloaddition. This is more pronounced for the silene where the calculated free energy of silylacetylene is 2.7 kcal/mol less than that of silacyclobutene, as compared to a free energy difference of 1.1 kcal/mol in the case of the germene.

Table 4.1 Calculated^a bond lengths, angles, and relative energies of the (a) metallacyclobutenes and (b) metallylacetylenes.



M	B3LYP							CCSD ^c		
	Bond Lengths (Å)				Angles (°)			Energy ^b		Energy ^b
	M-C1	M-C3	C1-C2	C2-C3	M-C3-C2	C2-C1-M	C1-M-C3	ΔH° (0 K)	ΔG° (298K)	ΔH° (0 K)
Si-a	1.916	1.867	1.527	1.347	91.0	84.0	76.3	-52.0	-55.6	-43.3
Si-b	1.880	1.838	-	1.209	179.4	-	110.6	-53.6	-57.0	-46.0
Ge-a	1.991	1.944	1.524	1.347	92.3	85.5	73.0	-47.6	-50.4	-38.8
Ge-b	1.963	1.917	-	1.209	179.2	-	109.4	-47.4	-50.4	-39.9

^a Using the 6-311++G(d,p) basis set. ^b Energies of the addition reaction in kcal/mol. ^c At the B3LYP geometries using B3LYP ZPE corrections.

The bond lengths and angles within the four-membered ring of the silacyclobutene agree well with the previously reported calculations,^{27e,g} as well as with previously reported crystal structures of related derivatives.^{26a,41} Some minor differences are present between the metrics measured by X-ray crystallography and those of the calculated structures; these are most likely due to the effects of bulky substituents.

4.3.3 Summary of Acetylene Addition Pathways

A brief overview of the addition of acetylene to silene and germene is presented (Figure 4.2, 4.3); a detailed description of each pathway follows in sections 4.3.4 – 4.3.6. To present the results clearly, only the free energies at 298 K and 1 atm are shown. The B3LYP and CCSD results provide the same qualitative description of the reaction pathways as the free energies.

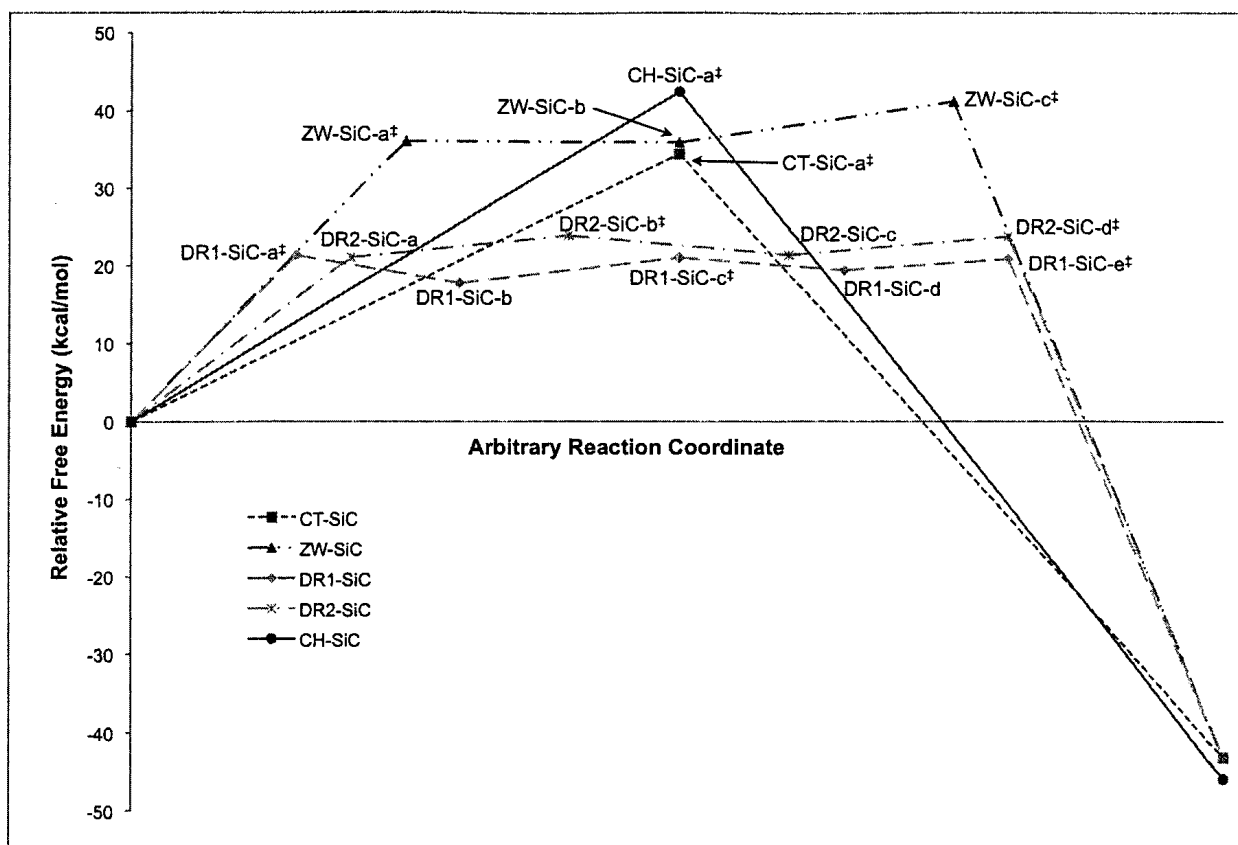


Figure 4.2 B3LYP gas-phase free energy profiles at 298 K and 1 atm for the addition of acetylene to silene. Energies are in kcal/mol relative to the sum of the energies of the separated reactants.

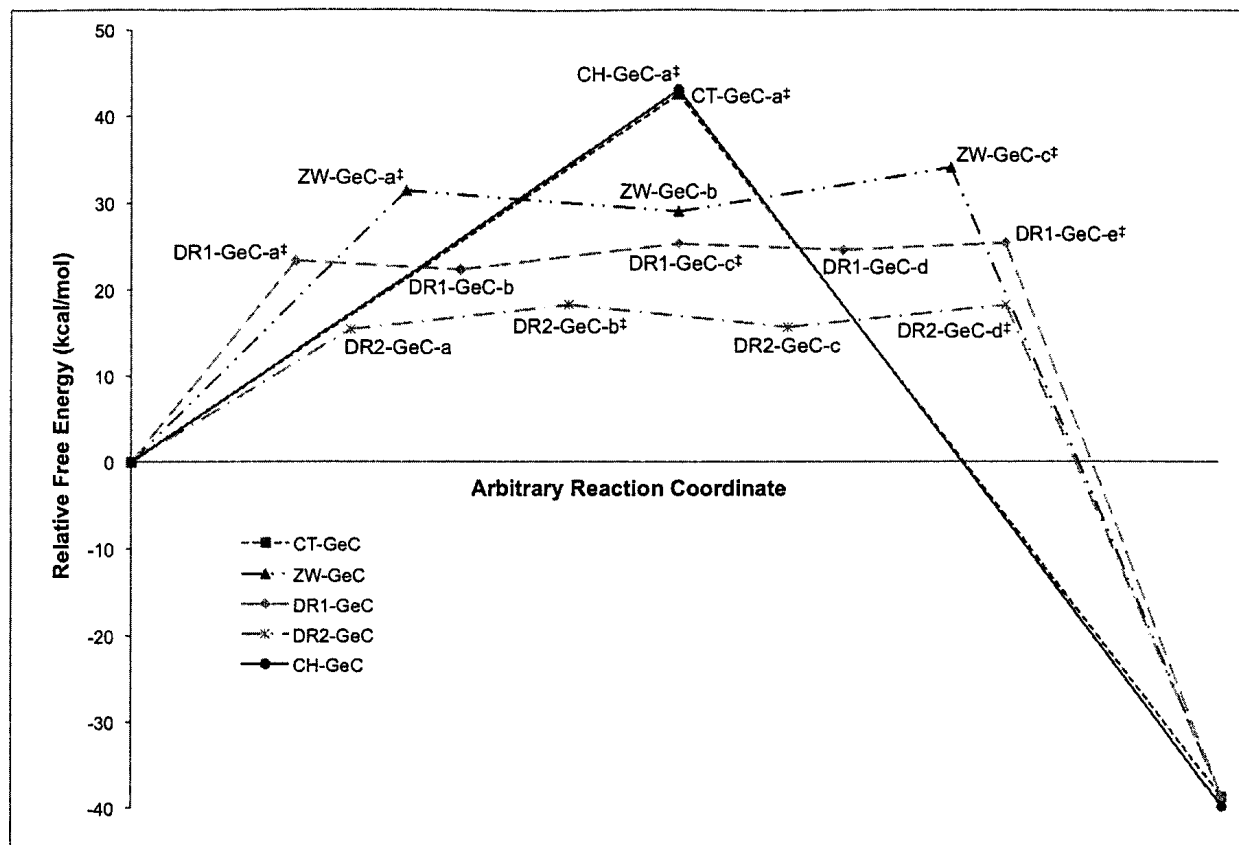


Figure 4.3 B3LYP gas-phase free energy profiles at 298 K and 1 atm for the addition of acetylene to germene. Energies are in kcal/mol relative to the sum of the energies of the separated reactants.

4.3.4 Open-Shell Cycloaddition Pathways

Two distinct reaction pathways involving the formation of a singlet diradical intermediate were located for the addition of acetylene to the metallenes. One diradical pathway begins with metalloïd-acetylenic carbon bond formation (**DR1**) and the second begins with the metallenic carbon-acetylenic carbon bond formation (**DR2**). The features of the **DR1** pathway for silene and germene are discussed together in section 4.3.4.1. The features of the **DR2** pathways are discussed in section 4.3.4.2.

4.3.4.1 Cycloaddition through Diradical Pathway 1 (DR1)

The formation of silacyclobutene and germacyclobutene follow diradical mechanisms that exhibit similar features when the initial step is the formation of the metalloid-acetylenic carbon bond. Consequently, the silene pathway (**DR1-SiC**) is described in detail, followed by any notable differences in the germene pathway (**DR1-GeC**). The pathways involve the progression of the reactants to the products as shown in Figure 4.2 (**DR1-SiC**) and Figure 4.3 (**DR1-GeC**). IRC calculations confirm that the transition states link the intermediates to the reactants and products. The structures of the transition states and intermediates are shown in Figure 4.4, whereas the energies along the potential energy surface relative to the reactants are given in Table 4.2.

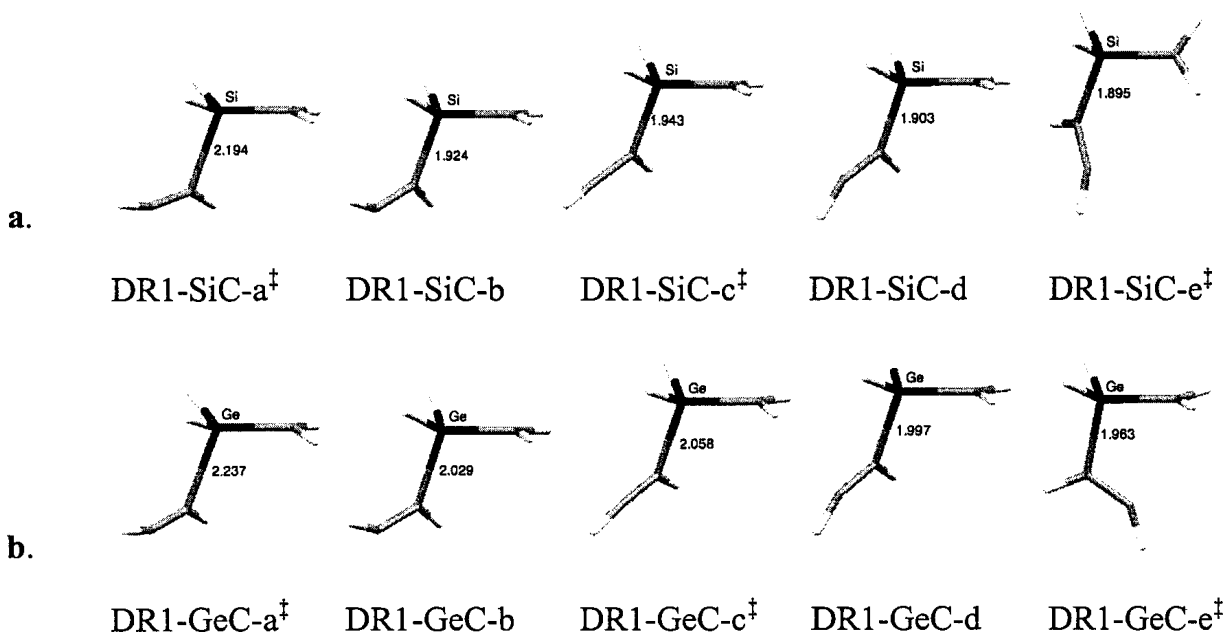
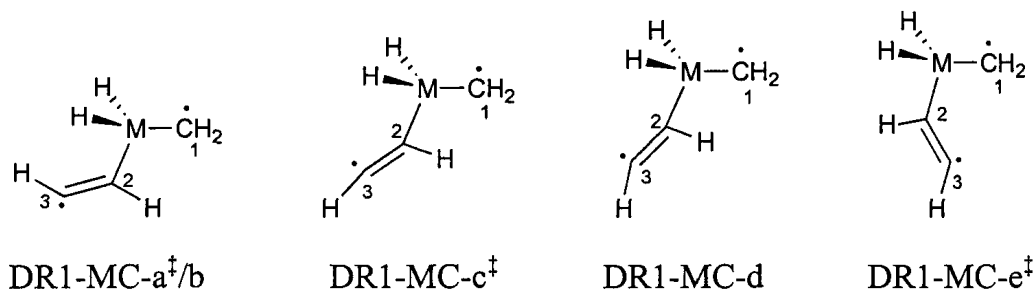


Figure 4.4 Optimized geometries of intermediates and transition states along **DR1** for the addition of acetylene to (a) silene and (b) germene. Bond lengths are in angstroms. Black = silicon/germanium, grey = carbon, white = hydrogen.

Table 4.2 Calculated^a energies and spin densities along **DR1** for the addition of acetylene to silene and germene.



Species	B3LYP ^b		CCSD ^{b,c}	Mulliken Spin Population ^d	
	ΔH° (0 K)	ΔG° (298 K)	ΔH° (0 K)	C1	C3
DR1-SiC-a [†]	14.0	21.3	19.6	-0.53	0.44
DR1-SiC-b	10.4	17.7	8.7	-1.01	0.87
DR1-SiC-c [†]	13.7	21.1	14.0	-0.98	0.92
DR1-SiC-d	12.3	19.4	9.9	-1.06	0.95
DR1-SiC-e [†]	13.2	20.9	10.3	-1.05	1.00
DR1-GeC-a [†]	16.0	23.4	20.6	-0.69	0.54
DR1-GeC-b	15.0	22.3	14.6	-0.99	0.83
DR1-GeC-c [†]	18.0	25.3	19.5	-0.96	0.87
DR1-GeC-d	17.4	24.6	16.0	-1.05	0.94
DR1-GeC-e [†]	19.2	25.4	16.9	-1.07	0.98

^a Using the 6-311++G(d,p) basis set. ^b Energies of the addition reaction in kcal/mol. ^c At the B3LYP geometries using B3LYP ZPE corrections. ^d From the B3LYP/6-311++G(d,p) determinant; positive values represent α spin, negative values represent β spin.

A singlet diradical has two unpaired electrons with opposite spin. The Mulliken net spin populations at both C₁ (or M for the DR2 pathways) and C₃ from the B3LYP calculations indicate the number of unpaired electrons at those atoms. A singlet diradical would have an approximate net α and net β spin of one, whereas a closed-shell species would have no net spin density.

The formation of the first diradical intermediate, **DR1-SiC-b**, from the separated reactants required the reaction to pass over an energy barrier corresponding to transition state **DR1-SiC-a[†]** (Figure 4.2, Figure 4.4a). The bonds formed between acetylene and

silene (Si-C2) were 18 % longer than the fully formed Si-C2 bonds in silacyclobutene (Figure 4.4a, Table 4.1). Furthermore, the former Si=C and C≡C bonds were lengthened by 3 – 4 %. Transition state **DR1-SiC-a[‡]** represented a significant energy barrier. The free energy (ΔG) of the species relative to the reactants was 21.3 kcal/mol, respectively (Table 4.2). A large portion of the free energy of each transition state structure was from the entropic contribution as the reactants came together. Upon examination of the net spin densities, it was apparent that **DR1-SiC-a[‡]** had an electronic structure intermediate between the closed-shell reactants and the open-shell singlet diradical intermediate **DR1-SiC-b**. The net Mulliken spins on C1 and C3 showed a moderate build-up of spin density centred on these atoms (Table 4.2) and an isosurface plot of the net spin density reveals the spin polarization localized on the two carbon centres (Figure 4.5a).

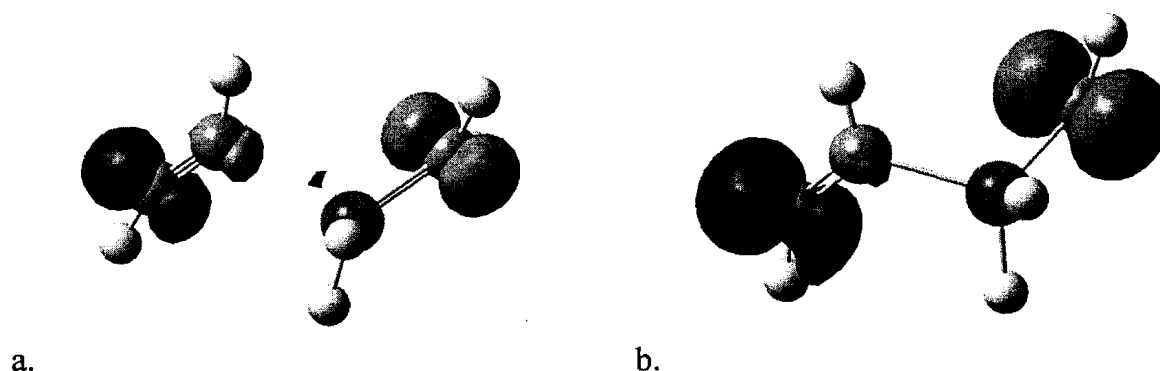


Figure 4.5 Isosurface plot of the net spin density of (a) **DR1-SiC-a[‡]** and (b) **DR1-SiC-b**. The dark grey isosurface represents the α -spin density and the light grey represents the β -spin density. The isosurface value plotted is 0.02 atomic units.

Progression to intermediate **DR1-SiC-b** (Figure 4.2, Figure 4.4a) involved shortening of the Si-C2 bond, now only 3 % longer than that in the final product, and rotation of the alkyne moiety relative to silene, thereby decreasing the C1-Si-C2-C3 dihedral angle by approximately 10°. The Si-C2 bond had a calculated bond order of 0.74

(Si-C2), in comparison with 0.85 in the cyclic product, which indicated that the Si-C2 bond is just about completely formed in **DR1-SiC-b**. A net spin corresponding to roughly one unpaired electron was observed at both of the radical centres (C1 and C3), each with opposite spin (Table 4.2). An isosurface plot of the net spin density is shown in Figure 4.5b. The results are consistent with the electronic structure of a singlet diradical intermediate species. The relative free energy of **DR1-SiC-b** corresponded to a stabilization of 3.6 kcal/mol from the preceding transition state (Table 4.2).

Before ring closure can occur, the hydrogen substituents on the alkene moiety need to be *cis* to each other. Thus, intermediate **DR1-SiC-b** progressed over a small energy barrier, **DR1-SiC-c[‡]**, to give a second diradical intermediate, **DR1-SiC-d**, in which the hydrogens are oriented appropriately (*cis*) for ring closure (Figure 4.2, Figure 4.4a). The *cis*-oriented intermediate was slightly higher in energy than the previous *trans*-oriented intermediate (Table 4.2). The results of the net spin analysis of transition state **DR1-SiC-c[‡]** and *cis*-oriented intermediate **DR1-SiC-d** are similar to the previous **DR1-SiC-b** intermediate and are consistent with singlet diradical species.

The final barrier along this diradical pathway corresponded to transition state **DR1-SiC-e[‡]** (Figure 4.2, Figure 4.4a). Silacyclobutene formation from intermediate **DR1-SiC-d** involved a significant decrease in the C1-Si-C2-C3 dihedral angle, which allows for the subsequent ring closure. A small relative free energy barrier of 2 kcal/mol (Table 4.2) to product formation indicates that the previous intermediates are likely transient species.

Progression from germene and acetylene to germacyclobutene through **DR1** (Figure 4.3, Figure 4.4b, Table 4.2) exhibits similar features to the silene pathway. One

notable difference lies in the structure of transition state **DR1-GeC-e[‡]**. The plane made by the CH₂ moiety on C1 was perpendicular to the Ge-C2 bond in **DR1-GeC-e[‡]**, while it was parallel to the Si-C2 bond in **DR1-SiC-e[‡]** (Figure 4.4).

4.3.4.2 Cycloaddition through Diradical Pathway 2 (DR2)

The formation of silacyclobutene and germacyclobutene also follow similar reaction pathways when the initial step is the formation of the metallenic carbon-acetylenic carbon bond. Again, the silene pathway (**DR2-SiC**) is described in detail, followed by any notable differences in the germene pathway (**DR2-GeC**). The pathways involve the progression of the reactants to the products as shown in Figure 4.2 (**DR2-SiC**) and Figure 4.3 (**DR2-GeC**). IRC calculations confirm that the transition states link the intermediates to the reactants and products. The transition states and intermediates are shown in Figure 4.6 and the energies along the potential energy surface relative to the reactants are given in Table 4.3.

The first stationary point found along the **DR2-SiC** corresponds to intermediate **DR2-SiC-a** (Figure 4.2, Figure 4.6a), where the bond between the silenic carbon and acetylene (C1-C2) has formed. A transition state structure preceding **DR2-SiC-a** may exist, but it could not be located. **DR2-SiC-a** had a *trans*-oriented double bond attached to the former silene and the newly formed C1-C2 bond in **DR2-SiC-a** was within 1% of the bond length in the final product indicating that the bond has fully formed (Figure 4.6a, Table 4.1). The diradical nature of the intermediates was confirmed by examination of the net spin densities. The B3LYP free energies of **DR2-SiC-a** was 21.0 kcal/mol higher than that of the separated reactants (Table 4.3).

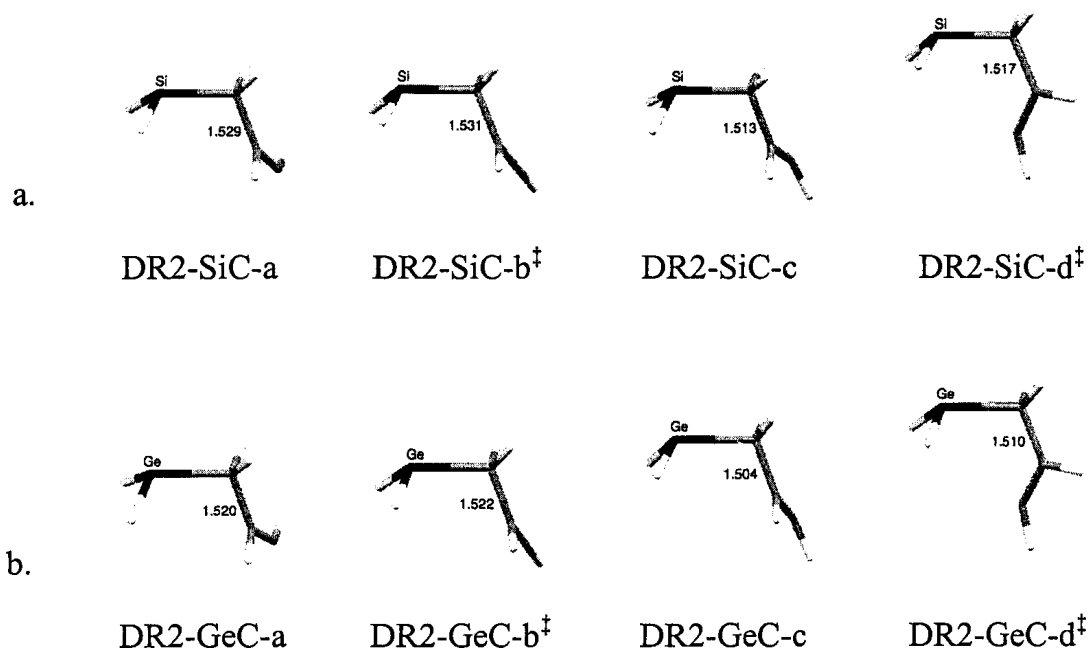


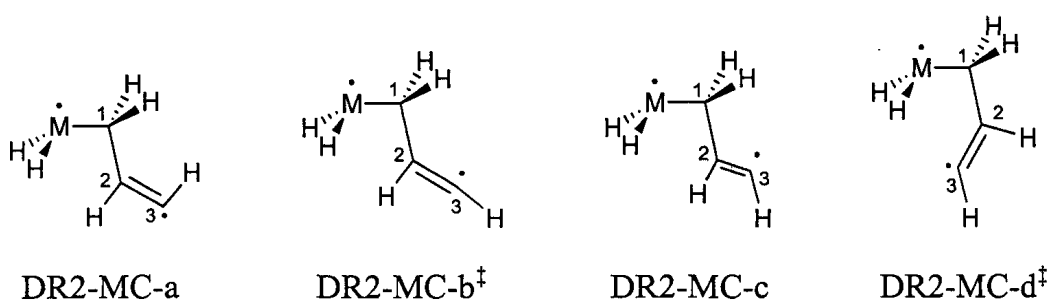
Figure 4.6 Optimized geometries of intermediates and transition states along **DR2** for the addition of acetylene to (a) silene and (b) germene. Bond lengths are in angstroms. Black = silicon/germanium, grey = carbon, white = hydrogen.

Again, the *trans*-oriented hydrogen substituents on the alkene moiety must be transformed to a *cis*-orientation before ring closure is possible. Progression from **DR2-SiC-a** to **DR2-SiC-c** over a modest energy barrier of 2.8 kcal/mol (Table 4.3), corresponding to transition state **DR2-SiC-b[‡]**, accomplished this necessary transformation (Figure 4.2, Figure 4.6a). **DR2-SiC-b[‡]** and **DR2-SiC-c** have structures that were consistent with diradical species.

The *cis*-oriented intermediate, **DR2-SiC-c**, then passed over transition state **DR2-MC-d[‡]** before formation of silacyclobutene. The most prominent structural feature of this transition state is the decrease in the Si-C1-C2-C3 dihedral angle from 105° to 44° in **DR2-SiC-d[‡]**. The smaller dihedral angle allows for the subsequent ring closure. The diradical nature was maintained upon progression to the transition state. The relative free energy barrier needed to overcome **DR2-SiC-d[‡]** was only 2.4 kcal/mol (Table 4.3). As

with **DR1-SiC**, the small barrier to ring formation indicates that the intermediates are likely very short-lived species.

Table 4.3 Calculated^a energies and spin densities along **DR2** for the addition of acetylene to silene and germene.



Species	B3LYP ^b		CCSD ^{b,c}	Mulliken Spin Population ^d	
	ΔH° (0 K)	ΔG° (298 K)	ΔH° (0 K)	M	C3
DR2-SiC-a	13.5	21.1	11.3	-0.98	0.91
DR2-SiC-b [†]	16.3	23.9	15.4	-0.98	1.03
DR2-SiC-c	13.9	21.4	11.3	-1.00	0.94
DR2-SiC-d [†]	15.8	23.8	12.7	-1.01	1.00
DR2-GeC-a	7.9	15.4	6.6	-0.86	0.90
DR2-GeC-b [†]	10.7	18.2	10.6	-0.86	1.02
DR2-GeC-c	8.1	15.7	6.5	-0.88	0.91
DR2-GeC-d [†]	10.3	18.2	8.0	-0.89	1.01

^a Using the 6-311++G(d,p) basis set. ^b Energies of the addition reaction in kcal/mol. ^c At the B3LYP geometries using B3LYP ZPE corrections. ^d From the B3LYP/6-311++G(d,p) determinant; positive values represent α spin, negative values represent β spin.

The stationary points along **DR2** for germene (Figure 4.3, Figure 4.6b, Table 4.3) exhibits similar structural features as those described for silene; however, the relative energetics of the germene pathway, compared to **DR1**, were markedly different from those of the silene pathway. **DR2-GeC** was lower in energy than **DR1-GeC** (by ~ 7 kcal/mol), while **DR2-SiC** was a slightly higher energy pathway (by ~ 3 kcal/mol) compared to **DR1-SiC**.

4.3.5 Closed-Shell Cycloaddition Pathways

Two different closed-shell pathways were located for the addition of acetylene to the metallenes. One pathway involved the formation of a zwitterionic intermediate (**ZW**), while the other proceeded in a concerted fashion to the metallacyclobutenes without the formation of an intermediate (**CT**). Both pathways were located for each metallene. The **ZW** pathway for silene and germene are discussed in section 4.3.5.1; the **CT** pathways are discussed in section 4.3.5.2.

4.3.5.1 Cycloaddition through a Zwitterionic Pathway (**ZW**)

For each metallene, a pathway was located for the addition of acetylene that involved the formation of a zwitterionic intermediate. The silene pathway (**ZW-SiC**) is described in detail, followed by any notable differences in the germene pathway (**ZW-GeC**). The zwitterionic pathways involve the progression of the reactants to the products as shown in Figure 4.2 (**ZW-SiC**) and Figure 4.3 (**ZW-GeC**). IRC calculations confirm that the transition states link the intermediates to the reactants and products. The relative energies of the stationary points along the reaction pathway as well as relevant bond orders are given in Table 4.4. The structures of the zwitterionic intermediate and transition states are shown in Figure 4.7.

The initial transition state, **ZW-SiC-a[‡]**, (Figure 4.2, Figure 4.7a) found on the potential energy surface was an adduct featuring a long C1-C2 bond distance, 21 % greater than the C1-C2 bond length in silacyclobutene (Figure 4.7a, Table 4.1). A small C1-C2 Wiberg bond order of 0.60 indicated that the C1-C2 bond has not yet fully formed. Progression towards the initial transition state also involved deformation of the

linear alkyne into a *trans* geometry as the C≡C bond lengthened from 1.20 to 1.26 Å in **ZW-SiC-a[‡]**. The Si=C bonds also stretched as the planar silene was distorted to a *trans*-bent geometry. Not surprisingly, the transition state represented a large energy barrier; the relative free energy of **ZW-SiC-a[‡]** was 36.1 kcal/mol greater than that of the separated reactants (Table 4.4).

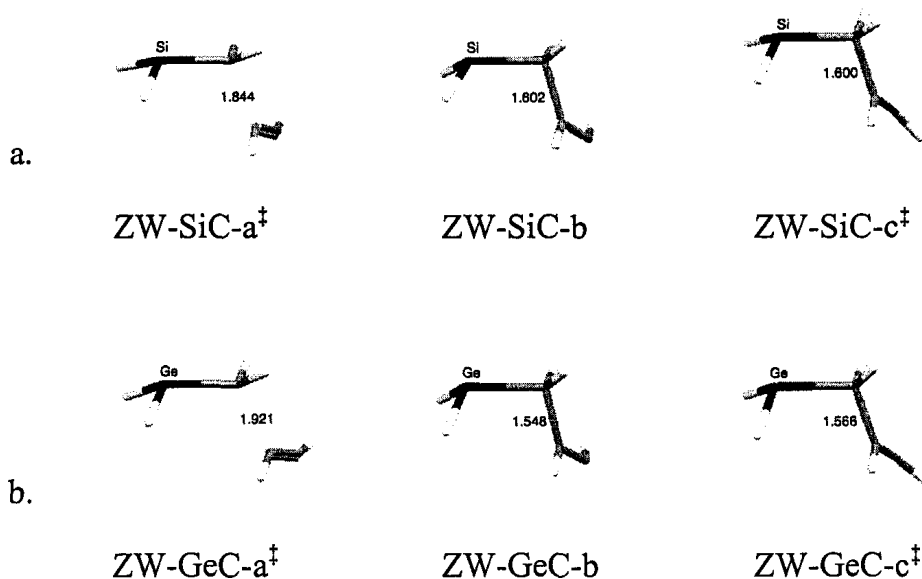
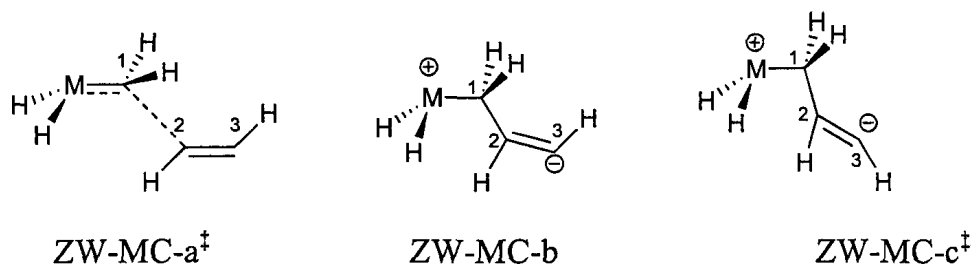


Figure 4.7 Optimized geometries of intermediates and transition states along **ZW** for the addition of acetylene to (a) silene and (b) germene. Black = silicon/germanium, grey = carbon, white = hydrogen.

Upon progression over the initial transition state, zwitterionic intermediate **ZW-SiC-b** formed as the C1-C2 bond distance decreased to within 5 % of that in the product with a bond order approaching 1. The intermediate was still a high-energy species, only stabilized by 0.2 kcal/mol from the preceding transition state (Table 4.4). The structure of **ZW-SiC-b** was consistent with a zwitterion; the bent geometry at C3 suggests that the negative charge was localized on this carbon, and thus, the positive charge on silicon. However, the HOMO and LUMO Kohn-Sham orbitals were best described as π and π^* -like orbitals.

Table 4.4 Calculated^a energies and bond orders along **ZW** for the addition of acetylene to silene and germene.



Species	B3LYP ^b		CCSD ^{b,c}	Bond Orders ^d		
	ΔH° (0 K)	ΔG° (298 K)	ΔH° (0 K)	M-C1	C1-C2	C2-C3
reactants ^e	0.0	0.0	0.0	1.82	-	2.99
ZW-SiC-a [‡]	28.6	36.1	31.9	1.20	0.60	2.43
ZW-SiC-b	28.4	35.9	28.6	0.93	0.88	2.09
ZW-SiC-c [‡]	33.3	41.2	33.0	0.90	0.90	2.10
product ^f	-52.0	-43.3	-55.6	0.82	1.04	1.93
reactants ^e	0.0	0.0	0.0	1.84	-	2.99
ZW-GeC-a [‡]	24.0	31.4	29.1	1.25	0.53	2.50
ZW-GeC-b	21.5	29.0	24.5	0.83	0.97	1.97
ZW-GeC-c [‡]	26.2	34.1	28.5	0.83	0.95	2.06
product ^f	-47.6	-38.8	-50.41	0.84	1.05	1.95

^a Using the 6-311++G(d,p) basis set. ^b Energies of the addition reaction in kcal/mol. ^c At the B3LYP geometries using B3LYP ZPE corrections. ^d Wiberg Bond orders. ^e The separate metallene and acetylene molecules. ^f The corresponding metallacyclobutene.

The reaction then proceeded over a second, larger free energy barrier, **ZW-SiC-c[‡]**, (Figure 4.2, Figure 4.7a) equal to 5.3 kcal/mol that connected the intermediate to the product (Table 4.4). Progress to the products through **ZW-SiC-c[‡]** involved rotation about the C1-C2 bond in order to bring the silicon closer to C3, allowing for eventual Si-C3 bond formation. In addition, the hydrogen substituents on the alkene adopt a *cis* orientation, which is necessary for ring closure.

As in the case of **DR2**, the zwitterionic pathway for germene (Figure 4.3, Figure 4.7b, Table 4.4) exhibits similar structural features as those described for silene. In

addition, both **ZW-SiC** and **ZW-GeC** pathways represent significant free energy barriers to reaction.

4.3.5.2 Cycloaddition through a Concerted Pathway (CT)

A pathway that did not involve a stable intermediate species was located for the cycloaddition of acetylene to silene and germene (Figure 4.2, Figure 4.3). The additions to silene and germene were similar and are discussed together as a general pathway with specific information given as necessary. IRC calculations confirm that the transition states link the reactants to the products. The relative energies of the stationary points along this pathway as well as relevant bond orders are given in Table 4.5. The general geometries of the transition state structures are given in Figure 4.8.

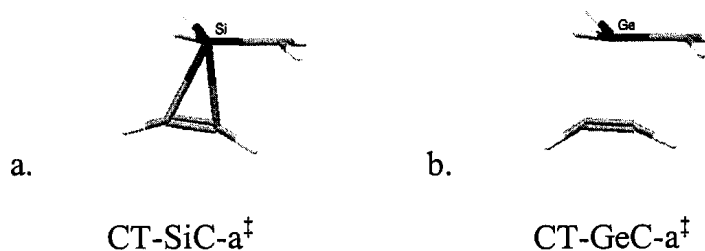
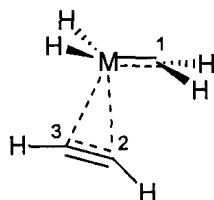


Figure 4.8 Optimized transition state geometries along **CT** for the addition of acetylene to (a) silene and (b) germene. Black = silicon/germanium, grey = carbon, white = hydrogen.

Table 4.5 Calculated^a energies and bond orders along CT for the addition of acetylene to silene and germene.



Species	B3LYP ^b		CCSD ^{b,c}	Bond Orders ^d				
	ΔH° (0 K)	ΔG° (298 K)	ΔH° (0 K)	M-C1	C1-C2	C2-C3	M-C3	M-C2
reactants ^e	0.0	0.0	0.0	1.82	-	2.99	-	-
CT-SiC-a [‡]	26.3	34.4	30.9	1.07	0.35	2.43	0.22	0.38
product ^f	-52.0	-43.3	-55.6	0.82	1.04	1.93	0.85	-
reactants ^e	0.0	0.0	0.0	1.84	-	2.99	-	-
CT-GeC-a [‡]	34.4	42.5	38.6	1.03	0.27	2.34	0.33	0.36
product ^f	-47.6	-38.8	-50.4	0.84	1.05	1.95	0.87	-

^a Using the 6-311++G(d,p) basis set. ^b Energies of the addition reaction in kcal/mol. ^c At the B3LYP geometries using B3LYP ZPE corrections. ^d Wiberg Bond orders. ^e The separate metallene and acetylene molecules. ^f The corresponding metallacyclobutene.

The concerted pathway for the silene was found to have high free energy barrier of 34.4 kcal/mol and that for the germene was 42.5 kcal/mol (Table 4.5). Although these pathways have been classified as concerted, our analysis of the two transition states and the corresponding IRC pathways suggest that these are not concerted pericyclic cyclizations; after initial coordination of the alkyne to the metalloid centre, the acetylenic moiety slowly moves towards C1 to enable ring formation. In agreement, the bond orders (Table 4.5) do not show the simultaneous formation of the M-C3 and C1-C2 bonds and breaking of the M-C1 and C2-C3 multiple bonds. Silene transition state **CT-SiC-a[‡]** and germene transition state **CT-GeC-a[‡]** both have a significant amount of charge transfer and are best described as pentacoordinate, zwitterionic species. For example, the silicon is more positively charged than in free silene (by 0.25 e) and C1 is more negatively

charged (by 0.09 e). The alkyne triple bond has also been polarized: the change in the natural atomic charge on C3 compared to free acetylene is -0.17 e. Many attempts were made to locate a transition state consistent with a concerted, antarafacial cycloaddition; however, no transition state structures consistent with a pericyclic process were found.

4.3.6 CH-insertion Pathways (CH)

The potential energy surface for the addition of acetylene to metallene was also examined for pathways that lead to the formation of CH-insertion products. A concerted pathway for the addition of the C-H bond of acetylene across the M=C bond of silene or germene was located (Figure 4.2, Figure 4.3). Abstraction of the acetylenic H in a stepwise manner, either via an ionic or radical mechanism, was also investigated; however, these pathways were not pursued in detail as the necessary, separated intermediate species were found to be very high in energy (in the gas phase). IRC calculations confirm that the transition states link the reactants to the products. The relative energies of the stationary points along this pathway as well as relevant bond orders are given in Table 4.6. The geometries of the transition state structures are shown in Figure 4.9.

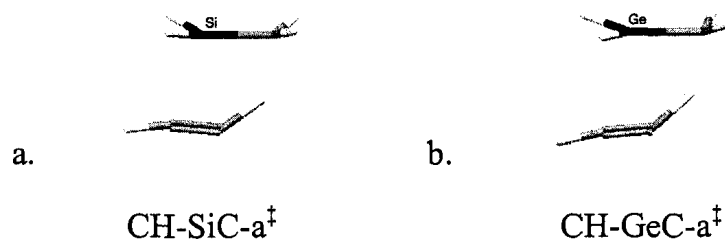
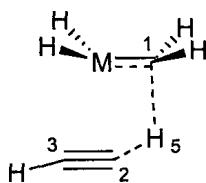


Figure 4.9 Optimized geometries of transition state along CH for the addition of acetylene to (a) silene and (b) germene. Black = silicon/germanium, grey = carbon, white = hydrogen.

The free energy barrier to CH-insertion was 42.4 and 43.0 kcal/mol for **CH-SiC-a[‡]** and **CH-GeC-a[‡]**, respectively (Table 4.6). Both transition states feature a severely distorted alkyne where the terminal hydrogen is approaching the metallenic carbon. Upon examination of the IRC pathway towards the products, it is clear that the new C1-H5 bond forms first followed by M-C2 formation and reestablishment of the linear alkyne moiety. The calculated natural atomic charges on **CH-SiC-a[‡]** are consistent with a significant amount of charge transfer in the transition state; the change in the natural atomic charges compared to the free reactants are + 0.28 e on Si and – 0.28 e on C1 as well as + 0.08 e on H5 and – 0.21 e on C2. Similar changes in the natural atomic charges were also noted for **CH-GeC-a[‡]**.

Table 4.6 Energies and bond orders along **CH** for the addition of acetylene to silene and germene.



Species	B3LYP ^b		CCSD ^{b,c}	Bond Orders ^d				
	ΔH° (0 K)	ΔG° (298 K)	ΔH° (0 K)	M-C1	C1-H5	C2-C3	M-C2	M-C3
reactants ^e	0.0	0.0	0.0	1.82	-	2.99	-	-
CH-SiC-a[‡]	34.8	42.4	38.5	1.06	0.25	2.64	0.23	0.21
product ^f	-53.6	-46.0	-57.0	0.86	0.93	2.93	0.85	-
reactants ^e	0.0	0.0	0.0	1.84	-	2.99	-	-
CH-GeC-a[‡]	35.3	43.0	38.7	1.09	0.30	2.71	0.21	0.17
product ^f	-47.4	-39.9	-50.4	0.88	0.94	2.94	0.86	-

^a Using the 6-311++G(d,p) basis set. ^b Energies of the addition reaction in kcal/mol. ^c At the B3LYP geometries using B3LYP ZPE corrections. ^d Wiberg Bond orders. ^e The separate metallene and acetylene molecules. ^f The corresponding metallacyclobutene.

4.4 Discussion of Pathway Selectivity

All reaction pathways presented (**DR1**, **DR2**, **ZW**, **CT**, **CH**) were located for the addition of acetylene to both silene and germene. This is in contrast to the addition of formaldehyde to silene and germene where fewer pathways were available for germene;³¹ only a concerted pathway was located for the addition of formaldehyde to germene, while diradical, zwitterionic, and concerted pathways were found for silene. The diradical and zwitterionic pathways for the addition of formaldehyde to silene involved initial formation of the Si-O bond. This bond was fully formed in the diradical intermediate species, while the intermediate in the zwitterionic pathway was a loosely bound silene-formaldehyde complex. The strength of the Si-O bond (122 – 136 kcal/mol)⁴² was noted as a major contributing factor for the low energy stepwise pathways for silene. In particular, the structure of the diradical intermediate was stabilized, relative to the zwitterionic complex, due to the fully formed Si-O bond. In contrast, the lower thermodynamic stability of the Ge-O bond (72 – 107 kcal/mol)⁴³ was not sufficient to stabilize an intermediate species, diradical or zwitterionic, between germene and formaldehyde.

Of the pathways located for the addition of acetylene to silene or germene, one of the diradical pathways (**DR1**) and the concerted pathway (**CT**) proceeded with initial M-C bond formation, whereas the remaining pathways involved initial C-C bond formation. A comparison between the bond strengths of Ge-C bonds (~76 kcal/mol) and Si-C bonds (~90 kcal/mol) reveals a much smaller difference than observed for Ge-O and Si-O bonds. The C-C bond strength is also comparable (~85 kcal/mol). As a result, the

pathway selectivity for the addition of acetylene to silene or germene does not depend as strongly on the strength of the initial bond formed.

The formation of a diradical species is favoured over the formation of a closed-shell species. There is not a significant bias towards initial M-C3 or C1-C2 bond formation; however, **DR1** (Si-C3 bond formation) is slightly favoured for silene (Figure 4.2) and **DR2** (C1-C2 bond formation) is favoured for germene (Figure 4.3). The larger size of germanium undoubtedly contributes to the stabilization of a germyl radical as opposed to an α -germyl carbon centred radical.

Upon examination of the pathways that lead to either initial M-C3 (**DR1** and **CT**) or C1-C2 (**ZW** and **DR2**) bond formation, it is of interest to consider what factors influence the pathway selectivity since the nuclear interactions between reactant molecules, when forming the same bond, are similar for both closed and open shell pathways. It may, in fact, be the manner in which the two reactant molecules approach one another that determines the nature of the pathway.

Initial M-C3 bond formation occurs via either a concerted (**CT**) or diradical (**DR1**) pathway. In the approach leading to the concerted pathway, the metallene and acetylene are parallel with one another and the acetylene is positioned directly under the metallene with a C1-Si-C2-C3 dihedral angle very close to 0° . This position would allow both acetylenic carbons to interact with the π^* orbital of the metallene. In such an alignment, the dipole of the metallene likely induces some polarization of the C \equiv C triple bond, which would facilitate the charge separation observed in the transition state. In addition, the ionic centres are in close proximity offering maximum electrostatic stabilization.

The approach that results in a diradical intermediate is quite different from that described for the concerted pathway; the C1-M-C2-C3 dihedral angle is much greater, close to 90°. Thus, the dipole from the metallene is perpendicular to the C≡C triple bond and does not induce polarization of acetylene. If the structures along **DR1** were to be ionic rather than diradical, an isolated positive charge would be placed on an sp² carbon. Furthermore, the distance between the ionic centres would be much larger than that in the concerted transition state, lowering the electrostatic stabilization of any charge accumulation.

The initial formation of the C1-C2 bond can proceed via a zwitterionic (**ZW**) or a diradical pathway (**DR2**). In the approach that leads to a zwitterion, the metallene acquires a *trans*-bent geometry and the metallene and acetylene are, again, almost parallel; however, acetylene is not aligned with the metallene dipole as the M-C1-C2-C3 dihedral angle is approaching 180°. Such an alignment is set up for nucleophilic attack from the metallenic carbon on acetylene. The developing ionic centres are not close together; however, presumably an sp² anion and a metalloid cation are better able to handle the charges than the opposite distribution of charge.

As the previously discussed diradical pathway (**DR1**), the approach for the other diradical pathway (**DR2**) has the metallene and acetylene nearly perpendicular, which leads to minimal polarization of the C≡C triple bond. Again, this approach is more suited to the formation of a diradical than a zwitterion.

Initial formation of a C-H bond, such as observed in the formation of the metallylacetylenes, also likely depends on the initial approach of the two reactants. The acetylenic C-H bond is aligned with the dipole of the M=C bond. Although this pathway

was concerted, a significant zwitterionic character developed during the course of the reaction, as was observed in the concerted cycloaddition pathway (CT). The alignment of the acetylenic C-H with the M=C may lead to a polarization of the C-H facilitating the formation the new C-H bond at the metallenic carbon.

4.5 Comparison to Experiment

A comparison of the reaction pathways for the addition of acetylene to silene and germene is presented in sections 4.5.1 and 4.5.2. The most probable mechanistic pathway based on the computational results is discussed along with a comparison to the experimental results.

4.5.1 Addition to Silene

Four competing cycloaddition pathways and a CH-insertion pathway were located for the addition of acetylene to silene. A comparison of the free energies of these pathways is shown in Figure 4.2. The calculated B3LYP and CCSD energy values (Tables 4.2 – 4.6) are in qualitative agreement with the relative free energies. The free energy profiles show that the two diradical pathways are competitive with DR1 being slightly favoured. The concerted, zwitterionic, and CH-insertion pathways have much higher free energy barriers to reaction.

Experimental evidence for a diradical intermediate has been reported by Milnes *et al.*²⁸ for the addition of alkynes to the relatively non-polar Brook silenes; the theoretical results presented here predict that a diradical mechanism is the lowest energy pathway for the addition of alkynes to polar silenes. This is surprising given the increased polarity of

the Si=C bond in the parent silene, as compared to a Brook silene.⁴⁰ It was hypothesized that the polarity would have a significant influence, and thus, a more polar silene would favour a zwitterionic mechanism of alkyne addition.²⁹

Ishikawa's group has investigated the addition of propyne to a model Brook silene, $(\text{H}_3\text{Si})_2\text{Si}=\text{C}(\text{OSiH}_3)\text{CH}_3$ at the B3LYP/6-31G* level. They located a single pathway of addition that was described as a "concerted but nonsynchronous process" that is more likely "viewed as a stepwise reaction with a diradical character";^{27e} however, it seems that spin-restricted DFT was used to calculate this pathway and a diradicaloid species may have been missed. Seemingly contradictory, this transition state, deemed diradical in character, was also described as possessing a significant charge transfer from the silene to the alkyne, consistent with a zwitterion. In fact, the transition state that was located by Ishikawa closely resembles that found for the concerted pathway (CT) of our study, in both structure and energy, in which a significant zwitterionic character was assigned to the transition state (CT-MC-a[‡]). In a later study by Ishikawa, the energies of isolated intermediate species from the addition of alkynes to the same model Brook silene were determined;^{27g} however, these intermediates were assigned to be diradicals without providing any evidence for an open-shell species (ie net spin densities) and no attempts were made to locate transition state structures. Although previous computational work on the addition of alkynes to silenes has been performed,^{27e,g} the results were ambiguous and incomplete. Here, the use of unrestricted DFT has enabled the location of lower energy, truly diradical pathways that may more accurately describe the addition of alkynes to silenes.

Insertion of the terminal C-H bond occurred preferentially during the reactions of 1,1-dimesitylneopentylsilene, a naturally polarized silene, with terminal alkynes; only a minor amount of cycloaddition was observed with phenylacetylene. Surprisingly, the CH-insertion pathway found computationally for the addition of acetylene to silene was the highest energy pathway located with a barrier of 42.4 kcal/mol as compared to 21.3 and 23.9 kcal/mol for the two diradical cycloaddition pathways. However, the presence of substituents and solvent may lower the energy required for CH-insertion.

4.5.2 Addition to Germene

The same four cycloaddition pathways as well as a CH-insertion pathway were located for the addition of acetylene to germene. A comparison of the free energies of these pathways is shown in Figure 4.3. The pathway involving the formation of a germyl radical (**DR2**) is the most energetically favourable, with all steps along the pathway being lower in energy than in the competitive routes. The B3LYP and CCSD energy values also indicate that the formation of a germyl radical along **DR2** is the favoured pathway. There have not been any previous computational investigations into the mechanism of alkyne additions to germenes for comparison; however, a zwitterionic mechanism was proposed in our previous reactivity study since cycloaddition was favoured with polar alkynes.³⁰ Although the free energy barrier of the zwitterionic pathway (**ZW**) for germene (31.4 kcal/mol) was lower than the analogous pathway for silene (36.1 kcal/mol), this energy barrier is significantly higher than either diradical pathway (25.4 and 18.2 kcal/mol). Interestingly, the nature of the zwitterionic intermediate located (**ZW-GeC-b**), with the anion localized on the alkenyl carbon (C3), matches that of the zwitterionic intermediate

proposed during the experimental study. Obviously, the substituents on the germene may have a significant impact on the mechanism of addition, but it is expected that the diradical pathway would still be competitive.

The free energy barrier for insertion of the acetylenic C-H bond across the germene is surprisingly high in energy (43.0 kcal/mol), as it was with silene. However, this mode of addition was prominent in the reactions between 1,1-dimesitylneopentylgermene and terminal alkynes.³⁰ Competition between cycloaddition and CH-insertion may be possible when the effects of substituents and solvent are considered.

4.6 Conclusions

We have examined the addition of acetylene to silene and germene in an effort to provide insight into the preferred mechanistic pathways for the addition of alkynes to polar metallenes. Both open- and closed-shell cycloaddition pathways were explored as well as a CH-insertion pathway. It was found that all pathways located for acetylene addition were available for both silene and germene. Contrary to our expectations, the two diradical pathways were more favoured energetically than either the zwitterionic or concerted pathway, and thus, are more probable. For silene, the two diradical cycloaddition pathways (**DR1** and **DR2**) were quite similar in energy in the gas phase, whereas for the germene, the diradical pathway involving the formation of a germyl radical (**DR2**) was the lowest energy route to cycloaddition. The CH-insertion reaction was found to be the highest energy pathway from the metallenes and acetylene. Alternative, lower energy pathways may exist for this reaction, but they could not be

located. Overall, the potential energy surface for acetylene addition is actually relatively flat, and thus, the substituents on the metallene and alkyne as well as the solvent may very well govern the pathway that is followed experimentally in solution.

The results of the current mechanistic study provide valuable insight into the nature of the pathways for the addition of alkynes to polar metallenes. Although the metallenes considered in this study are model systems, the examination of their reactivity provides a basis for comparison to future experimental results regarding the mechanism of addition of alkynes to silenes and germenenes.

4.7 References

1. West, R.; Fink, M. J.; Michl, J. *Science* **1981**, *214*, 1343.
2. (a) Brook, A. G.; Abdesaken, F.; Gutekunst, B.; Gutekunst, G.; Kallury, R. K. M. R. *J. Chem. Soc., Chem. Commun.* **1981**, 191; (b) Brook, A. G.; Nyburg, S. C.; Abdesaken, F.; Gutekunst, B.; Gutekunst, G.; Kallury, R. K. M. R.; Poon, Y. C.; Chang, Y. M.; Wong-Na, W. *J. Am. Chem. Soc.* **1982**, *104*, 5667.
3. Masamune, S.; Hanzawa, Y.; Williams, D. J. *J. Am. Chem. Soc.* **1982**, *104*, 6136.
4. Meyer, H.; Baum, G.; Massa, W.; Berndt, A. *Angew. Chem., Int. Ed. Engl.* **1987**, *26*, 798.
5. Couret, C.; Escudié, J.; Satgé, J. *J. Am. Chem. Soc.* **1987**, *109*, 4411.
6. For reviews on disilenes see: (a) West, R. *Angew. Chem., Int. Ed. Engl.* **1987**, *26*, 1201; (b) Weidenbruch, M. *Coord. Chem. Rev.* **1994**, *130*, 275; (c) Okazaki, R.; West, R. *Adv. Organomet. Chem.* **1996**, *39*, 231; (d) Weidenbruch, M. *The Chemistry of Organic Silicon Compounds*; Rappoport, Z.; Apeloig, Y., Eds.; Wiley & Sons: New York, 2001; Vol. 3, p391.

7. For reviews on digermenes see: (a) Barrau, J.; Escudié, J.; Satgé, J. *Chem. Rev.* **1990**, *90*, 283; (b) Escudié, J.; Couret, C.; Ranaivonjatovo, H.; Satgé, J. *Coord. Chem. Rev.* **1994**, *130*, 427; (c) Baines, K. M.; Stibbs, W. G. *Adv. Organomet. Chem.* **1996**, *39*, 275; (d) Escudié, J.; Ranaivonjatovo, H. *Adv. Organomet. Chem.* **1999**, *44*, 113; (e) Tokitoh, N.; Okazaki, R. *The Chemistry of Organic Germanium, Tin, and Lead Compounds*; Rappoport, Z., Ed.; Wiley & Sons: Chichester, 2002; Vol. 2, p843.

8. For reviews on silenes see: (a) Gusel'nikov, L. E.; Nametkin, N. S. *Chem. Rev.* **1979**, *79*, 529; (b) Raabe, G.; Michl, J. *Chem. Rev.* **1985**, *85*, 419; (c) Brook, A. G.; Baines, K. M. *Adv. Organomet. Chem.* **1986**, *25*, 1; (d) Brook, A. G.; Brook, M. A. *Adv. Organomet. Chem.* **1996**, *39*, 71; (e) Müller, T.; Ziche, W.; Auner, N. *The Chemistry of Organic Silicon Compounds*; Rappoport, Z.; Apeloig, Y., Eds.; Wiley & Sons: New York, 1998; Vol. 2, Chapter 16; (f) Morkin, T. L.; Owens, T. R.; Leigh, W. J. *The Chemistry of Organic Silicon Compounds*; Rappoport, Z.; Apeloig, Y., Eds.; Wiley & Sons: New York, 2001; Vol. 3, Chapter 17; (g) Ottosson, H.; Eklöf, A. M. *Coord. Chem. Rev.* **2008**, *252*, 1287.

9. For reviews on germenenes see: (a) Wiberg, N. *J. Organomet. Chem.* **1984**, *273*, 141; (b) Escudié, J.; Couret, C.; Ranaivonjatovo, J. *Coord. Chem. Rev.* **1998**, *180*, 565. Also, see reference 7a.

10. (a) Morkin, T. L.; Leigh, W. J. *Acc. Chem. Res.* **2001**, *34*, 129; (b) Owens, T. R.; Grinyer, J.; Leigh, W. J. *Organometallics* **2005**, *24*, 2307; (c) Leigh, W. J.; Owens, T. R.; Bendikov, M.; Zade, S. S.; Apeloig, Y. *J. Am. Chem. Soc.* **2006**, *128*, 10772.

11. (a) Toltl, N. P.; Leigh, W. J. *J. Am. Chem. Soc.* **1998**, *120*, 1172; (b) Leigh, W. J.; Potter, G. D.; Huck, L. A.; Bhattacharya, A. *Organometallics* **2008**, *27*, 5948.

12. Sakurai, J. *The Chemistry of Organic Silicon Compounds*; Rappoport, Z., Apeloig, Y., Eds.; Wiley & Sons: New York, 1998; Vol. 2, p 827.

13. (a) Dixon, C. E.; Hughes, D. W.; Baines, K. M. *J. Am. Chem. Soc.* **1998**, *120*, 11049; (b) Baines, K. M.; Dixon, C. E.; Samuel, M. S. *Phosphorus, Sulfur, Silicon Relat. Elem.* **1999**, *150-151*, 393; (c) Samuel, M. S.; Jenkins, H. A.; Hughes, D. W.; Baines, K. M.

Organometallics **2003**, *22*, 1603; (d) Samuel, M. S.; Baines, K. M. *J. Am. Chem. Soc.* **2003**, *125*, 12702; (e) Milnes, K. K.; Baines, K. M. *Organometallics* **2007**, *26*, 2392.

14. (a) Sluggett, G. W.; Leigh, W. J. *J. Am. Chem. Soc.* **1992**, *114*, 1195; (b) Leigh, W. J.; Bradaric, C. J.; Sluggett, G. W. *J. Am. Chem. Soc.* **1993**, *115*, 5332; (c) Leigh, W. J.; Sluggett, G. W. *Organometallics* **1994**, *13*, 269; (d) Toltl, N. P.; Leigh, W. J. *Organometallics* **1996**, *15*, 2554; (e) Bradaric, C. J.; Leigh, W. J. *Organometallics* **1998**, *17*, 645.

15. (a) Yu, T.; Deng, L.; Zhao, C.; Li, Z.; Xi, Z. *Tetrahedron Lett.* **2003**, *44*, 677; (b) Sun, X.; Wang, C.; Li, Z.; Zhang, S.; Xi, Z. *J. Am. Chem. Soc.* **2004**, *126*, 7172; (c) Jin, C. K.; Yamada, T.; Sano, S.; Shiro, M.; Nagao, Y. *Tetrahedron Lett.* **2007**, *48*, 3671; (d) Liu, J. H.; Zhang, W. X.; Xi, Z. *Chinese J. Org. Chem.* **2009**, *29*, 491.

16. Mohseni-Ala, J.; Auner, N. *Inorg. Chem. Acta* **2006**, *359*, 4677.

17. (a) Bamford, W. R.; Lovie, J. C.; Watt, J. A. C. *J. Chem. Soc. C* **1966**, 1137; (b) Nametkin, N. S.; Vdovin, V. M.; Finkel'shtein, E. S.; Yatsenko, M. S.; Ushakov, N. V. *Vysamol. Soedin., Ser. B.* **1969**, *11*, 207; (c) Fraenkel, G.; Winchester, W. R. *Organometallics* **1990**, *9*, 1314; (d) Theurig, M.; Weber, W. P. *Polym. Bull.* **1992**, *28*, 17.

18. Nakadaira, Y.; Sato, R.; Sakurai, H. *Chem. Lett.* **1985**, 643.

19. (a) De Young, D. J.; West, R. *Chem. Lett.* **1986**, *6*, 883; (b) De Young, D. J.; Fink, M. J.; West, R. *Main Group Met. Chem.* **1987**, *10*, 19.

20. Gottschling, S. E.; Grant, T. N.; Milnes, K. K.; Jennings, M. C.; Baines, K. M. *J. Org. Chem.* **2005**, *70*, 2686.

21. Gottschling, S. E.; Milnes, K. K.; Jennings, M. C.; Baines, K. M. *Organometallics* **2005**, *24*, 3811.

22. Gottschling, S. E.; Jennings, M. C.; Baines, K. M. *Can. J. Chem.* **2005**, *83*, 1568.

23. (a) Nefedov, O. M.; Egorov, M. P.; Gal'minas, A. M.; Kolesnikov, S. P.; Krebs, A.; Berndt, J. *J. Organomet. Chem.* **1986**, *301*, C21; (b) Batcheller, S. A.; Masamune, S.

Tetrahedron Lett. **1988**, *29*, 3383; (c) Ando, W.; Tsumuraya, T. *J. Chem. Soc., Chem. Commun.* **1989**, 770; (d) Tsumuraya, T.; Kabe, Y.; Ando, W. *J. Organomet. Chem.* **1994**, *482*, 131; (e) Weidenbruch, M.; Hagedorn, A.; Peters, K.; von Schnering, H. G. *Angew. Chem. Int. Ed. Engl.* **1995**, *34*, 1085.

24. Billeb, G.; Bauer, H.; Neumann, W. P.; Weisbeck, M. *Organometallics* **1992**, *11*, 2069.

25. Hurni, K. L. MSc Thesis, UWO, 2007.

26. (a) Brook, A. G.; Baumegger, A.; Lough, A. J. *Organometallics* **1992**, *11*, 3088; (b) Lassacher, P.; Brook, A. G.; Lough, A. J. *Organometallics* **1995**, *14*, 4359.

27. (a) Naka, A.; Ishikawa, M.; Matsui, S.; Ohshita, J.; Kunai, A. *Organometallics* **1996**, *15*, 5759; (b) Naka, A.; Ishikawa, M. *Organometallics* **2000**, *19*, 4921; (c) Naka, A.; Ishikawa, M. *J. Organomet. Chem.* **2000**, *611*, 248; (d) Naka, A.; Ikadai, J.; Shingo, M.; Yoshizawa, K.; Kondo, Y.; Kang, S.-Y.; Ishikawa, M. *Organometallics* **2002**, *21*, 2033; (e) Yoshizawa, K.; Kondo, Y.; Kang, S.-Y.; Naka, A.; Ishikawa, M. *Organometallics* **2002**, *21*, 3271; (f) Naka, A.; Ishikawa, M. *Chem. Lett.* **2002**, *3*, 364; (g) Naka, A.; Ohnishi, H.; Miyahara, I.; Hirotsu, K.; Shiota, Y.; Yoshizawa, K.; Ishikawa, M. *Organometallics* **2004**, *23*, 4277; (h) Naka, A.; Ohnishi, H.; Ohshita, J.; Ikadai, J.; Kunai, A.; Ishikawa, M. *Organometallics* **2005**, *24*, 5356; (i) Ohshita, J.; Ohnishi, H.; Naka, A.; Senba, N.; Ikadai, J.; Kunai, A.; Kobayashi, H.; Ishikawa, M. *Organometallics* **2006**, *25*, 3955; (j) Naka, A.; Motoike, S.; Senba, N.; Ohshita, J.; Kunai, A.; Yoshizawa, K.; Ishikawa, M. *Organometallics* **2008**, *27*, 2750.

28. (a) Milnes, K. K.; Jennings, M. C.; Baines, K. M. *J. Am. Chem. Soc.* **2007**, *128*, 2491; (b) Milnes, K. K.; Baines, K. M. *Can. J. Chem.* **2009**, *87*, 307.

29. Milnes, K. K.; Pavelka, L. C.; Baines, K. M. *manuscript in preparation*.

30. For details on the addition of alkynes to 1,1-dimesitylneopentylgermene see Chapter 3 of this thesis.

31. Mosey, N. J.; Baines, K. M.; Woo, T. K. *J. Am. Chem. Soc.* **2002**, *124*, 13306.

32. Stephens, P. J.; Devlin, F. J.; Chabalowski, C. F.; Frisch, M. J. *J. Phys. Chem.* **1994**, *98*, 11623.
33. Becke, A. D. *J. Chem. Phys.* **1993**, *98*, 5648.
34. Lee, C.; Yang, W.; Parr, R. G. *Phys. Rev. B* **1988**, *37*, 785.
35. *Gaussian 03*, Revision C.02, Frisch, M. J. *et al.* (Gaussian, Wallingford, CT, 2004).
36. Wiberg, K. B. *Tetrahedron* **1968**, *24*, 1083.
37. Glendening, E. D.; Reed, A. E.; Carpenter, J. E.; Weinhold, F. *NBO Version 3.1*.
38. Mulliken, R. S. *J. Chem. Phys.* **1955**, *23*, 1833.
39. Reed, A. E.; Weinstock, R. B.; Weinhold, F. *J. Chem. Phys.* **1985**, *83*, 735.
40. (a) Apeloig, Y.; Karni, M. *J. Am. Chem. Soc.* **1984**, *106*, 6676; (b) Bendikov, M.; Quadt, S. R.; Rabin, O.; Apeloig, Y. *Organometallics* **2002**, *21*, 3930; (c) Ottosson, H. *Chem. Eur. J.* **2003**, *9*, 4144.
41. (a) Dema, A. C.; Lukehart, C. M.; McPhail, A. T.; McPhail, D. R. *J. Am. Chem. Soc.* **1989**, *111*, 7615; (b) Auner, N.; Seidenschwarz, C.; Herdtweck, E. *Angew. Chem. Int. Ed. Engl.* **1991**, *30*, 1151; (c) Xi, Z.; Fischer, R.; Hara, R.; Sun, W.; Obora, Y.; Suzuki, N.; Nakajima, K.; Takahashi, T. *J. Am. Chem. Soc.* **1997**, *119*, 12842; (d) Yan, D.; Mohsseni-Ala, J.; Auner, N.; Bolte, M.; Bats, J. W. *Chem. Eur. J.* **2007**, *13*, 7204.
42. Becerra, R.; Walsh, R. In *The Chemistry of Organosilicon Compounds*; Rappoport, Z., Apeloig, Y., Eds.; Wiley & Sons: New York, 1998: Vol 2, p153.
43. (a) Shaulov, Y. K.; Federov, A. K.; Zueva, G. Y.; Borisjuk, G. V.; Genchel, V. G. *Russ. J. Phys. Chem. Engl. Ed.* **1970**, *44*, 1181; (b) Jackson, R. A. *J. Organomet. Chem.* **1979**, *166*, 17.

Chapter 5

Addition Polymerization of a Germene and Silene: Synthesis of a Polygermene and Polysilene *

5.1 Introduction

Addition polymerization of vinylic monomers, a standard protocol for the preparation of organic polymers, has only recently been applied to the synthesis of inorganic polymers. The development of this important method for inorganic-based polymers was hindered by the lack of or difficulty in the synthesis of suitable monomers. In fact, much of the research on unsaturated inorganic, primarily main group, compounds over the last 30 years has focussed on understanding how to *prevent* oligomerization reactions. One key strategy involves the use of bulky substituents to kinetically stabilize the doubly-bonded species;¹ it follows that such compounds would not be suitable as monomers for polymer synthesis. However, in a landmark series of papers, Gates *et al.* have shown that readily accessible stable phosphalkenes ($\text{RP}=\text{CR}_2$) with relatively bulky substituents can indeed undergo addition polymerization using radical or anionic initiators to form poly(methylenephosphines), a new and interesting class of polymers.² Furthermore, the phosphalkenes undergo living anionic polymerization at ambient temperatures using organolithium reagents as initiators.³ This discovery has opened up numerous exciting possibilities for the synthesis of novel copolymers containing the

* Versions of sections 5.2 and 5.3 of this chapter have been published. Laura C. Pavelka, Simon J. Holder, Kim M. Baines. Addition Polymerization of a Germene: Synthesis of a Polygermene. *Chem. Commun.* **2008**, 2346; Laura C. Pavelka, Kaarina K. Milnes, Kim M. Baines. Addition Polymerization of a Silene: Synthesis of a Polysilene. *Chem. Mat.* **2008**, *20*, 5948.

functional poly(methylenephosphine) block. Block copolymers, in general, and particularly those with inorganic segments, have been the subject of intense research of late due to the spontaneous self-assembly of the polymers into varied and interesting nanostructures.⁴

We have long been interested in the chemistry of multiply-bonded silicon and germanium derivatives and were intrigued by the possibility that silenes ($R_2Si=CR_2$) and germenes ($R_2Ge=CR_2$) may also be able to undergo addition polymerization, which would provide access to polymers with a regularly alternating silicon- or germanium-carbon backbone, which, based on the nature of the monomer, can be termed polysilenes, $[SiC]_n$, or polygermenes, $[GeC]_n$, respectively. Although silenes and germenes have been studied extensively for many years, there are no reports on their polymerization reactions.^{5,6}

The poly(silylenemethylene)s, $[R_2SiCH_2]_n$,⁷ are well-known and of particular interest due to the repeating stoichiometric ratio of silicon to carbon in the backbone, which has led to their use as effective thermal precursors to silicon carbide,^{8,9} an important technological material.¹⁰ High molecular weight poly(silylenemethylene)s are commonly obtained by the ring-opening polymerization of 1,3-disilacyclobutanes;⁷ however, this method is limited by the availability of appropriate ring systems. Furthermore, the linear polymers obtained using this method generally give low to moderate ceramic yields upon pyrolysis. Alternatively, low molecular weight polymers with broad polydispersities can be synthesized by the reductive coupling of chloromethylchlorosilanes¹¹ or dihalosilanes with dihalomethanes.¹² The highly cross-

linked polymers derived from chloromethylchlorosilanes have been shown to be excellent ceramic precursors.¹¹

In contrast, polymers with a regularly alternating germanium-carbon backbone are not known. The addition polymerization of germenes may provide an entry into a hitherto unknown $[\text{GeC}]_n$ polycarbogermane system. The information available on the pyrolysis of polycarbogermanes is relatively scarce in comparison to polycarbosilanes.¹³

With the high level of interest in the addition polymerization of main group alkene analogues and in the chemistry of inorganic polymers, we now report on the addition polymerization of a solution stable germene, 1,1-dimesitylneopentylgermene (**5.1**), and silene, 1,1-dimesitylneopentylsilene (**5.2**), as a new approach to polymers with a $[\text{GeC}]_n$ and $[\text{SiC}]_n$ backbone, respectively.

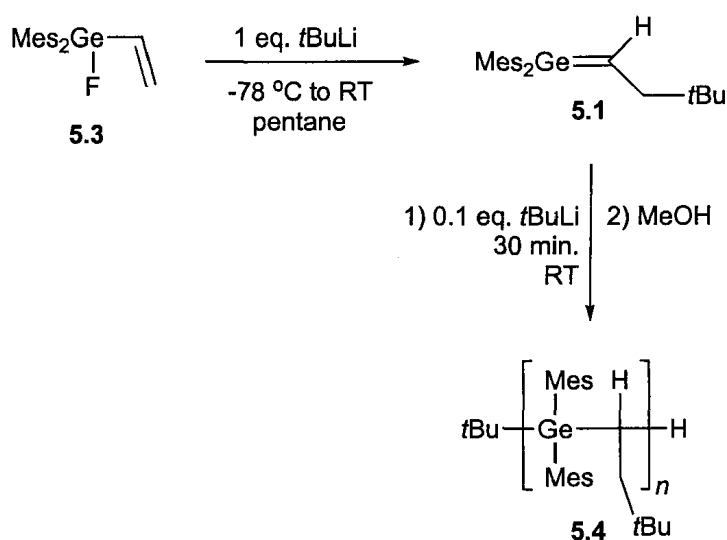
5.2 Synthesis of a Polygermene

The anionic addition polymerization of germene **5.1** was investigated using *t*BuLi as the initiator. The results are presented in section 5.2.1 (synthesis) and section 5.2.2 (NMR spectroscopic characterization). These sections are followed by a discussion of the polymerization mechanism in section 5.2.3 and the polymerization of germene **5.1** in the absence of an initiator in section 5.2.4.

5.2.1 Polymerization of 1,1-Dimesitylneopentylgermene (**5.1**)

A pale yellow pentane solution of 1,1-dimesitylneopentylgermene (**5.1**) was prepared from the addition of *t*-butyllithium (1 equiv) to a solution of fluorovinylgermane **5.3**.¹⁴ Germene **5.1** was stable in solution for several hours; however, upon addition of *t*-

butyllithium (0.1 equiv) to the solution (Scheme 5.1), the colour of the solution changed from pale to bright yellow. After 30 minutes, methanol was added and the bright yellow colour dissipated immediately. The solvents were removed and the residue was dissolved in CH_2Cl_2 . A white solid precipitated from the CH_2Cl_2 solution upon the addition of methanol; the solid was purified by re-precipitation. The air stable material (**5.4**) was isolated in 45% yield.



Scheme 5.1 Polymerization of germene **5.1**.

The ^1H NMR spectrum of the solid displayed broad resonances consistent with a polymeric substance. No resonances attributable to the methanol adduct of germene **5.1**¹⁴ were observed in the residue or the precipitated material, indicating that all of the germene had been consumed prior to the addition of methanol. The rapid polymerization of **5.1** is in contrast to the much slower polymerization of phosphalkenes.^{2,3} The molecular weight of the polymer was determined by GPC in THF; two distinct fractions were observed indicating a bimodal molecular weight distribution. The number-average molecular weights (M_n) were estimated to be 36 000 gmol^{-1} and 7 100 gmol^{-1} (vs.

polystyrene) with polydispersity indices ($PDI = M_w/M_n$) of 1.5 and 1.1, respectively. The bimodal molecular weight distribution was reproducible; similar M_n values were achieved. Polymer **5.4** was determined to be amorphous in nature based on the DSC results where only a glass transition was observed ($T_g = 144$ °C). The thermal stability of polymer **5.4** was determined using TGA. The material was stable to weight loss until 290 °C, at which point 87 % of the mass was lost.

Polymer **5.4** can also be synthesized in one step from the addition of excess *t*-butyllithium (1.1 equiv) to fluorovinylgermane **5.3** in pentane at -78 °C. Upon warming, germene **5.1** formed quantitatively as noted by the pale yellow colour of the solution. When the solution reached room temperature, germene **5.1** then reacted with the remainder of the *t*-butyllithium, as indicated when the colour of the solution changed from pale to bright yellow. Quantitative formation of germene **5.1** under these conditions was verified in a separate experiment in which methanol was added to the solution immediately upon reaching room temperature; the methanol adduct of **5.1** was the only product observed.

After precipitation, the polymer was obtained in 62% yield. The number-average molecular weight (M_n) of the polymer prepared by this method was higher than that prepared previously ($M_n = 39\ 000\ \text{g mol}^{-1}$, $PDI = 2.0$). The broad PDI is possibly a result of initiation over an extended time period during the start of the polymerization resulting from the gradual warming of the solution. The addition of one portion of *t*-butyllithium is the preferred method for the formation of polymer **5.4** since monomodal higher molecular weight polymer was isolated in greater yield with fewer experimental manipulations.

5.2.2 NMR Spectroscopic Characterization of Polygermene 5.4

The polymeric material (5.4) was characterized by one- and two- dimensional NMR spectroscopy. The ^{13}C NMR spectrum of 5.4 was particularly useful in elucidating the structure of the polymer. The signals in the ^{13}C NMR spectrum of 5.4 (Figure 5.1) were readily assigned by comparison of the chemical shifts with those of the model compound, $\text{Mes}_2\text{Ge}(t\text{Bu})\text{CH}_2\text{CH}_2t\text{Bu}$.⁸ For example, the $\text{Ge}\underline{\text{C}}\text{H}$ and $\text{GeCH}\underline{\text{C}}\text{H}_2$ carbons in polymer 5.4 were observed to resonate at 16.3 and 38.7 ppm, respectively, compared to 14.4 and 40.5 ppm in the model compound. Similarly, signals attributable to the $(\text{C}(\text{CH}_3)_3)$ moiety, the *o*- and *p*-methyls and the aromatic carbons of the mesityl groups could be assigned. However, in the polymer, two sets of mesityl signals are observed resulting from *meso* and *racemic* replacements between the stereogenic carbon centres. The assignments were confirmed by both 2D ^{13}C - ^1H correlation spectroscopy and DEPT spectroscopy. There were no remaining unassigned signals in the ^{13}C NMR spectrum of 5.4, indicating a regular alternating $[\text{GeC}]_n$ backbone.

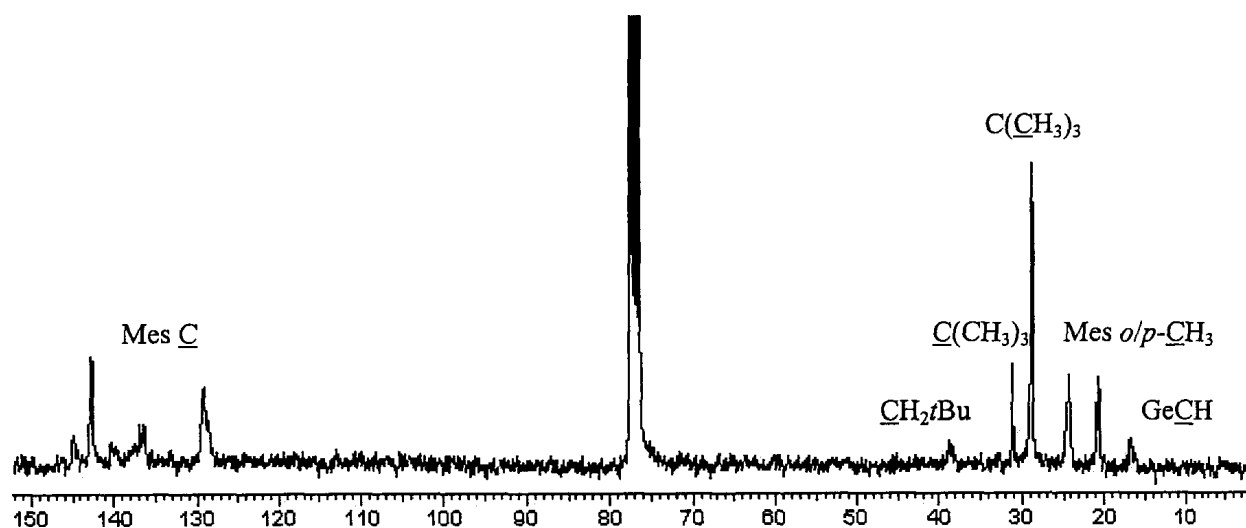


Figure 5.1 ^{13}C NMR spectrum of polygermene 5.4.

5.2.3 Polymerization Mechanism

The regioselective addition of *t*-butyllithium to germene **5.1** dissolved in ether has been reported; upon addition of water, only germane, $\text{Mes}_2\text{Ge}(t\text{Bu})\text{CH}_2\text{CH}_2t\text{Bu}$, was isolated.¹⁴ Presumably, the polymerization of **5.1** is initiated by the regioselective addition of *t*-butyllithium to the germene to give $\text{Mes}_2\text{Ge}(t\text{Bu})\text{CH}(\text{Li})\text{CH}_2t\text{Bu}$; in pentane, the carbanion rapidly adds to the germanium centre of another germene (**5.1**) to propagate the growth of the polymer. The decreased stability of the germene, along with a less sterically hindered propagating carbanion, likely contribute to the high reactivity. The bimodal distribution of polymer **5.4** synthesized by the addition of 0.1 equiv *t*BuLi to the germene is indicative of more than one polymerization mechanism. Other possible concurrent mechanisms may include radical polymerization by electron transfer to **5.1** or even ring-opening polymerization involving the intermediate formation of germene dimers (**5.5a** and **5.5b**, *vide infra*).¹⁵

5.2.4 Polymerization of Germene 5.1 in the Absence of an Initiator

Germene **5.1** slowly reacted to give head-to-tail cyclic dimers **5.5a** and **5.5b**, an isomeric germane (**5.6**), and polymeric material (Figure 5.2) when left in solution (C_6D_6) for several days. The head-to-head cyclic dimer was not observed. The two head-to-tail cyclic dimers (**5.5a,b**) were consistently formed in a 1:1 ratio. However, the relative ratio of **5.5a** and **b** to germane **5.6**, presumably formed via a hydride shift, varied depending on the concentration of the germene. Germane **5.6** was favoured when the initial solution was dilute, whereas in concentrated solutions, the cyclic dimers (**5.5a,b**) were formed almost exclusively. The *trans* dimer (**5.5a**) selectively crystallized from a concentrated

C₆D₆ solution. The molecular structure of **5.5a** was determined by X-ray crystallography (Figure 5.3). The 1,3-digermacyclobutane ring lies in a plane. The intracyclic bond angles are close to 90° and the intracyclic Ge – C bond lengths, 2.016(2) and 2.041(2) Å, are long but still well within the normal Ge – C single bond length range (1.90 – 2.05 Å).¹⁶ The metrics of **5.5a** are comparable to those of other crystallographically characterized 1,3-digermacyclobutanes.¹⁷ DSC analysis was performed on **5.5a** and on a mixture of **5.5a/5.5b**. An irreversible endotherm was observed in each sample with an onset temperature of 290.4 and 248.7 °C, respectively. Despite the irreversibility, the endotherms appear to be melting transitions. In the case of **5.5a**, the endotherm coincides with the observed melting point (280 °C), which was immediately followed by decomposition. No exotherm indicative of a thermal ring opening polymerization was observed.

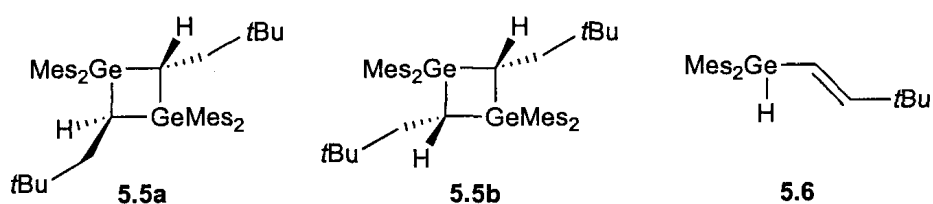


Figure 5.2 Cyclic dimers (**5.5a,b**) and isomeric germane (**5.6**) of germene **5.1**.

The polymerization of germene **5.1** in the absence of an anionic initiator occurred slowly; the polymer was formed as a minor component of the product mixture (25 wt%) under these conditions. The polymer was isolated from the mixture by precipitation from CH₂Cl₂ with methanol. The ¹H and ¹³C NMR spectra of the polymer obtained under these conditions were identical to the spectroscopic data of **5.4**. The exclusive formation of head-to-tail cyclic dimers (**5.5a,b**) under the same conditions was also taken as evidence

for a polymer with an alternating $[\text{GeC}]_n$ backbone. The molecular weight of the polymer was lower than that obtained using an anionic initiator and had a broader polydispersity ($M_n = 21\,000\text{ gmol}^{-1}$ vs. polystyrene; PDI = 2.5). This polymerization is presumably the result of a radical polymerization process, though further experiments are needed to verify this.¹⁸

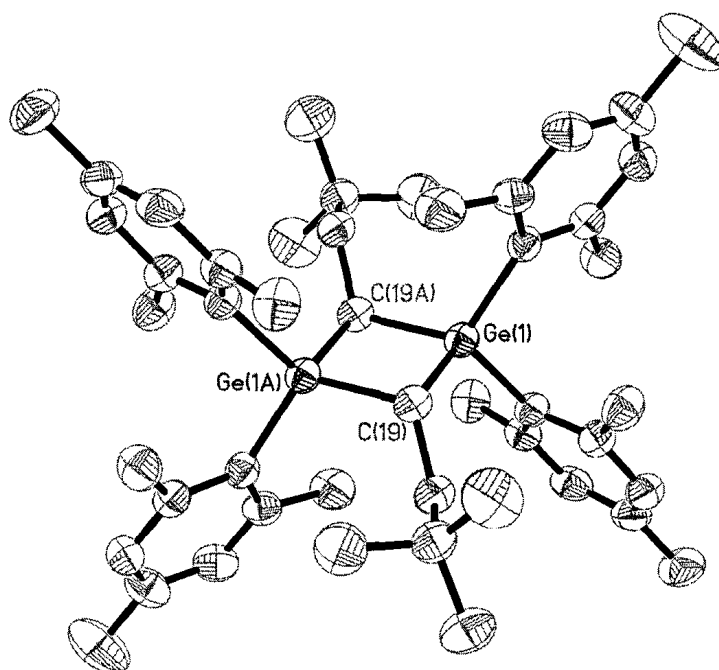


Figure 5.3 Thermal ellipsoid plot (50% probability surface) of **5.5a**. Two molecules of **5.5a** are present in the asymmetric unit; parameters are given for one of the two molecules. Atoms labeled with 'A' are located at equivalent positions ($-x, -y, -z$). Hydrogen atoms are omitted for clarity. Selected bond lengths (\AA) and angles (deg): $\text{Ge}(1)\text{-C}(19) = 2.041(2)$, $\text{Ge}(1)\text{-C}(19\text{A}) = 2.016(2)$, $\text{C}(19)\text{-Ge}(1)\text{-C}(19\text{A}) = 90.11(10)$.

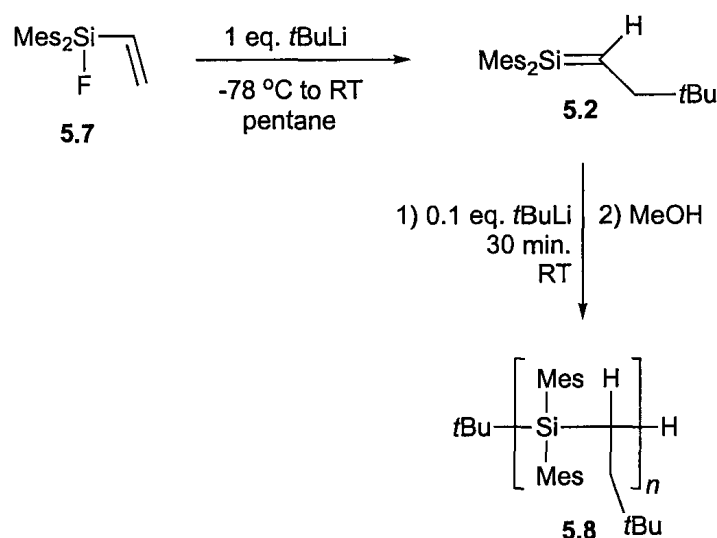
5.3 Synthesis of a Polysilene

The anionic addition polymerization of silene **5.2** was investigated using *t*BuLi as the initiator. The results are presented in section 5.3.1 (synthesis) and section 5.3.2 (NMR spectroscopic characterization). These sections are followed by a discussion of the

polymerization mechanism in section 5.3.3 and the polymerization of silene **5.2** in the absence of an initiator in section 5.3.4.

5.3.1 Polymerization of 1,1-Dimesitylneopentylsilene (**5.2**)

A pentane solution of fluorovinylsilane **5.7** was converted to 1,1-dimesitylneopentylsilene (**5.2**) upon the addition of *t*-butyllithium (1 equiv).¹⁹ Silene **5.2** is stable in pentane;¹⁹ however, upon the addition of *t*-butyllithium (0.1 equiv) the colour of the pale orange solution deepened and persisted until the reaction was quenched with methanol (Scheme 5.2).



Scheme 5.2 Polymerization of silene **5.2**.

The methanol adduct of the silene, $\text{Mes}_2\text{Si}(\text{OMe})\text{CH}_2\text{CH}_2t\text{Bu}$, was not observed in the crude product mixture, indicative of complete consumption of silene **5.2**. The product (**5.8**) was isolated as a white, air-stable solid after precipitation from a CH_2Cl_2 solution with methanol (50% yield). The ^1H NMR spectrum of the precipitate displayed several broad resonances consistent with polymeric material. The molecular weight of **5.8**

was estimated by GPC in THF. The M_n was determined to be 28 000 g mol^{-1} with a PDI of 1.2. DSC analysis of polymer **5.8** was performed; only a glass transition was observed ($T_g = 153\text{ }^\circ\text{C}$) indicative of an amorphous polymer. The thermal stability of polymer **5.8** was determined using TGA; weight loss was observed between 325 and 525 $^\circ\text{C}$. The weight of the residue remaining at 800 $^\circ\text{C}$ was 12 % of the original weight and is composed primarily of carbon as demonstrated by EDX analysis. The high carbon content is not surprising given the large organic substituents on the polymer backbone.

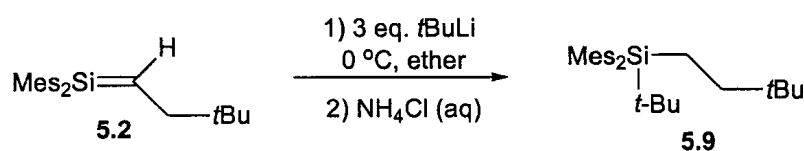
Polymer **5.8** can also be synthesized directly by the addition of excess *t*-butyllithium (1.1 equiv) to fluorovinylsilane **5.7** at $-78\text{ }^\circ\text{C}$. After warming to room temperature, the colour of the solution was pale orange and a precipitate formed (LiF) indicating the formation of silene **5.2**. Indeed, if methanol was added to the solution at this stage, the methanol adduct of the silene, $\text{Mes}_2\text{Si}(\text{OMe})\text{CH}_2\text{CH}_2t\text{Bu}$, was isolated as the only product. Without the addition of methanol, a deep orange colour developed indicating formation of the polymer.

The polymer was isolated in 65% yield after precipitation and purification. The number-average molecular weight of polymer synthesized in one step was similar to that prepared from the addition of *t*BuLi to silene **5.2** ($M_n = 32\ 000\ \text{g mol}^{-1}$; PDI = 1.1). The one step method for the preparation of polymer **5.8** from silane **5.7** is preferred since the polymer was isolated in higher yield with fewer experimental manipulations.

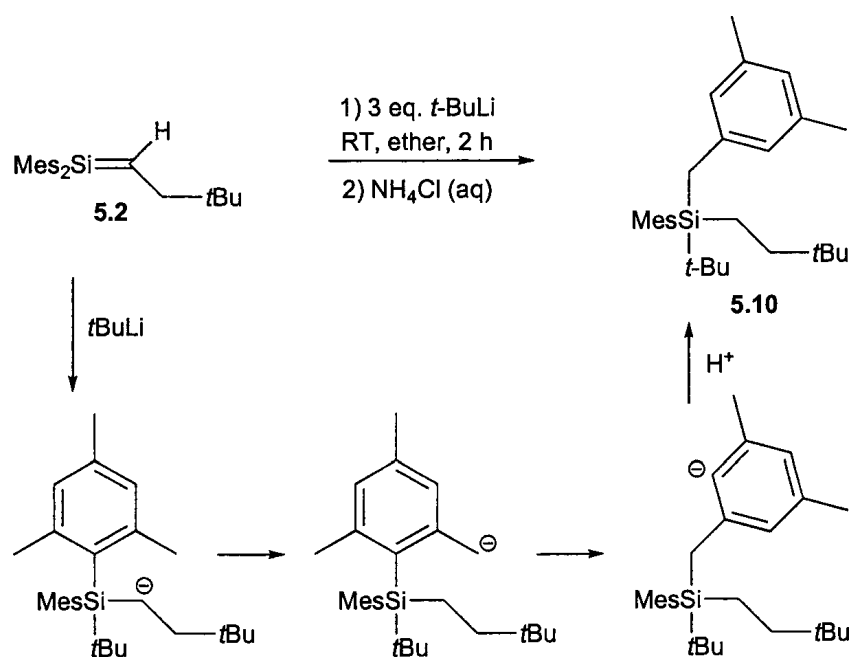
5.3.2 NMR Spectroscopic Characterization of Polysilene **5.8**

To aid in the spectroscopic analysis of **5.8**, $\text{Mes}_2\text{Si}(t\text{Bu})\text{CH}_2\text{CH}_2t\text{Bu}$ (**5.9**) was synthesized to model the repeating unit. When excess *t*-butyllithium (3 equiv) was added

to silene **5.2** in ether at 0 °C followed immediately by the addition of aqueous ammonium chloride, compound **5.9** was produced quantitatively (Scheme 5.3). In contrast, when the procedure for the synthesis of the analogous germanium compound was followed,¹⁴ where excess *t*-butyllithium was added to silene **5.2** in ether at room temperature, the isomeric *t*-butylsilane (**5.10**) was produced (Scheme 5.4). It seems likely that the initial α -silyl anion, formed by the regioselective addition of *t*-butyllithium to silene **5.2**,²⁰ deprotonates an *o*-methyl group to form a benzylic anion, which undergoes an anionic 1,3-silyl shift. Presumably, the additional steric strain around silicon, relative to germanium, promotes this unusual anionic 1,3-C,C silyl shift.



Scheme 5.3 Synthesis of silane **5.9**.



Scheme 5.4 Synthesis of silane **5.10**.

The polymeric material (**5.8**) was characterized by one- and two-dimensional NMR spectroscopy. All of the signals in the ^1H NMR spectrum of **5.8** could be assigned based on their chemical shift and integration and were consistent with the proposed structure. However, the broadness of the signals leads to significant overlap between many of the resonances, and so, detailed structural information could not be extracted.

The ^{29}Si and ^{13}C NMR spectra of **5.8** were more useful in elucidating the structure of the polymer. The strongest ^{29}Si signal observed in the $^1\text{H} - ^{29}\text{Si}$ gHMBC spectrum of **5.8** (-7.5 ppm) showed a correlation to the ^1H signal at 6.5 ppm assigned to the aromatic hydrogen of the mesityl group (Mes-H). No correlations to the Si-CH or Si-CHCH₂ hydrogens were observed presumably due to the broadness of the ^1H signals. Two weaker ^{29}Si signals, at 2.1 and 10.1 ppm, correlated to the ^1H signals at 0.87 and 0.89 ppm, respectively. These ^{29}Si signals could represent the two different types of end group silicon environments: Si-C(CH₃)₃ and Si-CH₂CH₂*t*Bu. The characteristics of the signal at 2.1 ppm are consistent with the ^{29}Si spectroscopic data of compound **5.9**, where the ^{29}Si signal (1.2 ppm) correlated strongly to the ^1H signal at 1.17 ppm, assigned to the Si-C(CH₃)₃ hydrogens. The chemical shift of the ^{29}Si signal at 10.1 ppm is similar to that of **5.10** (4.0 ppm) indicating a rearranged terminal mesityl group. The difference in the steric bulk of the substituents may account for the observed difference in the chemical shift. The ^{13}C NMR spectrum of **5.8** (Figure 5.4) was compared to that of compound **5.9** as well as to the ^{13}C NMR spectrum of the analogous germanium polymer **5.4**²¹ (Figure 5.1). All of the signals could be assigned on the basis of their chemical shifts. For example, the Si-CH and Si-CHCH₂ carbons in **5.8** were observed to resonate at 14.0 and 38.2 ppm, respectively, compared to 16.3 and 38.7 ppm in germanium polymer **5.4** and

11.9 and 39.9 ppm in compound **5.9**. Also, two sets of mesityl signals were observed in both **5.8** and **5.4** due to the chirality of the backbone carbon. The assignments were confirmed by both $^{13}\text{C} - ^1\text{H}$ correlation spectroscopy and DEPT spectroscopy. Both the ^{29}Si and ^{13}C NMR spectra of **5.8** are consistent with a dimesityl substituted silicon within a regular alternating silicon-carbon backbone.

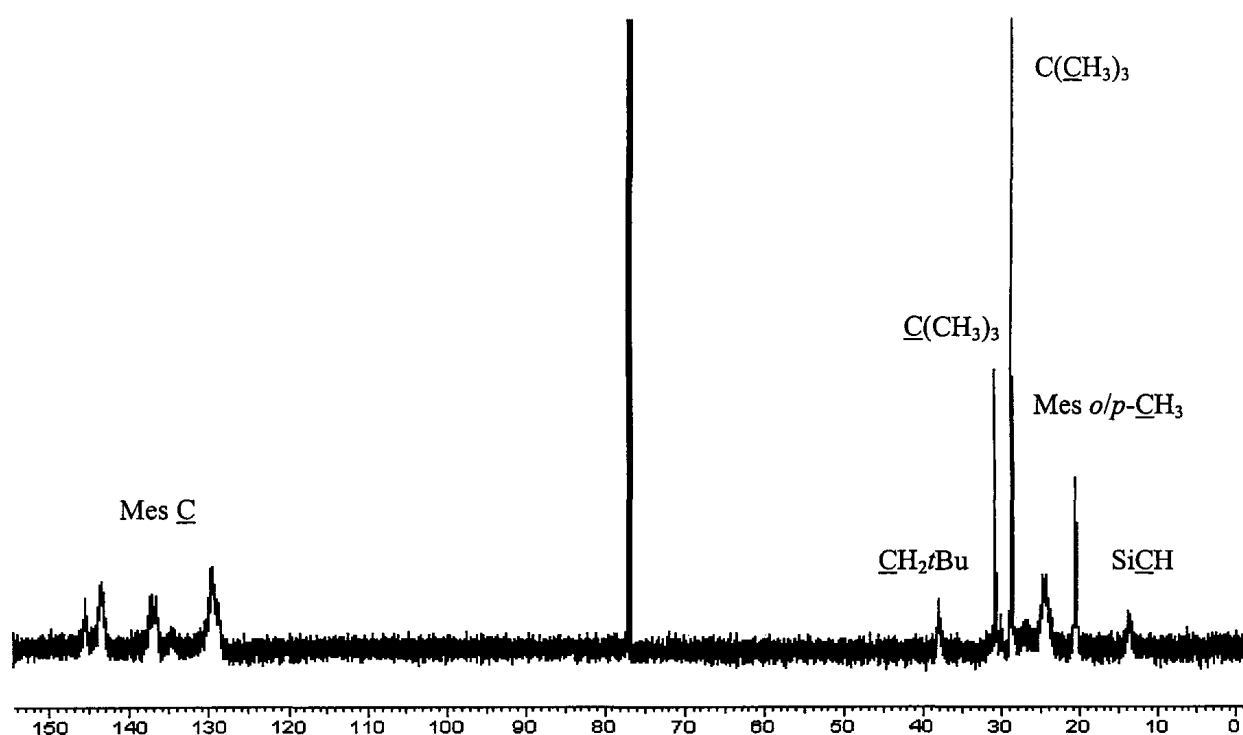


Figure 5.4 ^{13}C NMR spectrum of polysilene **5.8**.

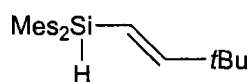
5.3.3 Polymerization Mechanism

The polymerization of silene **5.2** most likely proceeds via an anionic mechanism initiated by the regioselective addition of *t*-butyllithium to the electrophilic silicon of the silene.²⁰ The regioselective addition of an anionic reagent to the silene is known to occur in ether, as observed in the synthesis of **5.9**; however, in pentane, the initial carbanion,

$\text{Mes}_2\text{Si}(t\text{Bu})\text{CH}(\text{Li})\text{CH}_2t\text{Bu}$, appears to be more reactive and adds to the silicon of a second silene to propagate the growth of the polymer. The polymerization of silene **5.2** occurs rapidly, similar to the polymerization of 1,1-dimesitylneopentylgermene (**5.1**).²¹ The rapid reaction is most likely due to the high reactivity of silene **5.2** towards nucleophilic addition.

5.3.4 Polymerization of Silene **5.2** in the Absence of an Initiator

Polymeric material was also produced when silene **5.2** was left in solution (C_6D_6) for two days in the absence of an anionic initiator; isomeric vinylsilane **5.11** (Figure 5.5) and several other unidentified compounds were produced in minor amounts. The polymer was isolated in 40% yield after precipitation from a CH_2Cl_2 solution with methanol. The molecular weight of the polymer was determined by GPC in THF ($M_n = 37\,000\text{ gmol}^{-1}$; PDI = 1.2). The ^1H and ^{13}C NMR spectra of the polymer were identical to those of **5.8**, once again indicating a regular alternating silicon-carbon backbone. A radical polymerization mechanism is presumably occurring under these conditions; however, further investigation is required to confirm the mechanism of polymer formation.



5.11

Figure 5.5 Isomeric silane (**5.11**) of silene **5.2**.

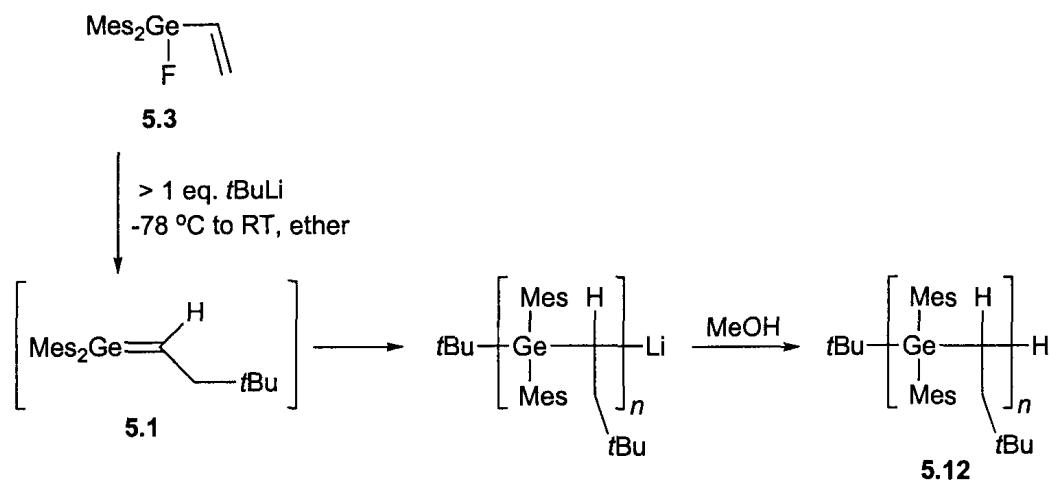
5.4 Towards the Living Polymerization of Germene 5.1

There are many advantages to developing a living polymer system, the main being the high level of control achieved over the molecular weight and PDI. To obtain living anionic polymerization, spontaneous termination must not occur and the rate of initiation must be much faster than the rate of propagation, to allow for complete initiation before propagation begins. If these criteria are met, polymers with predictable molecular weights and low PDI should be obtained. The molecular weight of the polymers can then easily be controlled by varying the concentration of initiator. Living polymerization allows for the controlled synthesis of block copolymers and other more elaborate polymer architectures (ie star polymers, polymer brushes).

The living anionic polymerization of germene **5.1** was investigated. The conditions that were described in section 5.2.1 for the anionic polymerization of germene **5.1** did not lead to living polymers; the molecular weights of the polymeric material obtained did not correlate with the concentration of initiator used. In pentane, it appears that the rate of polymer initiation, from the addition of *t*BuLi to germene **5.1**, was slow compared to the rate of propagation. Thus, other solvent systems were examined.

The 1:1 *t*BuLi adduct of germene **5.1**, $\text{Mes}_2\text{Ge}(t\text{Bu})\text{CHLiCH}_2t\text{Bu}$, could not be synthesized in high yield in pentane, but could be synthesized in ether.¹⁴ upon the addition of excess *t*BuLi to **5.1** in pentane, a significant amount of polymeric material was obtained. When the reaction was performed in ether, $\text{Mes}_2\text{Ge}(t\text{Bu})\text{CH}_2\text{CH}_2t\text{Bu}$ was formed quantitatively after work-up of the reaction mixture. Thus, the rate of *t*BuLi addition to **5.1** appears to be much faster in ether than in pentane, allowing for the

formation of the 1:1 adduct. The use of ether as a solvent for the polymerization of germene **5.1** was examined.



Scheme 5.5 Polymerization of germene **5.1** in ether.

As in pentane, germene **5.1** can be synthesized from fluorovinylgermane **5.3** in ether. This allows for the polymerization of **5.1** to be performed in one step from **5.3**, thereby avoiding excessive experimental manipulations (Scheme 5.5). Fluorovinylgermane **5.3** was treated with > 1 equivalent of *t*BuLi in ether at -78 °C. Upon warming to room temperature, germene **5.1** formed quantitatively. The remaining *t*BuLi then added to **5.1** to initiate polymerization. Several experiments were performed with different amounts of *t*BuLi. Although the ratio of monomer:initiator (M:I) was varied, the absolute amount of **5.1** remained constant. The resulting polymeric material (**5.12**) was isolated from the crude product mixture as a white, air-stable solid after precipitation from a CH₂Cl₂ solution with methanol. The molecular weights of the polymers were analyzed by GPC in THF. A bimodal molecular weight distribution was observed (Figure 5.6) in each case; in addition to the main fraction, a higher molecular weight fraction was present in the GPC trace. The M_n values of the lower molecular weight fraction from

representative samples are presented in Table 5.1 and compared to the calculated values based on the M:I ratio.

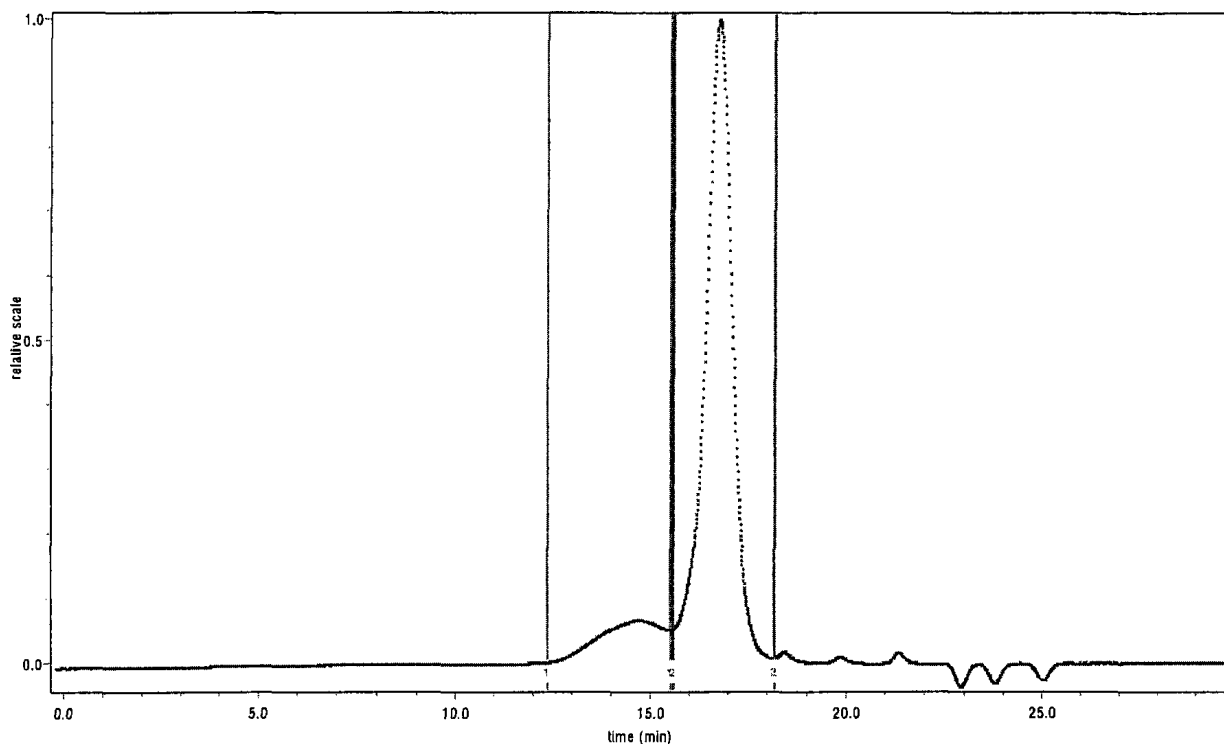


Figure 5.6 Representative GPC trace of polygermene **5.12**.

Despite the bimodal molecular weight distributions, the M_n values of the lower molecular weight fraction in samples of **5.12** did correlate better to the calculated values than those of **5.4** (synthesized in pentane); however, there was poor correlation of the molecular weights of samples of **5.12** obtained using very low amounts of initiator (100:1). Thus, ether offered some advantages as a solvent over pentane; however, a living system was still not achieved.

Table 5.1 Polymerization of germene **5.1** in ether.

Entry	M:I	Calc M_n	Obs M_n	PDI	Yield (%)
1	5:1	1980	1800	1.1	11
2	10:1	3950	3340	1.1	55
3	20:1	7900	7000	1.2	73
4	100:1	39500	12000	1.3	67

An ether-THF cosolvent system was then investigated in an attempt to avoid the undesirable bimodal molecular weight distributions. However, before any polymerization reactions could be performed it had to be determined whether germene **5.1** could be synthesized using an ether-THF cosolvent. Fluorovinylgermane **5.3** was treated with < 1 equivalent of *t*BuLi in ether-THF (3:1) at -78 °C. After warming to room temperature, methanol was added to the reaction mixture; quantitative formation of $\text{Mes}_2\text{Ge}(\text{OMe})\text{CH}_2\text{CH}_2t\text{Bu}$, the methanol adduct of **5.1**, indicated that germene **5.1** was indeed formed under these conditions.

The 1:1 *t*BuLi adduct of germene **5.1** could also be synthesized in ether-THF (3:1). When fluorovinylgermane **5.3** was treated with > 2 equivalent of *t*BuLi in ether-THF (3:1) at -78 °C followed by the addition of aqueous ammonium chloride solution at room temperature, $\text{Mes}_2\text{Ge}(t\text{Bu})\text{CH}_2\text{CH}_2t\text{Bu}$ was obtained in quantitative yield. Thus, the rate of addition of *t*BuLi to **5.1** in ether-THF appeared to be faster than the rate of propagation.

The polymerization of **5.1**, from the addition of > 1 equivalent of *t*BuLi to fluorovinylgermane **5.3**, was then investigated using the ether-THF cosolvent. To date, only two different ratios of monomer to initiator have been examined (10:1 and 20:1).

The resulting polymeric material (**5.13**) was isolated from the crude product mixture after precipitation from a CH_2Cl_2 solution with methanol and the molecular weights of the polymers were analyzed by GPC in THF. In each sample, a single molecular weight fraction was observed (Figure 5.7). The M_n values from samples of **5.13** are presented in Table 5.2 and compared to the calculated values based on the M:I ratio.

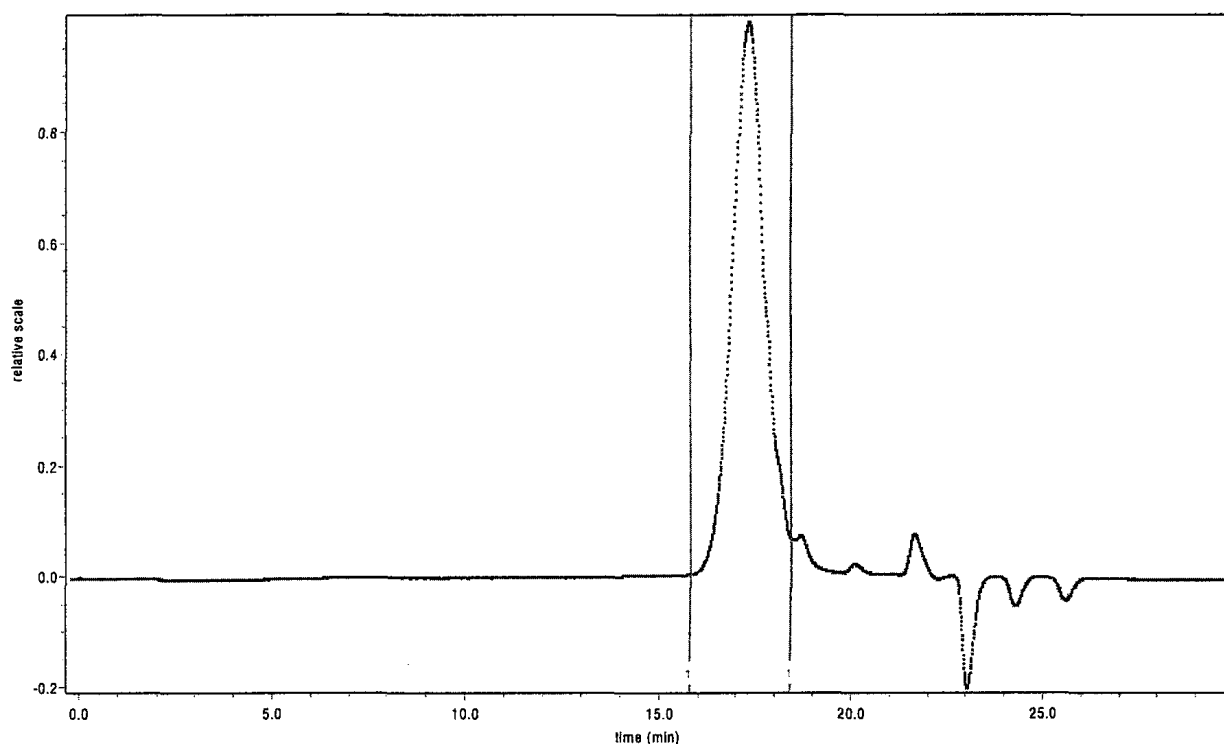


Figure 5.7 Representative GPC trace of polygermene **5.13**.

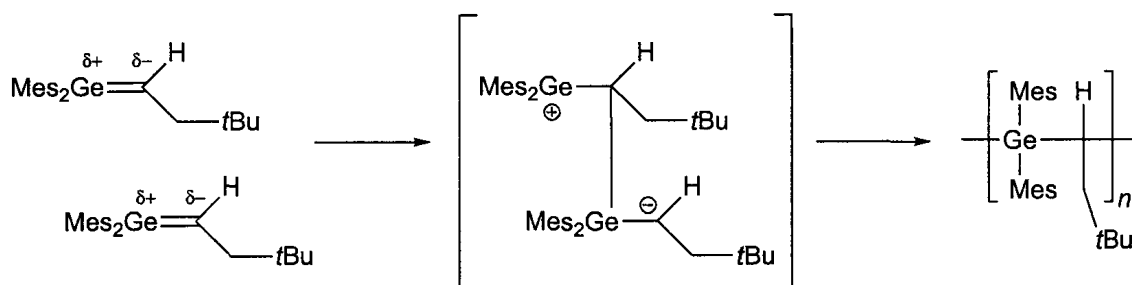
As was observed in ether, lower molecular weight polymers were obtained when germene **5.1** was polymerized in ether-THF as compared to pentane. Also, there appeared to be a correlation between the M:I ratio and the observed M_n values. In addition, a single molecular weight fraction was consistently observed in the GPC trace when an ether-THF cosolvent was used. Even a decrease in the amount of THF, from an ether:THF ratio of 3:1 to 6:1, lead to a monomodal molecular weight distribution. Thus, only a small amount

of THF is necessary. Although further work is required, it appears that the living polymerization of germene **5.1** may be possible using an ether-THF cosolvent system.

Table 5.2 Polymerization of germene **5.1** in ether-THF.

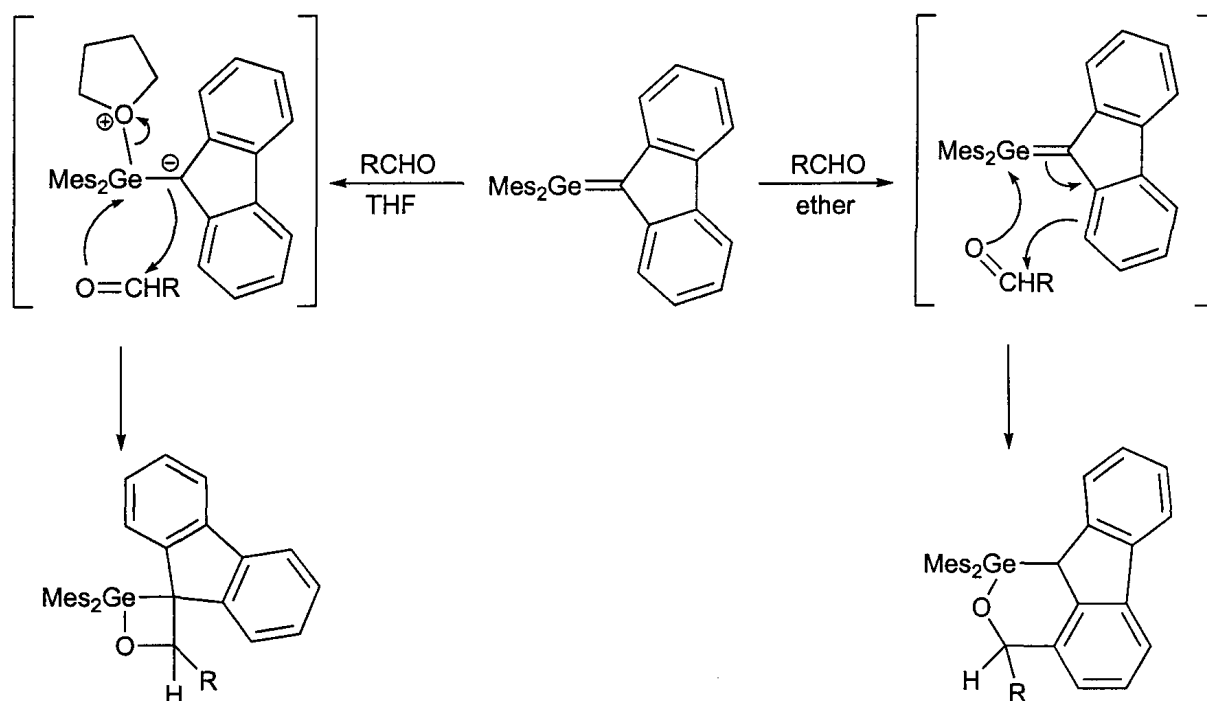
Entry	Ether:THF	M:I	Calc M_n	Obs M_n	PDI	Yield (%)
1	3:1	10:1	3950	3100	1.1	59
2	3:1	20:1	7900	6200	1.2	69
3	6:1	10:1	3950	2000	1.1	40

Bimodal molecular weight distributions were not observed when the polymeric material (**5.13**) was synthesized in an ether-THF cosolvent. The exact role of the THF is not known. A bimodal molecular weight distribution often indicates the presence of a second, competing polymerization mechanism. One possibility includes the uninitiated, ionic polymerization of germene **5.1** derived from a zwitterion formed by the reaction of two dipole aligned germene molecules (Scheme 5.6). Such zwitterionic species would be stabilized in a coordinating solvent (ether) more so than in a non-coordinating solvent (pentane, benzene).



Scheme 5.6 Uninitiated, ionic polymerization of germene **5.1**.

The formation of such a zwitterionic species may be inhibited in the presence of a strongly coordinating solvent, such as THF, that will complex with the germene. Presumably, in a solution with a significant excess of THF, all germene molecules would be complexed, and thus, it is unlikely that two germene-THF complexes would dimerize to initiate polymerization. Interestingly, we have recently observed dramatically different reactivity when dimesitylfluorenylidene-germane was allowed to react with an aldehyde in THF as compared to ether (Scheme 5.7).²² In ether, products derived from [4+2] cycloaddition were observed, while [2+2] cycloadducts were formed preferentially in THF. The difference in reactivity was attributed to the formation of a relatively stable germene-THF complex.



Scheme 5.7 Solvent effect on the reactivity of dimesitylfluorenylidene-germane.

Alternatively, the radical polymerization of germene **5.1** initiated by an electron transfer from *t*BuLi may explain the formation of the higher molecular weight fraction.

The complexation of THF to **5.1** would decrease the electron affinity of the system, and thus, electron transfer may be less likely in the presence of THF. Regardless of the exact nature of the second polymerization mechanism, it is apparent that THF has a significant influence on its viability.

5.5 Summary

We have reported the first addition polymerization of a stable germene and silene to yield new inorganic polymers, a polygermene and polysilene, respectively. The synthesis of a polygermene provides the first example of a polymer with a regularly alternating germanium-carbon backbone. The successful addition polymerization of the group 14 metallenes extends the list of known unsaturated inorganic species that can be utilized as polymeric precursors.

We have also investigated conditions for the living anionic polymerization of germene **5.1**. Initial results from the use of an ether-THF cosolvent seem promising; however, further work is required to optimize these conditions and investigate the potential for use in the synthesis of new block copolymers.

5.6 Experimental

5.6.1 General Experimental Details

All reactions were carried out under an inert atmosphere (argon) in flame-dried glassware. The C_6D_6 was distilled from $LiAlH_4$, stored over 4 Å molecular sieves, and degassed prior to use. Pentane was dried using a solvent purification system (Innovative Technologies Inc., Newburyport, Massachusetts) in which the solvent was passed

through an alumina-packed column. Dichloromethane and methanol were purchased from Caledon Laboratories Ltd. *t*-Butyllithium (1.7 M) was purchased from the Aldrich Chemical Co. and used without purification. 1,1-Dimesitylneopenylgermene (**5.1**),¹⁴ 1,1-dimesitylneopentylsilene (**5.2**),¹⁹ fluorovinylgermane **5.3**,¹⁴ and fluorovinylsilane **5.7**¹⁹ were prepared according to reported procedures.

The NMR spectra were recorded on a Varian Inova 400 or Inova 600 spectrometer. The internal NMR standards used were residual C₆D₅H (7.15 ppm) or CHCl₃ (7.25 ppm) for ¹H NMR spectra and the central signal of C₆D₆ (128.0 ppm) or CDCl₃ (77.0 ppm) for ¹³C NMR spectra. Thermal gravimetric analysis (TGA) was performed on a Mettler Toledo TGA/SDTA851^e instrument with a heating rate of 10 °C/min under nitrogen. Differential scanning calorimetry was performed on a Mettler Toledo DSC822^e instrument under nitrogen. The glass transitions (*T_g*) of the polymers were obtained from the second heating scan at a heating rate of 10 °C/min. The IR spectra were recorded on a Bruker Tensor 27 FT-IR spectrometer. Electron impact mass spectra were obtained using a MAT model 8400 mass spectrometer. Mass spectral data are reported in mass-to-charge ratios (*m/z*).

The molecular weight of polymer **5.4** (synthesized directly from **5.3**) was estimated relative to polystyrene standards by gel permeation chromatography (GPC) using equipment supplied by Polymer Laboratories Ltd. All determinations were carried out at 40 °C using a GPC system consisting of a Polymer Lab LC 1120 HPLC pump, a Polymer Labs Shodex Refractive Index detector, a Knauer K-2600 variable dual wavelength UV-vis detector and two 300 mm x 7.5 mm PLGel 5 μm mixed-C columns. THF (HPLC grade) was used as an eluent and was set to a flow rate of 1 mLmin⁻¹. All

GPC measurements were interpreted using the Cirrus GPC online computer software version 2.0.

Molecular weights of the remaining polymers were also estimated relative to polystyrene standards by size-exclusion chromatography at 40 °C. The GPC system consisted of a Waters 515 HPLC pump, a Wyatt Optilab rEX Refractive Index detector, a Wyatt miniDAWN TREOS triple-angle light scattering detector, and two 300 mm x 7.5 mm Resipore columns from Polymer Laboratories. THF (HPLC grade) was used as an eluent and was set to a flow rate of 0.75 mLmin⁻¹. All GPC measurements were interpreted using the Astra online computer software version 5.3.2.

5.6.2 Synthesis of Polygermene 5.4 from Germene 5.1

t-Butyllithium (1.7 M, 0.05 mL, 0.08 mmol) was added to a pale yellow solution of 5.1 (200 mg, 0.51 mmol) in pentane (6 mL) at room temperature. The colour of the solution changed from pale to bright yellow. After the solution was allowed to stir for 30 min, methanol (1 drop) was added and the bright yellow colour of the solution dissipated immediately. The solvents were removed under vacuum and the residue was dissolved in CH₂Cl₂ (10 mL). A white solid precipitated upon slow addition of methanol (10 mL) to the CH₂Cl₂ solution. The solid was purified by reprecipitation. The air stable material was isolated in 45% yield.

5.4: ¹H NMR (CDCl₃) δ 0.6 (br, 9 H, C(CH₃)₃), 0.8 – 1.5 (br, 3 H, GeCH, GeCHCH₂), 1.6 – 3.1 (br, 18 H, Mes *o/p*-CH₃), 6.5 (br, 4 H, Mes-H); ¹³C NMR (CDCl₃) δ 16.7 (br, Ge-CH), 20.6 (Mes *p*-CH₃), 20.9 (Mes *p*-CH₃), 24.3 (br, Mes *o*-CH₃), 28.9 (C(CH₃)₃), 31.1 (C(CH₃)₃), 38.7 (br, GeCHCH₂), 128.5 (br, Mes *m*-C), 129.2 (br, Mes *m*-C), 136.2

(br, Mes *p*-C), 136.8 (br, Mes *p*-C), 140.0 (br, Mes *i*-C), 142.6 (br, Mes *o*-C), 144.8 (br, Mes *o*-C); GPC (THF, vs. polystyrene) $M_n = 36\,000\text{ gmol}^{-1}$, PDI = 1.5; $M_n = 7\,100\text{ gmol}^{-1}$, PDI = 1.1.

5.6.3 Synthesis of Polygermene 5.4 from Vinylgermane 5.3

t-Butyllithium (1.7 M, 0.36 mL, 0.61 mmol) was added to a solution of **5.3** (200 mg, 0.56 mmol) in pentane (6 mL), cooled by a Dry Ice/acetone bath. The solution was allowed to warm to room temperature and then was stirred for 30 min. The colour of the solution changed from pale to bright yellow at room temperature. Methanol (1 drop) was added to the reaction mixture, at which point the colour dissipated. The pentane solution was washed with water, dried over MgSO_4 , and filtered. The solvent was removed on a rotary evaporator. The residue was dissolved in CH_2Cl_2 (10 mL) and a white solid precipitated upon dropwise addition of methanol (10 mL). The polymer was isolated in 62% yield. GPC (THF, vs. polystyrene) $M_n = 39\,000\text{ gmol}^{-1}$, PDI = 2.0.

5.6.4 Synthesis of Polygermene 5.4 from Germene 5.1 in the Absence of an Initiator

A solution of **5.3** (200 mg, 0.56 mmol) in pentane (6 mL) was cooled in Dry Ice/acetone. *t*-Butyllithium (1.7 M, 0.3 mL, 0.51 mmol) was added to the solution, which was then allowed to warm to room temperature. The pentane was removed under vacuum and the residue was dissolved in C_6D_6 (3 mL). The progress of the reaction was monitored by ^1H NMR spectroscopy. After 10 days, germene **5.1** was consumed. The C_6D_6 was removed under vacuum and the residue was dissolved in CH_2Cl_2 . The polymeric material (**5.4**) was precipitated with methanol (25 wt%); GPC (THF, vs.

polystyrene) $M_n = 21\,000\text{ gmol}^{-1}$, PDI = 2.5). The cyclic dimers (**5.5a,b**) and germane **5.6** remained in the mother liquor. Minor amounts of $(t\text{BuCH}_2\text{CH}_2\text{Mes}_2\text{Ge})_2\text{O}^{14}$ were also observed. The *trans* dimer (**5.5a**) was isolated from the mixture after crystallization from a concentrated C_6D_6 solution; attempts to separate the *cis* dimer (**5.5b**) from germane **5.6** and the digermoxane by chromatography were unsuccessful.

5.5a: mp 280 °C (decomp.); IR (cm^{-1}) 2950, 2867, 1605, 1560, 1450, 1408, 1368, 1036, 849; ^1H NMR (C_6D_6) δ 0.80 (s, 18 H, $\text{C}(\text{CH}_3)_3$), 1.71 (d, $J = 5.4$ Hz, 4 H, GeCHCH_2), 2.12 (s, 12 H, Mes *p*- CH_3), 2.47 (br, 24 H, Mes *o*- CH_3), 3.63 (t, $J = 5.4$ Hz, 2 H, GeCH), 6.76 (s, 8 H, Mes- H); ^{13}C NMR (C_6D_6) δ 20.94 (Mes *p*- CH_3), 26.23 (Mes *o*- CH_3), 29.88 ($\text{C}(\text{CH}_3)_3$), 32.04 ($\text{C}(\text{CH}_3)_3$), 37.66 (Ge- CH), 41.73 (Ge- CHCH_2), 129.39 (Mes *m*- C), 137.61 (Mes *i*- C), 138.00 (Mes *p*- C), 143.45 (Mes *o*- C); High-resolution EI-MS for $^{70}\text{Ge}^{72}\text{GeC}_{48}\text{H}_{68}$ m/z calcd 786.3784, found 786.3801.

5.5b: ^1H NMR (C_6D_6) δ 0.87 (s, 18 H, $\text{C}(\text{CH}_3)_3$), 2.09 (s, 6 H, Mes *p*- CH_3), 2.14 (s, 6 H, Mes *p*- CH_3), 2.28 (br, 12 H, Mes *o*- CH_3), 2.31 (d, $J = 6.0$ Hz, 4 H, GeCHCH_2), 2.49 (br, 12 H, Mes *o*- CH_3), 3.06 (t, $J = 6.0$ Hz, 2 H, GeCH), 6.74 (s, 4 H, Mes- H), 6.77 (s, 4 H, Mes- H); ^{13}C NMR (C_6D_6) δ 20.91 (Mes *p*- CH_3), 20.95 (Mes *p*- CH_3), 25.02 (Mes *o*- CH_3), 26.23 (Mes *o*- CH_3), 29.85 ($\text{C}(\text{CH}_3)_3$), 32.34 ($\text{C}(\text{CH}_3)_3$), 36.48 (Ge- CH), 43.89 (Ge- CHCH_2), 129.11 (Mes *m*- C), 129.85 (Mes *m*- C), 137.61 (Mes *p*- C), 138.11 (Mes *p*- C), 138.83 (Mes *i*- C), 142.18 (Mes *i*- C), 142.38 (Mes *o*- C), 143.20 (Mes *o*- C); EI-MS for $^{74}\text{Ge}_2\text{C}_{48}\text{H}_{68}$ m/z 790.5 (M^+ , 1.1), 622.2 ($^{74}\text{Ge}_2\text{Mes}_4$, 31).

5.6: ^1H NMR (C_6D_6) δ 0.93 (s, 9 H, $\text{C}(\text{CH}_3)_3$), 2.11 (s, 6 H, Mes *p*- CH_3), 2.41 (s, 12 H, Mes *o*- CH_3), 5.84 (d, $J = 2.4$ Hz, 1 H, Ge- H), 6.17 (AB, $J = 18$ Hz, 1 H, Ge- $\text{CH}=\text{CH}$), 6.20 (d of AB, $J = 18$ Hz, 3.0 Hz, Ge- $\text{CH}=\text{CH}$), 6.75 (s, 4 H, Mes- H); ^{13}C NMR (C_6D_6) δ

21.02 (Mes *p*-CH₃), 24.00 (Mes *o*-CH₃), 28.91 (C(CH₃)₃), 35.12 (C(CH₃)₃), 121.51 (Ge-CH=CH), 129.16 (Mes *m*-C), 133.72 (Mes *i*-C), 138.39 (Mes *p*-C), 143.63 (Mes *o*-C), 156.38 (Ge-CH=CH); High-resolution EI-MS for ⁷⁰GeC₂₄H₃₄ *m/z* calcd 392.1903, found 392.1899.

5.6.5 Synthesis of Polysilene 5.8 from Silene 5.2

t-Butyllithium (1.6 M, 0.04 mL, 0.06 mmol) was added to a pale orange solution of **5.2** (220 mg, 0.64 mmol) dissolved in pentane (6 mL) at room temperature. The colour of the solution changed from pale to dark orange. After the solution was allowed to stir for an hour, methanol (1 drop) was added and the dark orange colour of the solution dissipated immediately. The solvents were removed under vacuum and the residue was dissolved in CH₂Cl₂ (10 mL). A white solid precipitated upon slow addition of methanol (10 mL) to the CH₂Cl₂ solution. The solid was purified by reprecipitation. The air stable material was isolated in 50% yield.

5.8: ¹H NMR (CDCl₃) δ 0.7 (br, 9 H, C(CH₃)₃), 0.8 – 1.4 (br, 3 H, SiCH, SiCHCH₂), 1.5 – 3.0 (br, 18 H, Mes *o/p*-CH₃),²³ 6.5 (br, 4 H, Mes-H); ¹³C NMR (CDCl₃) δ 14.0 (br, SiCH), 20.6 (Mes *p*-CH₃), 20.9 (Mes *p*-CH₃), 25.0 (br, Mes *o*-CH₃), 27.2 (br, Mes *o*-CH₃), 28.9 (C(CH₃)₃), 31.0 (C(CH₃)₃), 38.2 (br, SiCHCH₂), 128.8 (br, Mes *m*-C), 129.7 (br, Mes *m*-C), 134.7 (br, Mes *i*-C), 136.6 (br, Mes *p*-C), 137.3 (br, Mes *p*-C), 143.4 (br, Mes *o*-C), 145.5 (br, Mes *o*-C); ²⁹Si NMR (CDCl₃) δ -7.5; GPC (THF, vs. polystyrene) *M_n* = 28 000, PDI = 1.2.

5.6.6 Synthesis of Polysilene 5.8 from Vinylsilane 5.7

t-Butyllithium (1.6 M, 0.44 mL, 0.70 mmol) was added to a solution of 5.7 (200 mg, 0.64 mmol) dissolved in pentane (6 mL), cooled by a Dry Ice/acetone bath. The solution was allowed to warm to room temperature and then was stirred for an hour. The colour of the solution changed from pale to dark orange after a few minutes at room temperature. Methanol (1 drop) was added to the reaction mixture, at which point the colour dissipated. The pentane solution was washed with water, dried over MgSO₄, and filtered. The solvent was removed under vacuum. The residue was dissolved in CH₂Cl₂ (10 mL); a white solid precipitated upon dropwise addition of methanol (10 mL). The polymer was isolated in 65% yield. GPC (THF, vs. polystyrene) $M_n = 32\,000\text{ gmol}^{-1}$, PDI = 1.1.

5.6.7 Synthesis of Mes₂Si(OMe)CH₂CH₂*t*Bu

t-Butyllithium (1.6 M, 0.13 mL, 0.20 mmol) was added to a solution of 5.7 (55 mg, 0.18 mmol) dissolved in pentane (2 mL), cooled by a Dry Ice/acetone bath. The solution was allowed to warm to room temperature and then was stirred for 10 min. Methanol was added to the solution. The pentane solution was washed with water, dried over MgSO₄, and filtered. The solvent was removed under vacuum. The residue was dissolved in hexanes and passed through a silica plug. After removal of the solvent, Mes₂Si(OMe)CH₂CH₂*t*Bu was obtained, contaminated with Mes₂Si(OMe)CH=CH₂ (7%), as a colourless oil (60 mg, 90%). Attempts to separate Mes₂Si(OMe)CH₂CH₂*t*Bu and Mes₂Si(OMe)CH=CH₂ by thin layer chromatography were unsuccessful.

Mes₂Si(OMe)CH₂CH₂*t*Bu: ¹H NMR (CDCl₃) δ 0.84 (s, 9 H, C(CH₃)₃), 1.14 – 1.17 (XX' portion of an AA'XX' spin system, 2 H, SiCH₂CH₂), 1.19 – 1.23 (AA' portion of an AA'XX' spin system, 2 H, SiCH₂CH₂), 2.24 (s, 6 H, Mes *p*-CH₃), 2.30 (s, 12 H, Mes *o*-CH₃), 3.32 (s, 3 H, SiOCH₃), 6.75 (s, 4 H, Mes H); ¹³C NMR (CDCl₃) δ 14.08 (SiCH₂CH₂), 21.00 (Mes *p*-CH₃), 23.55 (Mes *o*-CH₃), 28.85 (C(CH₃)₃), 30.95 (C(CH₃)₃), 37.29 (SiCH₂CH₂), 49.57 (SiOCH₃), 128.99 (Mes *m*-C), 131.98 (Mes *i*-C), 138.55 (Mes *p*-C), 144.05 (Mes *o*-C); ²⁹Si NMR (CDCl₃) δ 3.0; High-resolution EI-MS for SiC₂₅H₃₈O *m/z* calcd 382.2692, found 382.2689.

5.6.8 Synthesis of Silane 5.9

A solution of **5.7** (55 mg, 0.18 mmol) dissolved in pentane (2 mL) was cooled in Dry Ice/acetone. *t*-Butyllithium (1.6 M, 0.1 mL, 0.16 mmol) was added to the solution, which was then allowed to warm to room temperature. After 10 min at room temperature, the pentane was removed under vacuum and the residue was dissolved in diethyl ether (3 mL). The solution was cooled in an ice bath. A second portion of *t*-butyllithium (1.6 M, 0.3 mL, 0.48 mmol) was added to the cold solution, which was then quenched with aqueous ammonium chloride. After separation, the aqueous layer was washed with diethyl ether (x3) and the combined organic layers were dried over MgSO₄ and filtered. The solvents were removed under vacuum. The residue was dissolved in hexanes and then passed through a silica plug. After removal of the solvent, **5.9** was obtained as a waxy, colourless solid (62 mg, 95%).

5.9: mp 116 – 119 °C; ¹H NMR (CDCl₃) δ 0.79 (s, 9 H, C(CH₃)₃), 0.88 – 0.94 (br, 2 H, SiCH₂CH₂), 1.17 (s, 9 H, SiC(CH₃)₃), 1.23 – 1.28 (br, 2 H, SiCH₂CH₂), 2.19 (v. br, Mes

o-CH₃) and 2.22 (s, Mes *p*-CH₃, 18 H total), 6.72 (s, 4 H, Mes H); ¹³C NMR (CDCl₃) δ 11.91 (SiCH₂CH₂), 20.82 (Mes *p*-CH₃), 24.03 (SiC(CH₃)₃), 25.22 (br, Mes *o*-CH₃), 28.88 (C(CH₃)₃), 29.92 (SiC(CH₃)₃), 31.21 (C(CH₃)₃), 39.86 (SiCH₂CH₂), 129.04 (Mes *m*-C), 136.02 (Mes *i*-C), 137.22 (Mes *p*-C), 143.08 (Mes *o*-C); ²⁹Si NMR (CDCl₃) δ 1.2; High-resolution EI-MS for SiC₂₈H₄₄ (M⁺ - H) *m/z* calcd 407.3134, found 407.3130.

5.6.9 Synthesis of Silane 5.10

A solution of **5.7** (64 mg, 0.20 mmol) in pentane (2 mL) was cooled in Dry Ice/acetone. *t*-Butyllithium (1.6 M, 0.11 mL, 0.20 mmol) was added to the solution, which was then allowed to warm to room temperature. After 10 min at room temperature, the pentane was removed under vacuum and the residue was dissolved in diethyl ether (3 mL). A second portion of *t*-butyllithium (1.6 M, 0.35 mL, 0.6 mmol) was added to the solution, which was then allowed to stir at room temperature for 2 h. Aqueous ammonium chloride was added to the reaction solution; the resulting two layers were separated. The aqueous layer was washed with diethyl ether (x3) and the combined organic layers were dried over MgSO₄ and filtered. The solvents were removed under vacuum. *The residue was dissolved in hexanes and passed through a silica plug. After removal of the solvent, 5.10 was obtained, contaminated with 5.9 (8%), as a thick, colourless oil (76 mg, 93%). Attempts to separate 5.9 and 5.10 by thin layer chromatography were unsuccessful.*

5.10: ¹H NMR (CDCl₃) δ 0.70 (s, 9 H, C(CH₃)₃), 1.03 (s, 9 H, SiC(CH₃)₃), 0.78 – 0.93 (XX' portion of an AA'XX' spin system, 2 H, SiCH₂CH₂), 0.98 – 1.10 (AA' portion of an AA'XX' spin system, 2 H, SiCH₂CH₂), 2.20 (s, 6 H, Ar CH₃), 2.27 (s, 3 H, Mes *p*-CH₃),

2.51 (s, 6 H, Mes *o*-CH₃), 2.62 (AB, $J = 15$ Hz, 1 H, SiCH₂Ar), 2.66 (AB, $J = 15$ Hz, 1 H, SiCH₂Ar), 6.71 (s, 1 H, Ar *p*-H), 6.76 (s, 2 H, Ar *o*-H), 6.85 (s, 2 H, Mes H); ¹³C NMR (CDCl₃) δ 9.14 (SiCH₂CH₂), 20.81, 20.82 (SiC(CH₃)₃, Mes *p*-CH₃), 21.25 (Ar CH₃), 23.80 (SiCH₂Ar), 25.63 (Mes *o*-CH₃), 28.68 (SiC(CH₃)₃), 28.77 (C(CH₃)₃), 31.08 (C(CH₃)₃), 37.14 (SiCH₂CH₂), 126.00 (Ar *p*-C), 127.61 (Ar *o*-C), 129.67 (Mes *m*-C), 130.33 (Mes *i*-C), 137.22 (Ar *m*-C), 138.13 (Mes *p*-C), 140.44 (Ar *i*-C), 145.35 (Mes *o*-C); ²⁹Si NMR (CDCl₃) δ 4.0; High-resolution EI-MS for SiC₂₈H₄₄ (M⁺ - H) m/z calcd 407.3134, found 407.3126.

5.6.10 Synthesis of Polysilene 5.8 from Silene 5.2 in the Absence of an Initiator

A solution of 5.7 (55 mg, 0.18 mmol) in pentane (2 mL) was cooled in Dry Ice/acetone. *t*-Butyllithium (1.6 M, 0.1 mL, 0.16 mmol) was added to the solution, which was then allowed to warm to room temperature. After 10 min at room temperature, the pentane was removed under vacuum and the residue was dissolved in C₆D₆ (3 mL). The progress of the reaction was monitored by ¹H NMR spectroscopy. After 2 days, silene 5.2 was consumed. The C₆D₆ was removed under vacuum and the residue was dissolved in CH₂Cl₂. The polymeric material was precipitated with methanol (40% yield; GPC (THF, vs. polystyrene) $M_n = 37\,000$ gmol⁻¹, PDI = 1.2). The vinylsilane (5.11) and other unidentified compounds remained in the mother liquor as determined by ¹H NMR spectroscopy.

5.11: IR (cm⁻¹) 1651 (s, C=C), 2139 (m, Si-H); ¹H NMR (C₆D₆) δ 0.92 (s, 9 H, C(CH₃)₃), 2.10 (s, 6 H, Mes *p*-CH₃), 2.43 (s, 12 H, Mes *o*-CH₃), 5.75 (d, $J = 3.6$ Hz, ¹ $J_{\text{Si-H}} = 190$ Hz, 1 H, Si-H), 6.06 (dd, $J = 3.3, 18$ Hz, 1 H, SiCH=CH), 6.28 (dd, $J = 0.9, 18$ Hz, 1 H,

SiCH=CH), 6.74 (s, 4 H, Mes-H); ^{13}C NMR (C_6D_6) δ 23.10 (Mes *p*-CH₃), 23.86 (Mes *o*-CH₃), 28.76 (C(CH₃)₃), 35.17 (C(CH₃)₃), 120.32 (SiCH=CH), 129.30 (Mes *m*-C), 130.47 (Mes *i*-C), 139.10 (Mes *p*-C), 144.59 (Mes *o*-C), 159.20 (SiCH=CH); ^{29}Si NMR (C_6D_6) δ -34.8; High-Resolution EI-MS for $\text{C}_{24}\text{H}_{34}\text{Si}$ (M^+) m/z calcd 350.2430, found 350.2421.

5.7 References

1. For reviews see: (a) Cowley, A. H. *Acc. Chem. Res.* **1984**, *17*, 386; (b) Norman, N. C. *Polyhedron* **1993**, *12*, 2431; (c) Driess, M.; Grützmacher, H. *Angew. Chem. Int. Ed., Engl.* **1996**, *35*, 828; (d) Rivard, E.; Power, P. P. *Inorg. Chem.* **2007**, *46*, 10047.
2. (a) Tsang, C. W.; Yam, M.; Gates, D. P. *J. Am. Chem. Soc.* **2003**, *125*, 1480; (b) Tsang, C. W.; Baharloo, B.; Riendl, D.; Yam, M.; Gates, D. P. *Angew. Chem. Int. Ed.* **2004**, *43*, 5682; (c) Noonan, K. J. T.; Patrick, B. O.; Gates, D. P. *Chem. Commun.* **2007**, 3658.
3. Noonan, K. J. T.; Gates, D. P. *Angew. Chem. Int. Ed.* **2006**, *45*, 7271.
4. For reviews see: (a) Mark, J. E.; Allcock, H. R.; West, R. *Inorganic Polymers*; Oxford University Press: Oxford, **2005**; (b) Manners, I. *Angew. Chem.* **1996**, *108*, 1712; *Angew. Chem. Int. Ed., Engl.* **1996**, *35*, 1602; (c) Manners, I. *Angew. Chem. Int. Ed.* **2007**, *46*, 1565.
5. For reviews on silenes see: (a) Gusel'nikov, L. E.; Nametkin, N. S. *Chem. Rev.* **1979**, *79*, 529; (b) Raabe, G.; Michl, J. *Chem. Rev.* **1985**, *85*, 419; (c) Brook, A. G.; Baines, K. M. *Adv. Organomet. Chem.* **1986**, *25*, 1; (d) Brook, A. G.; Brook, M. A. *Adv. Organomet. Chem.* **1996**, *39*, 71; (e) Müller, T.; Ziche, W.; Auner, N. In *The Chemistry of Organosilicon Compounds*; Rappoport, Z.; Apeloig, Y., Eds.; Wiley and Sons Ltd.: New York, **1998**; Vol. 2, Chapter 16; (f) Morkin, T. L.; Owens, T. R.; Leigh, W. J. In *The Chemistry of Organosilicon Compounds*; Rappoport, Z.; Apeloig, Y., Eds.; Wiley and

Sons Ltd.: New York, 2001; Vol. 3, Chapter 17; (g) Ottosson, H.; Eklöf, A. M. *Coord. Chem. Rev.* **2008**, *22*, 1287.

6. For reviews on germenes see: (a) Wiberg, N. *J. Organomet. Chem.* **1984**, *273*, 141; (b) Barrau, J.; Escudié, J.; Satgé, J. *Chem. Rev.* **1990**, *90*, 283; (c) Escudie, J.; Couret, C.; Ranaivonjatovo, J. *Coord. Chem. Rev.* **1998**, *180*, 565.

7. For reviews on poly(silylenemethylene)s see: (a) Interrante, L. V.; Liu, Q.; Rushkin, I.; Shen, Q. *J. Organomet. Chem.* **1996**, *521*, 1; (b) Interrante, L. V.; Rushkin, I.; Shen, Q. *Appl. Organomet. Chem.* **1998**, *12*, 695; (c) Uhlig, W. *Organosilicon Chemistry IV: From Molecules to Materials* **2000**, 563; (d) Uhlig, W. *Prog. Polym. Sci.* **2002**, *27*, 255.

8. For reviews see: (a) Laine, R. M.; Babonneau, F. *Chem. Mater.* **1993**, *5*, 260; (b) Birot, M.; Pillot, J. P.; Dunoguès, J. *Chem. Rev.* **1995**, *95*, 1443; (c) Corriu, R. J. P. *Angew. Chem. Int. Ed.* **2000**, *39*, 1376; (d) Interrante, L. V.; Moraes, K.; Liu, Q.; Lu, N.; Puerta, A.; Sneddon, L. G. *Pure Appl. Chem.* **2002**, *74*, 2111; (e) Riedel, R.; Mera, G.; Hauser, R.; Klonczynski, A. *J. Ceram. Soc. Jpn.* **2006**, *114*, 425.

9. (a) Shen, Q. H.; Interrante, L. V. *J. Polym. Sci., Part A: Polym. Chem.* **1997**, *35*, 3193; (b) Lui, Q.; Wu, H. J.; Lewis, R.; Maciel, G. E.; Interrante, L. V. *Chem. Mater.* **1999**, *11*, 2038; (c) Cheng, Q. M.; Interrante, L. V.; Lienhard, M.; Shen, Q.; Wu, Z. *J. Eur. Ceram. Soc.* **2005**, *25*, 233.

10. Mélinon, P.; Masenelli, B.; Tournus, F.; Perez, A. *Nature Materials* **2007**, *6*, 479.

11. (a) Whitmarsh, C. K.; Interrante, L. V. *Organometallics* **1991**, *10*, 1336; (b) Whitmarsh, C. K.; Interrante, L. V. U. S. Patent No. 5,153,295, **1992**; (c) Rushkin, I. L.; Shen, Q.; Lehman, S. E.; Interrante, L. V. *Macromolecules* **1997**, *30*, 3141.

12. (a) Van Aefferden, B.; Habel, W.; Sartori, P. *J. Prakt. Chem. Chem-Ztg.* **1990**, *114*, 367; (b) Van Aefferden, B.; Habel, W.; Sartori, P. *Chem-Ztg.* **1991**, *115*, 173; (c) Habel, W.; Judenau, H. P.; Sartori, P. *J. Prakt. Chem. Chem-Ztg.* **1992**, *334*, 391; (d) Habel, W.; Judenau, H. P.; Sartori, P. *J. Prakt. Chem. Chem-Ztg.* **1993**, *335*, 61; (e) Uhlig, W. *J. Polym. Sci., Part A: Polym. Chem.* **1995**, *33*, 239.

13. Brefort, J. L.; Corriu, R. J. P.; Guerin, D.; Henner, B. J. L. *J. Organomet. Chem.* **1994**, *464*, 133.
14. Couret, C.; Escudié, J.; Delpon-Lacaze, G.; Satgé, J. *Organometallics* **1992**, *11*, 3176.
15. Any significant termination process in an ionic polymerization typically leads to broader monomodal molecular weight distributions rather than a bimodal molecular weight distribution: M. Szwarc, *Carbanions, Living Polymers and Electron Transfer Processes*, John Wiley and Sons, New York, 1969.
16. Baines, K. M.; Stibbs, W. G. *Coord. Chem. Rev.* **1995**, *145*, 157.
17. (a) Gusev, A. I.; Gar, T. K.; Los, M. G.; Alexeev, N. V. *J. Struct. Chem.* **1976**, *17*, 736; (b) Zemlyanskii, N. N.; Borisova, I. V.; Bel'skii, V. K.; Kolosova, N. D.; Beletskaya, I. P. *Izv. Akad. Nauk. SSSR, Ser. Khim.* **1983**, 959; (c) Toltl, N. P.; Stradiotto, M.; Morkin, T. L.; Leigh, W. J. *Organometallics* **1999**, *18*, 5643; (d) Wiberg, N.; Passler, T.; Wagner, S.; Polborn, K. *J. Organomet. Chem.* **2000**, *598*, 292; (e) Leung, W. P.; Wang, Z. X.; Li, H. W.; Yang, Q. C.; Mak, T. C. W. *J. Am. Chem. Soc.* **2001**, *123*, 8123; (f) Leung, W. P.; Wong, K. W.; Wang, Z. X.; Mak, T. C. W. *Organometallics* **2006**, *25*, 2037.
18. For details on the radical-initiated polymerization of 1,1-dimesitylneopentylgermene see Chapter 6.
19. Delpon-Lacaze, G.; Couret, C. *J. Organomet. Chem.* **1994**, *480*, C14.
20. Silenes are naturally polarized: $\delta^+ \text{Si}=\text{C}^{\delta-}$. In general, nucleophiles add to the silicon end of the silene.⁵
21. Pavelka, L. C.; Holder, S. J.; Baines, K. M. *Chem. Commun.* **2008**, 2346.
22. Allan, C. J.; Pavelka, L. C.; Baines, K. M. *manuscript in preparation*.
23. The ^1H chemical shift of the signals assigned to the methyl groups on the mesityl substituents occur over a large range, particularly in polymers (see reference 21) and hindered systems (see reference 24).

24. Gottschling, S. E.; Milnes, K. K.; Jennings, M. C.; Baines, K. M. *Organometallics* **2005**, *24*, 3811.

Chapter 6

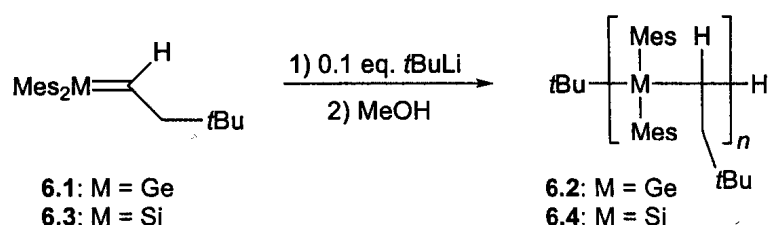
Radical Polymerization of a Germene: Synthesis of Polygermene Homopolymers and Copolymers with Styrene

6.1 Introduction

The free radical polymerization of alkenes has been a prominent method for the industrial synthesis of organic polymers because of the advantages this method offers, particularly in large scale production, over ionic or metal-catalyzed methods (i.e. the use of mild conditions and water as a solvent, tolerance to impurities and functional groups). However, the lack of control over the molecular weight and polydispersity of the materials are still serious drawbacks to free-radical methods. Recently, there has been resurgence of interest in laboratory-scale radical polymerization chemistry with the development of controlled radical polymerization techniques, which have allowed for the synthesis of polymers with predictable molecular weights and low polydispersities.¹ Thus, a variety of synthetic methods (radical, ionic, metal-catalyzed) are now available to prepare organic polymers from alkenes in a controlled manner. This allows for the synthesis of homopolymers with a seemingly endless array of functionality and the synthesis of copolymers from a multitude of different monomer combinations.

Recently, we reported the anionic addition polymerization of 1,1-dimesitylneopentylgermene **6.1**² ($\text{Mes}_2\text{Ge}=\text{C}(\text{H})\text{CH}_2t\text{Bu}$) to yield polygermene **6.2**, $[\text{R}_2\text{GeCR}'\text{R}'']_n$.³ Similarly, we have shown that the polymerization of 1,1-

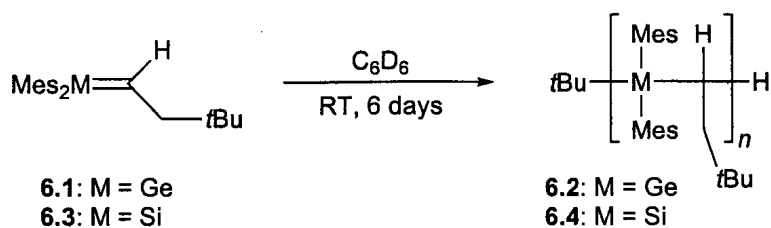
dimesitylneopentylsilene **6.3**⁴ ($\text{Mes}_2\text{Si}=\text{C}(\text{H})\text{CH}_2t\text{Bu}$) is a viable, alternate route to polycarbosilanes with a regularly alternating silicon-carbon backbone (Scheme 6.1).⁵



Scheme 6.1 Anionic polymerization of germene **6.1** and silene **6.3**.

With the successful demonstration of the anionic polymerization of a silene and germene,^{3,5} we were eager to investigate the use of radical initiators. Developing a radical polymerization method for silenes and germenes would provide a second synthetic route to polymeric material as well as introduce more flexibility in the types of polymers that may be made. The group 14 metallenes, when polymerized with alkenes under radical conditions, could be utilized to prepare inorganic-organic hybrid polymers. Organic polymers with silane or germane moieties incorporated in the backbone could easily be modified after polymerization to include new pendant side chains.

Germene **6.1** and silene **6.3** undergo slow polymerization without the addition of an initiator.^{3,5} We speculated that this may be occurring by a radical method; however, more work was needed to determine the nature of this reaction (Scheme 6.2). Although there have been no previous reports on the radical-initiated polymerization of a germene, recent work detailing the radical-initiated polymerization of a silene, $(\text{Me}_3\text{Si})_2\text{Si}=\text{Ad}$, has been reported.⁶



Scheme 6.2 Polymerization of germene **6.1** and silene **6.3** in the absence of an initiator.

Herein, we report on the radical-initiated polymerization of 1,1-dimesitylneopentylgermene, **6.1**, as an alternate route to polygermene **6.2**, and the copolymerization of germene **6.1** with styrene to afford new inorganic-organic hybrid polymers. The radical initiated polymerization of 1,1-dimesitylneopentylsilene, **6.3**, is currently under investigation.⁷

6.2 Synthesis of Germene Homopolymers

The radical-initiated polymerization of germene **6.1** was investigated under thermal and photochemical conditions using azobisisobutyronitrile (AIBN) as the free radical source. A summary of the results obtained are presented in Table 6.1. Details of these experiments follow in sections 6.2.1 and 6.2.2, characterization of the polymers is described in section 6.2.3, and a discussion of the polymerization mechanism is presented in section 6.2.4.

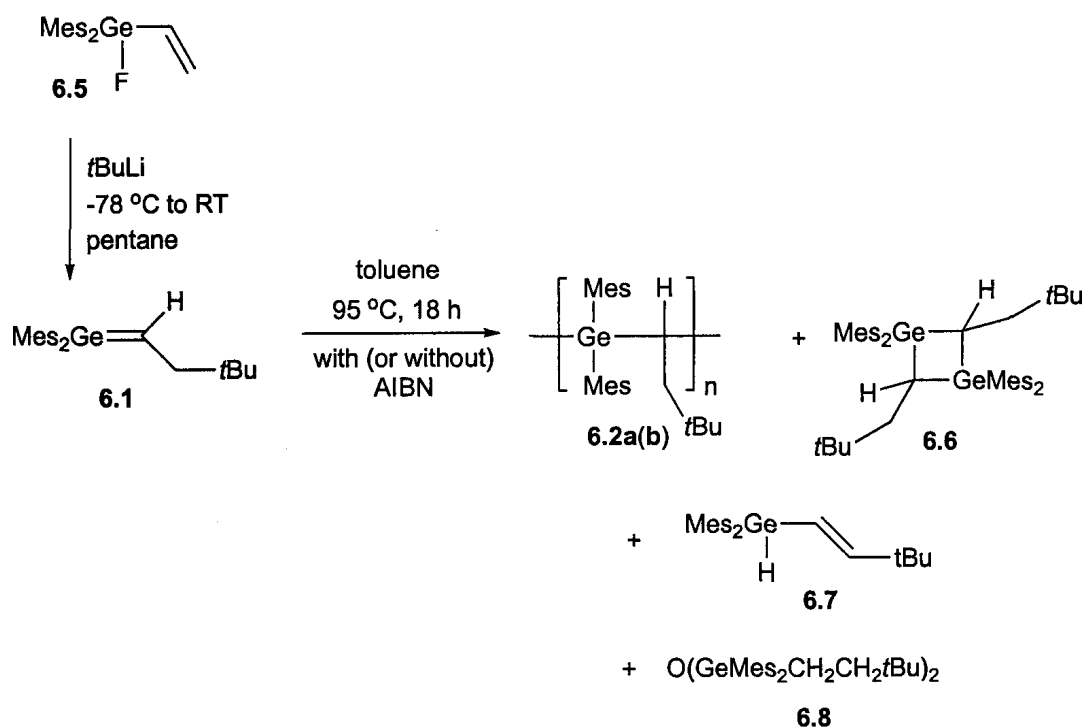
Table 6.1 Radical polymerization of germene 6.1.

Entry	Conditions		Time	M_w (g mol ⁻¹)	PDI	Yield (%)	
1	6.2a	Toluene	AIBN	18 h	80 000, 4 800	2.2, 1.2	20 – 30
2	6.2b	95 °C	no AIBN	18 h	72 000, 4 400	1.8, 1.1	10
3	6.2c	hν (> 350 nm)	AIBN	18 h	22 000	1.6	60 – 70
4	6.2d	C ₆ D ₆ , 20 °C	no AIBN	40 h	32 000	1.8	60 – 70
5	6.2e	C ₆ D ₆ , 20 °C	no AIBN	6 d	54 000	2.5	25

6.2.1 Radical-Initiated Polymerization of Germene 6.2: Thermal Conditions

A pentane solution of fluorovinylgermane **6.5** was treated with *t*BuLi to give germene **6.1**. The pentane was then removed under vacuum and the residue was dissolved in toluene. A trace amount of AIBN (5 mol %) was added to the solution and the reaction mixture was heated to 95 °C (Scheme 6.3). Methanol was added to the reaction mixture after heating for 18 h. Many of the signals in the ¹H NMR spectrum of the crude material were broad indicating polymer formation. Several molecular species were also identified in the crude product mixture including 1,3-digermacyclobutane **6.6**,³ presumably from dimerization of **6.1**, and vinylgermane **6.7**,³ from rearrangement of **6.1**, as well as a minor amount of digermoxane **6.8**² formed by the addition of adventitious water to germene **6.1**. The polymeric material (**6.2a**) was isolated by precipitation from a CH₂Cl₂ solution with methanol (yield = 20 – 30 %). The white, air-stable solid was analyzed by gel permeation chromatography (GPC) in THF; a bimodal molecular weight distribution was observed as evidenced by two distinct fractions. The weight-average molecular weights (M_w) of the two fractions were estimated to be 80 000 g mol⁻¹ and 4 800 g mol⁻¹ (vs. polystyrene) with polydispersity indices (PDI) of 2.2 and 1.2, respectively (Entry 1, Table 6.1). The

bimodal molecular weight distribution was reproducible; however, the M_w of the high molecular weight fraction varied from experiment to experiment ($\pm 5000 \text{ g}\cdot\text{mol}^{-1}$). The presence of a second molecular weight fraction is indicative of more than one polymerization mechanism. The possibility that polymeric material was also forming from the ring-opening polymerization of 1,3-digermacyclobutane **6.6** was considered; however, no exotherm was observed in the differential scanning calorimetric (DSC) scan of **6.6**, which would be typical of a ring-opening event, and thus, this possibility was eliminated. The nature of the competing mechanism is still under investigation.



Scheme 6.3 Synthesis of polygermene **6.2** under thermal conditions.

For comparison purposes, germene **6.1** was heated in toluene for 18 h in the absence of initiator (Scheme 6.3). In this case, the major product observed in the crude material was vinylgermane **6.7**.³ This product was observed in minor amounts in the

polymerization reactions in the presence of AIBN. The germene dimer **6.6** and digermoxane **6.8** were also present. A small amount of polymer (**6.2b**) was isolated from the mixture (yield = 10 %) and was analyzed by GPC ($M_w^1 = 72\,000\text{ g}\cdot\text{mol}^{-1}$, $\text{PDI}^1 = 1.8$; $M_w^2 = 4\,400\text{ g}\cdot\text{mol}^{-1}$, $\text{PDI}^2 = 1.1$; Entry 2, Table 6.1). A bimodal molecular weight distribution was also observed for the polymeric material synthesized in hot toluene without an initiator. This is in contrast to the slow, uninitiated polymerization of germene **6.1** in benzene- d_6 at room temperature (Scheme 6.2), where only one fraction was observed in the GPC trace ($M_w = 54\,000\text{ g}\cdot\text{mol}^{-1}$, $\text{PDI} = 2.5$; Entry 5, Table 6.1).³

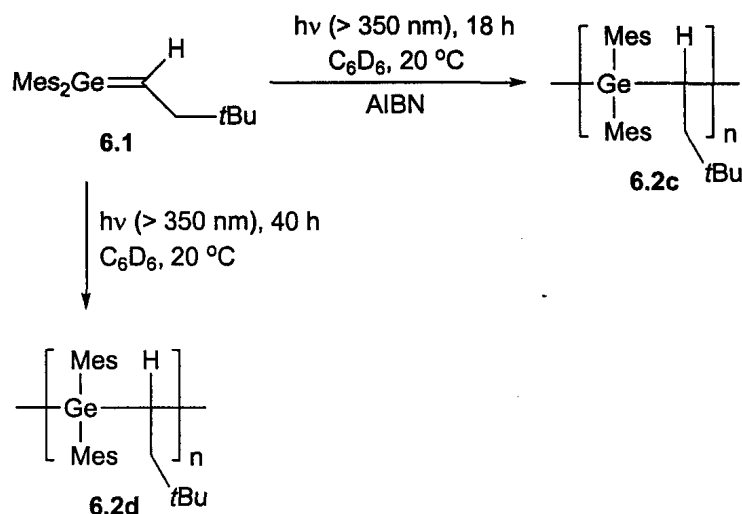
There was an increase in the amount of polymeric material produced from germene **6.1** when AIBN was included in the reaction mixture leading to the conclusion that the radical species generated from the thermal decomposition of AIBN were indeed acting as initiators for the polymerization of **6.1**. The thermal, uninitiated polymerization of germene **6.1** likely also proceeds via a radical mechanism; however, in the absence of AIBN, the other reactions (rearrangement and dimerization) are more competitive.

6.2.2 Radical-Initiated Polymerization of Germene 6.1: Photochemical Conditions

The synthesis of polygermene **6.2** using photochemically-generated radicals was also investigated. This method was employed in an attempt to avoid the problems associated with the radical-initiated polymerization of **6.1** under thermal conditions, specifically, the low isolated yields and the bimodal molecular weight distributions.

The irradiation of AIBN with long wavelength UV light leads to *trans-cis* isomerization of the N=N bond.⁸ The *cis* isomer has much lower thermal stability and

readily decomposes to $\text{Me}_2(\text{CN})\text{C}\cdot$ radicals at room temperature. Thus, AIBN can also act as a free-radical source under photochemical conditions.



Scheme 6.4 Synthesis of polygermene **6.2** under photochemical conditions.

Irradiation of a germene **6.1** solution (C_6D_6) in the presence of trace AIBN with long wavelength UV light ($> 350 \text{ nm}$) at $20 \text{ }^\circ\text{C}$ converted germene **6.1** to polymeric material (**6.2c**) over a period of 18 h (Scheme 6.4). The progress of the reaction was monitored by ^1H NMR spectroscopy. The crude product consisted primarily of polymeric material with few molecular contaminants; precipitation with methanol generally gave 60 – 70 % isolated yields of **6.2c**, representing a significant improvement over the yields obtained using AIBN under thermal conditions (20 – 30 %). The weight-average molecular weight (M_w) of polygermene **6.2c** was determined by GPC analysis; a molecular weight of $22\,000 \text{ g mol}^{-1}$ with a PDI of 1.6 was found (Entry 3, Table 6.1). Significantly, only one molecular weight fraction was present in the GPC trace, as compared to the bimodal molecular weight distribution seen previously when thermal conditions were used.

The UV-vis spectral data of transient diarylgermenes ($\text{Ar}_2\text{Ge}=\text{CH}_2$), generated by laser flash photolysis, have been studied.⁹ In addition to the absorptions from the aryl substituents, the UV-vis spectra of diarylgermenes contain an absorption centred at $\lambda_{\text{max}} \sim 330$ nm, which was assigned to the $\text{Ge}=\text{C}$ π to π^* transition. The UV-vis spectrum of germene **6.1** showed similar features. Not surprisingly, alkyl substitution at the germenic carbon does not significantly affect the position of the long wavelength λ_{max} of the germene. Although the λ_{max} of germene **6.1** is centred at ~ 310 nm, the absorption tails to ~ 450 nm with weak absorbance. Consequently, irradiation of germene **6.1** with long wavelength UV light (> 350 nm) could result in the excitation of the germene. Homolytic cleavage of the $\text{Ge}=\text{C}$ bond from an excited state would yield a diradical species, which could, in principle, initiate polymerization in the absence of an initiator.

To investigate this possibility, germene **6.1** was irradiated under the same photochemical conditions without AIBN (Scheme 6.4). Complete conversion to the polymer required 40 h using only UV light compared to 18 h under the same conditions in the presence of AIBN. After precipitation with methanol, the yield of polymeric material (**6.2d**) obtained from the irradiation of **6.1** was similar to that of polygermene **6.2c** obtained in the presence of AIBN ($\sim 60\%$). Analysis of the molecular weight of the polymer by GPC gave a M_w of $32\,000\text{ g}\cdot\text{mol}^{-1}$ with a PDI of 1.8 (Entry 4, Table 6.1). The absolute molecular weight values varied slightly between experiments ($\pm 5000\text{ g}\cdot\text{mol}^{-1}$). Samples of polygermene **6.2c**, synthesized in the presence of AIBN, generally had a lower molecular weight (M_w) and narrower PDI than those of **6.2d**. Also, in general, the molecular weight values of polymers **6.2c-d**, prepared using the photochemical methods, were lower than those obtained using the thermal methods (**6.2a-b**); however,

monomodal molecular weight distributions and higher yields were consistently observed in samples of **6.2c-d**. Thus, irradiation of germene **6.1** in the presence of AIBN is the preferred method for the radical-initiated synthesis of polygermene **6.2**.

Although the inclusion of AIBN does not improve the yield of polymeric material obtained under photochemical conditions, a significant decrease in time was noted for conversion to the polygermene. This suggests that the radicals generated from the decomposition of AIBN do indeed act as initiators for the polymerization of **6.1** under these conditions. It is also likely that the uninitiated polymerization of **6.1**, upon irradiation, proceeds via a radical mechanism beginning with homolytic cleavage of the Ge=C bond in an excited state germene; however, as indicated by the longer reaction times, this process is apparently less efficient at initiating polymerization than the addition of an AIBN radical.

The polymerization of germene **6.1** using long wavelength UV light in the absence of AIBN can also be compared to that using ambient light, also in the absence of AIBN. Germene **6.1** has been shown to polymerize slowly (over 6 days) without the addition of an initiator (Scheme 6.2; Entry 5, Table 6.1).⁵ The reaction time was shortened to 40 h and higher yields of polymers were obtained when **6.1** was exposed to more intense long wavelength UV irradiation. Assuming that polymerization of **6.1** begins with radical species generated from homolytic cleavage of the Ge=C bond in an excited state germene, it follows that this process would be much more efficient when germene **6.1** is subjected to more intense UV light, which would lead to shorter reaction times. These results demonstrate that UV light plays a critical role in the uninitiated polymerization of **6.1**.

6.2.3 Characterization of Polygermene 6.2

The polymeric materials (6.2) synthesized under thermal/photochemical conditions, in the presence or absence of AIBN, were characterized by ^1H and ^{13}C NMR spectroscopy. All spectra were identical to those obtained previously on polygermene 6.2 synthesized from the anionic polymerization of germene 6.1³ and were consistent with a regularly alternating germanium-carbon backbone.

The thermal stability of polygermene 6.2 was determined using thermal gravimetric analysis (TGA). Representative samples of 6.2, synthesized under thermal or photochemical conditions with AIBN as the free-radical source, were examined. All samples of 6.2 showed similar thermal characteristics; the material was stable to weight loss until 290 °C, at which point ~90 % of the mass was lost. The thermal stability of polygermene 6.2 prepared under radical conditions was remarkably similar to that of 6.2 synthesized from the anionic polymerization of germene 6.1,⁵ suggesting that the microscopic and macroscopic structures of the polymers are identical. Thus, the formation of a regularly alternating germanium-carbon backbone can be achieved under radical or anionic initiated addition polymerizations of germene 6.1.

6.2.4 Polymerization Mechanism

The radical polymerization of germene 6.1 to give a regularly alternating germanium-carbon chain could proceed via one of two possible mechanisms: radical addition to germanium followed by the propagation of a carbon-centred radical or radical addition to the germenic carbon followed by the propagation of a germyl radical. The addition of the electron poor radical ($\text{Me}_2(\text{CN})\text{C}\cdot$) to the electron rich germenic carbon

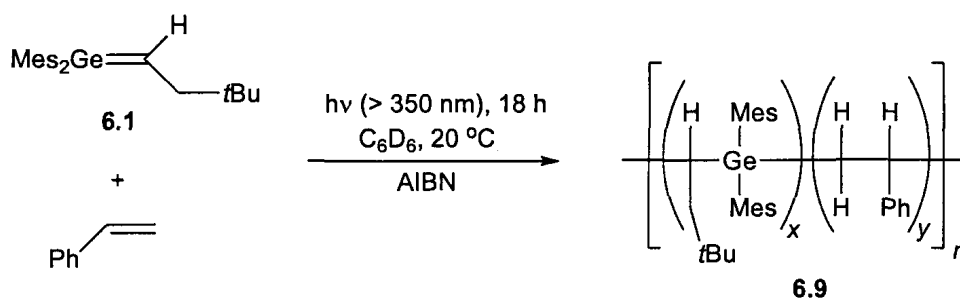
(CHCH_2tBu) to form a germyl radical should be kinetically favoured over addition to the electrophilic germanium (Mes_2Ge). Furthermore, steric interactions may play a role in directing the radical addition to the germylic carbon.

In an attempt to explore the mechanism of polymerization, the thermal and photochemical polymerization of **6.1** (without AIBN) was performed in the presence of butylated hydroxytoluene (BHT), a common alkyl radical trap. In the presence of 10 mol % BHT (relative to germene **6.1**), there was no significant difference in the amount of polymer formed. If a propagating carbon-centred radical existed during polymer formation, presumably it would be trapped by the BHT, which would effectively shut down propagation. In contrast, the more stable germyl radical would likely not be trapped. The inability of BHT to affect the amount of polygermene **6.2** formed is consistent with a propagating germanium-centred radical species in the polymerization of germene **6.1**. The use of carbon tetrachloride as a germyl radical trap was considered; however, germene **6.1** reacts with the reagent, so it could not be used in an attempt to provide evidence for the presence of germanium radicals. With a germyl radical as the propagating species, there is little possibility of backbiting or disproportionation and, consequently, linear polymers with an alternating germanium-carbon backbone are most likely, which is supported by the NMR spectroscopic data of the polymers and the high thermal stability.

6.3 Synthesis of Germene/Styrene Copolymers

With an efficient method for the radical polymerization of germene **6.1** in hand, the synthesis of copolymers was explored. Copolymerization of two different monomers

can potentially lead to materials with useful properties that are not readily obtained from the polymerization of a single monomer. A classic example is synthetic rubber made from the copolymerization of butadiene with styrene; polystyrene itself is too brittle and polybutadiene is too fluid for use as rubber materials.⁸



Scheme 6.5 Synthesis of copolymer **6.9**.

The copolymerization of **6.1** and styrene was performed in C_6D_6 using long wavelength UV irradiation ($> 350 \text{ nm}$) at $20 \text{ }^\circ\text{C}$ for 18 h in the presence of AIBN (5 mol %, relative to **6.1**) (Scheme 6.5). Several experiments were performed with different ratios of **6.1**:styrene. The absolute amount of **6.1** and AIBN remained constant. The resulting polymeric material (**6.9**) was isolated from the crude product mixture as a white, air-stable solid after precipitation from a CH_2Cl_2 solution with methanol. The solubility properties of **6.9** were similar to those of polygermene **6.2**: the polymer was soluble in most organic solvents (for example: CH_2Cl_2 , THF, hexanes, ether, toluene). The molecular weights of polymers **6.9a-d** were analyzed by GPC in THF and M_w values between 35 000 and 47 000 $\text{g}\cdot\text{mol}^{-1}$ (vs. polystyrene) were estimated with PDI's of 1.7 – 1.9 (Table 6.2). In each sample, a single molecular weight fraction was observed, providing strong evidence that **6.9a-d** are copolymers and not mixtures of segregated polygermene and polystyrene strands.

Table 6.2 Radical copolymerization of germene **6.1** with styrene.

Copolymer	6.1:styrene	T_g	M_w (g·mol ⁻¹)	PDI	Incorporated styrene (%)
6.2c	1:0	144	22 000	1.6	0
6.9a	1:1	142	31 000	1.7	16
6.9b	1:5	137	37 000	1.9	33
6.9c	1:10	138	40 000	1.7	43
6.9d	1:20	138	47 000	1.8	48

The thermal properties of copolymers **6.9a-d** were examined. The copolymers, like polygermene **6.2**, are amorphous solids with only a glass transition observed in the DSC trace. The values of the T_g ranged from 137 – 142 °C depending on the sample. These values are suppressed compared to that of **6.2c** ($T_g = 144$ °C), which is consistent with the incorporation of styrene. The presence of only one glass transition implies that there is no phase separation between polygermene and polystyrene segments in the bulk, solid phase. The thermal stability of **6.9a-d** was investigated using TGA. The material was stable to weight loss until 290 °C, at which point ~90 % of the mass was lost. The thermal stability of copolymers **6.9a-d** was very similar to that of polygermene **6.2**.

Regardless of the amount of styrene in the initial reaction mixture, some unreacted styrene remained after 18 h of irradiation; germene **6.1** was always completely consumed. Examination of the ¹H NMR spectrum of copolymer **6.9c** (Figure 6.1) revealed a new broad resonance in the aromatic region between 6.8 – 7.2 ppm, in addition to the signals assigned to the polygermene aromatic hydrogens. This signal was attributed to the *m*- and *p*-phenyl hydrogens from the styrene unit. Unfortunately, the *o*-phenyl hydrogen signal and the aliphatic CHCH_2 hydrogen signals expected from the styrene

moiety were not observed presumably due to overlap with the aromatic and aliphatic hydrogen signals from the germene unit. The degree of styrene incorporation was estimated from the ^1H NMR spectrum by analyzing the integration of the signals in the aromatic region. The relative amount of styrene incorporated in the copolymer increased significantly from 16 to 43 % upon increasing the ratio of styrene to germene from 1:1 to 10:1; however, only a modest additional increase was observed (48 %) when the ratio of styrene to germene was increased further to 20:1.

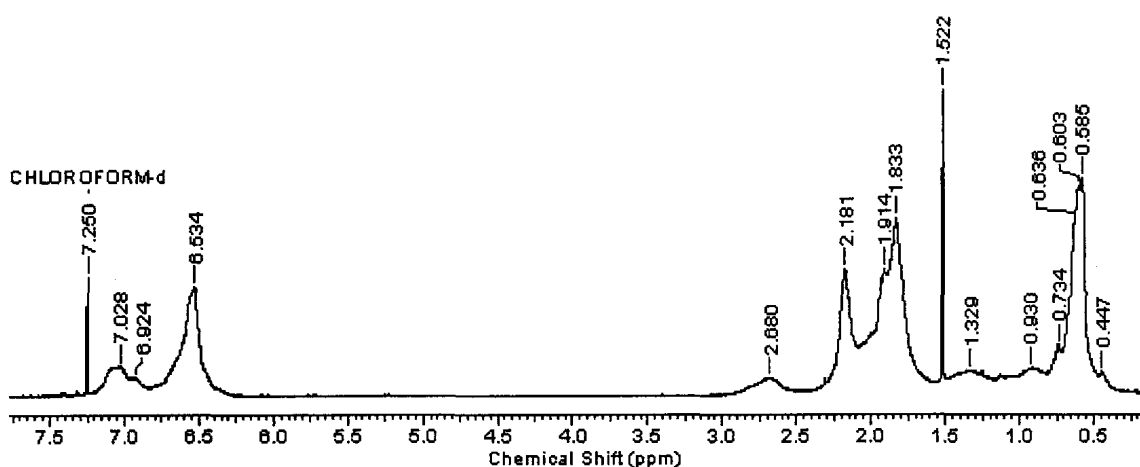


Figure 6.1 ^1H NMR spectrum of **6.9c**.

Copolymer **6.9** was also characterized by ^{13}C NMR spectroscopy (Figure 6.2). Given the degree of overlap in the ^1H NMR spectrum of **6.9**, the ^{13}C NMR spectrum gave much more insight into the structure of the copolymer. As in the ^1H NMR spectrum, all signals previously assigned to the polygermene carbons were present in the ^{13}C NMR spectrum of **6.9**. Two additional signals were present in the aliphatic region that were assigned to the $\underline{\text{C}}\text{H}$ and $\underline{\text{C}}\text{H}_2$ units within the styrene moieties and additional signals were present in the 120 – 130 ppm range, which were attributed to the phenyl carbons.

The exact nature of copolymer **6.9** is uncertain; however, the lack of any additional germene unit signals in the ^{13}C NMR spectrum of **6.9** suggests that the monomers may be grouped in blocks rather than in a random distribution. In fact, when the progress of the reaction was monitored by ^1H NMR spectroscopy, germene **6.1** was consumed before any evidence of styrene incorporation was observed. Upon continued irradiation of the reaction mixture, after the disappearance of **6.1**, polystyrene-like resonances appeared in the aromatic region of the ^1H NMR spectrum.

While monitoring the progress of the copolymerization reactions, it was noted that the consumption of germene **6.1** occurred faster when styrene was present than in the absence of styrene. When an equivalent of styrene was added, **6.1** was completely converted to polymeric material in 3 h. Recall, the photochemical polymerization of **6.1** with trace AIBN required 18 h. Furthermore, when the amount of styrene was increased, the consumption of **6.1** occurred even faster; in the extreme case, when a twenty-fold excess of styrene was used, **6.1** was consumed in less than an hour. The presence of styrene is most likely influencing the initiation stage of polymerization. The free radical produced from the decomposition of AIBN has a very short lifetime.¹⁰ With increasing concentrations of styrene, the free radical generated from AIBN may react with styrene rather than recombine and become dormant. The resulting benzyl radical may then act as a more efficient initiator. Since germene **6.1** is more reactive than styrene, the benzyl radical may then preferentially add to **6.1**, thereby initiating polygermene formation. The apparent increase in the rate of initiation in the presence of styrene suggests that the initiation of **6.1** with AIBN alone is quite slow, which would lead to the relatively long (18 h) reaction times observed in the absence of styrene.

6.4 Conclusions

We have demonstrated that germene **6.1** can undergo polymerization under radical conditions, in addition to the anionic polymerization methods presented previously. Both heating and irradiation of germene **6.1** in the presence of trace AIBN lead to the formation of polymeric material. Competitive reactions, namely dimerization and rearrangement of **6.1**, make the radical polymerization of **6.1** under thermal conditions inefficient. Irradiation of germene **6.1** under long wavelength UV light in the presence of trace AIBN leads to the highest yield of polygermene **6.2**; the milder, photochemical conditions yields fewer side products.

The photochemical route to polygermene has been applied in the synthesis of copolymers with styrene. Co-irradiation of germene **6.1** and styrene under long wavelength UV light in the presence of trace AIBN gives high yields of copolymer. This method gives an inorganic-organic polymer backbone containing germane functional groups. The aryl groups on germanium could easily be replaced with OTf groups upon treatment of the polymer with triflic acid. These Ge(OTf)₂ sites could then be utilized for further functionalization. Also, various substituted styrenes could be incorporated in place of styrene for additional functionalization of the polymers. The significant variation observed in the reaction times required for the consumption of germene **6.1** in the presence or absence of styrene suggests that different radical initiators should be surveyed to optimize the conditions for the radical polymerization of **6.1**.

Two viable experimental procedures for the synthesis of polygermene **6.2** in high yields have been developed: the anionic polymerization initiated with *t*BuLi and the radical polymerization initiated with AIBN under UV light. There are several advantages

to having multiple methods available to synthesize any given polymer; however, the main advantage is the added synthetic flexibility. Depending on the desired properties of the polymer, one method could be selected over another. For example, low molecular weight polygermene or block copolymers can only be synthesized in a controlled fashion anionically,¹¹ whereas higher molecular weight homopolymers and random copolymers are best synthesized via the radical polymerization protocol. Also, *t*BuLi is quite difficult to handle, whereas AIBN is not. Thus, the ease of the radical synthetic method offers an additional advantage over the anionic method.

6.5 Experimental

6.5.1 General Details

All reactions were carried out under an inert atmosphere (argon) in flame-dried glassware. The C₆D₆ was distilled from LiAlH₄, stored over 4 Å molecular sieves, and degassed prior to use. Pentane was dried using a solvent purification system (Innovative Technologies Inc., Newburyport, Massachusetts) in which the solvent was passed through an alumina-packed column. Dichloromethane and methanol were purchased from Caledon Laboratories Ltd. *t*-Butyllithium (1.7 M) was purchased from the Aldrich Chemical Co. and used without purification. 1,1-Dimesitylneopentylgermene (**6.1**) and fluorovinylgermane **6.5** were prepared according to reported procedures.²

The NMR spectra were recorded on a Varian Inova 400 or Inova 600 spectrometer. The internal NMR standards used were residual C₆D₅H (7.15 ppm) or CHCl₃ (7.25 ppm) for ¹H NMR spectra and the central signal of C₆D₆ (128.0 ppm) or CDCl₃ (77.0 ppm) for ¹³C NMR spectra. Thermal gravimetric analysis was performed on

a Mettler Toledo TGA/SDTA851^e instrument with a heating rate of 10 °C/min. Differential scanning calorimetry was performed on a Mettler Toledo DSC822^e instrument under nitrogen. The glass transition temperatures (T_g) were obtained from the second heating scan at a heating rate of 10 °C/min. Irradiations were carried out using three 100 W mercury spot lamps (Blak-Ray B-100AP series; $\lambda > 350$ nm); the NMR tubes were cooled in a cold water jacket (~ 6 °C).

The molecular weight of the polymers was estimated relative to polystyrene standards by gel-permeation chromatography (GPC) at 40 °C using a GPC system consisting of a Waters 515 HPLC pump, a Wyatt Optilab rEX Refractive Index detector, a Wyatt miniDAWN TREOS triple-angle light scattering detector, and two 300 mm x 7.5 mm Resipore columns from Polymer Laboratories. THF (HPLC grade) was used as an eluent and was set to a flow rate of 1 mLmin⁻¹. All GPC measurements were interpreted using the Astra online computer software version 5.3.2.

6.5.2 Polymerization of Germene 6.1 with AIBN under Thermal Conditions

t-Butyllithium (1.7 M, 0.15 mL, 0.26 mmol) was added to a colourless suspension of **6.5** (100 mg, 0.28 mmol) in pentane (3 mL) cooled in a Dry Ice/acetone bath. The colour of the solution changed from colourless to pale yellow upon warming to room temperature followed by the precipitation of a white solid (presumed to be LiF) indicating the formation of germene **6.1**. The pentane was removed under vacuum and the residue was dissolved in toluene. A trace amount of AIBN (2 mg, 0.01 mmol) was added to the germene solution, which was then heated to 95 °C for 18 h. After cooling, methanol (1 drop) was added to the reaction mixture. The solvents were removed under

vacuum and the residue was dissolved in ether (5 mL) and extracted with aqueous ammonium chloride solution. The organic layer was dried over MgSO₄, filtered and the solvent was removed by rotary evaporation. The crude product was dissolved in CH₂Cl₂ (5 mL) and a white solid precipitated upon slow addition of methanol (10 mL) to the CH₂Cl₂ solution. The solid was purified by reprecipitation. The air stable material was isolated in 20 – 30 % yield.

6.2a: ¹H NMR (CDCl₃) δ 0.6 (br, 9 H, C(CH₃)₃), 0.8 – 1.5 (br, 3 H, GeCHCH₂), 1.6 – 3.1 (br, 18 H, *o*- and *p*-Mes CH₃), 6.5 (br, 4 H, Mes-H); GPC (THF, vs. polystyrene) *M*_w = 80 000 g mol⁻¹, PDI = 2.2; *M*_w = 4 800 g mol⁻¹, PDI = 1.2.

6.5.3 Polymerization of Germene 6.1 with AIBN under Photochemical Conditions

t-Butyllithium (1.7 M, 0.15 mL, 0.26 mmol) was added to a colourless suspension of **6.5** (100 mg, 0.28 mmol) in pentane (3 mL) cooled in a Dry Ice/acetone bath. The colour of the solution changed from colourless to pale yellow upon warming to room temperature followed by the precipitation of a white solid (presumed to be LiF) indicating the formation of germene **6.1**. The pentane was removed under vacuum and the residue was dissolved in C₆D₆. A trace amount of AIBN (2 mg, 0.01 mmol) was added to the germene solution, which was transferred to an NMR tube and irradiated under long wavelength UV light for 18 h. The progress of the reaction was monitored periodically by ¹H NMR spectroscopy. Methanol (1 drop) was added to the reaction mixture after irradiation. The resulting solution was then dissolved in ether (5 mL) and extracted with aqueous ammonium chloride solution. The organic layer was dried over MgSO₄, filtered and the solvent was removed by rotary evaporation. The crude product

was dissolved in CH_2Cl_2 (5 mL) and a white solid precipitated upon slow addition of methanol (10 mL) to the CH_2Cl_2 solution. The solid was purified by reprecipitation. The air stable material was isolated in 60 – 70 % yield.

6.2c: ^1H NMR (CDCl_3) δ 0.6 (br, 9 H, $\text{C}(\underline{\text{CH}_3})_3$), 0.8 – 1.5 (br, 3 H, $\text{GeCH}\underline{\text{C}}\underline{\text{H}_2}$), 1.6 – 3.1 (br, 21 H, *o*- and *p*-Mes $\underline{\text{C}}\underline{\text{H}_3}$), 6.5 (br, 4 H, Mes- $\underline{\text{H}}$); ^{13}C NMR (CDCl_3) δ 16.6 (br, Ge- $\underline{\text{C}}\underline{\text{H}}$), 20.6 (*p*-Mes $\underline{\text{C}}\underline{\text{H}_3}$), 20.9 (*p*-Mes $\underline{\text{C}}\underline{\text{H}_3}$), 24.3 (br, *o*-Mes $\underline{\text{C}}\underline{\text{H}_3}$), 28.8 ($\text{C}(\underline{\text{C}}\underline{\text{H}_3})_3$), 31.1 ($\underline{\text{C}}(\underline{\text{C}}\underline{\text{H}_3})_3$), 38.7 ($\text{GeCH}\underline{\text{C}}\underline{\text{H}_2}$), 128.5 (br, *m*-Mes $\underline{\text{C}}$), 129.2 (br, *m*-Mes $\underline{\text{C}}$), 136.2 (br, *p*-Mes $\underline{\text{C}}$), 136.9 (br, *p*-Mes $\underline{\text{C}}$), 140.2 (br, *i*-Mes $\underline{\text{C}}$), 142.6 (br, *o*-Mes $\underline{\text{C}}$), 144.8 (br, *o*-Mes $\underline{\text{C}}$); GPC (THF, vs. polystyrene) $M_w = 22\,000\text{ g mol}^{-1}$, PDI = 1.6.

6.5.4 Irradiation of Germene 6.1 with Styrene and AIBN

t-Butyllithium (1.7 M, 0.15 mL, 0.26 mmol) was added to a colourless suspension of **6.5** (100 mg, 0.28 mmol) in pentane (3 mL) cooled in a Dry Ice/acetone bath. The colour of the solution changed from colourless to pale yellow upon warming to room temperature followed by the precipitation of a white solid (presumed to be LiF) indicating the formation of germene **6.1**. The pentane was removed under vacuum and the residue was dissolved in C_6D_6 . Styrene (30 μL – 0.3 mL, 0.26 – 2.6 mmol) and a trace amount of AIBN (2 mg, 0.01 mmol) was added to the germene solution, which was transferred to an NMR tube and irradiated under long wavelength UV light for 18 h. The progress of the reaction was monitored periodically by ^1H NMR spectroscopy. Methanol (1 drop) was added to the reaction mixture after irradiation. The resulting solution was then dissolved in ether (5 mL) and extracted with aqueous ammonium chloride solution. The organic layer was dried over MgSO_4 , filtered and the solvent was removed by rotary

evaporation. The crude product was dissolved in CH₂Cl₂ (5 mL) and a white solid precipitated upon slow addition of methanol (10 mL) to the CH₂Cl₂ solution. The solid was purified by reprecipitation.

6.9: ¹H NMR (CDCl₃) δ 0.6 (br, 9 H, C(CH₃)₃), 0.8 – 1.5 (br, 3 H, GeCHCH₂), 1.6 – 3.1 (br, 21 H, *o*- and *p*-Mes CH₃, CHCH₂), 6.3 – 6.8 (br, 6 H, Mes-H, *o*-Ph H), 6.9 – 7.2 (br, 3 H, *m*- and *p*-Ph H); ¹³C NMR (CDCl₃) δ 15.7 (br, Ge-CH), 19.6 (*p*-Mes CH₃), 19.9 (*p*-Mes CH₃), 23.3 (br, *o*-Mes CH₃), 27.8 (C(CH₃)₃), 30.1 (C(CH₃)₃), 37.7 (GeCHCH₂), 39.3 (CH₂), 42.8 (br, CHPh), 124.6 (br, Ph), 126.9 (br, Ph), 127.5 (br, *m*-Mes C), 128.1 (br, *m*-Mes C), 135.3 (br, *p*-Mes C), 135.8 (br, *p*-Mes C), 138.9 (br, *i*-Mes C), 141.6 (br, *o*-Mes C), 143.8 (br, *o*-Mes C).

6.9a: GPC (THF, vs. polystyrene) $M_n = 31\ 000\ \text{g}\cdot\text{mol}^{-1}$, PDI = 1.7.

6.9b: GPC (THF, vs. polystyrene) $M_n = 37\ 000\ \text{g}\cdot\text{mol}^{-1}$, PDI = 1.9.

6.9c: GPC (THF, vs. polystyrene) $M_n = 40\ 000\ \text{g}\cdot\text{mol}^{-1}$, PDI = 1.7.

6.9d: GPC (THF, vs. polystyrene) $M_n = 47\ 000\ \text{g}\cdot\text{mol}^{-1}$, PDI = 1.8.

6.5 References

1. Braunecker, W. A.; Matyjaszewski, K. *Prog. Polym. Sci.* **2007**, *32*, 93.
2. Couret, C.; Escudié, J.; Delpon-Lacaze, G.; Satgé, J. *Organometallics*, **1992**, *11*, 3176.
3. Pavelka, L. C.; Holder, S. J.; Baines, K. M. *Chem. Commun.* **2008**, 2346.
4. (a) Delpon-Lacaze, G.; Couret, C. *J. Organomet. Chem.* **1994**, *480*, C14; (b) Delpon-Lacaze, G.; de Battisti, C.; Couret, C. *J. Organomet. Chem.* **1996**, *514*, 59.
5. Pavelka, L. C.; Milnes, K. K.; Baines, K. M. *Chem. Mat.* **2008**, *20*, 5948.

6. Bravo-Zhivotovskii, D.; Melamed, S.; Molev, V.; Sigal, N.; Tumanskii, B.; Botoshansky, M.; Molev, G.; Apeloig, Y. *Angew. Chem. Int. Ed.* **2009**, *48*, 1834.
7. Guo, J.; Baines, K. M. *unpublished work*.
8. Moad, G.; Solomon, D. H. *The Chemistry of Free Radical Polymerization*, 1st ed.; Elsevier Science Inc.: New York, 1995.
9. (a) Toltl, N. P.; Leigh, W. J. *J. Am. Chem. Soc.* **1998**, *120*, 1172; (b) Leigh, W. J. *Pure Appl. Chem.* **1999**, *71*, 453; (c) Leigh, W. J.; Potter, G. D.; Huck, L. A.; Bhattacharya, A. *Organometallics* **2008**, *27*, 5948.
10. Denisov, E. T.; Denisova, T. G.; Pokidova, T. S. *Handbook of Free Radical Initiators*; Wiley & Sons: Hoboken, NJ, 2003.
11. For details on the controlled anionic polymerization of 1,1-dimesitylneopentylgermene see Chapter 5 of this thesis.

Chapter 7

Summary and Future Directions

7.1 Summary

This thesis has examined two areas of E=C compound chemistry: their reactivity towards alkynes and their use as monomers in the synthesis of inorganic polymers. Alkyne addition is an important reaction of silenes ($R_2Si=CR_2$)¹ and other dimetallenes ($R_2M=MR_2$)^{2,3} and yet is relatively unexplored for the phosphalkenes and germenenes. This is surprising given the depth of research that has been dedicated to the study of these species.^{4,5}

In chapter 2, the addition of alkynes to phosphalkenes was described. Several terminal alkynes were added to three different phosphalkenes with varying electronic properties. Adducts were only formed in the reactions between the aromatic alkynes and $MesP=CPh_2$; 1,2-dihydrophosphinines **2.4a-c** were obtained quantitatively. These adducts arise from [4+2] cycloaddition rather than [2+2] cycloaddition. The phosphalkene acted as the 4π component by the participation of the C-phenyl substituent, along with the P=C bond, in the reaction. Following cycloaddition, a H-shift allowed for re-aromatization of the fused six-membered ring. A concerted cycloaddition mechanism was proposed as only one diastereomer was formed in each reaction; stepwise pathways would potentially lead to a mixture of diastereomers. The propensity of phosphalkenes to prefer [4+2] over [2+2] cycloaddition under thermal conditions indicates that their reactivity towards alkynes mirrors that of alkenes more so than that of

silenes. The behaviour of phosphalkenes has also been noted to be similar to alkenes in a wide variety of other pericyclic reactions.⁴ The low polarity of the P=C bond has been linked to the close relation observed between phosphalkene and alkene chemistry. Evidently, the electronic nature of the organic substituents on the phosphalkene does not have a significant influence over the [2+2] cycloaddition reactivity.

The reactivity of a naturally polarized germene, $\text{Mes}_2\text{Ge}=\text{C}(\text{H})\text{CH}_2t\text{Bu}$,⁶ towards alkynes was described in chapter 3. The increased polarity of the Ge=C bond compared to the P=C bond had a great influence on the reactivity. With no C-aryl substituent, [4+2] cycloaddition was not possible with $\text{Mes}_2\text{Ge}=\text{C}(\text{H})\text{CH}_2t\text{Bu}$;⁷ however, products derived from formal [2+2] cycloaddition as well as ene-addition and CH-insertion were observed. A stepwise, zwitterionic cycloaddition pathway was proposed due to the polarity of the germene and the absence of cycloaddition with non-polar alkynes. $\text{Mes}_2\text{Ge}=\text{C}(\text{H})\text{CH}_2t\text{Bu}$ participated in ene-reactions with alkynes quite readily; the presence of an α -CH allowed the germene to act as the ene-component. Ene-addition products were also prominent in reactions of $\text{Mes}_2\text{Ge}=\text{C}(\text{H})\text{CH}_2t\text{Bu}$ with carbonyl compounds.⁸ The ability of the alkynyl C-H bond to insert across the Ge=C bond has been attributed to the polarity of the germene. Similar reactivity was also observed, almost exclusively, with the more polar, analogous silene, $\text{Mes}_2\text{Si}=\text{C}(\text{H})\text{CH}_2t\text{Bu}$, upon addition of terminal alkynes.

The mechanism of alkyne addition to polar metallenes was investigated computationally to gain a better understanding of their reactivity. The parent silene and germene, $\text{H}_2\text{M}=\text{CH}_2$, were used to model naturally polarized silenes and germenes, respectively, and acetylene was used to model a terminal alkyne. Both cycloaddition and CH-insertion pathways were examined. Two different diradical pathways as well as a

zwitterionic and concerted pathway were located for the cycloaddition of acetylene to silene/germene. A concerted CH-insertion pathway was also located for both silene and germene. The diradical cycloaddition pathways were found to be the lowest energy routes for alkyne addition to both silene and germene. Experimentally, the relatively non-polar Brook silenes, $(\text{Me}_3\text{Si})_2\text{Si}=\text{C}(\text{OSiMe}_3)\text{R}$, have also been shown to undergo cycloaddition with alkynes via a stepwise, diradical mechanism.⁹ The similarity between the model, naturally polarized silene, $\text{H}_2\text{Si}=\text{CH}_2$, and the Brook silenes was surprising given the increased polarity of the parent silene. The more polar Si=C bond was expected to favour a zwitterionic pathway of alkyne addition. Likewise, a zwitterionic mechanism was expected to be the lowest energy pathway for acetylene addition to the parent germene since cycloaddition between $\text{Mes}_2\text{Ge}=\text{C}(\text{H})\text{CH}_2t\text{Bu}$ and alkynes was favoured with polar alkynes. Although the zwitterionic pathway was high in energy, the structure of the zwitterionic intermediate located on the potential energy surface for the parent germene was the same as that proposed in the experimental study. The CH-insertion pathway was high in energy for both silene and germene; however, products from CH-insertion were prominent in the experimental work with $\text{Mes}_2\text{M}=\text{C}(\text{H})\text{CH}_2t\text{Bu}$. A lower energy, stepwise CH-insertion pathway may be available in solution that could not be located in the gas phase calculations. Overall, the potential energy surface for the addition of acetylene to silene/germene was relatively flat, and thus, the solvent and the presence of substituents will affect the energetics of the reaction mechanism and may dictate the pathway followed in solution. The calculations performed on these model systems do, however, provide a basis for comparison to the more complex experimental systems.

The addition polymerization of unsaturated monomers is commonplace in organic polymer chemistry; however, it was not until recently that the first unsaturated, inorganic compound, a phosphalkene, was successfully polymerized.¹⁰

In chapter 5, the addition polymerization of $\text{Mes}_2\text{Ge}=\text{C}(\text{H})\text{CH}_2t\text{Bu}$ and $\text{Mes}_2\text{Si}=\text{C}(\text{H})\text{CH}_2t\text{Bu}$ using anionic initiators was described.^{11,12} Polymeric material was obtained from both monomers in moderate yield (45 – 55 %). The polymers were determined to have a regularly alternating metalloid-carbon backbone, derived from head-to-tail propagation. Conditions for the controlled anionic polymerization of $\text{Mes}_2\text{Ge}=\text{C}(\text{H})\text{CH}_2t\text{Bu}$ were also explored. Changing the solvent from pentane to an ether-THF cosolvent gave the most encouraging results.

Conditions for the radical polymerization of the germene were also explored. Both heating and irradiation of $\text{Mes}_2\text{Ge}=\text{C}(\text{H})\text{CH}_2t\text{Bu}$ in the presence of AIBN lead to the formation of polymeric material; however, higher yields of polygermene were obtained using photochemical conditions. Several side reactions occurred at elevated temperatures, which lowered the yield of polymer under these conditions. The photochemical conditions were then employed in the synthesis of copolymers with styrene; polymers with 16 – 48 % styrene incorporation were prepared by varying the initial amount of styrene. The exact microscopic structures of the copolymers are not known; however, the evidence suggests that the polymers resemble block copolymers more so than a random distribution of germene and styrene units.

7.2 Conclusions

The examination of phosphalkene, germene, and silene reactivity together has proven to be synergistic. By utilizing similar conditions and reagents with each system, direct comparisons were possible, and thus, a greater understanding of the chemistry was obtained. Although this concept seems simple, comparative studies of E=C compound reactivity are rare, especially between species from different groups in the Periodic Table. This comparative study has shown that the reactivity of an E=C compound appears to be more dependent on the polarity of the double bond rather than the valency of the main group element (E). Thus, phosphalkenes, not silenes, are the better mimics of alkenes due to the low polarity of the P=C bond.

A general trend was observed in the reactivity these compounds towards alkynes that followed the polarity of the E=C bond: phosphalkenes are less reactive than germenes, which, in turn, are less reactive than silenes. In addition to the overall reactivity, the types of products formed also reflected the differences in E=C bond polarity. The naturally polarized 1,1-dimesitylneopentylsilene preferred to react with the terminal C-H bond rather than the less polar C≡C triple bond, whereas the slightly less polar 1,1-dimesitylneopentylgermene showed an increased preference for reaction with the C≡C triple bond (cycloaddition and ene-addition). The relatively non-polar MesP=CPh₂ reacted exclusively with the C≡C bond as a 4π component in a [4+2] cycloaddition, behaving like a diene. Although alkyne addition is just one class of reactions, the results aptly reflect the inherent differences between phosphalkenes, germenes, and silenes.

The results from the alkyne addition studies suggest that the heavy alkene analogues do indeed obey the Woodward-Hoffmann rules for pericyclic reactions.¹³ Those compounds that undergo formal [2+2] cycloaddition do so through a stepwise pathway, and when a stepwise pathway is inaccessible, formal [2+2] cycloaddition does not occur. Although no direct experimental evidence for an intermediate species was obtained, the computational study suggests that stepwise pathways are lower in energy than concerted pathways for silenes and germenenes. Furthermore, the lack of [2+2] cycloaddition between organo-substituted phosphalkenes and alkynes suggests that neither stepwise nor concerted mechanisms of addition are available for these systems.

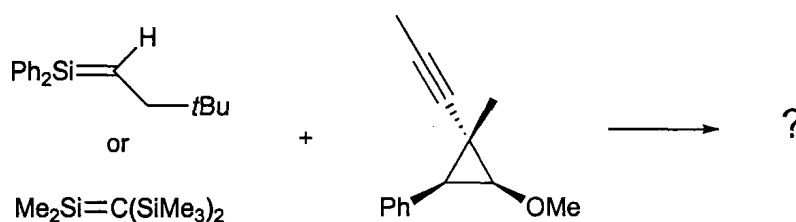
Silenes and germenenes are readily polymerized to give inorganic polymers with a regularly alternating metalloid-carbon backbone. The ease of the polymerization reactions was surprising given that stable group 14 metallenes have been studied for nearly thirty years and there have been no previous reports on their polymerization. Despite the importance of the addition polymerization of alkenes, reactivity studies on heavy alkene analogues have primarily focused on molecular chemistry. The ability of phosphalkenes, and now silenes and germenenes, to undergo addition polymerization suggests that this may be a general route to inorganic polymers and provides the motivation to examine the use of other inorganic multiply bonded species as monomers.

The steadfast, regioselective head-to-tail propagation that occurs during the synthesis of these polymers is also quite interesting; both anionic and radical conditions yield the same, linear polymers with an [MC] repeat unit. This is not commonly observed with organic monomers. Free-radical techniques are known to be less selective and a combination of head-to-tail and head-to-head propagation can occur. Also, back-biting to

produce branched chains is common in the free-radical polymerization of alkenes. The presence of an electrophilic main group element promotes the regular, head-to-tail propagation. As a consequence, the metalloid and substituents are distributed evenly throughout the polymer chain. The periodic distribution of functional sites could be advantageous in the preparation of new polymeric derivatives as well as higher ordered materials.

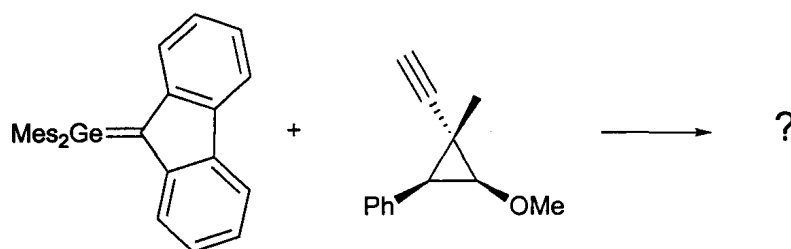
7.3 Future Work

The cycloaddition of alkynes to silenes or germenes was proposed to proceed by a stepwise, diradical pathway; however, this was based on computational results from a model system. The presence of substituents and solvent could alter the nature of the pathway. These results could not be verified experimentally with $\text{Mes}_2\text{Si}=\text{C}(\text{H})\text{CH}_2t\text{Bu}$ or $\text{Mes}_2\text{Ge}=\text{C}(\text{H})\text{CH}_2t\text{Bu}$ due to the lack of cycloaddition with alkyl-substituted terminal alkynes. Ene-adducts and CH-insertion adducts were the only products observed. Previously, in an attempt to shut down CH-insertion, a methylated alkynyl probe was synthesized and added to $\text{Mes}_2\text{Si}=\text{C}(\text{H})\text{CH}_2t\text{Bu}$.¹⁴ Unfortunately, the internal alkyne did not react with the silene; however, it may react with a less hindered transient silene, such as $\text{Me}_2\text{Si}=\text{C}(\text{SiMe}_3)_2$ ¹⁵ or $\text{Ph}_2\text{Si}=\text{C}(\text{H})\text{CH}_2t\text{Bu}$ (Scheme 7.1).¹⁶



Scheme 7.1 Addition of methylated alkynyl probe to transient polar silenes.

To investigate the mechanism of alkyne addition experimentally for the germenes, another naturally polarized germene, 1,1-dimesitylfluorenylidene-germane ($\text{Mes}_2\text{Ge}=\text{CR}_2$), could be examined. This germene does not possess any α -hydrogens, and thus, cannot participate as an ene-component upon treatment with alkynes. Elimination of the ene pathway could potentially favour cycloaddition with alkynes. The preference of $\text{Mes}_2\text{Ge}=\text{CR}_2$ to participate in cycloaddition reactions has already been demonstrated with carbonyl compounds; $\text{Mes}_2\text{Ge}=\text{CR}_2$ gives cycloadducts upon addition of reagents that exclusively yielded ene-adducts with $\text{Mes}_2\text{Ge}=\text{C}(\text{H})\text{CH}_2t\text{Bu}$.¹⁷ The potential for increased cycloaddition reactivity could enable the use of the alkynyl mechanistic probe with this germene (Scheme 7.1). Thus, experimental insight into the mechanism of alkyne addition to a polar silene and germene may be possible with these alternative systems.



Scheme 7.2 Addition of Alkynyl Probe to 1,1-Dimesitylfluorenylidene-germane.

There are a number of directions that could be pursued with our new polymer systems. To begin with, the living polymerization of $\text{Mes}_2\text{Ge}=\text{C}(\text{H})\text{CH}_2t\text{Bu}$ and $\text{Mes}_2\text{Si}=\text{C}(\text{H})\text{CH}_2t\text{Bu}$ should be developed and optimized. The use of an ether-THF cosolvent, using $t\text{BuLi}$ as the initiator, seems promising for the germene, but further work

is required to determine whether these conditions actually yield living polymers. Appropriate conditions have yet to be found for the silene.

The ability to synthesize living anionic polymers should enable the synthesis of a variety of block copolymer architectures. Amphiphilic block copolymers are known to self-assemble in solution as well as in the solid phase. The synthesis of polysilene/germene-*block*-poly(polar monomer) may yield self assembled structures. Ordered, solid-state structures, such as nanoparticle arrays and nanowires, containing silicon/germanium could have potential use in semiconductor materials. Cross-linking followed by pyrolysis of the polysilene/germene block could deposit silicon/germanium carbide in structured patterns. The preparation of ordered, inorganic nanomaterials from self-assembled block copolymers has already been successfully demonstrated with poly(ferrocenylsilane) block copolymers to yield iron-containing nanostructures.¹⁸

The most significant advantage of our polysilene and polygermene systems is the presence of a regularly distributed functional site. The substituents at silicon/germanium can easily be modified to tune the properties of the polymer. Furthermore, the increased size of silicon/germanium compared to carbon should enable the integration of bulky substituents not possible in organic polymers, while maintaining a pseudo organic backbone. This property has been demonstrated in the polymers we have already synthesized, which contain two mesityl groups and a neopentyl group in the repeat unit. The addition of bulky substituents with specialized characteristics, such as chirality, fluorescence, or other electronic features, could yield polymers with unique properties. In addition, the increased steric congestion around the main chain may also have a significant effect on the morphology, of both homopolymer and copolymer systems. One

example of a bulky, functional substituent is a carborane. The synthesis of carborane containing polymers has received much attention due to their potential use in radiation shielding materials.¹⁹ Boron has an extremely high neutron capture ability.²⁰ Attachment of pendant carborane groups to organic polymers requires significant linker/spacer units due to steric constraints, whereas the carborane could potentially be attached directly to silicon/germanium. Without the need for long linker segments, fewer experimental manipulations and reagents would be required in the synthesis of these polymers. Also, a more densely packed carborane material may be possible. This could be extremely beneficial for applications in radiation shielding.

The polygermene, in particular, may be a viable precursor for germanium carbide, after some post polymerization modifications. There is already an incredibly efficient polymeric precursor for silicon carbide,²¹ but there is nothing comparable for germanium carbide. Furthermore, our polygermene is the only example of a polymer with a regularly alternating germanium-carbon backbone, which has the appropriate stoichiometry for use as a GeC precursor. The cleavage of the mesityl groups with triflic acid followed by reduction with lithium aluminum hydride should give polymers with a $[\text{GeH}_2\text{CHR}]_n$ backbone. The presence of Ge-H sites should lead to higher ceramic yields upon pyrolysis due to the lower portion of carbon and the potential cross-linking of the Ge-H groups during heating.

As an alternative to post polymerization modifications, new monomers could also be synthesized and polymerized to introduce different substituents at silicon/germanium. This technique would be particularly useful for larger aromatic substituents, such as naphthyl or anthryl groups, which may yield fluorescent polymers. The preparation of

these new metallenes should be straight forward, following the procedure for the synthesis of $\text{Mes}_2\text{M}=\text{C}(\text{H})\text{CH}_2t\text{Bu}$ (Scheme 1.20), with a modification on the aryl lithium/Grignard utilized. The size of the metalloid should enable the inclusion of two naphthyl/anthryl groups per repeat unit, which could increase the fluorescence intensity of these polymers compared to organic polymers with the same type of substituent.

The addition polymerization of silenes and germenes has opened up several directions for future research including the synthesis of block copolymers and functional polymers. Although much work still remains to be done, there is significant potential to prepare inorganic polymers with unique properties from these systems.

7.4 References

1. For reviews on silenes see: (a) Gusel'nikov, L. E.; Nametkin, N. S. *Chem. Rev.* **1979**, *79*, 529; (b) Raabe, G.; Michl, J. *Chem. Rev.* **1985**, *85*, 419; (c) Brook, A. G.; Baines, K. M. *Adv. Organomet. Chem.* **1986**, *25*, 1; (d) Brook, A. G.; Brook, M. A. *Adv. Organomet. Chem.* **1996**, *39*, 71; (e) Müller, T.; Ziche, W.; Auner, N. *The Chemistry of Organic Silicon Compounds*; Rappoport, Z.; Apeloig, Y., Eds.; Wiley & Sons: New York, 1998; Vol. 2, Chapter 16; (f) Morkin, T. L.; Owens, T. R.; Leigh, W. J. *The Chemistry of Organic Silicon Compounds*; Rappoport, Z.; Apeloig, Y., Eds.; Wiley & Sons: New York, 2001; Vol. 3, Chapter 17; (g) Ottosson, H.; Eklöf, A. M. *Coord. Chem. Rev.* **2008**, *252*, 1287.
2. For reviews on disilenes see: (a) West, R. *Angew. Chem., Int. Ed. Engl.* **1987**, *26*, 1201; (b) Weidenbruch, M. *Coord. Chem. Rev.* **1994**, *130*, 275; (c) Okazaki, R.; West, R. *Adv. Organomet. Chem.* **1996**, *39*, 231; (d) Weidenbruch, M. *The Chemistry of Organic Silicon Compounds*; Rappoport, Z.; Apeloig, Y., Eds.; Wiley & Sons: New York, 2001; Vol. 3, p391.

3. For reviews on digermenes see: (a) Barrau, J.; Escudié, J.; Satgé, J. *Chem. Rev.* **1990**, *90*, 283; (b) Escudié, J.; Couret, C.; Ranaivonjatovo, H.; Satgé, J. *Coord. Chem. Rev.* **1994**, *130*, 427; (c) Baines, K. M.; Stibbs, W. G. *Adv. Organomet. Chem.* **1996**, *39*, 275; (d) Escudié, J.; Ranaivonjatovo, H. *Adv. Organomet. Chem.* **1999**, *44*, 113; (e) Tokitoh, N.; Okazaki, R. *The Chemistry of Organic Germanium, Tin, and Lead Compounds*; Rappoport, Z., Ed.; Wiley & Sons: Chichester, 2002; Vol. 2, p843.
4. For reviews on phosphalkenes: (a) Mathey, F. *Acc. Chem. Res.* **1992**, *25*, 90; (b) Dillon, K. B.; Mathey, F.; Nixon, J. F. *Phosphorus: The Carbon Copy*; John Wiley & Sons: New York, 1998; (c) Mathey, F. *Angew. Chem. Int. Ed.* **2003**, *42*, 1578; (d) Gates, D. *Top. Curr. Chem.* **2005**, *250*, 107.
5. For reviews on germenes see: (a) Wiberg, N. *J. Organomet. Chem.* **1984**, *273*, 141; (b) Escudié, J.; Couret, C.; Ranaivonjatovo, J. *Coord. Chem. Rev.* **1998**, *180*, 565. Also, see reference 3a.
6. Couret, C.; Escudié, J.; Delpon-Lacaze, G.; Satgé, J. *Organometallics*, **1992**, *11*, 3176.
7. Although an aryl substituent (mesityl) was present on germanium, [4+2] cycloaddition was unlikely due to the poor delocalization between the Ge=C and the mesityl group as well as the increased steric hinderence.
8. Delpon-Lacaze, G.; Couret, C.; Escudié, J.; Satgé, J. *Main Group Metal Chemistry* **1993**, *16*, 419.
9. (a) Milnes, K. K.; Jennings, M. C.; Baines, K. M. *J. Am. Chem. Soc.* **2006**, *128*, 2491; (b) Milnes, K. K.; Baines, K. M. *Can. J. Chem.* **2009**, *87*, 307.
10. Tsang, C. W.; Yam, M.; Gates, D. P. *J. Am. Chem. Soc.* **2003**, *125*, 1480.
11. Pavelka, L. C.; Holder, S. J.; Baines, K. M. *Chem. Commun.* **2008**, 2346.
12. Pavelka, L. C.; Milnes, K. K.; Baines, K. M. *Chem. Mat.* **2008**, *20*, 5948.
13. (a) Woodward, R. B.; Hoffman, R. *J. Am. Chem. Soc.* **1965**, *87*, 395. (b) Woodward, R. B.; Hoffman, R. *Conservation of Orbital Symmetry*; Academic: New York, 1970.

14. Milnes, K. K.; Pavelka, L. C.; Baines, K. M. *manuscript in preparation*.
15. Wiberg, N.; Preiner, G. *Angew. Chem. Int. Ed. Engl.* **1977**, *16*, 328.
16. Auner, N.; Ziche, W.; Herdtweck, E. *J. Organomet. Chem.* **1992**, *426*, 1.
17. Lazraq, M.; Couret, C.; Escudié, J.; Satgé, J. *Organometallics* **1991**, *10*, 1771.
18. (a) Manners, I. *Angew. Chem., Int. Ed. Engl.* **1996**, *35*, 1602; (c) Manners, I. *Angew. Chem., Int. Ed.* **2007**, *46*, 1565.
19. Herzog, A.; Maderna, A.; Harakas, G. N.; Knoblen, C. B.; Hawthorne, M. J. *Chem. Eur. J.* **1999**, *5*, 1212.
20. Taylor, H. J.; Goldhaber, M. *Nature (London)* **1935**, *135*, 341.
21. (a) Whitmarsh, C. K.; Interrante, L. V. *Organometallics* **1991**, *10*, 1336; (b) Whitmarsh, C. K.; Interrante, L. V. U. S. Patent No. 5,153,295, **1992**.

Appendix 1

Molecular Structure Analysis

A1.1 X-Ray Structures of 2.6a

Crystals of **2.6a** were grown by slow diffusion of hexanes into a concentrated Et₂O/C₆D₆ solution containing **2.6a**. A colourless crystal was mounted on a glass fibre. Data were collected at low temperature (150(2) K) on a Nonius Kappa-CCD area detector diffractometer with COLLECT (Nonius B.V., 1997-2002). The unit cell parameters were calculated and refined from the full data set. Crystal cell refinement and data reduction were carried out using HKL2000 DENZO-SMN.¹ The absorption correction was applied using HKL2000 DENZO-SMN (SCALEPACK). The crystal data and refinement parameters are listed in Tables A1.1. The reflection data and systematic absences were consistent with a triclinic space group: P $\bar{1}$.

The SHELXTL/PC V6.14 for Windows NT (Sheldrick, G. M., 2001) suite of programs was used to solve the structure by direct methods. Subsequent difference Fourier syntheses allowed the remaining atoms to be located. All of the non-hydrogen atoms were refined with anisotropic thermal parameters. The hydrogen atom positions were calculated geometrically and were included as riding on their respective carbon atoms. Full-matrix least squares refinement of F² gave R₁ = 6.19 for 2σ data and wR₂ = 20.02 for all data (GOOF = 1.070).

Table A1.1 X-Ray Crystallographic Data for **2.6a**

Formula	C ₃₁ H ₂₆ F ₃ PS
Fw	518.61
Wavelength	0.71073
<i>T</i> (K)	150(2)
Crystal system	triclinic
Space group	<i>P</i> $\bar{1}$
<i>a</i> (Å)	10.6836(5)
<i>b</i> (Å)	10.8849(5)
<i>c</i> (Å)	13.1140(5)
α (deg)	69.316(3)
β (deg)	74.491(2)
γ (deg)	74.934(2)
<i>V</i> (Å ³)	1351.41(11)
<i>Z</i>	2
<i>D</i> _{calc} (g cm ⁻³)	1.274
Absorption coefficient (mm ⁻¹)	0.217
<i>F</i> (000)	540
Crystal size (mm ³)	0.125 x 0.3 x 0.35
θ range for data collection (deg)	2.04 to 27.48
Reflections collected	10114
Independent reflections	6195; R(int) = 0.037
Completeness (%)	98.1
Absorption correction	Semi-empirical from equivalents
Data/restraints/parameters	6195/0/328
Goodness-of-fit <i>F</i> ²	1.070
Final R indices [<i>I</i> > 2 σ (<i>I</i>)]	R ₁ = 0.0619; wR ₂ = 0.1743
R indices (all data)	R ₁ = 0.1064; wR ₂ = 0.2002
Largest diff. peak and hole (e Å ⁻³)	0.517; -0.422

A1.2 X-Ray Structure of 2.6b

Crystals of **2.6b** were grown by slow diffusion of hexanes into a concentrated Et₂O/C₆D₆ solution containing **2.6b**. A colourless crystal was mounted on a glass fibre. Data were collected at low temperature (150(2) K) on a Nonius Kappa-CCD area detector diffractometer with COLLECT (Nonius B.V., 1997-2002). The unit cell parameters were calculated and refined from the full data set. Crystal cell refinement and data reduction were carried out using HKL2000 DENZO-SMN.¹ The absorption correction was applied using HKL2000 DENZO-SMN (SCALEPACK). The crystal data and refinement parameters are listed in Table A1.2. The reflection data and systematic absences were consistent with a triclinic space group: P $\bar{1}$.

The SHELX/PC V6.14 for Windows NT (Sheldrick, G. M., 2001) suite of programs was used to solve the structure by direct methods. Subsequent difference Fourier syntheses allowed the remaining atoms to be located. All of the non-hydrogen atoms were refined with anisotropic thermal parameters. The hydrogen atom positions were calculated geometrically and were included as riding on their respective carbon atoms. Full-matrix least squares refinement of F² gave R₁ = 5.60 for 2σ data and wR₂ = 15.04 for all data (GOOF = 1.045).

Table A1.2 X-Ray Crystallographic Data for **2.6b**

Formula	C ₃₀ H ₂₇ PS
Fw	450.61
Wavelength	0.71073
<i>T</i> (K)	150(2)
Crystal system	triclinic
Space group	<i>P</i> $\bar{1}$
<i>a</i> (Å)	11.3067(3)
<i>b</i> (Å)	11.8222(3)
<i>c</i> (Å)	20.3297(6)
α (deg)	87.8245(14)
β (deg)	76.1635(12)
γ (deg)	62.4285(13)
<i>V</i> (Å ³)	2330.59(11)
<i>Z</i>	4
<i>D</i> _{calc} (g cm ⁻³)	1.284
Absorption coefficient (mm ⁻¹)	0.224
<i>F</i> (000)	952
Crystal size (mm ³)	0.3 x 0.35 x 0.375
θ range for data collection (deg)	2.04 to 30.03
Reflections collected	16932
Independent reflections	13308; R(int) = 0.031
Completeness (%)	97.1
Absorption correction	Semi-empirical from equivalents
Data/restraints/parameters	13308/0/583
Goodness-of-fit <i>F</i> ²	1.045
Final R indices [<i>I</i> > 2 σ (<i>I</i>)]	R ₁ = 0.0560; wR ₂ = 0.1377
R indices (all data)	R ₁ = 0.0795; wR ₂ = 0.1504
Largest diff. peak and hole (e Å ⁻³)	1.757; -1.004

A1.3 X-Ray Structure of 2.6c

Crystals of **2.6c** were grown by slow diffusion of hexanes into a concentrated Et₂O/C₆D₆ solution containing **2.6c**. A colourless crystal was mounted on a glass fibre. Data were collected at low temperature (150(2) K) on a Nonius Kappa-CCD area detector diffractometer with COLLECT (Nonius B.V., 1997-2002). The unit cell parameters were calculated and refined from the full data set. Crystal cell refinement and data reduction were carried out using HKL2000 DENZO-SMN.¹ The absorption correction was applied using HKL2000 DENZO-SMN (SCALEPACK). The crystal data and refinement parameters are listed in Table A1.3. The reflection data and systematic absences were consistent with a monoclinic space group: P2(1)/c.

The SHELXTL/PC V6.14 for Windows NT (Sheldrick, G. M., 2001) suite of programs was used to solve the structure by direct methods. Subsequent difference Fourier syntheses allowed the remaining atoms to be located. All of the non-hydrogen atoms were refined with anisotropic thermal parameters. The hydrogen atom positions were calculated geometrically and were included as riding on their respective carbon atoms. Full-matrix least squares refinement of F² gave R₁ = 4.63 for 2σ data and wR₂ = 12.48 for all data (GOOF = 1.046).

Table A1.3 X-Ray Crystallographic Data for **2.6c**

Formula	C ₃₁ H ₂₉ OPS
Fw	480.64
Wavelength	0.71073
<i>T</i> (K)	150(2)
Crystal system	monoclinic
Space group	<i>P</i> 2(1)/ <i>c</i>
<i>a</i> (Å)	10.1635(3)
<i>b</i> (Å)	14.1370(4)
<i>c</i> (Å)	17.8587(4)
α (deg)	90.000
β (deg)	102.1929(14)
γ (deg)	90.000
<i>V</i> (Å ³)	2508.08(12)
<i>Z</i>	2
<i>D</i> _{calc} (g cm ⁻³)	1.273
Absorption coefficient (mm ⁻¹)	0.215
<i>F</i> (000)	1016
Crystal size (mm ³)	0.3 x 0.325 x 0.45
θ range for data collection (deg)	2.04 to 27.48
Reflections collected	19121
Independent reflections	6004; R(int) = 0.047
Completeness (%)	99.9
Absorption correction	Semi-empirical from equivalents
Data/restraints/parameters	6004/0/311
Goodness-of-fit <i>F</i> ²	1.046
Final R indices [<i>I</i> > 2 σ (<i>I</i>)]	R ₁ = 0.0463; wR ₂ = 0.1124
R indices (all data)	R ₁ = 0.0720; wR ₂ = 0.1248
Largest diff. peak and hole (e Å ⁻³)	0.206; -0.376

A1.4 X-Ray Structure of 5.5a

Crystals of **5.5a** were grown by slow evaporation of a concentrated C₆D₆ solution containing **5.5a**, **5.5b**, and **5.6**. A colourless crystal was mounted on a glass fibre. Data were collected at low temperature (150(2) K) on a Nonius Kappa-CCD area detector diffractometer with COLLECT (Nonius B.V., 1997-2002). The unit cell parameters were calculated and refined from the full data set. Crystal cell refinement and data reduction were carried out using HKL2000 DENZO-SMN.¹ The absorption correction was applied using HKL2000 DENZO-SMN (SCALEPACK). The crystal data and refinement parameters are listed in Table A1.4. The reflection data and systematic absences were consistent with a triclinic space group: P $\bar{1}$.

The SHELXTL/PC V6.14 for Windows NT (Sheldrick, G. M., 2001) suite of programs was used to solve the structure by direct methods. Subsequent difference Fourier syntheses allowed the remaining atoms to be located. There were two nearly identical half molecules in the asymmetric unit each lying about a centre of inversion. As a result, the symmetry generated digermacyclobutane rings are exactly planar. All of the non-hydrogen atoms were refined with anisotropic thermal parameters. The hydrogen atom positions were calculated geometrically and were included as riding on their respective carbon atoms.

Full-matrix least squares refinement of F² gave R₁ = 3.98 for 2σ data and wR₂ = 10.16 for all data (GOOF = 1.047). The final solution was submitted to the IUCR checkCIF program and had no Alert Levels A or B.

Table A1.4 X-Ray Crystallographic Data for **5.5a**

Formula	C ₄₈ H ₆₈ Ge ₂
Fw	790.20
Wavelength	0.71073
<i>T</i> (K)	150(2)
Crystal system	triclinic
Space group	<i>P</i> $\bar{1}$
<i>a</i> (Å)	12.5026(4)
<i>b</i> (Å)	13.2978(4)
<i>c</i> (Å)	14.0760(4)
α (deg)	102.1924(16)
β (deg)	104.8630(15)
γ (deg)	92.3110(14)
<i>V</i> (Å ³)	2199.83(12)
<i>Z</i>	2
<i>D</i> _{calc} (g cm ⁻³)	1.193
Absorption coefficient (mm ⁻¹)	1.396
<i>F</i> (000)	840
Crystal size (mm ³)	0.38 x 0.23 x 0.18
θ range for data collection (deg)	2.04 to 27.48
Reflections collected	17043
Independent reflections	10107; R(int) = 0.037
Completeness (%)	99.5
Absorption correction	Semi-empirical from equivalents
Data/restraints/parameters	10107/0/469
Goodness-of-fit <i>F</i> ²	1.047
Final R indices [<i>I</i> > 2 σ (<i>I</i>)]	R ₁ = 0.0398; wR ₂ = 0.0909
R indices (all data)	R ₁ = 0.0691; wR ₂ = 0.1016
Largest diff. peak and hole (e Å ⁻³)	0.444; -0.565

A1.5 References

1. Z. Otwinowski and W. Minor in *Methods in Enzymology, Vol. 276: Macromolecular Crystallography, Part A*. Edited by C. W. Carter Jr. and R. M. Sweet; Academic Press: New York, 1997; p. 307.

Appendix 2

Energies and Coordinates of Calculated Structures

A2.1 Reactants

Acetylene

E (B3LYP):	-77.356644	E (CCSD):	-77.127593
Free Energy (B3LYP):	-77.348434	ZPE (B3LYP):	0.025224
C	0.000000	0.000000	0.000000
C	0.000000	0.000000	1.199308
H	0.015473	0.000000	-1.062907
H	0.015491	0.000136	2.262215

Silene

E (B3LYP):	-329.98425	E (CCSD):	-329.36012
Free Energy (B3LYP):	-329.96810	ZPE (B3LYP):	0.04003
Si	0.000000	0.000000	0.000000
C	0.000000	0.000000	1.707919
H	1.243539	0.000000	-0.795551
H	-1.243511	0.000047	-0.795595
H	0.916925	-0.000018	2.286187
H	-0.916892	-0.000014	2.286233

Germene

E (B3LYP):	-2117.47259	E (CCSD):	-2115.73973
Free Energy (B3LYP):	-2117.45920	ZPE (B3LYP):	0.03864
Ge	0.000000	0.000000	0.000000
C	0.000000	0.000000	1.778883
H	1.286489	0.000000	-0.818890
H	-1.286489	0.000217	-0.818890
H	0.923660	-0.000140	2.343197
H	-0.923659	-0.000005	2.343196

A2.2 Products

Silacyclobutene:

E (B3LYP):	-407.43394	E (CCSD):	-406.58656
Free Energy (B3LYP):	-407.38549	ZPE (B3LYP):	0.07543
Si	0.000000	0.000000	1.915931
C	0.000000	0.000000	0.000000
C	1.814026	0.000000	1.473920
C	1.518648	0.000000	0.159402
H	-0.395674	-0.886312	-0.503969
H	-0.395675	0.886313	-0.503970
H	-0.555949	-1.202411	2.595866
H	-0.555949	1.202411	2.595866
H	2.801622	0.000000	1.918360
H	2.224070	0.000000	-0.672697

Silylacetylene

E (B3LYP):	-407.43361	E (CCSD):	-406.58593
Free Energy (B3LYP):	-407.38989	ZPE (B3LYP):	0.07257
Si	0.000000	0.000000	1.879521
C	0.000000	0.000000	0.000000
C	1.721005	0.000000	2.526130
C	2.857368	0.000000	2.939485
H	0.508452	-0.884975	-0.390357
H	-1.025196	0.000000	-0.381084
H	-0.555949	-1.202411	2.595866
H	-0.688312	1.206254	2.404875
H	-0.688312	-1.206254	2.404875
H	3.855980	0.000000	3.306962

Germacyclobutene

E (B3LYP):	-2194.91496	E (CCSD):	-2192.95754
Free Energy (B3LYP):	-2194.86941	ZPE (B3LYP):	0.07366
Ge	0.000000	0.000000	0.000000
C	0.000000	0.000000	2.011636
C	1.516753	0.000000	1.888908
C	1.869703	0.000000	0.592315
H	-0.536180	-1.255053	-0.714647
H	-0.536180	1.255052	-0.714647
H	-0.415322	-0.887787	2.495175
H	-0.415322	0.887786	2.495174
H	2.194389	0.000000	2.743688
H	2.872689	0.000000	0.182126

Germylacetylene

E (B3LYP):	-2194.91189	E (CCSD):	-2192.95474
Free Energy (B3LYP):	-2194.87115	ZPE (B3LYP):	0.07093
Ge	0.000000	0.000000	1.963437
C	0.000000	0.000000	0.000000
C	1.808309	0.000000	2.601201
C	2.953646	0.000000	2.987050
H	0.512818	-0.887369	-0.373760
H	-1.025957	0.000000	-0.373093
H	0.512802	0.887377	-0.373760
H	-0.690068	1.254189	2.520476
H	-0.690061	-1.254203	2.520455
H	3.960547	0.000000	3.330945

A2.3 Intermediates and Transition States

DR1-SiC-a[‡]

E (B3LYP):	-407.32051	E (CCSD):	-406.45843
Free Energy (B3LYP):	-407.28253	ZPE (B3LYP):	0.06719
Si	0.000000	0.000000	1.758438
C	0.000000	0.000000	0.000000
C	2.063747	0.000000	2.502613
C	2.251295	0.831946	3.411280
H	0.250465	-0.890163	-0.569342
H	0.025690	0.922011	-0.572316
H	-0.554404	1.192222	2.434682
H	-0.406299	-1.260896	2.422023
H	2.598527	-0.793363	2.008524
H	2.032727	1.660980	4.049223

DR1-SiC-b

E (B3LYP):	-407.32752	E (CCSD):	-406.47698
Free Energy (B3LYP):	-407.28833	ZPE (B3LYP):	0.06841
Si	0.000000	0.000000	1.834962
C	0.000000	0.000000	0.000000
C	1.793492	0.000000	2.530972
C	2.211741	0.937507	3.328549
H	0.151518	-0.904273	-0.582902
H	-0.005626	0.915824	-0.583950
H	-0.674161	1.205936	2.375129
H	-0.660068	-1.231411	2.343697
H	2.424250	-0.847308	2.259693
H	1.855425	1.869657	3.743802

DR1-SiC-c[‡]

E (B3LYP):	-407.32013	E (CCSD):	-406.46660
Free Energy (B3LYP):	-407.28298	ZPE (B3LYP):	0.06636
Si	0.000000	0.000000	1.829113
C	0.000000	0.000000	0.000000
C	1.807666	0.000000	2.540625
C	2.226228	0.938196	3.311148
H	0.225904	-0.888654	-0.582882
H	-0.062870	0.914688	-0.582162
H	-0.628407	-1.244214	2.348973
H	-0.685680	1.193606	2.377930
H	2.409155	-0.876098	2.267660
H	2.651260	1.666589	3.962837

DR1-SiC-d

E (B3LYP):	-407.32375	E (CCSD):	-406.47445
Free Energy (B3LYP):	-407.28562	ZPE (B3LYP):	0.06777
Si	0.000000	0.000000	1.847005
C	0.000000	0.000000	0.000000
C	1.772638	0.000000	2.540053
C	2.245254	0.979307	3.254506
H	0.173153	-0.897231	-0.587745
H	-0.088289	0.911745	-0.583517
H	-0.703591	1.195897	2.368283
H	-0.660900	-1.239440	2.338726
H	2.386816	-0.882852	2.318764
H	3.129972	1.277506	3.798920

DR1-SiC-e[‡]

E (B3LYP):	-407.32211	E (CCSD):	-406.47358
Free Energy (B3LYP):	-407.28330	ZPE (B3LYP):	0.06748
Si	0.000000	0.000000	1.846955
C	0.000000	0.000000	0.000000
C	1.769660	0.000000	2.525910
C	2.641033	0.919590	2.220933
H	-0.815464	-0.412046	-0.587411
H	0.814817	0.425541	-0.577737
H	-0.704688	-1.206254	2.360434
H	-0.713866	1.194579	2.379770
H	2.047101	-0.819721	3.203132
H	3.663187	1.208050	2.423047

DR2-SiC-a

E (B3LYP):	-407.32541	E (CCSD):	-406.47575
Free Energy (B3LYP):	-407.28298	ZPE (B3LYP):	0.07132
Si	1.205231	1.753978	3.066300
C	0.023694	-0.069579	1.225680
C	1.278226	0.131020	2.076813
C	-0.009336	-0.029810	-0.081389
H	0.656392	0.180360	-0.905743
H	-0.890083	-0.272563	1.783593
H	2.172084	0.140811	1.448932
H	1.378469	-0.706161	2.775666
H	-0.036880	1.825206	3.887986
H	1.268301	2.937802	2.163935

DR2-SiC-b[‡]

E (B3LYP):	-407.31912	E (CCSD):	-406.46743
Free Energy (B3LYP):	-407.27848	ZPE (B3LYP):	0.06952
Si	0.000222	-0.000530	-0.000386
C	-0.001135	-0.000701	1.902561
C	1.418017	0.001988	2.478106
C	2.001495	1.006413	3.054303
H	0.799099	-1.141046	-0.535097
H	0.552096	1.275621	-0.536224
H	-0.529310	-0.893649	2.252920
H	-0.555032	0.871914	2.254512
H	1.944846	-0.952724	2.364866
H	2.495687	1.820866	3.529852

DR2-SiC-c

E (B3LYP):	-407.32471	E (CCSD):	-406.47556
Free Energy (B3LYP):	-407.28248	ZPE (B3LYP):	0.07115
Si	1.527548	1.734330	2.951638
C	1.224406	0.009861	2.192699
C	-0.003218	0.001384	1.308256
C	-0.007562	-0.012507	-0.000649
H	-0.717242	-0.036901	-0.812664
H	-0.963191	0.032048	1.836712
H	2.108812	-0.279799	1.620880
H	1.104455	-0.711115	3.007304
H	0.340714	2.186770	3.733570
H	1.836054	2.737019	1.894468

DR2-SiC-d[‡]

E (B3LYP):	-407.32108	E (CCSD):	
Free Energy (B3LYP):	-407.27867	ZPE (B3LYP):	0.07068
Si	0.000227	0.003840	0.000363
C	-0.000431	0.000034	1.907802
C	1.394705	-0.001921	2.503535
C	2.406931	0.732098	2.110311
H	0.760888	-1.162571	-0.529013
H	0.562444	1.270147	-0.544873
H	-0.555460	-0.873316	2.260150
H	-0.556963	0.877294	2.254862
H	1.557305	-0.685721	3.346580
H	3.439052	0.893557	2.380742

ZW-SiC-a[‡]

E (B3LYP):	-407.29900	E (CCSD):	-406.44047
Free Energy (B3LYP):	-407.25896	ZPE (B3LYP):	0.06889
Si	0.000000	0.000000	1.807850
C	0.000000	0.000000	0.000000
C	1.687008	0.000000	-0.743813
C	1.980731	-0.938846	-1.522662
H	0.740585	1.119709	2.448001
H	0.370169	-1.291018	2.443476
H	-0.388638	0.901860	-0.472201
H	-0.475528	-0.877336	-0.430980
H	2.152878	0.918760	-0.433137
H	1.775341	-1.904836	-1.936324

ZW-SiC-b

E (B3LYP):	-407.30085	E (CCSD):	-406.44731
Free Energy (B3LYP):	-407.25935	ZPE (B3LYP):	0.07049
Si	0.000000	0.000000	0.000000
C	0.000000	0.000000	1.859943
C	1.539905	0.000000	2.300195
C	2.012125	0.996590	2.984612
H	0.860640	-1.065689	-0.585633
H	0.412340	1.308653	-0.578234
H	-0.469228	-0.882097	2.299139
H	-0.502004	0.889335	2.238040
H	2.042906	-0.940088	2.108974
H	1.725842	2.036244	3.082783

ZW-SiC-c[‡]

E (B3LYP):	-407.29204	E (CCSD):	-406.43922
Free Energy (B3LYP):	-407.25089	ZPE (B3LYP):	0.06938
Si	0.000000	0.000000	1.866618
C	0.000000	0.000000	0.000000
C	1.518279	0.000000	-0.505035
C	1.997547	-1.053762	-1.058371
H	0.911608	1.022555	2.455035
H	0.357679	-1.318478	2.457174
H	-0.482188	0.882286	-0.424419
H	-0.505958	-0.891487	-0.368655
H	1.998717	0.962836	-0.334169
H	2.720223	-1.413693	-1.768240

CT-SiC-a[‡]

E (B3LYP):	-407.30182	E (CCSD):	-406.44143
Free Energy (B3LYP):	-407.26172	ZPE (B3LYP):	0.06815
Si	0.000000	0.000000	1.757379
C	0.000000	0.000000	0.000000
C	1.976112	0.000000	2.788095
C	2.166704	0.000062	1.561194
H	-0.439675	1.242031	2.434265
H	-0.439604	-1.242051	2.434280
H	0.216080	0.915627	-0.542611
H	0.216100	-0.915623	-0.542612
H	2.720990	0.000153	0.645716
H	2.249698	-0.000055	3.824311

CH-SiC-a[‡]

E (B3LYP):	-407.28496	E (CCSD):	-406.42587
Free Energy (B3LYP):	-407.24891	ZPE (B3LYP):	0.06470
Si	0.000000	0.000000	1.772325
C	0.000000	0.000000	0.000000
C	2.239829	0.000000	2.525197
C	2.356437	0.000063	1.297787
H	-0.282143	-0.914790	-0.514210
H	-0.282490	0.914499	-0.514589
H	-0.281195	-1.225237	2.557181
H	-0.281227	1.225061	2.557440
H	1.619828	0.000101	0.282963
H	2.351478	-0.000051	3.586217

DR1-GeC-a[‡]

E (B3LYP):	-2194.80516	E (CCSD):	-2192.83603
Free Energy (B3LYP):	-2194.77040	ZPE (B3LYP):	0.06533
Ge	0.000000	0.000000	1.853410
C	0.000000	0.000000	0.000000
C	2.101140	0.000000	2.619990
C	2.358703	0.859734	3.495171
H	0.251140	-0.899604	-0.552543
H	0.095969	0.928516	-0.552884
H	-0.586055	1.246224	2.521903
H	-0.493904	-1.296582	2.508159
H	2.626396	-0.819233	2.155726
H	2.126580	1.717960	4.091182

DR1-GeC-b

E (B3LYP):	-2194.80787	E (CCSD):	-2192.84672
Free Energy (B3LYP):	-2194.77202	ZPE (B3LYP):	0.06642
Ge	0.000000	0.000000	1.909441
C	0.000000	0.000000	0.000000
C	1.901489	0.000000	2.618261
C	2.324664	0.942120	3.395146
H	0.158303	-0.910979	-0.568414
H	0.050866	0.923106	-0.568182
H	-0.675750	1.254523	2.478151
H	-0.662585	-1.278431	2.450166
H	2.498645	-0.860135	2.323138
H	1.992733	1.876909	3.820814

DR1-GeC-c[‡]

E (B3LYP):	-2194.80119	E (CCSD):	-2192.83682
Free Energy (B3LYP):	-2194.76732	ZPE (B3LYP):	0.06445
Ge	0.000000	0.000000	1.902153
C	0.000000	0.000000	0.000000
C	1.922293	0.000000	2.636782
C	2.337491	0.953346	3.374314
H	0.217881	-0.899444	-0.567099
H	0.022821	0.926485	-0.564436
H	-0.627866	-1.291782	2.454841
H	-0.683718	1.242316	2.483763
H	2.479237	-0.895503	2.350149
H	2.822319	1.659077	4.009798

DR1-GeC-d

E (B3LYP):	-2194.80340	E (CCSD):	-2192.84379
Free Energy (B3LYP):	-2194.76846	ZPE (B3LYP):	0.06578
Ge	0.000000	0.000000	1.924319
C	0.000000	0.000000	0.000000
C	1.869061	0.000000	2.627672
C	2.336872	0.992594	3.315081
H	0.147906	-0.908175	-0.575503
H	-0.020475	0.922860	-0.570288
H	-0.710189	1.243696	2.470679
H	-0.669881	-1.287162	2.439216
H	2.455328	-0.896206	2.398290
H	3.210756	1.331515	3.850870

DR1-GeC-e[†]

E (B3LYP):	-2194.80042	E (CCSD):	-2192.84211
Free Energy (B3LYP):	-2194.76715	ZPE (B3LYP):	0.06559
Ge	0.000000	0.000000	1.939383
C	0.000000	0.000000	0.000000
C	1.913513	0.000000	2.378339
C	2.691821	0.000188	1.328548
H	-0.016291	-0.920403	-0.573414
H	-0.017110	0.920366	-0.573445
H	-0.692080	-1.254647	2.505941
H	-0.692074	1.254656	2.505918
H	2.300043	-0.000127	3.402829
H	3.740713	0.000266	1.061559

DR2-GeC-a

E (B3LYP):	-2194.82274	E (CCSD):	-2192.86295
Free Energy (B3LYP):	-2194.78308	ZPE (B3LYP):	0.06992
Ge	1.220806	1.789536	3.098699
C	1.289264	0.082351	2.062150
C	0.031490	-0.089367	1.226705
C	-0.011866	-0.026234	-0.080832
H	0.647325	0.205048	-0.904900
H	-0.879578	-0.298810	1.786714
H	2.183368	0.103217	1.438072
H	1.384939	-0.741613	2.773902
H	-0.098573	1.867986	3.908549
H	1.278925	2.998951	2.132716

DR2-GeC-b[‡]

E (B3LYP):	-2194.81647	E (CCSD):	-2192.85469
Free Energy (B3LYP):	-2194.77858	ZPE (B3LYP):	0.06812
Ge	-0.490275	-0.197262	-0.962089
C	-0.386695	-0.147758	1.033678
C	1.052364	0.012906	1.503218
C	1.571579	1.092285	2.004032
H	0.467066	-1.283706	-1.517109
H	-0.065315	1.172705	-1.547313
H	-0.801624	-1.085230	1.412494
H	-1.009106	0.676181	1.382824
H	1.664388	-0.889414	1.389047
H	1.997612	1.977771	2.414225

DR2-GeC-c

E (B3LYP):	-2194.82214	E (CCSD):	-2192.86281
Free Energy (B3LYP):	-2194.78267	ZPE (B3LYP):	0.06974
Ge	0.000000	0.000000	0.000000
C	0.000000	0.000000	2.005188
C	1.411218	0.000000	2.526513
C	2.051287	1.032904	3.017930
H	0.815298	-1.209321	-0.526898
H	0.648526	1.304274	-0.524900
H	-0.537740	-0.891360	2.334934
H	-0.546113	0.882720	2.338609
H	1.939792	-0.958153	2.458394
H	3.010903	1.263033	3.453644

DR2-GeC-d[‡]

E (B3LYP):	-2194.81818	E (CCSD):	-2192.86006
Free Energy (B3LYP):	-2194.77860	ZPE (B3LYP):	0.06924
Ge	1.342213	-1.287675	-0.740339
C	1.062241	0.000000	2.279886
C	0.000000	0.000000	1.509934
C	0.000000	0.000000	0.000000
H	1.140289	-2.680081	-0.095216
H	2.780619	-0.789410	-0.463447
H	-0.986449	-0.262548	-0.385378
H	0.248418	0.990091	-0.391085
H	-0.984350	-0.000464	1.996366
H	1.294231	-0.000864	3.333809

ZW-GeC-a[‡]

E (B3LYP):	-2194.79444	E (CCSD):	-2192.82428
Free Energy (B3LYP):	-2194.75753	ZPE (B3LYP):	0.06724
Ge	0.000000	0.000000	1.888303
C	0.000000	0.000000	0.000000
C	1.723089	0.000000	-0.848986
C	1.859470	-0.860975	-1.735300
H	0.834547	1.142396	2.513495
H	0.460966	-1.337604	2.508270
H	-0.379943	0.908946	-0.464066
H	-0.477524	-0.877695	-0.426481
H	2.239425	0.839757	-0.426051
H	1.619047	-1.727467	-2.311067

ZW-GeC-b

E (B3LYP):	-2194.80042	E (CCSD):	-2192.83375
Free Energy (B3LYP):	-2194.76142	ZPE (B3LYP):	0.06923
Ge	0.000000	0.000000	0.000000
C	0.000000	0.000000	1.982786
C	1.503905	0.000000	2.351318
C	1.969636	1.003320	3.055785
H	1.015459	-1.049338	-0.533848
H	0.520767	1.368267	-0.520825
H	-0.493266	-0.882251	2.392094
H	-0.510666	0.899380	2.321470
H	2.030649	-0.929126	2.167800
H	1.659440	2.043437	3.083501

ZW-GeC-c[‡]

E (B3LYP):	-2194.79158	E (CCSD):	-2192.82598
Free Energy (B3LYP):	-2194.75332	ZPE (B3LYP):	0.06790
Ge	0.000000	0.000000	1.983217
C	0.000000	0.000000	0.000000
C	1.481812	0.000000	-0.507569
C	1.893563	-1.037505	-1.146361
H	1.145904	0.900895	2.527886
H	0.326360	-1.418364	2.526511
H	-0.499497	0.886341	-0.393877
H	-0.523638	-0.895246	-0.333992
H	2.019268	0.924783	-0.298601
H	2.530249	-1.405450	-1.929931

CT-GeC-a[‡]

E (B3LYP):	-2194.77673	E (CCSD):	-2192.80813
Free Energy (B3LYP):	-2194.73991	ZPE (B3LYP):	0.06617
Ge	0.000000	0.000000	1.848733
C	0.000000	0.000000	0.000000
C	2.234999	0.000000	1.380922
C	2.153518	0.000000	2.631428
H	0.233955	-0.922954	-0.518393
H	0.233952	0.922945	-0.518410
H	-0.398462	-1.294337	2.565632
H	-0.398462	1.294336	2.565631
H	2.716249	0.000000	3.550225
H	2.712468	0.000000	0.422639

CH-GeC-a[‡]

E (B3LYP):	-2194.77221	E (CCSD):	-2192.80486
Free Energy (B3LYP):	-2194.73905	ZPE (B3LYP):	0.06309
Ge	0.000000	0.000000	1.871064
C	0.000000	0.000000	0.000000
C	2.437263	0.000000	1.165372
C	2.540193	-0.007140	2.391950
H	-0.388636	-0.912778	-0.447603
H	-0.389113	0.912615	-0.447557
H	-0.145933	-1.269649	2.722810
H	-0.141637	1.270549	2.722076
H	1.552996	0.001231	0.217477
H	2.766669	-0.012794	3.433907

Appendix 3

Copyrighted Material and Permissions

A3.1 Royal Society of Chemistry: Rights Retained by Journal Authors¹

When the author signs the exclusive Licence to Publish for a journal article, he/she retains certain rights that may be exercised without reference to the RSC. He/she may:

Reproduce/republish portions of the article (including the abstract)

Photocopy the article and distribute such photocopies and distribute copies of the PDF of the article that the RSC makes available to the corresponding author of the article upon publication of the article for personal or professional use only, provided that any such copies are not offered for sale.

Adapt the article and reproduce adaptations of the article for any purpose other than the commercial exploitation of a work similar to the original

Reproduce, perform, transmit and otherwise communicate the article to the public in spoken presentations (including those which are accompanied by visual material such as slides, overheads and computer projections)

¹ This material is available at: <http://pubs.rsc.org/AboutUs/Copyright/RightsRetainedbyJournalauthors.asp>

A3.2 American Chemical Society's Policy on Theses and Dissertations²

Thank you for your request for permission to include **your** paper(s) or portions of text from **your** paper(s) in your thesis. Permission is now automatically granted; please pay special attention to the implications paragraph below. The Copyright Subcommittee of the Joint Board/Council Committees on Publications approved the following:

Copyright permission for published and submitted material from theses and dissertations: ACS extends blanket permission to students to include in their theses and dissertations their own articles, or portions thereof, that have been published in ACS journals or submitted to ACS journals for publication, provided that the ACS copyright credit line is noted on the appropriate page(s).

Publishing implications of electronic publication of theses and dissertation material: Students and their mentors should be aware that posting of theses and dissertation material on the Web prior to submission of material from that thesis or dissertation to an ACS journal may affect publication in that journal. Whether Web posting is considered prior publication may be evaluated on a case-by-case basis by the journal's editor. If an ACS journal editor considers Web posting to be "prior publication", the paper will not be accepted for publication in that journal. If you intend to submit your unpublished paper to ACS for publication, check with the appropriate editor prior to posting your manuscript electronically.

If your paper has **not** yet been published by ACS, we have no objection to your including the text or portions of the text in your thesis/dissertation in **print and microfilm formats**; please note, however, that electronic distribution or Web posting of the unpublished paper as part of your thesis in electronic formats might jeopardize

² This material is available at: <http://pubs.acs.org/page/copyright/permissions.html>

publication of your paper by ACS. Please print the following credit line on the first page of your article: "Reproduced (or 'Reproduced in part') with permission from [JOURNAL NAME], in press (or 'submitted for publication'). Unpublished work copyright [CURRENT YEAR] American Chemical Society." Include appropriate information.

If your paper has already been published by ACS and you want to include the text or portions of the text in your thesis/dissertation in **print or microfilm formats**, please print the ACS copyright credit line on the first page of your article: "Reproduced (or 'Reproduced in part') with permission from [FULL REFERENCE CITATION.] Copyright [YEAR] American Chemical Society." Include appropriate information.

Submission to a Dissertation Distributor: If you plan to submit your thesis to UMI or to another dissertation distributor, you should not include the unpublished ACS paper in your thesis if the thesis will be disseminated electronically, until ACS has published your paper. After publication of the paper by ACS, you may release the entire thesis (**not the individual ACS article by itself**) for electronic dissemination through the distributor; ACS's copyright credit line should be printed on the first page of the ACS paper.

Use on an Intranet: The inclusion of your ACS unpublished or published manuscript is permitted in your thesis in print and microfilm formats. If ACS has published your paper you may include the manuscript in your thesis on an intranet that is not publicly available. Your ACS article cannot be posted electronically on a publicly available medium (i.e. one that is not password protected), such as but not limited to, electronic archives, Internet, library server, etc. The only material from your paper that can be posted on a public electronic medium is the article abstract, figures, and tables,

and you may link to the article's DOI or post the article's author-directed URL link provided by ACS. This paragraph does not pertain to the dissertation distributor paragraph above.